High-order numerical methods for integral fractional Laplacian: algorithm and analysis

Zhaopeng Hao
Worcester Polytechnic Institute

High-order numerical methods for integral fractional Laplacian: algorithm and analysis

by

Zhaopeng Hao

A Dissertation

Submitted to the Faculty

of the

WORCESTER POLYTECHNIC INSTITUTE

in partial fulfillment of the requirements for the

Degree of Doctor of Philosophy

in

Mathematical Sciences

by

_____

April 2020

APPROVED:

_____

Dr. Zhongqiang Zhang, Advisor
Department of Mathematical Sciences
Worcester Polytechnic Institute

Dr. Vladimir Druskin
Department of Mathematical Sciences
Worcester Polytechnic Institute

Dr. Akil Narayan
Department of Mathematics
Utah University

Dr. Nikolaos A. Gatsonis
Department of Mechanical Engineering
Worcester Polytechnic Institute

Dr. Marcus Sarkis-Martins
Department of Mathematical Sciences
Worcester Polytechnic Institute

Dr. Darko Volkov
Department of Mathematical Sciences
Worcester Polytechnic Institute

Dr. Vadim V. Yakovlev
Department of Mathematical Sciences
Worcester Polytechnic Institute

Acknowledgements

I wish to thank the members of my dissertation committee, Dr. Vladimir Druskin, Dr. Akil Narayan, Dr. Nikolaos A. Gatsonis, Dr. Marcus Sarkis, Dr. Darko Volkov, Dr. Vadim V. Yakovlev, Dr. Zhongqiang Zhang, for generously offering their time, support, guidance and good will throughout the preparation and review of this document.

Time flies as if it just happened tomorrow when I was so excited to hear that I was admitted to WPI. Since then, almost three years have past. When I look back upon my PhD study at WPI, I was lucky to get so many help from the nice people around me.

First, I would like to express my gratitude to my advisor Dr. Zhongqiang Zhang who provided me a lot of useful comments and suggestions when I am writing this dissertation on the fractional Laplacian. To me, the research does need the interest, passion, energy and particularly the time. In the course of pursing my PhD degree at WPI, I am extremely grateful to my advisor who provided me two and a half years research assistant position so that I have ample time for research, and sponsored me to attend academic conferences.

Second, I am particularly grateful for those who have ever imparted the knowledge to me during my study at WPI. For example, Dr. Nikolaos A. Gatsonis taught me CFD, Dr. Burt S. Tilley taught me analytical methods on fluid dynamics, and particularly Dr. Marcus Sarkis not only taught me advanced finite elements method but also was always willing to provide me the help, whenever I reached out to him, and gave me many useful comments on my current research.

I would like to thank my academic brother, Ph.D candidate Yuchen Dong for his several times helpful and kind supports in daily life. In passing, I would like to acknowledge the help to those who have helped me but are not named here at the department of Mathematical Sciences, the faculties, my lovely collegues and the staffs. I appreciate your help and will keep them in mind forever.

In addition, I would like to thank my former advisor, collaborator and future mentor Dr. Zhiqiang Cai from Purdue University for the caring, help and sharing of his own advice on my

Abstract

The fractional Laplacian is a promising mathematical tool due to its ability to capture the anomalous diffusion and model the complex physical phenomenon with long range interaction, such as fractional quantum mechanics, image processing, jump process etc. One of important applications of fractional Laplacian is a turbulence intermittency model of fractional Navier-Stokes equation which is derived from Boltzmann's theory. However efficient computation of this model on bounded domains is challenging as highly accurate and efficient numerical methods are not yet available.

The bottleneck for efficient computation lies in the low accuracy and high computational cost of discretizing the fractional Laplacian operator.

Although many state-of-the-art numerical methods have been proposed and some progress has been made for the existing numerical methods to achieve quasi-optimal complexity, some issues are still fully unresolved: i) Due to nonlocal nature of the fractional Laplacian, the implementation of algorithm is still complicated and the computational cost for preparation of algorithms is still high, e.g., as pointed out by Acosta et al [2] 'Over 99% of the CPU time is devoted to assembly routine' for finite element method;

ii) Due to the intrinsic singularity of the fractional Laplacian, the convergence orders in the literature (e.g. [4, 6]) are still unsatisfactory for many applications including turbulence intermittency simulations.

To reduce the complexity and computational cost, we consider two numerical methods, finite difference and spectral method with quasi-linear complexity, which are summarized as follows.

- We develop spectral Galerkin methods to accurately solve the fractional advection-diffusion-reaction equations and apply the method to fractional Navier-Stokes equations. In spectral methods on a ball, the evaluation of fractional Laplacian operator can be straightforward thanks to the pseudo-eigen relation. For general smooth computational domains, we propose the use of spectral methods enriched by singular functions which characterizes the inherent boundary singularity of the fractional Laplacian.

- We develop a simple and easy-to-implement fractional centered difference approximation to the fractional Laplacian on a uniform mesh using generating functions. The weights or coefficients of the fractional centered formula can be readily computed using the *fast Fourier transform*. Together with singularity subtraction, we propose high-order finite difference methods without any graded mesh.

With the use of the presented results, it may be possible to solve fractional Navier-Stokes equations, fractional quantum Schrodinger' equations and stochastic fractional equations with high accuracy. All numerical simulations will be accompanied with stability and convergence analysis.

Contents

List of Figures

List of Tables

XIII

Chapter 1

Introduction

1.1 The fractional Laplacian

Nonlocal operators have been applied to model real-world phenomenon in many fields, e.g., fluid dynamics [38, 69], quantum mechanics [51, 63], finance [28], in phase transitions [8, 9], material science [14], etc. However, the difficulty lies in how to efficiently discretize nonlocal operators on which partial differential equations are based and how to justify the convergence order of the algorithms when they are applied to these models. Prior to getting to these important questions, we first recall the definitions and some properties of fractional Laplacian.

1.1.1 Nonlocal pseudo-differential operator

Let $\alpha \in (0,2)$ and $u \in \mathbb{R}^d \to \mathbb{R}$ be smooth enough (belongs to Schwartz class $\mathscr{C}$) A very popular nonlocal operator is given by integral representation: the integral is defined in the sense of principle value

$$(-\Delta)^{\alpha/2} u(x) = c_{d,\alpha} \int_{\mathbb{R}^d} \frac{u(x) - u(y)}{|x - y|^{d+\alpha}}\, dy, \quad c_{d,\alpha} = \frac{2^\alpha \Gamma(\frac{\alpha+d}{2})}{\pi^{d/2}|\Gamma(-\alpha/2)|}, \tag{1.1.1}$$

where $c_{d,\alpha}$ is a normalization constant involving the Gamma function. One of the very important properties which we will use in our work later is Fourier transform:

$$\mathcal{F}((-\Delta)^\alpha u)(k) = |k|^\alpha \mathcal{F}(u)(k). \tag{1.1.2}$$

The fractional Laplace operator is consistent with the integer ones. In particular we have the following pointwise limits

$$\lim_{\alpha \to 0} (-\Delta)^{\alpha/2} u(x) = u(x)$$

$$\lim_{\alpha \to 2} (-\Delta)^{\alpha/2} u(x) = -\Delta u(x)$$

Except above integral definition studied in this work, there are other equivalent definitions which are intensively investigated in the literature, e.g., see Refs. [62] and [1].

A variant of the fractional Laplacian (1.1.1) consists in restricting the domain of integration to a subset of $\mathbb{R}^n$. In these direction, an interesting operator is defined by the following singular integral:

$$(-\Delta)^s_\Omega u(x) := \int_\Omega \frac{u(x) - u(y)}{|x - y|^{n+2s}} dy. \tag{1.1.3}$$

1

When $\Omega = \mathbb{R}^n$, the regional fractional Laplacian is reduced to the standard fractional Laplacian. Here we should point out that they are different operators although they are similarly defined.

Another natural but inequivalent (see [78]) fractional operator is defined through taking fractional powers of the eigenvalues:

$$(-\Delta)^s_{D,\Omega} u(x) = \sum_{k=0}^{\infty} \lambda_k^s u_k \phi_k(x). \tag{1.1.4}$$

where ϕ_k is normalized eigenfunction corresponding to the Dirichlet Laplacian with the kth eigenvalue $0 \le \lambda_0 < \lambda_1 \le \lambda_2 \le \cdots$, namely

$$-\Delta u = \lambda_k \phi_k, \quad x \in \Omega \subset \mathbb{R}^d, \tag{1.1.5}$$
$$u(x) = 0, \quad x \in \partial\Omega. \tag{1.1.6}$$

Furthermore, other types of fractional operators can be defined in terms of different boundary conditions: for example, a spectral decomposition with respect to the eigenfunctions of Laplacians with Neumann boundary data naturally leads to an operator $(-\Delta)^s_{N,\Omega}$. An interesting observation, spectral definition is equivalent to the regional one up to a constant. Furthermore, for periodic functions, or functions defined on the flat torus, namely, if $u(x + k) = u(x)$ for any $x \in \mathbb{R}^n$ and $k \in \mathbb{Z}^n$, then $(-\Delta)^s_{N,\Omega} = \text{const}(-\Delta)^s_\Omega$. The proofs for these equivalence can be seen from [1].

1.1.2 Other equivalent definitions

Except the hyper-singular form definitions, there are other equivalent ones. In [62] the author discussed ten equivalent definitions and provided their proof. We list three of them as follows. Here we only provide a loosely description. For rigorous discussion of equivalent definitions, we recommend the readers to consult [62].

Let $u \in L^p$ with $p \in [1, \infty]$ or u belongs to the space of continuous functions vanishing at the infinity or the space bounded uniformly continuous functions.

- Bochner's definition:

$$(-\Delta)^{\alpha/2} u(x) = \frac{1}{|\Gamma(-\frac{\alpha}{2})|} \int_0^\infty (e^{t\Delta} u - u) t^{-1-\alpha/2} dt, \tag{1.1.7}$$

- Balakrishnan's definition:

$$(-\Delta)^{\alpha/2} u(x) = \frac{\sin(\frac{\alpha\pi}{2})}{\pi} \int_0^\infty \Delta(sI - \Delta)^{-1} u s^{\alpha/2-1} ds, \tag{1.1.8}$$

- Caffarelli–Silvestre'definition through harmonic extensions:

$$\Delta_x v(x, y) + \alpha^2 c_\alpha^{2/\alpha} y^{2-2/\alpha} \partial_y^2 v(x, y) = 0, \forall y > 0,$$
$$v(x, 0) = u(x),$$
$$\partial_y v(x, 0) = (-\Delta)^{\alpha/2} u(x), \tag{1.1.9}$$

- For $\alpha \in (1, 2)$, the fractional Laplacian can also rewritten as [73, 77]

$$(-\Delta)^{\alpha/2}u(x) = c_\alpha \int_0^{2\pi} D_\theta^\alpha u(x)d\theta, \tag{1.1.10}$$

where D_θ^α is fractional directional derivative,

$$D_\theta^\alpha = \frac{1}{\Gamma(2-\alpha)}(\theta \cdot \nabla)^2 \int_0^\infty \xi^{1-\alpha}u(x-\xi\zeta(\theta))d\xi, \tag{1.1.11}$$

where $\zeta(\theta) \in \mathbb{R}^d$, $\zeta(\theta) = \cos(\theta)$ for $\theta = 0, \pi$ in 1D; $\zeta(\theta) = [\cos(\theta), \sin(\theta)]^T$ for $\theta \in [0, 2\pi]$ in 2D; $\zeta(\theta) = [\sin(\phi)\cos(\theta), \sin(\phi)\sin(\theta), \cos(\phi)]^T$ for $\theta \in [0, 2\pi]$ and $\phi \in [0, \pi]$. In particular in two-dimensional case, we have $c_\alpha = \frac{\Gamma(\frac{1-\alpha}{2})\Gamma(\frac{2+\alpha}{2})}{2\pi^{3/2}}$.

These definitions provide different starting points for constructing the numerical methods for the fractional Laplacian. We will discuss them later in the literature review of existing numerical methods.

1.1.3 Long jump random walk

Such nonlocal operators are related to Levy process. We next briefly show a possible probabilistic interpretation. For detailed derivation, readers can refer to the note by Enrico Valdinoci in [86].

Consider a random walk [1] of particle on the lattice $h\mathbb{Z} := \{hz, z \in \mathbb{Z}\}$ along the real line. Let $u(x, t)$ be the probability that our particle lies at $x \in h\mathbb{Z}$ at time $t \in \tau\mathbb{Z}$. Then for local jump random walk, at each time step of size τ, the particle jumps to the left or right with the probability $1/2$.

$$u(x, t+\tau) = \frac{1}{2}u(x+h, t) + \frac{1}{2}u(x-h, t)$$
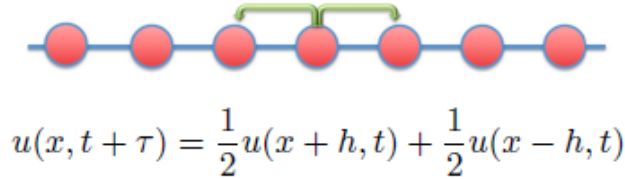
Figure 1.1: Local jump

If we consider $2\tau = h^2$, then we obtain

$$\frac{u(x, t+\tau) - u(x, t)}{\tau} = \frac{u(x-h, t) - 2u(x, t) + u(x, t+\tau)}{h^2}.$$

Letting $h, \tau \to 0$ yields the second order diffusion equation

$$u_t = \Delta u.$$

For the long jump walk [86], the particle can move everywhere, both near and far fields, although the probability could be very small for the far field. In the long jump walk, we assume the probability that the particle jumps from the point $hk \in h\mathbb{Z}$ to the point $hm \in h\mathbb{Z}$ is $\mathcal{K}(k-m) = \mathcal{K}(m-k)$.

$$u(x, t + \tau) = \sum_{k \in \mathbb{Z}} \mathcal{K}(k) u(x + hk, t).$$

Figure 1.2: Long jump

Here $u(x, t + \tau)$ equals the sum of all the probabilities of the possible positions $x + hk$ at time t weighted by the probability of jumping from $x + hk$ to x. Since $\sum_{k \in \mathbb{Z}} \mathcal{K}(k) = 1$ this yields

$$u(x, t + \tau) - u(x, t) = \sum_{k \in \mathbb{Z}} \mathcal{K}(k)(u(x + kh, t) - u(x, t).$$

If $\mathcal{K}(y) \approx |y|^{-(1+\alpha)}$ for $y \to \infty$ (For example we can take the kernel function $k(y) = \frac{4^{\alpha/2} \Gamma(1/2 + \alpha/2)}{\sqrt{\Pi} |\Gamma(-\alpha/2)|} \cdot \frac{(|y| - \alpha/2)}{|y| + 1 + \alpha/2}$; see [25].) with $\alpha \in (0, 2)$ and $\tau = h^\alpha$ then $\frac{\mathcal{K}(k)}{\tau} = h\mathcal{K}(kh)$. Letting $h, \tau \to 0$ gives the fractional order diffusion equation

$$\partial_t u = \int_{\mathbb{R}} \frac{u(x + y, t) - u(x, t)}{|y|^{1+\alpha}} dy \Leftrightarrow \partial_t u + (-\Delta)^{\alpha/2} u = 0.$$

Except the above derivation, recently, the authors in [38] have derived the fractional Laplacian operator as a means to represent the ensembleaveraged friction force arising in a turbulent flow. For the convenience of readers, we leave its brief derivation on the Appendix.

1.1.4 Anomalous diffusion as super-diffusion

Anomalous diffusion phenomena are ubiquitous in the natural sciences and social sciences. Fractional Laplacian can be used to describe the anomalous diffusion and the related equation corresponds to the super-diffusion. In order to get a good sense of the diffusion equation with fractional Laplacian, here we illustrate it by taking one-dimensional case for example. Imagine we have a long thin tube filling with medium. We inject an drop of tracer and observe the evolution of the density. Suppose at the certain time, the density of tracer obeys the law as $\exp(-|x|)$. Then this diffusion process can be modeled by fractional diffusion equation:

$$\partial_t u(x, t) = -(-\Delta)^{\alpha/2} u(x, t), \quad x \in \mathbb{R}, \ t > 0,$$
$$\lim_{x \to \infty} u(x, t) = 0, \quad u(x, 0) = \exp(-|x|),$$

where $0 < \alpha \leq 2$.

The comparison of the profile between second-order and fractional-order equations is illustrated in Figure 1.3. From the picture, we can see the solution of fractional diffusion equations spread faster than the integer counterpart. This partially explain why we call the fractional diffusion as super-diffusion or fast-diffusion.

---

[1]The Figures local jump and long jump comes from the Nochetto's talk: Numerical methods for fractional diffusion.
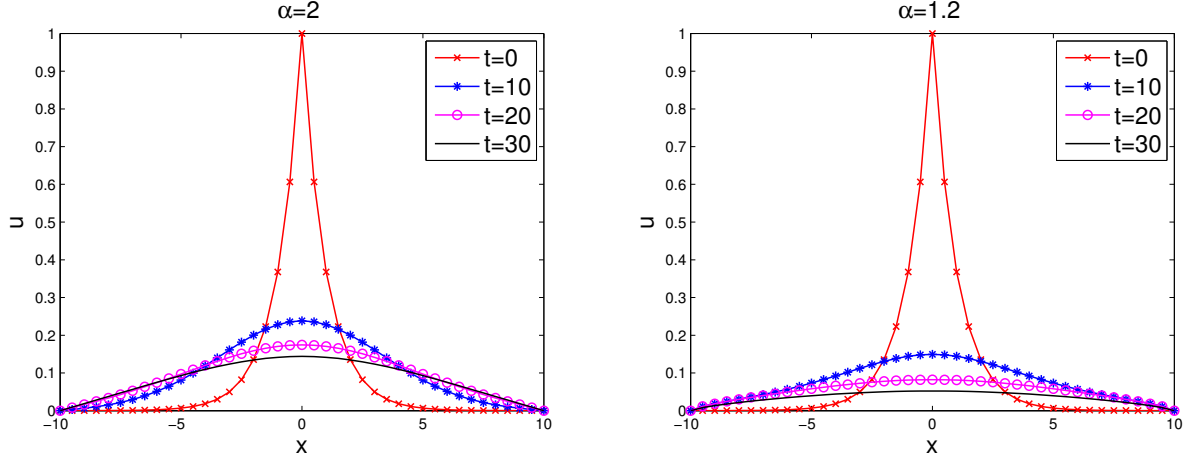
Figure 1.3: Comparison of the profile between second-order and fractional-order equations. Here u the density function of the space variable x and α denotes the order of equation.

1.2 Well posedness for the model problem

In this work, we consider finite difference schemes for the following diffusion equation with fractional Laplacian

$$(-\Delta)^{\alpha/2}u + \mu u = f(x), \quad x \in \Omega \subset \mathbb{R}^d, \qquad \alpha \in (0,2), \tag{1.2.1}$$
$$u(x) = 0, \quad x \in \Omega^c, \tag{1.2.2}$$

where μ is non-negative, $f(x)$ is a given function, Ω is rectangular domain and Ω^c is the complement of Ω in $\mathbb{R}^d$.

Let Ω^c be the complement of the unit disk $\Omega = \{(x_1, x_2) \,|\, x_1^2 + x_2^2 \leq 1\}$. Define

$$\rho(x) = c_{2,\alpha} \int_{\Omega^c} \frac{1}{|x-y|^{2+\alpha}}\, dy, \tag{1.2.3}$$

where $c_{2,\alpha}$ is defined in (1.1.1).

For u, v vanish outside of Ω, we have

$$
\begin{aligned}
((-\Delta)^{\alpha/2}u, v) &= c_{d,\alpha} \iint_{\mathbb{R}\otimes\mathbb{R}} \frac{v(x)(u(x)-u(y))}{|x-y|^{1+\alpha}}\, dy dx = c_{d,\alpha} \iint_{\mathbb{R}\otimes\mathbb{R}} \frac{v(y)(u(y)-u(x))}{|x-y|^{1+\alpha}}\, dx dy \\
&= \frac{1}{2}\left(c_{d,\alpha} \iint_{\mathbb{R}\otimes\mathbb{R}} \frac{v(x)(u(x)-u(y))}{|x-y|^{1+\alpha}}\, dy dx + c_{d,\alpha} \iint_{\mathbb{R}\otimes\mathbb{R}} \frac{v(y)(u(y)-u(x))}{|x-y|^{1+\alpha}}\, dx dy \right).
\end{aligned}
$$

Rearranging this equality, we obtain the formula of integration by parts for fractional Laplacian.

Lemma 1.2.1 (Integration by parts, [4, 7, 93])**.** *Assume that u, v vanish on $\Omega^c \subseteq \mathbb{R}^2$ almost everywhere. Then it holds that*

$$\int_\Omega v(-\Delta)^{\alpha/2}u(x)\, dx = \frac{c_{d,\alpha}}{2} \iint_{\Omega\otimes\Omega} \frac{(u(x)-u(y))(v(x)-v(y))}{|x-y|^{n+\alpha}}\, dy\, dx + \int_\Omega u(x)v(x)\rho(x)\, dx,$$

when all the integrals are well-defined. Here $\rho(x)$ is defined in (1.2.3).

Lemma 1.2.2 ([68]). *Let $\Omega \subset \mathbb{R}^n$ be a convex set and $1 < \alpha < 2$. For any $v \in C_0^\infty(\Omega)$, it holds*

$$\iint_{\Omega \otimes \Omega} \frac{|v(x) - v(y)|^2}{|x - y|^{n+\alpha}} dx dy \geq k_{n,\alpha} \int_\Omega \frac{|v(x)|^2}{d_\Omega(x)^\alpha} dx,$$

where $k_{n,\alpha}$ is a positive constant which only depends on dimension n and α, and $d_\Omega(x)$ denotes the distance from the point $x \in \Omega$ to the boundary of the Ω.

Take $d = 2$ for example. For $x = (x_1, x_2) \in \Omega$, we have

$$\frac{1}{d_\Omega(x)^\alpha} = \frac{\alpha}{2\pi} \int_{|y-x| \geq d_\Omega(x)} \frac{1}{|x - y|^{2+\alpha}} dy \geq \frac{\alpha}{2\pi} \int_{\Omega^c} \frac{1}{|x - y|^{2+\alpha}} dy = \frac{\alpha}{2\pi c_{d,\alpha}} \rho(x).$$

Thus using Lemma 1.2.2 and by the standard density argument we have

$$\iint_{\Omega \otimes \Omega} \frac{|v(x) - v(y)|^2}{|x - y|^{2+\alpha}} dx dy \geq \frac{\alpha k_{2,\alpha}}{2\pi c_{2,\alpha}} \int_\Omega |v(x)|^2 \rho(x) dx, \quad \forall v \in H_0^{\alpha/2}(\Omega). \tag{1.2.4}$$

By Lemma 1.2.1 and (1.2.4), we have the following conclusion that is crucial to build the wellposedness of the problem (1.2.1)-(1.2.2).

Lemma 1.2.3. *For any $v \in H_0^{\alpha/2}(\Omega)$ with $1 < \alpha \leq 2$, there exist constants depending on the order α such that*

$$C_{1,\alpha} |v|^2_{H^{\alpha/2}(\Omega)} \leq ((-\Delta)^{\alpha/2} v, v) \leq C_{2,\alpha} |v|^2_{H^{\alpha/2}(\Omega)}.$$

By Lax-Milgram's Theorem, Lemmas 1.2.1 and 1.2.3, the well-posedness of the problem (1.2.1)-(1.2.2) can be established.

1.3 Motivation

This work is mainly motivated by a promising turbulence intermittency model of fractional Navier-Stokes equation [38], which is one of important applications of fractional Laplacian [67]. This model is derived from Boltzmann's theory while efficient computation of this model on bounded domains is challenging as high-order numerical methods are not yet available. The challenge arises from the intrinsic singularity and nonlocal nature of the fractional Laplacian. Many attempts have been made to accommodate the singularity, nonlocality and the complication of these two issues. For example, [70] has applied a singularity subtraction to achieve similar complexity using a collocation method. However, the stability and convergence of their method is not clear. [7] has applied banded and hierarchical matrices with finite element methods to achieve quasi-optimal complexity. As finite element method involves too much complexity to compute the singular integrals which is difficult for extension to high-dimension or high-order methods.

1.3.1 Motivation for the spectral method

In literature only very mild assumption on regularity of solutions has been made in [7] while many other numerical methods for fractional Laplacian either assume high regularity or achieve very slow convergence without the strong assumption on regularity, see e.g. finite element methods (e.g., [3, 19, 30, 83]), finite difference methods (e.g., [34, 35, 58, 59])

In spectral methods, the evaluation of fractional Laplacian operator (1.1.1) can be straightforward thanks to the pseudo-eigen relation (see Lemma 2.3.1, which can be derived from similar conclusions in [36]), while the high computational cost of discretizing the fractional Laplacian operator (1.1.1) for many other methods in computing solutions to equations with the fractional Laplacian can be very high. According to the pseudo-eigen relation in Lemma 2.3.1, it is natural to represent the solution to (2.0.2) by $u = (1-x^2)^{\alpha/2} \sum_{n=0}^{\infty} \hat{u}_n P_n^{\alpha/2}(x)$, where $P_n^{\alpha/2}$ is the n-th order Jacobi polynomial (see (2.1.4)). When $\mu_1 = \mu_2 = 0$, the regularity of $(1-x)^{-\alpha/2}u$ can be high as it can be analytic if f is analytic [4]; and the regularity index for $(1-x)^{-\alpha/2}u$ is $r + \alpha$ if the regularity index for f is r in weighted Sobolev spaces [93]. However, it is shown in [93] that when $\mu_2 > 0$, the regularity index for $(1-x)^{-\alpha/2}u$ is $\alpha + \min(\alpha + 1 - \epsilon, r)$ for $\epsilon > 0$, which implies limited regularity and only an algebraic convergence of spectral methods. The algebraic convergence order has been verified by numerical results in [93]. However, we observe an even higher convergence order of the spectral Galerkin method (3.4.1); see Figure 1.4. The convergence order of the spectral Galerkin method (3.4.1) in [93] is $2\alpha + 1$ in a weighted L^2-norm while we observe the order of $5\alpha/2 + 1$ in a similar weighted L^2-norm.
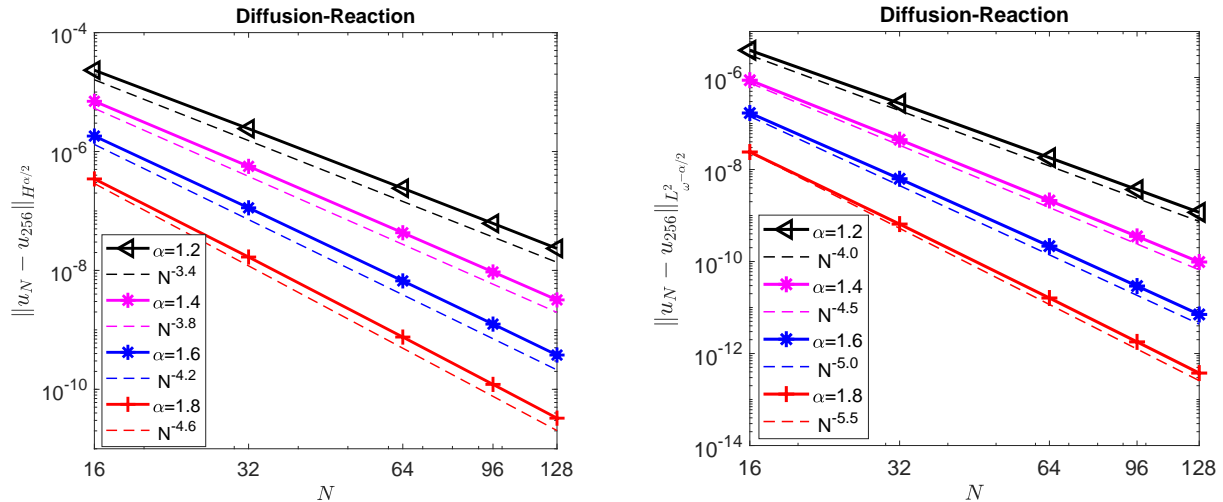
Figure 1.4: For the diffusion-reaction equation $(-\Delta)^{\alpha/2}u + u = \sin x$ with u vanishing outside of $(-1, 1)$, the convergence order of the spectral Galerkin method (3.4.1) is $2\alpha + 1 - \epsilon$ in $H^{\alpha/2}$-norm and $5\alpha/2 + 1 - \epsilon$ in $L^2_{\omega^{-\alpha/2}}$-norm.

Unfortunately, we were not able to prove the regularity index $5\alpha/2 + 1 - \epsilon$ using the analysis in [93] and thus failed to obtain the optimal convergence order $5\alpha/2 + 1 - \epsilon$ even when f is analytic.

This goal is an important step toward high-order numerical methods for this problem and more general fractional advection-diffusion equations on general smooth domains such as the quasi-geostrophic equation [27] and the fractional Navier-Stokes equation [38].

.

However, the convergence orders in these papers are still unsatisfactory for many applications including turbulence intermittency simulations. Along the line of our earlier work on high-order spectral methods for fractional advection-diffusion equations in one dimension [57, 93] with order $5\alpha/2 + 1$ in L^2-norm (compared to an order 2 in [7]), we are employing weighted orthogonal polynomials for fractional Laplacian on a disk. In fact, the evaluation of fractional Laplacian

7

operator (1.1.1) on a disk is straightforward, thanks to the pseudo-eigen relation (see Lemma 3.3.1), and it is natural to represent the solution to Equation (1.2.1) by the pseudo-eigenfunctions (generalized Zernike polynomials), which form a complete orthogonal system. The resulting stiffness matrix is diagonal and thus we can easily compute the fractional Laplacian. This approach has been reported in [92] for fractional Poisson equation on a unit disk where there is no reaction ($\mu = 0$) and an exponential convergence is reported when f is analytic. The exponential convergence arises from the regularity estimate for (1.2.1) when $\mu = 0$: the solution to equation (1.2.1) with $\mu = 0$ can be written by $(1 - r^2)^{\alpha/2}v$ and v is analytic if f is analytic [75].

1.3.2 Motivation for the finite/spectral based fictitious method

For the rectangles and circular domain, we proposed the efficient and accurate finite difference and spectral methods, respectively. For the structure domain, using the spectral method for the circular domain leads to the high-order convergence or using the finite difference methods leads to high efficiency of numerical solution. A natural question arise when it comes to the general domain. This motivates us to think about the extended or fictitious methods.

1.3.3 Motivation for the finite difference method

Given the wide application of fractional Laplacian and its ability to capture the anomalous diffusion and model the complex physical phenomenon with long range interaction, see e.g., [38, 42, 49, 64, 89], many numerical methods have been proposed, e.g., finite difference-quadrature method in [34, 35, 59, 70] and finite element method [3, 7, 30, 88], spectral methods [57, 54, 92]. We refer the readers to [18, 67, 29] for a review of many definitions of fractional Laplacian and their numerical methods.

While there are several methods with linear solvers of quasilinear complexity, see e.g. [7, 35, 70], the implementation of algorithm is still complicated, especially the computation of entries of resulting linear systems in finite element method [3, 7, 30, 88] or construction of the weights in finite difference method [34, 35, 59, 70] or finding the modes in terms of orthogonal expansion basis in spectral method [54, 92]. In particular, as pointed out in [2], over 99% of the CPU time is devoted to assembly routine in a finite element algorithm. The following example based on the variational finite element method allows one to feel the level of computational complexity:

$$
\begin{aligned}
a_{i,j} &= \int_\Omega \left(\int_\Omega \frac{(\phi_i(x) - \phi_i(y))(\phi_j(x) - \phi_j(y))}{|x - y|^{1+\alpha}} dy \right) dx \\
&= \sum_m \sum_l \int_{I_m} \left(\int_{I_l} \frac{(\phi_i(x) - \phi_i(y))(\phi_j(x) - \phi_j(y))}{|x - y|^{1+\alpha}} dy \right) dx \\
&= \left(\sum_{m=l} + 2 \sum_{m<l} \right) \int_{I_m} \left(\int_{I_l} \frac{(\phi_i(x) - \phi_i(y))(\phi_j(x) - \phi_j(y))}{|x - y|^{1+\alpha}} dy \right) dx.
\end{aligned}
$$

Thus a simple and efficient solver is still urgent in need although many numerical methods have been developed. This motivates us to rethink about the finite difference methods. In Chapter 5, we will *present a simple-and-easy implementation scheme for the numerical approximation of fractional Laplacian operator and finite difference method for high-dimensional fractional diffusion equations.*

8

1.4 Outline

The outline of this document is as following:

In Chapter 2, we investigate a spectral Galerkin method for the fractional advection-diffusion-reaction equations in one dimension. We first prove sharp regularity estimates of solutions in non-weighted and weighted Sobolev spaces. Then we obtain optimal convergence orders of the spectral Galerkin methods for both fractional advection-diffusion and diffusion-reaction equations. We also present an iterative solver with a quasi-optimal complexity. Numerical results are presented to verify the theoretical analysis.

In Chapter 3, we investigate a spectral Galerkin method for the two-dimensional fractional diffusion-reaction equations on a disk. We first prove regularity estimates of solutions in the weighted Sobolev space. Then we obtain optimal convergence orders of a spectral Galerkin method for the fractional diffusion-reaction equations in the L^2 and energy norm. Numerical results are presented to verify the theoretical analysis.

In Chapter 4, we propose an efficient fictitious domain methods based on the spectral-solver and finite difference solvers. The rational of fictitious domain method in the fractional context will be offered and a large of numerical examples will be provided.

In Chapter 5, we study the finite difference method for the fractional diffusion equation with high dimensional hyper-singular integral fractional Laplacian. We first propose a simple-and-easy discrete approximation, i.e., fractional centered difference scheme with second-order convergence for the fractional operator. Based on the established approximation, we then construct a finite difference scheme to solve fractional diffusion equations and analyze the stability and convergence in discrete energy norm. We further present a fast solver for the linear system which is obtained by discretization on rectangular domain and use the fictitious domain method to extend the fast solver to the non-rectangular one. Several numerical results are provided to support our theoretical results.

In Chapter 6, we first concentrate on the model problem of two-term fractional Laplacian on the unit disk. Specifically, we investigate in detail the regularity and accuracy of the two-term fractional Laplacian model problem, starting from one-dimensional case and then moving on to the two dimensional one later. Next, we describe the procedure of the implementation for the steady fractional Stokes Problems. We also include the discussion of time dependent fractional Navier-Stokes problems.

In the last chapter, we summarize the main results presented in this work and discuss the further works.

Chapter 2

Spectral method for fractional Laplacian in 1D

In this chapter [1], we consider one of the nonlocal models, advection-diffusion-reaction (ADR) equations with fractional Laplacian, which is a simplified model from the fractional Navier-Stokes equation [38]. While our ultimate goal is efficient spectral and spectral element methods for the fractional Navier-Stokes equation (nonlinear ADR), our goal here is to *investigate the convergence order of a spectral Galerkin method for a one-dimensional fractional ADR equation.* As a simplified model, the following one-dimensional problem provides views on potential advantage and disadvantages on designed numerical methods for advection diffusion equations which navier stokes is in nature [21]. Specifically, we consider the following problem

$$(-\Delta)^{\alpha/2}u + \mu_1 Du + \mu_2 u = f(x), \quad x \in \Omega = (-1,1), \qquad \alpha \in (1,2), \qquad (2.0.1)$$
$$u(x) = 0, \quad x \in \Omega^c, \qquad (2.0.2)$$

where D is the first-order derivative in x, $\mu_1 \in \mathbb{R}$, $\mu_2 \geq 0$ and $f(x)$ is a given function.

We apply a different approach than that in [93] and obtain the optimal regularity index of $(1-x)^{-\alpha/2}u$ in a weighted Sobolev space; see Section 3.3. Moreover, we are able to prove the regularity index when $\mu_1 \neq 0$, where the regularity index of $(1-x)^{-\alpha/2}u$ is $\alpha + \min(3\alpha/2 - 1 - \epsilon, r)$. Though the regularity is still limited in weighted Sobolev spaces, our results are better than the classical analysis in non-weighted Sobolev spaces when $r > 0$; see Table 2.1 for conclusions of regularity index on the fractional ADR equations in one dimension in literature.

With the established higher regularity estimates, we consider the spectral Galerkin method (3.4.1) using the approximation $(1-x)^{\alpha/2}\tilde{u}_N = (1-x^2)^{\alpha/2}\sum_{n=0}^{N}\hat{u}_n P_n^{\alpha/2}(x)$. The approximation of u using $(1-x)^{\alpha/2}\tilde{u}_N$ provides a different view than those in the classical numerical methods such as in [30, 3] for finite element methods and [34, 59] for finite difference methods. In these classical methods, the convergence order is low as the solution is usually weakly singular along the boundary; and the computational cost is high, mainly because of the dense matrix resulting from the discretization of fractional Laplacian.

We observe that the effectiveness of factorization of the solution as a weak singular function and a regular function $\tilde{u}$ has been also pointed out in [75] in the regularity analysis of the fractional

---

Table 2.1: Regularity indices for u in the standard Sobolev space H^s and for $\tilde{u} = (1 - x^2)^{-\alpha/2}u$ in the weighted Sobolev space $B^s_{\omega^{\alpha/2}}$. Here r is regularity index for f in standard or the weighted Sobolev spaces. The letter 'P' is an abbreviation for Poisson ($\mu_1 = \mu_2 = 0$); the letters 'DR' means Diffusion-Reaction ($\mu_1 = 0$ and $\mu_2 > 0$); and 'ADR' represents Advection-Diffusion-Reaction ($\mu_1 \neq 0$ and $\mu_2 > 0$).

	s (u in the Sobolev space)	s ($\tilde{u}$ in the weighted Sobolev space)
P	$\alpha + \min(1/2 - \alpha/2 - \epsilon, r)$ ([3, 47], Lem 2.2.1)	$\alpha + r$ ([4, 93])
DR	$\alpha + \min(1/2 - \alpha/2 - \epsilon, r)$	$\alpha + \min(\alpha + 1 - \epsilon, r)$ ([93])
	$-$	$\alpha + \min(3\alpha/2 + 1 - \epsilon, r)$ (Thm 2.2.10)
ADR	$\alpha + \min(1/2 - \alpha/2 - \epsilon, r)$ (Thm 2.2.2)	$\alpha + \min(3\alpha/2 - 1 - \epsilon, r)$ (Thm 6.1.4)

Poisson equation. The high regularity for $\tilde{u}$ is verified by high convergence orders using the spectral methods (3.4.1). For example, for the diffusion-reaction (DR) equation (2.0.2) where $\mu_1 = 0$, the convergence order for $\tilde{u}_N$ in weighted $L^2_{\omega^{-\alpha/2}}$-norm (stronger one than standard non-weighted L^2-norm) can be $5\alpha/2 + 1 - \epsilon$ when $f = \sin x$; see Theorem 3.4.3. In contrast, the convergence order of finite element/difference method is expected to be no higher than $(\alpha + 1)/2 - \epsilon$ unless some adaptive mesh or graded mesh is applied; see e.g., [3, 7]. Thus, the spectral method presented in this work can provide a reliable reference solution for other numerical methods.

The outline of this chapter is arranged as follows. In Section 2.1, we introduce some necessary notations and recall weighted Sobolev spaces. Some long but important auxiliary lemmas are presented in Appendix. In Section 2.2, we present and prove the regularity of fractional ADR equations in non-weighted and weighted Sobolev spaces. In Section 2.3, we consider a spectral Galerkin method for (2.0.1)-(2.0.2) and prove its optimal convergence. In Section 2.4, we present both direct and iterative solvers and verify the theoretical convergence orders with several numerical examples. In Section 2.5, we apply the regularity results to fractional equations driven by random noise. In Section 2.6, we discuss the two-term Laplacian before we make concluding remarks and discussions on possible extensions of this work. Throughout the chapter C and c denote generic constants and are independent of any functions and of the truncation parameter N.

2.1 Weighted Sobolev spaces

In this section, we introduce weighted Sobolev spaces. Denote by $L^2_{\omega^\beta}(\Omega)$ the space with inner product and associated norm defined by

$$(u, v)_{\omega^\beta} = \int_\Omega uv\omega^\beta dx, \quad \|u\|_{\omega^\beta} = \left((u, u)_{\omega^\beta}\right)^{1/2}, \tag{2.1.1}$$

where $\omega^\beta = (1 - x^2)^\beta$ with a real number β. To simplify the notation we abbreviate $L^2_{\omega^\beta}(\Omega)$ as $L^2_{\omega^\beta}$ and the similar treatment is done for other spaces. To incorporate singularities at the endpoints, we introduce the following weighted Sobolev space (see e.g. [13, 50]),

$$B^m_{\omega^\beta} := \left\{ u \mid D^k u \in L^2_{\omega^{\beta+k}}, \ k = 0, 1, \ldots, m \right\}, \quad m \text{ is a nonnegative integer}, \tag{2.1.2}$$

which is equipped with the following norm

$$\|u\|_{B^m_{\omega^\beta}} = \left(\sum_{k=0}^m |u|^2_{B^k_{\omega^\beta}}\right)^{1/2}, \quad |u|_{B^k_{\omega^\beta}} = \|D^k u\|_{\omega^{\beta+k}}, . \tag{2.1.3}$$

When $m = s$ is not an integer, the space can be defined via classical interpolation method, e.g. K-method; see [5].

These weighted Sobolev spaces are closely related to the Jacobi polynomials. The Jacobi polynomials $P_n^\beta(x)$ are mutually orthogonal as

$$\int_{-1}^{1} (1-x^2)^\beta P_m^\beta(x) P_n^\beta(x)\, dx = h_n^\beta \delta_{nm}, \quad \beta > -1. \tag{2.1.4}$$

Here δ_{nm} is equal to 1 if $n = m$ and zero otherwise and

$$h_n^\beta = \left\| P_n^\beta \right\|_{\omega^\beta}^2 = \frac{2^{2\beta+1}(\Gamma(n+\beta+1))^2}{(2n+2\beta+1)\Gamma(n+2\beta+1)\Gamma(n+1)}. \tag{2.1.5}$$

The following asymptotic formula for a ratio of two gamma functions holds

$$\lim_{n\to\infty} \frac{\Gamma(n+\delta)}{n^{\delta-\gamma}\Gamma(n+\gamma)} = \lim_{n\to\infty} [1 + \frac{(\delta-\gamma)(\delta+\gamma-1)}{2n} + \mathcal{O}(n^{-2})] = 1. \tag{2.1.6}$$

By (2.1.6), we know that $h_n^\beta \approx \frac{1}{2n+2\beta+1}$. The following relations hold for Jacobi polynomials $P_n^\beta(x)$ (see e.g. Chapter 2 in [11])

$$D\left((1-x^2)^\beta P_{n-1}^\beta\right) = -2n(1-x^2)^{\beta-1}P_n^{\beta-1}, \quad \beta > 0. \tag{2.1.7}$$

We say that a_n is equivalent to b_n if there exist c_1 and c_2 such that $c_1 a_n \le b_n \le c_2 a_n$ asymptotically and denote the equivalence by $a_n \approx b_n$. For functions in $B_{\omega^\beta}^s$ with $s \ge 0$, we can introduce a equivalent fractional norm in discrete form (see [13]):

$$\|\|u\|\|_{B_{\omega^\beta}^s}^2 = \sum_{n=0}^{\infty} (u_n^\beta)^2 h_n^\beta (1+n^2)^s, \quad \beta > -1, \tag{2.1.8}$$

where u_n^β are the coefficients of Jacobi-Fourier expansion for u in terms of P_n^β.

2.2 Regularity

In this section, we present our regularity results in the weighted and non-weighted Sobolev spaces as well as their proofs.

We recall the non-weighted Sobolev space H^s (e.g. in [5]) with the semi-norm $|\cdot|_{H^s}$

$$|v|_{H^s} = \left(\iint_{\Omega\otimes\Omega} \frac{|v(x)-v(y)|^2}{|x-y|^{1+2s}}\, dxdy \right)^{1/2}.$$

The weak formulation of the problem (2.0.1)-(2.0.2) is to find $u \in H_0^{\alpha/2}$, such that

$$a(u,v) := ((-\Delta)^{\alpha/2}u, v) + \mu_1(Du, v) + \mu_2(u, v) = (f, v), \quad \forall v \in H_0^{\alpha/2}. \tag{2.2.1}$$

13

2.2.1 Regularity in non-weighted Sobolev spaces

The following theorem describes the Sobolev regularity properties of the fractional Poisson equation (2.0.1) with $\mu_1 = \mu_2 = 0$.

Theorem 2.2.1 ([3, 46]). *Suppose $f \in H^r$ for $r \geq -\alpha/2$ and $u \in H^{\alpha/2}$ be the solution of fractional Poisson equation, i.e., (2.0.1) with $\mu_1 = \mu_2 = 0$. Then $u \in H^{\alpha+\min(1/2-\alpha/2-\epsilon,r)}$ with $\epsilon > 0$ arbitrarily small.*

In this work, we use the bootstrapping technique (see, e.g. [39], Chapter 6) to obtain the optimal regularity for the problem (2.0.1)-(2.0.2) with the lower order terms in non-weighted Sobolev spaces.

Theorem 2.2.2. *For the problem (2.0.1)-(2.0.2) with $\mu_1 \in \mathbb{R}, \mu_2 \geq 0$, if $f \in H^r$ with $r \geq -\alpha/2$, then $u \in H^{\alpha+\min(1/2-\alpha/2-\epsilon,r)}$ with $\epsilon > 0$ arbitrarily small.*

Proof Denote $\min(a,b)$ by $a \wedge b$. By Lax-Milgram Theorem, we know $u \in H_0^{\alpha/2}$ from $f \in H^{-\alpha/2}$. Thus $Du \in H^{\alpha/2-1}$. Then it follows that $(-\Delta)^{\alpha/2}u = f - \mu_1 Du - \mu_2 u \in H^{(\alpha/2-1)\wedge r}$. By Theorem 2.2.1, we have $u \in H^{\alpha+(\alpha/2-1)\wedge r\wedge(1/2-\alpha/2-\epsilon)}$.

If $\alpha \geq 3/2$ then $\alpha/2 - 1 \geq 1/2 - \alpha/2$ and $u \in H^{\alpha+r\wedge(1/2-\alpha/2-\epsilon)}$. If $\alpha < 3/2$ and $r < \alpha/2 - 1$, then we also have $u \in H^{\alpha+r} = H^{\alpha+r\wedge(1/2-\alpha/2-\epsilon)}$.

If $\alpha < 3/2$ and $r \geq \alpha/2 - 1$, then $u \in H^{3\alpha/2-1}$. In this case we will lift the regularity index of u from $3\alpha/2 - 1$ to $\alpha + r \wedge (1/2 - \alpha/2 - \epsilon)$. In fact, from $u \in H^{3\alpha/2-1}$ we have $Du \in H^{3\alpha/2-2}$. It follows that $(-\Delta)^{\alpha/2}u = f - \mu_1 Du - \mu_2 u \in H^{(3\alpha/2-2)\wedge r}$. By Theorem 2.2.1, we have $u \in H^{\alpha+(3\alpha/2-2)\wedge r\wedge(1/2-\alpha/2-\epsilon)}$.

If either $\alpha \geq 5/4$ or $\alpha < 5/4$ and $r < 3\alpha/2-2$, then $(3\alpha/2-2) \wedge r \wedge (1/2-\alpha/2-\epsilon) = r \wedge (1/2-\alpha/2-\epsilon)$. That is $u \in H^{\alpha+r\wedge(1/2-\alpha/2-\epsilon)}$. Otherwise if $\alpha < 5/4$ and $r \geq 3\alpha/2-2$, $u \in H^{5\alpha/2-2}$ and thus $Du \in H^{5\alpha/2-3}$. Following the similar argument above, we have $u \in H^{\alpha+(5\alpha/2-3)\wedge r\wedge(1/2-\alpha/2-\epsilon)}$.

Repeating above procedures k times, we have $u \in H^{\alpha+(k(\alpha-1)-\alpha/2)\wedge r\wedge(1/2-\alpha/2-\epsilon)}$. When k is the smallest integer number such that $k \geq \frac{1}{2(\alpha-1)}$, we have

$$u \in H^{\alpha+(k(\alpha-1)-\alpha/2)\wedge r\wedge(1/2-\alpha/2-\epsilon)} = H^{\alpha+r\wedge(1/2-\alpha/2-\epsilon)}.$$

This completes the proof. □

Remark 2.2.3. *Here is the key step of the proof. Suppose that we obtain $u \in H^\beta$, $\beta < \alpha + r \wedge (1/2 - \alpha/2 - \epsilon)$. Then by the fact $(-\Delta)^{\alpha/2}u = f - \mu_1 Du - \mu_2 u \in H^{(\beta-1)\wedge r}$ and Theorem 2.2.1, we have $u \in H^{\beta'}$, where $\beta' = \alpha + (\beta - 1) \wedge r \wedge (1/2 - \alpha/2 - \epsilon)$. Then $\beta' = \alpha + (\beta - 1) > \beta$. If $\beta' < \alpha + r \wedge (1/2 - \alpha/2 - \epsilon)$, then we can repeat the above processes many times to conclude $u \in H^{\alpha+r\wedge(1/2-\alpha/2-\epsilon)}$.*

2.2.2 Regularity in weighted Sobolev spaces

For the fractional Poisson equation (2.0.1), where $\mu_1 = \mu_2 = 0$, we consider the regularity of $\tilde{u} = \omega^{-\alpha/2}u$.

Theorem 2.2.4 ([93]). *For the problem (2.0.1)-(2.0.2) with $\mu_1 = \mu_2 = 0$, if $f \in B^r_{\omega^{\alpha/2}}$ with $r \geq 0$, then $\omega^{-\alpha/2}u \in B^{\alpha+r}_{\omega^{\alpha/2}}$.*

However, the nice property of full regularity in above theorem does not hold anymore for the fractional Laplace equations with lower order terms, which we will see shortly. Before presenting our regularity results for fractional ADR equations, we need two technical lemmas, which play an essential role in the analysis of regularity of the fractional ADR equations. For proofs, please see Appendix.

Lemma 2.2.5. *If $v \in B^s_{\omega^{\alpha/2-1}}$ with $s \geq 0$, then $v\omega^{\alpha/2-1} \in B^{\min(s,3\alpha/2-1-\epsilon)}_{\omega^{\alpha/2}}$ with arbitrarily small $\epsilon > 0$.*

Lemma 2.2.6. *If $v \in B^s_{\omega^{\alpha/2}}$ with $s \geq 0$, then $v\omega^{\alpha/2} \in B^{\min(s,3\alpha/2+1-\epsilon)}_{\omega^{\alpha/2}}$ with arbitrarily small $\epsilon > 0$.*

We are now at the position to present the regularity of the fractional ADR (2.0.1).

Theorem 2.2.7 (**Regularity in weighted Sobolev spaces**). *For the problem (2.0.1)-(2.0.2) with $\mu_1 \neq 0$ and $\mu_2 > 0$, if $f \in H^{1/2-\alpha/2} \cap B^r_{\omega^{\alpha/2}}$ with $r \geq 0$, then we have $\omega^{-\alpha/2}u \in B^{\alpha+\min(3\alpha/2-1-\epsilon,r)}_{\omega^{\alpha/2}}$ with $\epsilon > 0$ arbitrarily small.*

Proof Denote $a \wedge b$ as $\min(a,b)$ and recall $\tilde{u} = \omega^{-\alpha/2}u$. Since if $f \in H^{1/2-\alpha/2}$, by Theorem 2.2.2 we have $u \in H_0^{\alpha/2+1/2-\epsilon}$ and $Du \in H_0^{\alpha/2-1/2-\epsilon}$.

Now we use the bootstrapping technique to lift the regularity of solution $\tilde{u}$. Note that $H_0^{\alpha/2-1/2-\epsilon} \subset B^{\alpha/2-1/2-\epsilon}_{\omega^{\alpha/2}}$ thus $Du \in B^{\alpha/2-1/2-\epsilon}_{\omega^{\alpha/2}}$. Then it follows that

$$(-\Delta)^{\alpha/2}u = f - \mu_1 Du - \mu_2 u \in B^{(\alpha/2-1/2-\epsilon)\wedge r}_{\omega^{\alpha/2}}.$$

By Theorem 2.2.4, we have $\tilde{u} \in B^{\alpha+(\alpha/2-1/2-\epsilon)\wedge r}_{\omega^{\alpha/2}}$.

If $r \geq \alpha/2 - 1/2$ then $\tilde{u} \in B^{3\alpha/2-1/2-\epsilon}_{\omega^{\alpha/2}}$. In this case we proceed to lift the regularity. Let $\tilde{u} = \sum_{n=0}^{\infty} \hat{u}_n P_n^{\alpha/2}$. Then by the formula (2.1.7), we have

$$Du = D(\omega^{\alpha/2}\tilde{u}) = -2\sum_{n=0}^{\infty} \hat{u}_n(n+1)P_{n+1}^{\alpha/2-1}\omega^{\alpha/2-1}.$$

Denote $v = -2\sum_{n=0}^{\infty} \hat{u}_n(n+1)P_{n+1}^{\alpha/2-1}$. Then $Du = v\omega^{\alpha/2-1}$ and by the equivalent definition (2.1.8), we have $v \in B^{3\alpha/2-3/2-\epsilon}_{\omega^{\alpha/2-1}}$. It follows from Lemma 2.2.5 that we have $Du \in B^{3\alpha/2-3/2-\epsilon}_{\omega^{\alpha/2}}$. Recall $u = \omega^{\alpha/2}\tilde{u}$ with $\tilde{u} \in B^{3\alpha/2-1/2-\epsilon}_{\omega^{\alpha/2}}$. Then by Lemma .3.1, we have $u \in B^{3\alpha/2-1/2-\epsilon}_{\omega^{\alpha/2}}$. Thus it follows that $(-\Delta)^{\alpha/2}u = f - \mu_1 Du - \mu_2 u \in B^{(3\alpha/2-3/2-\epsilon)\wedge r}_{\omega^{\alpha/2}}$. By Theorem 2.2.4 we have $\tilde{u} \in B^{\alpha+(3\alpha/2-3/2-\epsilon)\wedge r}_{\omega^{\alpha/2}}$.

If $r > 3/2(\alpha-1)$, we can follow a similar argument to lift the regularity. Suppose that k is the smallest integer number such that $(k+1/2)(\alpha-1) > 3\alpha/2 - 1$. After repeating the lifting procedure k times as above, we have

$$\tilde{u} \in B^{\alpha+(k+1/2)(\alpha-1)\wedge(3\alpha/2-1-\epsilon)\wedge r}_{\omega^{\alpha/2}} = B^{\alpha+(3\alpha/2-1-\epsilon)\wedge r}_{\omega^{\alpha/2}}.$$

This completes the proof. $\qquad\qquad\qquad\qquad\qquad\qquad\qquad\qquad\qquad\qquad\square$

Remark 2.2.8. *For $r \geq \alpha/2$, the assumption $f \in B^r_{\omega^{\alpha/2}}$ implies that $f \in H^{1/2-\alpha/2}$ by Lemma .1.4. The condition $f \in H^{1/2-\alpha/2} \cap B^r_{\omega^{\alpha/2}}$ becomes $f \in B^r_{\omega^{\alpha/2}}$ when $r \geq \alpha/2$.*

Remark 2.2.9. *The key step in the proof is to show that if $\tilde{u} \in B^{\beta}_{\omega^{\alpha/2}}$, then $\tilde{u} \in B^{\beta'}_{\omega^{\alpha/2}}$, where $\beta' = \alpha + (\beta - 1) \wedge r \wedge (3/2\alpha - 1 - \epsilon)$. In fact, we have $(-\Delta)^{\alpha/2} u = f - \mu_1 Du - \mu_2 u \in B^{r \wedge [(\beta-1) \wedge (3/2\alpha - 1 - \epsilon)]}_{\omega^{\alpha/2}}$ as $Du \in B^{(\beta-1) \wedge (3/2\alpha - 1 - \epsilon)}_{\omega^{\alpha/2}}$ according to Lemma 2.2.5 and thus by Theorem 2.2.1, we reach the desired conclusion. Observe that $\beta' = \beta$ if $\beta \geq \alpha + r \wedge (3/2\alpha - 1 - \epsilon)$; and $\beta' > \beta$ if $\beta < \alpha + r \wedge (3/2\alpha - 1 - \epsilon)$, in which case we can repeat the key step many times until the new regularity index β' is equal to $\alpha + r \wedge (3/2\alpha - 1 - \epsilon)$.*

Theorem 2.2.10 (**Regularity in weighted Sobolev spaces with reaction-only term**). *For the problem (2.0.1)-(2.0.2) with $\mu_1 = 0$ and $\mu_2 > 0$, if $f \in B^r_{\omega^{\alpha/2}}$ with $r \geq 0$, then we have $\omega^{-\alpha/2} u \in B^{\alpha + \min(3\alpha/2 + 1 - \epsilon, r)}_{\omega^{\alpha/2}}$ with $\epsilon > 0$ arbitrarily small.*

Proof By Theorem 2.2.4 we have $\omega^{-\alpha/2} u \in B^{\alpha + \min(r, \alpha)}_{\omega^{\alpha/2}}$. If $r \geq \alpha$ then $\omega^{-\alpha/2} u \in B^{2\alpha}_{\omega^{\alpha/2}}$. By Lemma .3.1 we that $u \in B^{2\alpha - \epsilon}_{\omega^{\alpha/2}}$. Then it follows that $(-\Delta)^{\alpha/2} u = f - \mu_2 u \in B^{(2\alpha - \epsilon) \wedge r}_{\omega^{\alpha/2}}$. Using Theorem 2.2.4 we have $\omega^{-\alpha/2} u \in B^{\alpha + (2\alpha - \epsilon) \wedge r}_{\omega^{\alpha/2}}$. If $r \geq 2\alpha$, then $\omega^{-\alpha/2} u \in B^{3\alpha}_{\omega^{\alpha/2}}$. By Lemma .3.1 we know that $u \in B^{3\alpha/2 + 1 - \epsilon}_{\omega^{\alpha/2}}$. Then it follows that $(-\Delta)^{\alpha/2} u = f - \mu_2 u \in B^{(3\alpha/2 + 1 - \epsilon) \wedge r}_{\omega^{\alpha/2}}$. Using Theorem 2.2.4 again we get the desired result. $\qquad\square$

2.3 Error estimate of spectral Galerkin method

In this section, we consider a spectral Galerkin method and carry out its error analysis based on the obtained regularity in Section 2.2.

We first present the spectral Galerkin method. Define

$$U_N := \omega^{\alpha/2} \mathbb{P}_N = \text{Span}\{\phi_0, \phi_1, \ldots, \phi_N\},$$

where $\phi_k(x) := \omega^{\alpha/2} P_k^{\alpha/2}(x)$ for $0 \leq k \leq N$, and $\mathbb{P}_N$ is the set of all algebraic polynomials of degree at most N. The spectral Galerkin method is to find $u_N \in U_N$ such that

$$a(u_N, v_N) = (f, v_N), \quad \forall v_N \in U_N, \tag{2.3.1}$$

with $a(u_N, v_N) = ((-\Delta)^{\alpha/2} u_N, v_N) + \mu_1(Du_N, v_N) + \mu_2(u_N, v_N)$.

The following *pseudo-eigenfunctions* for fractional diffusion operator are essential to analyse and implement the spectral Galerkin method.

Lemma 2.3.1 ([4, 93]). *For the n-th order Jacobi polynomial $P_n^{\alpha/2}(x)$, it holds that*

$$(-\Delta)^{\alpha/2}[\omega^{\alpha/2} P_n^{\alpha/2}(x)] = \lambda_n^{\alpha} P_n^{\alpha/2}(x), \quad \lambda_n^{\alpha} = \frac{\Gamma(\alpha + n + 1)}{n!}. \tag{2.3.2}$$

The well-posedness of discrete problem (2.3.1) can be readily shown by the Lax-Milgram theorem. We omit the statement.

Next, we introduce two necessary lemmas which play the key role in the error estimate. The first one is a version of Cea's Lemma.

Lemma 2.3.2. *Let u and u_N solve the equations (2.2.1) and (2.3.1) respectively. Then it holds*

$$\|u - u_N\|_{H^{\alpha/2}} \leq C \inf_{v_N \in U_N} \|u - v_N\|_{H^{\alpha/2}}. \tag{2.3.3}$$

For $u \in H_0^{\alpha/2}$ we have $\omega^{-\alpha/2}u \in L_{\omega^{\alpha/2}}^2$ by the inequality (1.2.4). Thus it is legitimate to write $u = \omega^{\alpha/2}\sum_{n=0}^{\infty}\hat{u}_n P_n^{\alpha/2}(x)$. Introduce the projection $\Pi_N^{\alpha/2}: H_0^{\alpha/2} \to U_N$ such that $\Pi_N^{\alpha/2}u = \omega^{\alpha/2}\sum_{n=0}^{N}\hat{u}_n P_n^{\alpha/2}(x)$.

The following lemma is about the approximation property of the projection $\Pi_N^{\alpha/2}u$.

Lemma 2.3.3. *Let $u \in H_0^{\alpha/2}$ and $\omega^{-\alpha/2}u \in B_{\omega^{\alpha/2}}^s$. Then for $s \geq \alpha/2$ we have*

$$\|u - \Pi_N^{\alpha/2}u\|_{H^{\alpha/2}} \leq cN^{\alpha/2-s}|\omega^{-\alpha/2}u|_{B_{\omega^{\alpha/2}}^s}. \tag{2.3.4}$$

Proof. Let $u = \omega^{\alpha/2}\sum_{n=0}^{\infty}\hat{u}_n P_n^{\alpha/2}(x)$. Then $u - \Pi_N^{\alpha/2}u = \omega^{\alpha/2}\sum_{n=N+1}^{\infty}\hat{u}_n P_n^{\alpha/2}(x)$. From Lemma 1.2.3, we have the following norm equivalence

$$\|v\|_{H^{\alpha/2}}^2 \approx ((-\Delta)^{\alpha/2}v, v), \quad \forall v \in H_0^{\alpha/2}. \tag{2.3.5}$$

Using the pseudo-eigen relation in Lemma 2.3.1 gives

$$\|u - \Pi_N^{\alpha/2}u\|_{H^{\alpha/2}}^2 \approx ((-\Delta)^{\alpha/2}(u - \Pi_N^{\alpha/2}u), (u - \Pi_N^{\alpha/2}u)) = \sum_{n=N+1}^{\infty}\lambda_n^{\alpha}|\hat{u}_n|^2 h_n^{\alpha/2}. \tag{2.3.6}$$

Note that by (2.1.6), $\lambda_n^{\alpha} \approx n^{\alpha}$. It follows that

$$\begin{aligned}\|u - \Pi_N^{\alpha/2}u\|_{H^{\alpha/2}}^2 &\approx \sum_{n=N+1}^{\infty}n^{\alpha}|\hat{u}_n|^2 h_n^{\alpha/2} = \sum_{n=N+1}^{\infty}n^{\alpha-2s}n^{2s}|\hat{u}_n|^2 h_n^{\alpha/2} \\ &\leq N^{\alpha-2s}\sum_{n=N+1}^{\infty}n^{2s}|\hat{u}_n|^2 h_n^{\alpha/2}.\end{aligned} \tag{2.3.7}$$

Using the norm definition (2.1.8) leads to the desired result. $\square$

We are ready to state the convergence order of the spectral Galerkin method (2.3.1).

Theorem 2.3.4 (Optimal convergence order). *Suppose that u and u_N satisfy the problems (2.2.1) and (2.3.1), respectively. Suppose that f satisfies the assumption in Theorems 6.1.4 and 2.2.10 we have the following error estimates:*

$$\|u - u_N\|_{L_{\omega^{-\alpha/2}}^2} + N^{-\alpha/2}\|u - u_N\|_{H^{\alpha/2}} \leq CN^{-s}\left|\omega^{-\alpha/2}u\right|_{B_{\omega^{\alpha/2}}^s},$$

where s is the regularity index of the solution defined in Theorem 6.1.4 (ADR, $s = \alpha + \min(3\alpha/2 - 1 - \epsilon, r)$) and Theorem 2.2.10 (DR, $s = \alpha + \min(3\alpha/2 + 1 - \epsilon, r)$).

Proof. Denote $e = u - u_N$. By Cea's Lemma 2.3.2, we have

$$\|e\|_{H^{\alpha/2}} \leq C\|u - \Pi_N^{\alpha/2}u\|_{H^{\alpha/2}}.$$

Applying the approximation property in Lemma 2.3.3 yields

$$\|e\|_{H^{\alpha/2}} \leq C\|u - \Pi_N^{\alpha/2}u\|_{H^{\alpha/2}} \leq CN^{\alpha/2-s}|\omega^{-\alpha/2}u|_{B_{\omega^{\alpha/2}}^s}. \tag{2.3.8}$$

Next we apply the duality argument to obtain the convergence order for $\|e\|_{L^2_{\omega^{-\alpha/2}}}$. We introduce the following auxiliary problem

$$(-\Delta)^{\alpha/2}w - \mu_1 Dw + \mu_2 w = \omega^{-\alpha/2}e, \quad x \in \Omega,$$
$$w(x) = 0, \quad x \in \Omega^c.$$

Then the weak formulation is to find $w \in H_0^{\alpha/2}$ such that

$$a^*(w,v) := ((-\Delta)^{\alpha/2}w, v) - \mu_1(Dw, v) + \mu_2(w, v) = (\omega^{-\alpha/2}e, v), \ \forall v \in H_0^{\alpha/2}.$$

The corresponding discrete problem is to find $w_N \in U_N$ such that

$$a^*(w_N, v_N) = (\omega^{-\alpha/2}e, v_N), \quad \forall v_N \in U_N.$$

By Theorems 6.1.4 and 2.2.10, we have the following regularity estimate

$$\|\omega^{-\alpha/2}w\|_{B^\alpha_{\omega^{\alpha/2}}} \le C\|\omega^{-\alpha/2}e\|_{L^2_{\omega^{\alpha/2}}} = C\|e\|_{L^2_{\omega^{-\alpha/2}}}. \tag{2.3.9}$$

Then applying Galerkin orthogonality $a^*(v_N, e) = a(e, v_N) = 0$, $\forall v_N \in U_N$, we have

$$\|e\|^2_{L^2_{\omega^{-\alpha/2}}} = a^*(w,e) = a^*(w - \Pi_N^{\alpha/2}w, e) \le c\|w - \Pi_N^{\alpha/2}w\|_{H^{\alpha/2}}\|e\|_{H^{\alpha/2}}. \tag{2.3.10}$$

Using the approximation property in Lemma 2.3.3, (2.3.10) and (2.3.8), we have

$$\|e\|^2_{L^2_{\omega^{-\alpha/2}}} \le CN^{-\alpha/2}\|\omega^{-\alpha/2}w\|_{B^\alpha_{\omega^{\alpha/2}}}\|e\|_{H^{\alpha/2}}$$
$$\le CN^{-s}\|\omega^{-\alpha/2}w\|_{B^\alpha_{\omega^{\alpha/2}}}\|\omega^{-\alpha/2}u\|_{B^s_{\omega^{\alpha/2}}}.$$

Then by (2.3.9), we have

$$\|e\|_{L^2_{\omega^{-\alpha/2}}} \le CN^{-s}\|\omega^{-\alpha/2}u\|_{B^s_{\omega^{\alpha/2}}}. \tag{2.3.11}$$

The conclusion follows by combining (2.3.11) and (2.3.8). $\qquad\square$

2.4 Numerical experiments

In this section, we present three examples with different source terms f: smooth (Example 2.4.1), weakly singular at an interior point (Example 2.4.2) and weakly singular at boundary (Example 2.4.3). Since exact solutions are unavailable, we use reference solutions u_{ref}, which are computed with a very fine resolution using the same methods for computing u_N. In the computation, we take $\mu_1 = \mu_2 = 1$ and measure the error as follows

$$E(N) = \|u_{\text{ref}} - u_N\|_{L^2_{\omega^{-\alpha/2}}}, \quad E^*(N) = ((-\Delta)^{\alpha/2}(u_{\text{ref}} - u_N), (u_{\text{ref}} - u_N))^{1/2}.$$

Here $u_N = \sum_{n=0}^N \hat{u}_n \omega^{\alpha/2}P_n^{\alpha/2}$ and $u_{\text{ref}} =: u_{256}$ unless otherwise stated. Recall from Lemma 1.2.3 that $E^*(N) \approx \|u_{\text{ref}} - u_N\|_{H^{\alpha/2}}$. We also test the case for u_{512} and find the convergence errors and orders behave almost the same.

2.4.1 Numerical implementation

We first describe the numerical implementation of spectral Galerkin method.

Plugging $u_N = \sum_{n=0}^{N} \hat{u}_n \phi_n(x)$ into (2.3.1) and taking $v_N = \phi_k(x)$ for $k = 0, 1, \ldots, N$, we obtain the following linear equation from the orthogonality of Jacobi polynomials and Lemma 2.3.1 that

$$A\hat{u} = \hat{f}, \tag{2.4.1}$$

where $\hat{u} = (\hat{u}_0, \hat{u}_1, \ldots, \hat{u}_N)^T$, $\hat{f} = (\hat{f}_0, \hat{f}_1, \ldots, \hat{f}_N)^T$ with $\hat{f}_k = (f, \phi_k)$. Here the matrix $A = S + \mu_1 M^a + \mu_2 M^r$, where S is a diagonal matrix with

$$S = \text{diag}(\lambda_0^\alpha h_0^{\alpha/2}, \lambda_1^\alpha h_1^{\alpha/2}, \cdots, \lambda_N^\alpha h_N^{\alpha/2}),$$

and the entries of matrices M^a and M^r are

$$M_{k,n}^a = -2(n+1) \int_{-1}^{1} \omega^{\alpha-1}(x) P_{n+1}^{\alpha/2-1}(x) P_k^{\alpha/2}(x)\, dx, \tag{2.4.2}$$

$$M_{k,n}^r = \int_{-1}^{1} \omega^\alpha(x) P_n^{\alpha/2}(x) P_k^{\alpha/2}(x)\, dx. \tag{2.4.3}$$

Here we have applied (2.1.7) to obtain $M_{k,n}^a$.

If a direct solver is applied to (2.4.1), we then need to find $M_{k,n}^a$ and $M_{k,n}^r$. Here we apply Gauss-Jacobi quadrature rules as follows. For $M_{k,n}^r$, we obtain

$$M_{k,n}^r = \int_{-1}^{1} \omega^\alpha(x) P_n^{\alpha/2}(x) P_k^{\alpha/2}(x)\, dx = \sum_{j=0}^{N} P_n^{\alpha/2}(x_j) P_k^{\alpha/2}(x_j) w_j,$$

where x_j's are the zeros of Jacobi polynomial $P_{N+1}^\alpha(x)$ and w_j's are the corresponding quadrature weights. The quadrature rule here is exact since $n + k \leq 2N$ while the quadrature rule is exact for all $(2N + 1)$-th order polynomials. The integral in $M_{k,n}^a$ can be calculated similarly. To find $\hat{f}_k = (f, \phi_k)$, we use a different Gauss-Jacobi quadrature rule: $\hat{f}_k \approx \sum_{j=0}^{N} f(x_j) P_k^{\alpha/2}(x_j) w_j$. Here x_j's are the roots of Jacobi polynomial $P_{N+1}^{\alpha/2}(x)$ and w_j's are the corresponding quadrature weights. We then can solve (2.4.1) using any efficient direct solver.

A fast iterative solver with a quasilinear complexity

As the resulting system (2.4.1) is dense, a direct solver will require $\mathcal{O}(N^2)$ storage while the complexity is $\mathcal{O}(N^3)$. In the following, we present a matrix-free iterative solver with $\mathcal{O}(N)$ storage and $\mathcal{O}(N \log^2(N))$ computational complexity. This iterative solver consists of a fixed-point iteration and fast polynomial transforms.

The fixed-point iteration we use [2] is

$$\hat{u}^{(m+1)} = \hat{u}^{(m)} + P^{-1}(\hat{f} - A\hat{u}^{(m)}) \tag{2.4.4}$$

where $P = S + \mu_2 I$ is a diagonal matrix. In each iteration, we compute the matrix-vector product $A\hat{u}$ without forming a matrix. To illustrate the idea, we present how to compute $M^r \hat{u}$. Recall that

---

[2]Iterative methods based on Krylov subspaces can also be developed but proper preconditioners are needed.

in (6.1.21), $(M^r \hat{u})_k = (u_N, (1-x^2)^{\alpha/2} P_k^{\alpha/2})$. This quantity is to compute Jacobi-Fourier expansions of u_N up to its N-th mode, which is obtained by applying fast polynomial transforms.

Given the modes $\hat{u}_N$ for $\tilde{u}_N$. We can evaluate $\tilde{u}_N$ at the Chebyshev collocation points $\mathbf{x}_j$'s ($1 \leq j \leq M$, $M \geq N$) as well as $u_N = (1-x^2)^{\alpha/2} \tilde{u}_N$ by a fast transformation from Jacobi-Fourier expansion coefficients to Chebyshev-Fourier expansion coefficients (FJCT [3], see e.g. [84], with a cost at $\mathcal{O}(N \log^2(N))$) and the fast Chebyshev transform (FCT, see e.g. [21], with a cost at $\mathcal{O}(N \log(N))$). In fact, by FJCT, $\tilde{u}_N = \sum_{n=0}^{N} \hat{u}_n P_n^{\alpha/2} = \sum_{n=0}^{N} \hat{u}_n^{-1/2} P_n^{-1/2}$ and $\tilde{u}_N(\mathbf{x}_j)$ can be computed with FCT. Then $u_N(\mathbf{x}_j) = (1-\mathbf{x}_j^2)^{\alpha/2} \tilde{u}_N(\mathbf{x}_j)$ and thus by the inverse FCT, we can obtain $u_N \approx \sum_{n=0}^{M} \hat{u}_n^{-1/2} P_n^{-1/2}$ and further by a fast transform from Cheyshev-Fourier expansion coefficients to Jacobi-Fourier expansion coefficients (FCJT, see e.g. [84]) $u_N \approx \sum_{n=0}^{M} \hat{u}_n^{-1/2} P_n^{-1/2} = \sum_{n=0}^{M} \hat{u}_n^{\alpha/2} P_n^{\alpha/2}$. Finally, we obtain from the orthogonality (2.1.4) that for $0 \leq k \leq N$,

$$(M^r \hat{u})_k = (u_N, (1-x^2)^{\alpha/2} P_k^{\alpha/2}) \approx (\sum_{n=0}^{M} \hat{u}_n^{\alpha/2} P_n^{\alpha/2}, (1-x^2)^{\alpha/2} P_k^{\alpha/2}) = \hat{u}_k^{\alpha/2} h_k^{\alpha/2}.$$

The total computational cost in this process is $\mathcal{O}(N \log^2(N))$ and the storage is $\mathcal{O}(N)$, where we take $M = 2N$ so that the approximation errors in the calculations can be ignored. The above process of obtaining $(M^r \hat{u})_k$ is summarized in the following chart.

$$\{\hat{u}_n\} \xrightarrow{FJCT} \{\hat{u}_n^{-1/2}\} \xrightarrow{FCT} \{\tilde{u}_N(\mathbf{x}_j)\} \longrightarrow \{u_N(\mathbf{x}_j)\} \xrightarrow{FCT} \{\hat{u}_n^{-1/2}\} \xrightarrow{FCJT} \{\hat{u}_n^{\alpha/2}\}.$$

To compute $M^a \hat{u}$, we apply the procedure as above after performing integration-by-parts. In fact, by integration-by-parts and (2.1.7)

$$\begin{aligned} (M^a \hat{u})_k &= (Du_N, (1-x^2)^{\alpha/2} P_k^{\alpha/2}) = -(u_N, D(1-x^2)^{\alpha/2} P_k^{\alpha/2}) \\ &= 2(k+1)(u_N, (1-x^2)^{\alpha/2-1} P_{k+1}^{\alpha/2-1}), \quad 0 \leq k \leq N. \end{aligned}$$

Here we present the flow chart to compute the $(M^a \hat{u})_k \approx 2(k+1) \hat{u}_{k+1}^{\alpha/2-1} h_{k+1}^{\alpha/2-1}$:

$$\{\hat{u}_n\} \xrightarrow{FJCT} \{\hat{u}_n^{-1/2}\} \xrightarrow{FCT} \{\tilde{u}_N(\mathbf{x}_j)\} \longrightarrow \{u_N(\mathbf{x}_j)\} \xrightarrow{FCT} \{\hat{u}_n^{-1/2}\} \xrightarrow{FCJT} \{\hat{u}_n^{\alpha/2-1}\}.$$

The right hand side $\hat{f}_k = (f, (1-x^2)^{\alpha/2} P_k^{\alpha/2})$ can be computed as $(M^r \hat{u})_k$ and the calculation is done only once.

The initial guess of the iterative method can be chosen as the numerical solution obtained by solving (2.4.1) with a direct method and $N = 8$. The iterations stop either it reaches the maximum iteration number 100 or meets the condition $\|\hat{u}^{(m+1)} - \hat{u}^{(m)}\|_{l^2} / \|\hat{u}^{(m+1)}\|_{l^2} < \epsilon$, where we take $\epsilon = 10^{-7}$. We will numerically check the performance of the proposed iterative solver in Table 2.4 for Example 3.5.2.

2.4.2 Numerical results

Throughout the following tables, "Order" is short for the estimated convergence order for the numerical method (2.3.1).

---

[3] These fast transforms may not be exact but they are highly accurate and the errors from these fast transforms can be ignored in many applications, as in all the computations in this section.

Example 2.4.1. *Consider $f = \sin x$. Here f belongs to $B^{\infty}_{\omega^{\alpha/2}}$.*

By Theorem 6.1.4, $\omega^{-\alpha/2}u \in B^{5\alpha/2-1-\epsilon}_{\omega^{\alpha/2}}$ for the problem (2.0.1)-(2.0.2) with $\mu_1 \neq 0$. According to Theorem 3.4.3, the convergence orders are expected to be $2\alpha-1-\epsilon$ in $H^{\alpha/2}$-norm and $5\alpha/2-1-\epsilon$ in $L^2_{\omega^{-\alpha/2}}$-norm. The convergence orders are observed and verified in Table 2.2 with the $H^{\alpha/2}$-norm and in Table 2.3 with the $L^2_{\omega^{-\alpha/2}}$-norm.

When $\mu_1 = 0$, the problem (2.0.1)-(2.0.2) becomes the reaction-diffusion equation and by Theorem 2.2.10, $\omega^{-\alpha/2}u \in B^{5\alpha/2+1-\epsilon}_{\omega^{\alpha/2}}$. Theorem 2.3.4 suggests that the convergence order in $H^{\alpha/2}$-norm is $2\alpha + 1 - \epsilon$ and the order in $L^2_{\omega^{-\alpha/2}}$-norm is $5\alpha/2 + 1 - \epsilon$. The orders are observed in Figure 1.4.

The numerical results verify the regularity index $5\alpha/2 - 1 - \epsilon$ and $5\alpha/2 + 1 - \epsilon$ for the solution with advection and reaction-only term, respectively, as suggested in Theorems 6.1.4 and 2.2.10.

Table 2.2: Convergence orders and errors of the spectral Galerkin method (2.3.1) for the equation $(-\Delta)^{\alpha/2}u + Du + u = \sin x$ (Example 2.4.1). The estimated convergence order is $2\alpha - 1 - \epsilon$ in $H^{\alpha/2}$-norm.

N	$\alpha = 1.2$		$\alpha = 1.4$		$\alpha = 1.6$		$\alpha = 1.8$	
	$E^*(N)$	rate	$E^*(N)$	rate	$E^*(N)$	rate	$E^*(N)$	rate
16	6.04e-03		1.10e-03		2.07e-04		3.19e-05	
32	2.64e-03	1.19	3.42e-04	1.69	5.01e-05	2.05	6.12e-06	2.38
64	1.10e-03	1.27	1.02e-04	1.74	1.16e-05	2.11	1.10e-06	2.48
128	4.18e-04	1.39	2.88e-05	1.82	2.55e-06	2.19	1.87e-07	2.55
Order		1.40		1.80		2.20		2.60

Table 2.3: Convergence orders and errors of the spectral Galerkin method (2.3.1) for the equation $(-\Delta)^{\alpha/2}u + Du + u = \sin x$ (Example 2.4.1). The estimated convergence order is $5\alpha/2 - 1 - \epsilon$ in $L^2_{\omega^{-\alpha/2}}$-norm.

N	$\alpha = 1.2$		$\alpha = 1.4$		$\alpha = 1.6$		$\alpha = 1.8$	
	$E(N)$	rate	$E(N)$	rate	$E(N)$	rate	$E(N)$	rate
16	8.96e-04		1.24e-04		1.74e-05		2.00e-06	
32	2.68e-04	1.74	2.46e-05	2.34	2.54e-06	2.77	2.18e-07	3.19
64	7.49e-05	1.84	4.63e-06	2.41	3.47e-07	2.87	2.17e-08	3.33
128	1.97e-05	1.93	8.32e-07	2.47	4.52e-08	2.94	2.03e-09	3.42
Order		2.00		2.50		3.00		3.50

In Tables 2.2 and 2.3, we have tested convergence orders using a direct solver for (2.4.1). We now check the performance of the proposed iterative solver. Here we take the reference solution as $u_{\text{ref}} =: u_{2^{14}}$. In Table 2.4, we observe the order of $5\alpha/2 - 1$ in the $L^2_{\omega^{-\alpha/2}}$-norm as in Theorem 6.1.4. The number of iterations is less than 20 for various α's listed in the table. However, the iteration numbers decrease with α: when $\alpha = 1.2$, the iteration number is 19 while the number is 5 for $\alpha = 1.8$. These iteration numbers suggest the need of better iterative methods for small α's (or independent of α). Intuitively, the matrix $P^{-1} = (S + \mu_2 I)^{-1}$ contains no information from the advection term while it becomes more pronounced when α is closer to 1. The choice of P is then a subtle issue and deserves further explorations in future work. From Table 2.4 we conclude

that the CPU time increases roughly as $\mathcal{O}(N \log^2 N)$. Here the CPU time is obtained by averaging three runs of the code in MATLAB R2019a, performed on a laptop with the configuration of AMD A10-8700p Radeon R6, 10 Compute Cores 4C+6G 1.80GHz and 12 GB memory.

Table 2.4: Tests of the proposed fast iterative solver with the complexity $\mathcal{O}(N \log^2 N)$ in convergence and computational time: spectral Galerkin method (2.3.1) for the equation $(-\Delta)^{\alpha/2}u + Du + u = \sin x$. The estimated convergence order is $5\alpha/2 - 1$ in $L^2_{\omega^{-\alpha/2}}$-norm. Here 'iter #' represents the iteration number and 'CPU(s)' stands for the computational time measured in seconds.

	$\alpha = 1.2$				$\alpha = 1.4$			
N	$E(N)$	rate	iter #	CPU (s)	$E(N)$	rate	iter #	CPU(s)
512	1.50e-06		19	0.82	3.09e-08		12	0.55
1024	3.84e-07	1.97	19	1.56	5.48e-09	2.49	12	1.02
2048	9.76e-08	1.98	19	3.18	9.71e-10	2.50	12	2.21
4096	2.48e-08	1.98	19	8.53	1.72e-10	2.50	12	5.56
	$\alpha = 1.6$				$\alpha = 1.8$			
N	$E(N)$	rate	iter #	CPU (s)	$E(N)$	rate	iter #	CPU(s)
512	8.91e-10		8	0.40	2.17e-11		5	0.27
1024	1.12e-10	2.99	8	0.73	1.94e-12	3.49	5	0.53
2048	1.41e-11	3.00	8	1.71	1.72e-13	3.49	5	1.20
4096	1.76e-12	3.00	8	4.81	1.53e-14	3.49	5	4.09

Example 2.4.2. *Consider* $f = |\sin x|$. *The function* f *has a weak singularity at* $x = 0$ *and* $f \in B^{1.5-\epsilon}_{\omega^{\alpha/2}}$ *with* $\epsilon > 0$ *arbitrarily small.*

By Theorem 6.1.4, $\omega^{-\alpha/2}u \in B^{\alpha+\min(3\alpha/2-1,1.5)-\epsilon}_{\omega^{\alpha/2}}$ for (2.0.1) with $\mu_1 = \mu_2 = 1$. According to Theorem 2.3.4, the convergence order for the spectral Galerkin method (2.3.1) is expected to be $\alpha + \min(3\alpha/2 - 1, 1.5 - \epsilon)$ in $L^2_{\omega^{-\alpha/2}}$-norm.

From Table 2.5, we can observe that the convergence order for the spectral Galerkin method (2.3.1) is $\alpha + \min(3\alpha/2 - 1, 1.5 - \epsilon)$, which is in agreement with the theoretical prediction and verifies the regularity result in Theorem 6.1.4.

Next, we test the reaction-only case $\mu_1 = 0$ in (2.0.1). From Table 2.6, we can observe that the convergence order is $\alpha + 1.5 - \epsilon$ for the spectral Galerkin method (2.3.1), which is in agreement with the estimate order $\alpha + \min(3\alpha/2 + 1, 1.5 - \epsilon)$. This verifies the regularity result in Theorem 2.2.10.

The performance of the proposed iterative solver (2.4.4) in this example is similar to that in Example 3.5.2 and thus is not presented.

Example 2.4.3 (Boundary singularity for the function f)**.** *Consider* $f = (1 - x^2)^\beta \sin x$.

We test the different β's in Tables 2.7-2.8 ($\beta = 0.5$) and in Tables 2.9-2.10 ($\beta = -0.4$).

It can readily verified that $f \in B^r_{\omega^{\alpha/2}}$ with $r = \alpha/2 + 2\beta + 1 - \epsilon$; see e.g. in the appendix of [55] for a proof. By Theorems 6.1.4 and 2.3.4, the theoretical order for the spectral Galerkin method is $\alpha + \min(3\alpha/2 - 1 - \epsilon, r)$. If $\mu_1 = 0$, by Theorems 2.2.10 and 2.3.4 the theoretical order for the Galerkin method is $\alpha + \min(3\alpha/2 + 1 - \epsilon, r)$.

We first test the case $\beta = 0.5$, where the derivative of f has a weak singularity and f vanishes at both endpoints ± 1. When $\mu_1 \neq 0$, we observe the convergence order is about $5\alpha/2 - 1$ in Table 2.7

Table 2.5: Convergence orders and errors of the spectral Galerkin method (2.3.1) for the equation $(-\Delta)^{\alpha/2}u + Du + u = |\sin x|$ (Example 2.4.2). The estimated convergence order is $\alpha + \min(3\alpha/2 - 1, 1.5 - \epsilon)$ in $L^2_{\omega^{-\alpha/2}}$-norm.

| N | $\alpha = 1.2$ | | $\alpha = 1.4$ | | $\alpha = 1.6$ | | $\alpha = 1.8$ | |
	$E(N)$	rate	$E(N)$	rate	$E(N)$	rate	$E(N)$	rate
16	2.74e-03		4.47e-04		1.25e-04		5.94e-05	
32	8.00e-04	1.78	8.27e-05	2.43	1.78e-05	2.82	7.51e-06	2.98
64	2.21e-04	1.86	1.47e-05	2.49	2.31e-06	2.95	8.56e-07	3.13
128	5.79e-05	1.93	2.55e-06	2.53	2.84e-07	3.02	9.16e-08	3.22
Order		2.00		2.50		3.00		3.30

Table 2.6: Convergence orders and errors of the spectral Galerkin method (2.3.1) for the equation $(-\Delta)^{\alpha/2}u + u = |\sin x|$ (Example 2.4.2). The estimated convergence order is $\alpha + 1.5 - \epsilon$ in $L^2_{\omega^{-\alpha/2}}$-norm.

| N | $\alpha = 1.2$ | | $\alpha = 1.4$ | | $\alpha = 1.6$ | | $\alpha = 1.8$ | |
	$E(N)$	rate	$E(N)$	rate	$E(N)$	rate	$E(N)$	rate
16	3.85e-04		2.06e-04		1.10e-04		5.89e-05	
32	7.00e-05	2.46	3.32e-05	2.63	1.57e-05	2.81	7.46e-06	2.98
64	1.18e-05	2.57	4.90e-06	2.76	2.04e-06	2.95	8.52e-07	3.13
128	1.87e-06	2.65	6.84e-07	2.84	2.50e-07	3.03	9.14e-08	3.22
Order		2.70		2.90		3.10		3.30

which matches with the expected one, $\alpha + \min(3\alpha/2 - 1 - \epsilon, r)$. We further test the reaction-only case, $\mu_1 = 0$. We observe that the convergence orders displayed in Table 2.8 are $3\alpha/2 + 2$, which is exactly $\alpha + \min(3\alpha/2 + 1 - \epsilon, r)$.

We then consider the singular $f = (1 - x^2)^\beta \sin x$ with $\beta = -0.4$. For the equation (2.0.1) with $\mu_1 \neq 0$, we can see that the convergence orders are about $3\alpha/2 + 0.2 - \epsilon$ in Table 2.9. For the case $\mu_1 = 0$, the observed orders are $3\alpha/2 + 0.2$ which can be seen in Table 2.10.

In this example, the observed convergence orders for Galerkin method are following the theoretical ones when f has both weak boundary singularity ($\beta = 0.5$) or stronger boundary singularity ($\beta = -0.4$). The numerical results verify the regularity estimates and also show that the error estimates for the Galerkin method are optimal.

The performance of the proposed iterative solver (2.4.4) in this example is similar to that in Example 3.5.2 and thus is not presented. The only difference here is that $\hat{f}$ cannot be computed with the fast transforms because of the singularity at both endpoints. We apply a proper Gauss-Jacobi quadrature rule as in the direct solver. Though the use of a quadrature rule leads to an increase of computational cost, $\hat{f}$ can be computed offline.

In summary, we observe in Examples 2.4.1-2.4.3 that the convergence order of spectral Galerkin method 2.3.1 in $L^2_{\omega^{-\alpha/2}}$-norm is $\alpha + \min(3\alpha/2 - 1 - \epsilon, r)$ for advection-diffusion-reaction and $\alpha + \min(3\alpha/2 + 1 - \epsilon, r)$ for diffusion-reaction equation respectively, which verify the regularity estimates in Theorems 6.1.4 and 2.2.10.

Table 2.7: Convergence orders and errors of the spectral Galerkin method (2.3.1) for the equation $(-\Delta)^{\alpha/2}u + Du + u = (1 - x^2)^{0.5}\sin x$ (Example 2.4.3). The estimated convergence order is $5\alpha/2 - 1 - \epsilon$ in $L^2_{\omega^{-\alpha/2}}$-norm.

| | $\alpha = 1.2$ | | $\alpha = 1.4$ | | $\alpha = 1.6$ | | $\alpha = 1.8$ | |
N	$E(N)$	rate	$E(N)$	rate	$E(N)$	rate	$E(N)$	rate
16	4.38e-04		5.88e-05		8.29e-06		1.64e-06	
32	1.35e-04	1.70	1.23e-05	2.25	1.29e-06	2.68	1.29e-07	3.67
64	3.80e-05	1.83	2.36e-06	2.39	1.81e-07	2.83	1.20e-08	3.43
128	1.00e-05	1.92	4.26e-07	2.47	2.38e-08	2.93	1.12e-09	3.42
Order		2.00		2.50		3.00		3.50

Table 2.8: Convergence orders and errors of the spectral Galerkin method (2.3.1) for the equation $(-\Delta)^{\alpha/2}u + u = (1 - x^2)^{0.5}\sin x$ (Example 2.4.3). The estimated convergence order is $3\alpha/2 + 2 - \epsilon$ in $L^2_{\omega^{-\alpha/2}}$-norm.

| | $\alpha = 1.2$ | | $\alpha = 1.4$ | | $\alpha = 1.6$ | | $\alpha = 1.8$ | |
N	$E(N)$	rate	$E(N)$	rate	$E(N)$	rate	$E(N)$	rate
16	1.44e-05		6.85e-06		3.21e-06		1.49e-06	
32	1.18e-06	3.61	4.66e-07	3.88	1.81e-07	4.15	6.97e-08	4.42
64	9.11e-08	3.69	2.96e-08	3.98	9.39e-09	4.27	2.97e-09	4.55
128	6.81e-09	3.74	1.80e-09	4.04	4.66e-10	4.33	1.20e-10	4.63
Order		3.80		4.10		4.40		4.70

Table 2.9: Convergence orders and errors of the spectral Galerkin method (2.3.1) for the equation $(-\Delta)^{\alpha/2}u + Du + u = (1 - x^2)^{-0.4}\sin x$ (Example 2.4.3). The estimated convergence order is $3\alpha/2 + 0.2 - \epsilon$ in $L^2_{\omega^{-\alpha/2}}$-norm.

| | $\alpha = 1.2$ | | $\alpha = 1.4$ | | $\alpha = 1.6$ | | $\alpha = 1.8$ | |
N	$E(N)$	rate	$E(N)$	rate	$E(N)$	rate	$E(N)$	rate
16	3.23e-03		7.79e-04		2.65e-04		1.07e-04	
32	9.54e-04	1.76	1.65e-04	2.24	4.74e-05	2.48	1.62e-05	2.73
64	2.65e-04	1.85	3.38e-05	2.29	8.15e-06	2.54	2.30e-06	2.81
128	6.97e-05	1.93	6.69e-06	2.34	1.35e-06	2.59	3.15e-07	2.87
Order		2.00		2.30		2.60		2.90

2.5 Extension to fractional diffusion equations driven by random noise

Stochastic mathematical models have received increasing attention for their ability of representing intrinsic uncertainty in complex systems, e.g., representing various scales in particle simulations at molecular and mesoscopic scales, as well as extrinsic uncertainty, e.g., stochastic external forces, stochastic initial conditions, or stochastic boundary conditions. One important class of stochastic mathematical models is stochastic partial differential equations (SPDEs), which can be seen as

Table 2.10: Convergence orders and errors of the spectral Galerkin method (2.3.1) for the equation $(-\Delta)^{\alpha/2}u + u = (1-x^2)^{-0.4}\sin x$ (Example 2.4.3). The estimated convergence order is $3\alpha/2 + 0.2$ in $L^2_{\omega^{-\alpha/2}}$-norm.

	$\alpha = 1.2$		$\alpha = 1.4$		$\alpha = 1.6$		$\alpha = 1.8$	
N	$E(N)$	rate	$E(N)$	rate	$E(N)$	rate	$E(N)$	rate
16	1.47e-03		6.03e-04		2.51e-04		1.06e-04	
32	3.92e-04	1.91	1.33e-04	2.18	4.59e-05	2.45	1.61e-05	2.72
64	1.01e-04	1.96	2.81e-05	2.24	7.97e-06	2.53	2.30e-06	2.81
128	2.49e-05	2.02	5.71e-06	2.30	1.33e-06	2.58	3.15e-07	2.87
Order		2.00		2.30		2.60		2.90

deterministic partial differential equations (PDEs) with finite or infinite dimensional stochastic processes either with color noise or white noise. Though white noise is a purely mathematical construction, it can be a good model for rapid random fluctuations, and it is also the limit of color noise when the correlation length goes to zero.

For simplicity we will study the fractional diffusion equations driven by low regularity random noise as following:

$$(-\Delta)^{\alpha/2}u + u = f(x) \tag{2.5.1}$$

with $f(x) = \sum_{k=0}^{\infty} k^{-\beta/2}m_k(x)\chi_k$. Here $m_k(x)$ is orthonormal basis in $L^2(\Omega)$ and χ_k are i.i.d standard normal distribution. If $\beta = 0$ we call it white noise, $\beta = 1$ for pink noise and $\beta = 2$ for brown noise.

Consider the fractional Poisson with $1/f^\beta$ noise.

$$(-\Delta)^{\frac{\alpha}{2}}u + \mu u = \dot{W}^\beta(x). \tag{2.5.2}$$

Here

$$\dot{W}^\beta(x) = \sum_{k=1}^{\infty} k^{-\frac{\beta}{2}}e_k(x)\xi_k. \tag{2.5.3}$$

where $e_k(x) = \sin(k\pi\frac{x+1}{2})$, $x \in (-1,1)$. When $0 \leq \beta \leq 2$, the noise is called $1/f^\beta$ noise. The following are common discussed in the literature.

- (white noise) $\beta = 0$, $t < -\frac{1}{2}$

- (Pink noise) $\beta = 1$, $t < 0$

- (Brownian noise) $\beta = 2$, $t < \frac{1}{2}$

Next we describe the regularity of noise (2.5.3). To this end, we introduce the space $\mathbb{L}^2(\Omega; B^s_{\alpha/2})$

$$\mathbb{L}^2(\Omega; B^s_\beta) = \{u : \|u\|_{\mathbb{L}^2(\Omega;B^s_\beta)} < \infty\} \tag{2.5.4}$$

$$\|u\|^2_{\mathbb{L}^2(\Omega;B^s_\beta)} = \sum_{n=0}^{\infty} \mathbb{E}(u_n^\beta)^2 h_n^\beta(1+n^2)^s, \quad \beta > -1, \tag{2.5.5}$$

where u_n^β are the coefficients of Jacobi-Fourier expansion for u in terms of P_n^β.

$$\mathbb{E}[\left\|\dot{W}^\beta\right\|_{\dot{H}^t}^2] = \sum_{k=1}^\infty k^{2t-\beta} < \infty, \quad \text{when } t < \frac{\beta}{2} - \frac{1}{2}. \tag{2.5.6}$$

Recall the space

$$\dot{H}^s = \dot{H}^s(\mathcal{D}) = \mathcal{D}((-\Delta)^{s/2}) = \left\{ v | \; \|v\|_s = \left\|(-\Delta)^{s/2}v\right\| = (\sum_{k=1}^\infty \lambda_k^s [(v, e_k)]^2)^{1/2} < \infty \right\}.$$

For the color noise $\dot{W}^\beta(x)$, we have

$$\dot{W}^\beta(x) = \sum_k k^{-\beta/2} e_k(x)\xi_k(\theta) = \sum_n a_n^{\alpha/2}(\theta) P_n^{\alpha/2}(x), \tag{2.5.7}$$

$$a_n^{\alpha/2}(\theta) = \sum_k k^{-\beta/2} a_{n,k}^{\alpha/2} \xi_k(\theta), \quad a_{n,k}^{\alpha/2} = \frac{1}{h_n^{\alpha/2}} \int_{-1}^1 e_k(x)(1-x^2)^{\alpha/2} P_n^{\alpha/2}(x)dx. \tag{2.5.8}$$

where ξ_k are standard Gauss Random variables which obey independently identical distribution. It is clear that

$$\mathbb{E}(a_n^{\alpha/2})^2 = \sum_{k=0}^\infty k^{-\beta} |a_{n,k}^{\alpha/2}|^2. \tag{2.5.9}$$

Thus it suffices to estimate $|a_{n,k}^{\alpha/2}|$ in (2.5.8), which will be shown in the Appendix .2

As to the orthogonal basis e_k we have myriad of choices. For example, we can take $e_k(x) = P_k^0(x)$ or $\omega^{\alpha/4} P_k^{\alpha/2}(x)$, and the traditional eigenfunctions for Dirichlet type boundary value problems.

With the regularity of noise, the regularity of the solution can be shown readily. Actually, when $-\frac{\alpha}{2} \le -\frac{1}{2} \le \frac{\beta-1}{2} \le \frac{1-\alpha}{2}$ ($0 \le \beta \le 2-\alpha$ and $\alpha \ge 1$), we have

$$\mathbb{E}[\left\|\mathcal{T}\dot{W}^\beta\right\|_{H^{\alpha+\frac{\beta-1}{2}-\epsilon}}^2] \le C\mathbb{E}[\left\|\dot{W}^\beta\right\|_{H^{\frac{\beta-1}{2}-\epsilon}}^2] \le C. \tag{2.5.10}$$

Then we obtain $\mathcal{T}\dot{W}^\beta \in \mathbb{L}^2(\Omega; H^{\alpha+\frac{\beta-1}{2}-\epsilon})$.

When $\beta > 2 - \alpha > 0$, we have $\frac{\beta-1}{2} > \frac{1-\alpha}{2}$ and thus

$$\mathbb{E}[\left\|\mathcal{T}\dot{W}^\beta\right\|_{H^{\frac{\alpha+1}{2}-\epsilon}}^2] \le C\mathbb{E}[\left\|\dot{W}^\beta\right\|_{H^{\frac{1-\alpha}{2}}}^2] \le C. \tag{2.5.11}$$

If we used the weighted Sobolev space

$$\omega^{-\frac{\alpha}{2}} \mathcal{T}\dot{W}^\beta \in \mathbb{L}^2(\Omega; B_{\frac{\alpha}{2}}^{\alpha+\frac{\beta-1}{2}-\epsilon}),$$

Then we expect the convergence order $\alpha + \frac{\beta-1}{2}$ ($\beta > 1$).

With the establishment of the regularity of solution, we can the discuss the convergence of numerical methods.

Based on the approximations properties, the error estimates can be expected as

$$
\begin{aligned}
\left\|\mathcal{T}\dot{W}^\beta - \mathcal{T}_N\dot{W}^\beta_M\right\| &\leq \left\|\mathcal{T}\dot{W}^\beta - \mathcal{T}\dot{W}^\beta_M\right\| + \left\|\mathcal{T}\dot{W}^\beta_M - \mathcal{T}_N\dot{W}^\beta_M\right\| \\
&\leq CM^{-(\alpha+\frac{\beta-1}{2})} + CN^{-(\alpha+\frac{\beta-1}{2}-)}\left\|\dot{W}^\beta_M\right\|_{\alpha+\frac{\beta-1}{2}-}.
\end{aligned}
$$

By the fact $\mathbb{E}[\left\|\dot{W}^\beta_M\right\|^2_{\alpha+\frac{\beta-1}{2}-}] \leq \mathbb{E}[\left\|\dot{W}^\beta\right\|^2_{\alpha+\frac{\beta-1}{2}-}]$, we have

$$
\mathbb{E}[\left\|\mathcal{T}\dot{W}^\beta - \mathcal{T}_N\dot{W}^\beta_M\right\|^2] \leq CM^{-2(\alpha+\frac{\beta-1}{2})} + CN^{-2(\alpha+\frac{\beta-1}{2}-)}.
$$

Thus taking $M = N$ leads to the order of $\alpha + \frac{\beta-1}{2} - \epsilon$ with $\epsilon > 0$. We will check the findings by the following numerical experiments, where we take 20000 samples and the $M = 1000$.

Table 2.11: Convergence orders and errors of the spectral Galerkin method for the equation $(-\Delta)^{\alpha/2}u + u = f(x)$ with the white noise. The estimated convergence order is $\alpha - 0.5$ in L^2-norm.

| N | $\alpha = 1.2$ | | $\alpha = 1.4$ | | $\alpha = 1.6$ | | $\alpha = 1.8$ | |
	$E(N)$	rate	$E(N)$	rate	$E(N)$	rate	$E(N)$	rate
8	1.41e-01		7.68e-02		4.27e-02		2.42e-02	
16	1.05e-01	0.43	4.99e-02	0.62	2.39e-02	0.84	1.15e-02	1.07
32	7.42e-02	0.50	3.21e-02	0.63	1.40e-02	0.77	6.19e-03	0.90
64	4.77e-02	0.64	1.85e-02	0.80	7.23e-03	0.95	2.87e-03	1.11
128	2.61e-02	0.87	8.54e-03	1.11	2.83e-03	1.35	9.47e-04	1.60
256	1.58e-02	0.73	4.49e-03	0.93	1.29e-03	1.13	3.79e-04	1.32
Order		0.70		0.90		1.10		1.30

Table 2.12: Convergence orders and errors of the spectral Galerkin method for the equation $(-\Delta)^{\alpha/2}u + u = f(x)$ with the white noise. The estimated convergence order is $\alpha - 0.5$ in L^2-norm.

| N | $\alpha = 1.0$ | | $\alpha = 1.1$ | | $\alpha = 1.9$ | | $\alpha = 2.0$ | |
	$E(N)$	rate	$E(N)$	rate	$E(N)$	rate	$E(N)$	rate
8	2.62e-01		1.92e-01		1.83e-02		1.40e-02	
16	2.18e-01	0.27	1.51e-01	0.35	8.04e-03	1.19	5.65e-03	1.31
32	1.70e-01	0.35	1.13e-01	0.43	4.14e-03	0.96	2.78e-03	1.02
64	1.23e-01	0.47	7.66e-02	0.56	1.81e-03	1.19	1.16e-03	1.27
128	7.94e-02	0.63	4.56e-02	0.75	5.51e-04	1.72	3.23e-04	1.84
256	5.49e-02	0.53	2.95e-02	0.63	2.07e-04	1.41	1.14e-04	1.51
Order		0.50		0.60		1.40		1.50

Table 2.13: Convergence orders and errors of the spectral Galerkin method for the equation $(-\Delta)^{\alpha/2}u + u = f(x)$ with the pink noise. The estimated convergence order is α in L^2-norm.

	$\alpha = 1.2$		$\alpha = 1.4$		$\alpha = 1.6$		$\alpha = 1.8$	
N	$E(N)$	rate	$E(N)$	rate	$E(N)$	rate	$E(N)$	rate
8	4.02e-02		2.32e-02		1.35e-02		7.93e-03	
16	2.01e-02	1.00	9.84e-03	1.24	4.85e-03	1.48	2.41e-03	1.72
32	1.13e-02	0.83	5.02e-03	0.97	2.26e-03	1.10	1.03e-03	1.23
64	5.51e-03	1.03	2.19e-03	1.20	8.82e-04	1.36	3.59e-04	1.52
128	2.00e-03	1.46	6.78e-04	1.69	2.32e-04	1.93	8.01e-05	2.16
256	8.50e-04	1.24	2.49e-04	1.44	7.42e-05	1.64	2.25e-05	1.83
Order		1.20		1.40		1.60		1.80

Table 2.14: Convergence orders and errors of the spectral Galerkin method for the equation $(-\Delta)^{\alpha/2}u + u = f(x)$ with the pink noise. The estimated convergence order is α in L^2-norm.

	$\alpha = 1.0$		$\alpha = 1.1$		$\alpha = 1.9$		$\alpha = 2.0$	
N	$E(N)$	rate	$E(N)$	rate	$E(N)$	rate	$E(N)$	rate
8	7.02e-02		5.31e-02		6.10e-03		4.70e-03	
16	4.11e-02	0.77	2.87e-02	0.89	1.70e-03	1.84	1.21e-03	1.96
32	2.55e-02	0.69	1.70e-02	0.76	6.97e-04	1.29	4.75e-04	1.35
64	1.39e-02	0.87	8.75e-03	0.95	2.30e-04	1.60	1.48e-04	1.68
128	6.00e-03	1.22	3.46e-03	1.34	4.73e-05	2.28	2.81e-05	2.40
256	2.93e-03	1.03	1.58e-03	1.13	1.25e-05	1.93	6.93e-06	2.02
Order		1.00		1.10		1.90		2.00

Table 2.15: Convergence orders and errors of the spectral Galerkin method for the equation $(-\Delta)^{\alpha/2}u + u = f(x)$ with the brown noise. The estimated convergence order is $\alpha + 0.5$ in L^2-norm.

	$\alpha = 1.2$		$\alpha = 1.4$		$\alpha = 1.6$		$\alpha = 1.8$	
N	$E(N)$	rate	$E(N)$	rate	$E(N)$	rate	$E(N)$	rate
8	1.31e-02		7.75e-03		4.60e-03		2.74e-03	
16	4.13e-03	1.66	2.07e-03	1.91	1.04e-03	2.15	5.24e-04	2.39
32	1.85e-03	1.16	8.40e-04	1.30	3.86e-04	1.43	1.79e-04	1.55
64	6.79e-04	1.44	2.75e-04	1.61	1.13e-04	1.78	4.66e-05	1.94
128	1.67e-04	2.02	5.79e-05	2.25	2.03e-05	2.48	7.15e-06	2.70
256	4.94e-05	1.76	1.49e-05	1.96	4.55e-06	2.16	1.41e-06	2.34
Order		1.70		1.90		2.10		2.30

2.6 Two-term Laplacian in 1D

For the fractional diffusion equations, we have high convergence rate by using the non-polynomial basis but it does not apply to the equations with second order Laplacian term as the principle term. In fact, as the inclusion of the advection term in the diffusion equations will degrade the convergence by two. It is natural to conjecture that the convergence order will further degrade

Table 2.16: Convergence orders and errors of the spectral Galerkin method for the equation $(-\Delta)^{\alpha/2}u+u = f(x)$ with the brown noise. The estimated convergence order is $\alpha+0.5$ in L^2-norm.

N	$\alpha = 1.0$ $E(N)$	rate	$\alpha = 1.1$ $E(N)$	rate	$\alpha = 1.9$ $E(N)$	rate	$\alpha = 2.0$ $E(N)$	rate
8	2.20e-02		1.70e-02		2.12e-03		1.65e-03	
16	8.25e-03	1.41	5.84e-03	1.54	3.74e-04	2.51	2.68e-04	2.62
32	4.07e-03	1.02	2.74e-03	1.09	1.23e-04	1.61	8.43e-05	1.67
64	1.68e-03	1.27	1.07e-03	1.36	3.01e-05	2.03	1.95e-05	2.11
128	4.87e-04	1.79	2.85e-04	1.90	4.27e-06	2.82	2.56e-06	2.93
256	1.66e-04	1.55	9.05e-05	1.66	7.89e-07	2.44	4.43e-07	2.53
Order		1.50		1.60		2.40		2.50

Table 2.17: Convergence orders and errors of the spectral Galerkin method for the equation $(-\Delta)^{\alpha/2}u+u = f(x)$ with the brown noise. The estimated convergence order is $\alpha+0.5$ in weighted L^2-norm.

N	$\alpha = 1.0$ $E(N)$	rate	$\alpha = 1.1$ $E(N)$	rate	$\alpha = 1.9$ $E(N)$	rate	$\alpha = 2.0$ $E(N)$	rate
8	2.56e-02		2.04e-02		3.68e-03		3.01e-03	
16	1.04e-02	1.30	7.74e-03	1.40	8.10e-04	2.18	6.19e-04	2.28
32	4.74e-03	1.13	3.31e-03	1.23	2.09e-04	1.95	1.51e-04	2.04
64	1.97e-03	1.27	1.30e-03	1.35	5.34e-05	1.97	3.64e-05	2.05
128	6.23e-04	1.66	3.86e-04	1.75	9.61e-06	2.47	6.15e-06	2.57
256	1.91e-04	1.71	1.08e-04	1.84	1.40e-06	2.78	8.35e-07	2.88
Order		1.50		1.60		2.40		2.50

with appearance of second order terms. We will not pursue theory along this line but give some numerical examples to demonstrate the idea.

Next we will examine the two terms by comparing the non-polynomial basis with the traditional Legendre polynomial basis to compute the equations. To this end, we need the following Lemma.

$$_{-1}D_x^\mu L_n(x) = \frac{\Gamma(n+1)}{\Gamma(n+1-\mu)}(1+x)^{-\mu}P_n^{\mu,-\mu}, \qquad (2.6.1)$$

$$_xD_1^\mu L_n(x) = \frac{\Gamma(n+1)}{\Gamma(n+1-\mu)}(1-x)^{-\mu}P_n^{-\mu,\mu} \qquad (2.6.2)$$

In our numerical test, the basis is taken as $\phi_n(x) = L_n(x) - L_{n+2}(x)$. To compute the stiff matrix for fractional operator, we have the following steps.

- Step 1, for $0 < \alpha < 2$, generate the inner product $A_{k,n} = (_{-1}D_x^\alpha L_n, L_k) = (_{-1}D_x^{\alpha/2}L_n,\ _xD_1^{\alpha/2}L_k)$ for $0 \le k, n, \le N$. We use the Gauss-Jacobi quadrature to compute

$$\int_{-1}^1 (1-x)^{-\alpha/2}(1+x)^{-\alpha/2}P_n^{-\alpha/2,\alpha/2}P_k^{\alpha/2,-\alpha/2}dx.$$

- Step 2, let $S^0 = -1/(2\cos(\alpha\pi/2))(A + A^T)$.

- Let connection matrix $C = diag(ones(N + 1), 0) - diag(ones(N - 1), 2)$ and $C(N, N) = 0$ and $C(N + 1, N + 1) = 0$. Then $S^1 = CS^0C^T$.

- Take the $(N - 1) \times (N - 1)$ matrix $S^\alpha = S^1(1 : N - 1; 1 : N - 1)$.

The stiff matrix for second order diffusion operator is diagonal with entries $S^2_{k,k} = (4k + 6)$. How to compute the mass matrix (see Page 146 in [79]). Mass matrix is symmetrical Penta-diagonal whose non-zero elements are

$$m_{j,k} = m_{k,j} = \begin{cases} \frac{2}{2k+1} + \frac{2}{2k+5}, & k = j \\ -\frac{2}{2k+5}, & j = k + 2. \end{cases}$$

We test the equation with the exact solution $(1 - x^2)^{1+\alpha/2}$ and the right hand side function $f = -\mu_0 D^\alpha u - \mu_1 D^2 u + \mu_2 u$, where

$$D^\alpha(1 - x^2)^{1+\alpha/2} = (C_0 \lambda_0 P_0^{\alpha/2} + C_2 \lambda_2 P_2^{\alpha/2}). \tag{2.6.3}$$

Here

$$C_0 = -\frac{1}{(\alpha + 3)}, \quad C_2 = -\frac{8}{(\alpha + 3)(\alpha + 4)}, \quad \lambda_n^\alpha = \frac{\Gamma(n + \alpha + 1)}{n!}$$

and

$$P_0^{\alpha/2} = 1, \quad P_2^{\alpha/2} = \frac{\alpha + 4}{8}[(\alpha + 3)x^2 + 1].$$

By calculation we have

$$D^2(1 - x^2)^{1+\alpha/2} = (2 + \alpha)(1 - x^2)^{\alpha/2-1}((\alpha + 1)x^2 - 1). \tag{2.6.4}$$

Thus $f = f_1 + f_2$ with

$$f_1 = -\mu_0 D^\alpha u, \quad f_2 = (1 - x^2)^{\alpha/2-1}[-\mu_1(2 + \alpha)((\alpha + 1)x^2 - 1) + \mu_2(1 - x^2)^2].$$

We show the numerical comparison of the computation between using non polynomials and polynomials in Figures 2.1 and 2.2. From these figures, we can see the convergence order using the polynomials is higher than the non-polynomials, which suggests different regularity behavior between the fractional-term and integer-term dominant diffusion equations. We will study this regularity in our future work.

2.7 Conclusion and discussion

In this paper, we study regularity and a spectral Galerkin method for a fractional advection-diffusion-reaction equation with fractional Laplacian. By factorizing the solution as $u = (1 - x^2)^{\alpha/2}\tilde{u}$, we show that the regularity of solution $\tilde{u}$ in weighted Sobolev spaces can be greatly improved compared to u in non-weighted Sobolev spaces. For the fractional reaction-diffusion equations with or without advection term, the regularity can be essentially different in weighted Sobolev spaces, with the regularity indices being $5/2\alpha + 1 - \epsilon$ and $5/2\alpha - 1 - \epsilon$, respectively. Here $\alpha \in (1, 2)$ is the order of equation and $\epsilon > 0$ is arbitrarily small. These regularity results are sharp in the weighted Sobolev spaces. Based on the obtained regularity, we prove optimal
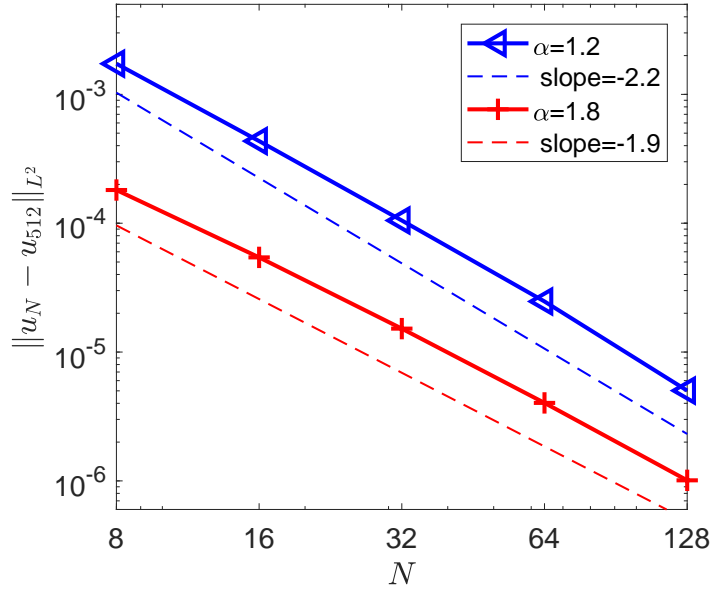
Figure 2.1: For two term Laplace equation $-\Delta u + (-\Delta)^{\alpha/2}u + u = \sin(x)$, $\quad x \in (-1, 1)$, the convergence order using non-polynomial bases is about second order.
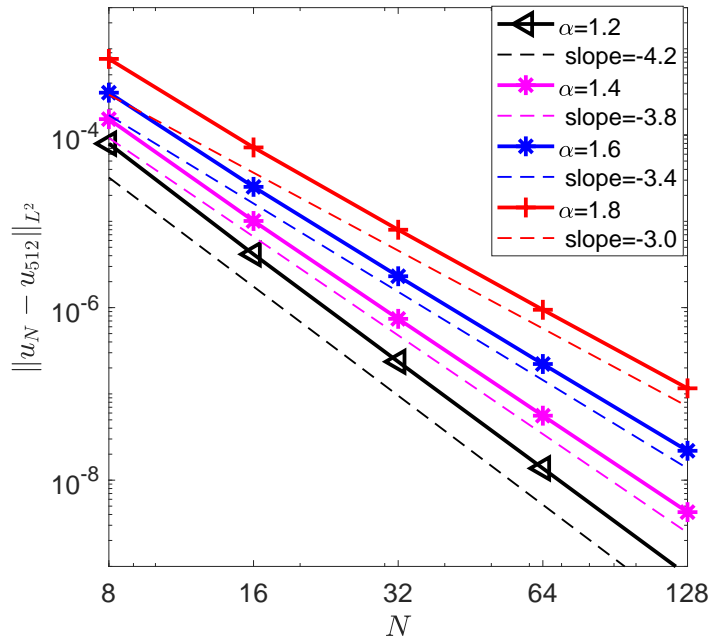
Figure 2.2: For two term Laplace equation $-\Delta u + (-\Delta)^{\alpha/2}u + u = \sin(x)$, $x \in (-1, 1)$, the convergence order using Lendendre polynomial bases is about $6.5 - 2\alpha$.

error estimates of a spectral Galerkin method in the $H^{\alpha/2}$-norm and the weighted L^2-norm. We applied our method to stochastic differential equations with fractional Laplacian in 1D and showed the regularity estimates in weighted norm. Moreover, we further discussed the two-term Laplacian with second-order Laplaician as a principle term. Numerical results verify our theoretical regularity estimates and convergence orders.

Our regularity analysis can be directly applied to equations with Riesz-type derivatives [55], which coincides with the fractional Laplacian in 1D. The analysis can be further extended to time-dependent nonlinear advection-diffusion-reaction equations with fractional Laplacian in 1D. In higher dimensions, the solutions to equations with fractional Laplacian can still be represented by the product of a weakly singular function and a regular function [75]. On a disk, a pseudo-eigendecomposition similar to that in Lemma 2.3.1 also holds; see [37]. We are currently working on the analysis of similar spectral methods and applying fictitious domain methods for general smooth domains other than disks. Numerical results show that extension of current work is promising in two dimensions.

Chapter 3

Spectral method for fractional Laplacian in 2D

3.1 Introduction

In this chapter [1], we consider the following diffusion-reaction equation 1.2.1-1.2.2 with fractional Laplacian on a disk. Our goal here is to *show the convergence order of a spectral Galerkin method for this two-dimensional fractional diffusion-reaction equation on a disk.*

In this chapter, we show that with a reaction term ($\mu > 0$ in (1.2.1)) the exponential convergence cannot be obtained but an order $5\alpha/2 + 1$ in L^2-norm is obtained when f is smooth; see Theorem 3.4.3. The high-order convergence is due to the use of approximation basis in the form of $(1-r^2)^{\alpha/2} \times$ polynomials, in which the factor $(1 - r^2)^{\alpha/2}$ is exactly the boundary singularity of the solution, even though we lose the regularity lifting.

Even the exponential convergence of spectral methods is lost when $\mu > 0$, the spectral methods can still lead to high-order convergence compared to finite element methods. In Table 3.1, we list the convergence rates of piecewise linear finite element methods and the spectral method we use in this paper.

Table 3.1: The estimated convergence order in L^2-norm for finite element method (FEM) and spectral method (SM) corresponding to different right hand side function f. Here $r^2 = x_1^2 + x_2^2$ and h is the mesh size of the linear finite element and N is the number of modes in the radial direction (it is enough to take 200 modes in θ direction). Also, DOF refers to degree of freedom.

$f(x_1, x_2)$	$\sin(x_1) + 2x_2$	$\|0.25 - r^2\| \sin(x_1)$	$(1 - r^2)^{-0.4} \sin(x_1)$
FEM ([3])	$h^{\alpha/2+0.5}$	$h^{\alpha/2+0.5}$	$h^{\alpha/2+0.5}$
SM (this work)	$N^{-(5\alpha/2+1)}$	$N^{-(\alpha+1.5)}$	$N^{-(3\alpha/2+0.2)}$
FEM ([7], adaptive)	$\mathrm{DOF}^{-(1+\alpha)/2}$	$\mathrm{DOF}^{-(1+\alpha)/2}$	$-$

To derive the convergence order as empirically observed in Section 2.4, we need to find a proper theoretical framework, which is not fully available in 2D. In [92], the Hölder space is used but it

---

[1]Zhaopeng Hao, Huiyuan Li, Zhimin Zhang, Zhongqiang Zhang, Sharp error estimates of a spectral Galerkin method for a diffusion-reaction equation with integral fractional Laplacian on a disk, Mathematics of Computation (submitted).

is too coarse for our settings. Using the same tool as in our earlier work [57, 93], we define a weighted space through expansions of functions using the aforementioned pseudo-eigenfunctions and we show that this space is equivalent to the space in [65] when the regularity indexes are integers. Subsequently, we prove the weighted Sobolev regularity of equations on a disk with or without the reaction term and provide the convergence of spectral Galerkin methods. There are several advantages of this theoretical framework: 1) our analysis allows us to deal with solutions with low regularity, e.g. when f is in L^2 or even rougher data; 2) we can explain the convergence orders observed empirically, such as those in Section 2.4; 3) the regularity indexes we obtain can be informative for choosing truncation parameters.

In addition to the theoretical contribution, we present a simpler numerical implementation for spectral Galerkin method than that in [92], especially when truncation numbers M, N are large.

We remark that there are many other choices of orthogonal bases for fractional Laplacian but we won't discuss in this work due to the length limit of the paper. For Poisson equations ($\alpha = 2$), a comprehensive comparison between many basis expansions has been presented in [20]. The simplest extension from Poisson equations is to apply generalized Zernike polynomials leading to diagonal stiffness matrix while the rest of expansions leads to complicated computations of fractional Laplacian. Unfortunately, the complexity of spectral methods using the Zernike polynomials is at the order of N^3 (in storage and the amount of operations) as no fast algorithms are available, where $(N + 1)(N + 2)/2$ modes are used. Similar cost is for generalized Zernike polynomials: we need $\mathcal{O}(N^2 M)$ operations but only $\mathcal{O}(NM)$ storage as we identify the special structure of the mass matrix even when we use $(N + 1)(2M + 1)$ modes; see Section 2.4.

The rest of this paper is arranged as follows. In Section 2, we introduce some necessary notations and weighted Sobolev spaces and basic facts about the well-posedness of (1.2.1)-(1.2.2). In Section 3, we present and prove the regularity of fractional diffusion-reaction equations in weighted Sobolev spaces. In Section 4, we consider a spectral Galerkin method for (1.2.1)-(1.2.2) and prove its optimal convergence. Numerical results are shown in Section 5 to verify the theoretical convergence order before some concluding remarks and discussions on extensions of this work.

3.2 Preliminary

In this section, we present the well-posedness of the problem in non-weighted Sobolev spaces and introduce an weighted Sobolev space for our regularity analysis and error estimates.

Throughout the paper we consider the unit disk $\Omega = \{(x_1, x_2) \,|\, x_1^2 + x_2^2 < 1\}$. Let $x_1 = r \cos(\theta)$ and $x_2 = r \sin(\theta)$. Then in polar coordinate we will use (r, θ) where $\Omega = \{(r, \theta) \,|\, 0 \leq r < 1, \, 0 \leq \theta \leq 2\pi\}$. The notations C and c denote generic constants and are independent of any functions and of the truncation parameters M and N. We say that a_n is equivalent to b_n if there exist c_1 and c_2 independent of n such that $c_1 a_n \leq b_n \leq c_2 a_n$ for large n and denote them by $a_n \approx b_n$.

3.2.1 Well-posedness

We recall the standard Sobolev space $H^s(\Omega)$ (e.g. in [5]) with the semi-norm $|\cdot|_{H^s(\Omega)}$ when $0 < s < 1$, which is defined by $H^s(\Omega) = \left\{ v| \, \|v\|_{L^2(\Omega)} + |v|_{H^s(\Omega)} < \infty \right\}$, where $\|u\|_{H^{\alpha/2}(\Omega)} = (\|u\|_{L^2(\Omega)}^2 +$

$|u|^2_{H^{\alpha/2}(\Omega)})^{1/2}$ and

$$\|v\|_{L^2(\Omega)} = \left(\int_\Omega v^2(x) \, dx \right)^{1/2}, \quad \text{and } |v|_{H^s(\Omega)} = \left(\iint_{\Omega\otimes\Omega} \frac{|v(x) - v(y)|^2}{|x - y|^{2+2s}} \, dxdy \right)^{1/2}.$$

The weak formulation of the problem (1.2.1)-(1.2.2) is to find $u \in H_0^{\alpha/2}(\Omega)$, such that

$$a(u,v) := ((-\Delta)^{\alpha/2}u, v) + \mu(u,v) = (f,v), \quad \forall v \in H_0^{\alpha/2}(\Omega). \tag{3.2.1}$$

Theorem 3.2.1. *For the problem (1.2.1)-(1.2.2) with $\mu \geq 0$ and $f \in H^{-\alpha/2}(\Omega)$, there exists a unique solution $u \in H_0^{\alpha/2}(\Omega)$ such that $\|u\|_{H^{\alpha/2}(\Omega)} \leq \|f\|_{H^{-\alpha/2}(\Omega)}$, where $H^{-\alpha/2}(\Omega)$ is the dual space of $H_0^{\alpha/2}(\Omega)$ with respect to the inner product $(u,v)_{L^2(\Omega)} = \int_\Omega uv \, dx$.*

The proof of Theorem 3.2.1 is based on a fractional Hardy inequality, and integration-by-parts formula as well as Lax-Milgram Theorem. We will present the proof in Appendix 1.2.

Proposition 3.2.2 (Regularity in non-weighted Sobolev space, [57])**.** *Suppose $f \in H^s(\Omega)$ for $s \geq -\alpha/2$ and $u \in H^{\alpha/2}(\Omega)$ be the solution of the problem (1.2.1)-(1.2.2) with $\mu \geq 0$. Then $u \in H^{\alpha+\min(1/2-\alpha/2-\epsilon,s)}(\Omega)$ with $\epsilon > 0$ arbitrarily small.*

The proof is based on the boostrapping technique and the regularity estimate in [46, 75] where $\mu = 0$.

3.2.2 Weighted Sobolev spaces

We introduce weighted Sobolev spaces which we use extensively in this work. The weighted space $L^2_\beta(\Omega)$ is endowed with the inner product and the associated norm $\|\cdot\|_{L^2_\beta(\Omega)}$ as follows.

$$(u,v)_\beta = \int_\Omega u(x)v(x)(1-|x|^2)^\beta \, dx, \quad \|u\|^2_{L^2_\beta(\Omega)} = (u,u)_\beta, \tag{3.2.2}$$

where $x = (x_1, x_2)$ and $|x|^2 = x_1^2 + x_2^2$. When $\beta = 0$, we omit the subscript, e.g. $(u,v) = \int_\Omega u(x)v(x) \, dx$ and $\|u\|^2 = (u,u)$.

Let $P_n^{\beta,m}$ be conventional notation for the Jacobi polynomials; see Appendix B. In the disk, one complete orthogonal basis in $L^2_\beta(\Omega)$ ([66, 91]) is

$$\{\cos(m\theta)Q_n^{\beta,m}(r), \sin(m\theta)Q_n^{\beta,m}(r)\}, \qquad Q_n^{\beta,m}(r) := r^m P_n^{\beta,m}(2r^2 - 1). \tag{3.2.3}$$

Then $v \in L^2_\beta(\Omega)$ can be written as

$$v = \sum_{m=0}^\infty \sum_{n=0}^\infty (a_{m,n}^\beta \cos(m\theta) + b_{m,n}^\beta \sin(m\theta))Q_n^{\beta,m}(r). \tag{3.2.4}$$

where

$$a_{m,n}^\beta = \frac{1}{h_{m,n}^\beta} \int_0^{2\pi} \int_0^1 v\cos(m\theta)Q_n^{\beta,m}(r)(1-r^2)^\beta r dr d\theta, \tag{3.2.5}$$

$$b_{m,n}^\beta = \frac{1}{h_{m,n}^\beta} \int_0^{2\pi} \int_0^1 v\sin(m\theta)Q_n^{\beta,m}(r)(1-r^2)^\beta r dr d\theta, \tag{3.2.6}$$

and $h_{m,n}^{\beta}$ is a normalized constant

$$h_{m,n}^{\beta} = \int_0^{2\pi} \int_0^1 (\cos(m\theta)Q_n^{\beta,m}(r))^2(1-r^2)^{\beta}rdrd\theta. \tag{3.2.7}$$

Introduce the anisotropic weighted space $\mathbf{B}_{\beta}^{s_1,s_2}(\Omega)$ for any $s_1, s_2 > 0$ as

$$\mathbf{B}_{\beta}^{s_1,s_2}(\Omega) := \left\{ v \,|\, v \in L_{\beta}^2(\Omega) \text{ and } |v|_{\mathbf{B}_{\beta}^{s_1,s_2}(\Omega)} < \infty \right\}, \tag{3.2.8}$$

where the semi-norm $|\cdot|_{\mathbf{B}_{\beta}^{s_1,s_2}(\Omega)}$ is given by

$$|v|^2_{\mathbf{B}_{\beta}^{s_1,s_2}(\Omega)} = \sum_{m=0}^{\infty}\sum_{n=0}^{\infty}(m^{2s_1} + n^{2s_2})(|a_{m,n}^{\beta}|^2 + |b_{m,n}^{\beta}|^2)h_{m,n}^{\beta}. \tag{3.2.9}$$

The norm in this space is defined for any $s_1, s_2 > 0$ as $\|\cdot\|_{\mathbf{B}_{\beta}^{s_1,s_2}(\Omega)}$, i.e.,

$$\|v\|^2_{\mathbf{B}_{\beta}^{s_1,s_2}(\Omega)} = \sum_{m=0}^{\infty}\sum_{n=0}^{\infty}(1 + m^{2s_1} + n^{2s_2})(|a_{m,n}^{\beta}|^2 + |b_{m,n}^{\beta}|^2)h_{m,n}^{\beta}. \tag{3.2.10}$$

The weighted space (3.2.8) is well-defined and independent of choices of bases. In fact, the weighted space can be characterized by the one defined only through derivatives. We will show that the weighted space (3.2.8) is equivalent to the weighted Sobolev space $\mathbf{H}_{*,\beta}^s$ introduced in [65]. The space $\mathbf{H}_{*,\beta}^s$ is defined as

$$\mathbf{H}_{*,\beta}^s = \left\{ u \in L_{\omega^{\beta}}^2(\Omega) \,|\, \sum_{|\mathbf{k}|=s} \binom{s}{\mathbf{k}} \left\| \partial_{x_1}^{k_1}\partial_{x_2}^{k_2}(x_1\partial_{x_2} - x_2\partial_{x_1})^{k_3} u \right\|_{L_{\beta+k_1+k_2}^2} < \infty \right\}, \tag{3.2.11}$$

where s is an integer. For example, when $s = 1$, we have

$$\mathbf{H}_{*,\beta}^1 = \left\{ u \in L_{\beta}^2(\Omega)|\partial_{x_1}u, \partial_{x_2}u \in L_{\beta+1}^2(\Omega), x_2\partial_{x_1}u - x_1\partial_{x_2}u \in L_{\beta}^2(\Omega) \right\}. \tag{3.2.12}$$

The proof of equivalence of these two spaces will be presented in Appendix .8, where $s_1 = s_2 = s$ are positive integers.

In Table 3.2, we present some functions with corresponding regularity indexes s_1 and s_2 for space $\mathbf{B}_{\alpha/2}^{s_1,s_2}(\Omega)$ and s for $\mathbf{H}_{*,\alpha/2}^s(\Omega)$. We are not aware of any calculations of regularity indexes of these functions even for the integer-order problems ($\alpha = 2$) in the literature. We present the details of calculations in Appendix .4-.5 for interested readers, except for the function $\sin(x_1)+2x_2$, whose regularity can be readily checked from the definition (3.2.11). It can be readily shown that the functions in Table 3.2 have the regularity index $s = \min(s_1, s_2)$. Here we use the classical space interpolation theory [85] to extend the definition (3.2.11) for any $s > 0$ and we omit the details of calculations.

Remark 3.2.3. *The use of the space $\mathbf{B}_{\alpha/2}^{s_1,s_2}(\Omega)$ is informative for computations as it is defined through its expansion coefficients which are computed in practice. When $s_1 \gg s_2$, it suggests that much fewer modes in θ may be used than in the radial direction to achieve a given accuracy. For example, the function $(1-r^2)^{-0.4}\sin(x_1)$ is analytic in θ and thus the approximation of such a function will require only a few modes in θ while it is not straightforward to acquire such information in $\mathbf{H}_{*,\alpha/2}^s(\Omega)$.*

However, when s is small, the calculation of indexes might be simpler using the space $\mathbf{H}_{*,\alpha/2}^s(\Omega)$ as only derivatives in x_1, x_2 are involved. The use of two spaces depends on the forms of functions.

Table 3.2: Regularity indexes of functions $f(x_1, x_2)$ in two different spaces. Here $\epsilon > 0$ is an arbitrarily small number.

$f(x_1, x_2)$	$\sin(x_1) + 2x_2$	$|x_1|^3 + x_2$	$|r^2 - 0.25|\sin(x_1)$	$(1 - r^2)^{-0.4}\sin(x_1)$
(s_1, s_2) for $\mathbf{B}_{\alpha/2}^{s_1, s_2}(\Omega)$	(∞, ∞)	$(3.5 - \epsilon, 3.5 - \epsilon)$	$(\infty, 1.5 - \epsilon)$	$(\infty, \alpha/2 + 0.2)$
s for $\mathbf{H}_{*,\alpha/2}^s(\Omega)$	∞	$3.5 - \epsilon$	$1.5 - \epsilon$	$\alpha/2 + 0.2$

3.3 Regularity of the solution in weighted Sobolev spaces

In this section, we present our regularity results in weighted Sobolev spaces and their proofs.

The following *pseudo-eigenfunctions* for the fractional Laplacian in [37] are essential to analyze the regularity.

Lemma 3.3.1 ([37]). *It holds that*

$$(-\Delta)^{\alpha/2}[\cos(m\theta)Q_n^{\alpha/2,m}(r)(1-r^2)^{\alpha/2}] = \lambda_{n,m}^\alpha \cos(m\theta)Q_n^{\alpha/2,m}(r), \qquad (3.3.1)$$

$$(-\Delta)^{\alpha/2}[\sin(m\theta)Q_n^{\alpha/2,m}(r)(1-r^2)^{\alpha/2}] = \lambda_{n,m}^\alpha \sin(m\theta)Q_n^{\alpha/2,m}(r), \qquad (3.3.2)$$

where $m, n = 0, 1, \ldots$, $Q_n^{\alpha/2,m}(r) = r^m P_n^{\alpha/2,m}(2r^2 - 1)$ and $\lambda_{n,m}^\alpha = \frac{2^\alpha \Gamma(\alpha/2+n+1)\Gamma(\alpha/2+n+m+1)}{n!\Gamma(n+m+1)}$.

The functions $Q_n^{\alpha/2,m}(r)\cos(m\theta)$ and $Q_n^{\alpha/2,m}(r)\sin(m\theta)$ are known as the generalized Zernike or disc polynomials [91].

We first consider the regularity of solution to the fractional Poisson problem (1.2.1)-(1.2.2) with $\mu = 0$ in weighted Sobolev spaces. We can obtain full regularity for the solution $\tilde{u} = (1 - r^2)^{-\alpha/2}u$ instead of u, as stated in the following theorem.

Theorem 3.3.2. *For the problem (1.2.1)-(1.2.2) with $\mu = 0$, if $f \in \mathbf{B}_{\alpha/2}^{s_1, s_2}(\Omega) \cap H^{-\alpha/2}(\Omega)$ with $s_1, s_2 \geq 0$, then $(1 - r^2)^{-\alpha/2}u \in \mathbf{B}_{\alpha/2}^{s_1+\alpha/2, s_2+\alpha}(\Omega)$.*

Proof For $f \in \mathbf{B}_{\alpha/2}^{s_1, s_2}(\Omega)$, we write

$$f = \sum_{m=0}^\infty \sum_{n=0}^\infty \left(f_{m,n}^{(1)}\cos(m\theta) + f_{m,n}^{(2)}\sin(m\theta) \right) Q_n^{\alpha/2,m}(r). \qquad (3.3.3)$$

Then by the norm (3.2.10), we have

$$\|f\|_{\mathbf{B}_{\alpha/2}^{s_1,s_2}(\Omega)}^2 = \sum_{m=0}^\infty \sum_{n=0}^\infty (1 + m^{2s_1} + n^{2s_2})(|f_{m,n}^{(1)}|^2 + |f_{m,n}^{(2)}|^2)h_{m,n}^{\alpha/2} < \infty. \qquad (3.3.4)$$

For $f \in H^{-\alpha/2}(\Omega)$, we know $u \in H_0^{\alpha/2}(\Omega)$ from Lemma 3.2.1. By the fractional Hardy inequality (1.2.4), we have $(1 - r^2)^{-\alpha/2}u \in L_{\alpha/2}^2(\Omega)$. Then it is legitimate to write

$$u = (1-r^2)^{\alpha/2} \sum_{m=0}^\infty \sum_{n=0}^\infty \left(u_{m,n}^{(1)}\cos(m\theta) + u_{m,n}^{(2)}\sin(m\theta) \right) Q_n^{\alpha/2,m}(r). \qquad (3.3.5)$$

Substituting (3.3.3) and (3.3.5) into Equation (1.2.1), and using Lemma 3.3.1 gives

$$u_{m,n}^{(1)} = f_{m,n}^{(1)}/\lambda_{m,n}^{\alpha}, \quad u_{m,n}^{(2)} = f_{m,n}^{(2)}/\lambda_{m,n}^{\alpha}. \tag{3.3.6}$$

Denote $\tilde{u} = (1 - r^2)^{-\alpha/2}u$. It follows from (3.3.4)-(3.3.6) and the norm (3.2.10) that

$$
\begin{aligned}
\|\tilde{u}\|_{\mathbf{B}_{\alpha/2}^{s_1+\alpha/2,s_2+\alpha}(\Omega)}^2 &= \sum_{m=0}^{\infty}\sum_{n=0}^{\infty}(1 + m^{2s_1+\alpha} + n^{2s_2+2\alpha})(|u_{m,n}^{(1)}|^2 + |u_{m,n}^{(2)}|^2)h_{m,n}^{\alpha/2} \\
&= \sum_{m=0}^{\infty}\sum_{n=0}^{\infty}\left[(1 + m^{2s_1+\alpha} + n^{2s_2+2\alpha})/(\lambda_{m,n}^{\alpha})^2\right](|f_{m,n}^{(1)}|^2 + |f_{m,n}^{(2)}|^2)h_{m,n}^{\alpha/2}.
\end{aligned}
\tag{3.3.7}
$$

Using the following asymptotic formula for a ratio of two gamma functions

$$\lim_{n\to\infty}\frac{\Gamma(n+\delta)}{n^{\delta-\gamma}\Gamma(n+\gamma)} = \lim_{n\to\infty}\left[1 + \frac{(\delta-\gamma)(\delta+\gamma-1)}{2n} + \mathcal{O}(n^{-2})\right] = 1, \tag{3.3.8}$$

we have the asymptotic estimate

$$\lambda_{n,m}^{\alpha} \approx n^{\alpha/2}(n+m)^{\alpha/2}. \tag{3.3.9}$$

Substituting (3.3.9) into (3.3.7), we obtain

$$\|\tilde{u}\|_{\mathbf{B}_{\alpha/2}^{s_1+\alpha/2,s_2+\alpha}(\Omega)}^2 \leq C\sum_{m=0}^{\infty}\sum_{n=0}^{\infty}(1 + m^{2s_1} + n^{2s_2})(|f_{m,n}^{(1)}|^2 + |f_{m,n}^{(2)}|^2)h_{m,n}^{\alpha/2} < \infty. \tag{3.3.10}$$

This completes the proof. □

However, the property of full regularity in above theorem does not hold for the equation (1.2.1)-(1.2.2) when $\mu > 0$. The loss of full regularity is similar to that in 1D [57, 93].

Theorem 3.3.3 (Regularity in weighted Sobolev spaces). *For the problem (1.2.1)-(1.2.2) with $\mu > 0$, and $f \in \mathbf{B}_{\alpha/2}^{s_1,s_2}(\Omega) \cap H^{-\alpha/2}(\Omega)$ with $s_1, s_2 \geq 0$, we have for any arbitrarily small $\epsilon > 0$ that*

$$(1 - r^2)^{-\alpha/2}u \in \mathbf{B}_{\alpha/2}^{s_1+\alpha/2,\min(s_2,3\alpha/2+1-\epsilon)+\alpha}(\Omega).$$

Before presenting the proof, we need one technical lemma, which plays an essential role in the analysis of regularity for the equation (1.2.1)-(1.2.2) when $\mu \neq 0$. The proof of this lemma is given in Appendix .3.

Lemma 3.3.4. *If $v \in \mathbf{B}_{\alpha/2}^{s_1,s_2}(\Omega)$ with $s_1, s_2 \geq 0$, then $(1 - r^2)^{\alpha/2}v \in \mathbf{B}_{\alpha/2}^{s_1,\min(s_2,3\alpha/2+1-\epsilon)}(\Omega)$ with $\epsilon > 0$.*

Proof of Theorem 3.3.3. Denote $a \wedge b = \min(a,b)$ and $\tilde{u} = (1 - r^2)^{-\alpha/2}u$. We use the bootstrapping technique to prove this theorem. First, by Theorem 3.2.2, we have $u \in L_{\alpha/2}^2(\Omega)$. Then it follow that $\tilde{f} = f - \mu u \in \mathbf{B}_{\alpha/2}^{0,0}(\Omega)$. Using the conclusion without a reaction term in Theorem 3.3.2 and $(-\Delta)^{\alpha/2}u = \tilde{f}$, we have $\tilde{u} \in \mathbf{B}_{\alpha/2}^{s_1\wedge 0+\alpha/2,s_2\wedge 0+\alpha}(\Omega)$. Then by Lemma 3.3.4, we have $u \in \mathbf{B}_{\alpha/2}^{s_1\wedge 0+\alpha/2,s_2\wedge 0+\alpha}(\Omega)$. Repeating the above procedure if $s_1, s_2 > 0$, we then have $\tilde{f} = f - \mu u \in \mathbf{B}_{\alpha/2}^{s_1\wedge\alpha/2,s_2\wedge\alpha}(\Omega)$ and thus by Theorem 3.3.2 and $(-\Delta)^{\alpha/2}u = \tilde{f}$, we obtain $\tilde{u} \in$

$\mathbf{B}_{\alpha/2}^{s_1 \wedge \alpha/2 + \alpha/2, s_2 \wedge \alpha + \alpha}(\Omega)$. If we further have $s_1 \geq \alpha/2$ and $s_2 \geq \alpha$, we repeat the above procedure again and obtain $\tilde{u} \in \mathbf{B}_{\alpha/2}^{s_1 \wedge \alpha + \alpha/2, s_2 \wedge 2\alpha + \alpha}(\Omega)$. If $s_2 \geq 2\alpha$, we can lift the regularity further to $\tilde{u} \in \mathbf{B}_{\alpha/2}^{s_1 \wedge \alpha + \alpha/2, s_2 \wedge (3\alpha/2 + 1 - \epsilon) + \alpha}(\Omega)$ by using Lemma 3.3.4. If s_1 is large enough, we can repeat the above procedure k times and obtain $\tilde{u} \in \mathbf{B}_{\alpha/2}^{s_1 \wedge k\alpha/2 + \alpha/2, s_2 \wedge (3\alpha/2 + 1 - \epsilon) + \alpha}(\Omega)$ until $k \geq 2s_1/\alpha$. Then by Lemma 3.3.4, we get the desired conclusion. □

3.4 Error estimate of spectral Galerkin method

In this section, we consider a spectral Galerkin method and carry out its error analysis based on the obtained regularity in Section 3.3 .

We first present the spectral Galerkin method using the basis from the pseudo-eigenfunction in Lemma 3.3.1. Define the finite dimensional space

$$U_{M,N} := \text{Span}\{(1-r^2)^{\alpha/2} \cos(m\theta) Q_n^{\alpha/2,m}(r), (1-r^2)^{\alpha/2} \sin(m\theta) Q_n^{\alpha/2,m}(r), 0 \leq m \leq M, 0 \leq n \leq N\},$$

where $Q_n^{\alpha/2,m}(r)$'s are from Lemma 3.3.1. The spectral Galerkin method is to find $u_{M,N} \in U_{M,N}$ such that

$$a(u_{M,N}, v_{M,N}) = (f, v_{M,N}), \quad \forall v_{M,N} \in U_{M,N}, \tag{3.4.1}$$

with $a(u_{M,N}, v_{M,N}) := ((-\Delta)^{\alpha/2} u_{M,N}, v_{M,N}) + \mu(u_{M,N}, v_{M,N})$.

The well-posedness of the discrete problem (3.4.1) can be readily shown by Lax-Milgram's Theorem as in the proof of Theorem 3.2.1 and is thus omitted here. The implementation of this method will be described in Section 3.5.

Introduce the projection $\Pi_{M,N}^{\alpha/2} : L_{-\alpha/2}^2(\Omega) \to U_{M,N}$ such that for $v \in L_{-\alpha/2}^2(\Omega)$,

$$\Pi_{M,N}^{\alpha/2} v = (1-r^2)^{\alpha/2} \sum_{m=0}^{M} \sum_{n=0}^{N} \left[v_{m,n}^{(1)} \cos(m\theta) + v_{m,n}^{(2)} \sin(m\theta) \right] Q_n^{\alpha/2,m}(r), \tag{3.4.2}$$

where $u_{m,n}^{(1)}$'s and $u_{m,n}^{(2)}$'s are the expansion coefficients as in (3.2.5) and (3.2.6) respectively. The error estimates of the projection $\Pi_{M,N}^{\alpha/2} v$ are stated in the following lemmas.

Lemma 3.4.1. Let $(1-r^2)^{-\alpha/2} v \in \mathbf{B}_{\alpha/2}^{s_1,s_2}(\Omega)$ with $s_1, s_2 \geq 0$. Then we have the following estimate

$$\|v - \Pi_{M,N}^{\alpha/2} v\|_{L_{-\alpha/2}^2(\Omega)} \leq (M^{-s_1} + N^{-s_2}) |(1-r^2)^{-\alpha/2} v|_{\mathbf{B}_{\alpha/2}^{s_1,s_2}(\Omega)}. \tag{3.4.3}$$

Proof. Let v be of the form (3.3.5). By the orthogonality of generalized Zernike polynomials and

39

completeness of basis functions in $L^2_{\alpha/2}(\Omega)$, we have

$$\|v - \Pi^{\alpha/2}_{M,N} v\|^2_{L^2_{-\alpha/2}(\Omega)}$$

$$= \|(\sum_{m=0}^{\infty}\sum_{n=0}^{\infty} - \sum_{m=0}^{M}\sum_{n=0}^{N})[v^{(1)}_{m,n}\cos(m\theta) + v^{(2)}_{m,n}\sin(m\theta)]Q^{\alpha/2,m}_n(r)\|^2_{L^2_{\alpha/2}(\Omega)}$$

$$= (\sum_{m=M+1}^{\infty}\sum_{n=0}^{\infty} + \sum_{m=0}^{\infty}\sum_{n=N+1}^{\infty} - \sum_{m=M+1}^{\infty}\sum_{n=N+1}^{\infty})(|v^{(1)}_{m,n}|^2 + |v^{(2)}_{m,n}|^2)h^{\alpha/2}_{m,n}$$

$$\leq (\sum_{m=M+1}^{\infty}\sum_{n=0}^{\infty} + \sum_{m=0}^{\infty}\sum_{n=N+1}^{\infty})(|v^{(1)}_{m,n}|^2 + |v^{(2)}_{m,n}|^2)h^{\alpha/2}_{m,n}.$$

Using the facts

$$M^{2s_1} \leq m^{2s_1} + n^{2s_2}, \quad m \geq M+1, n \geq 0,$$
$$N^{2s_2} \leq m^{2s_1} + n^{2s_2}, \quad m \geq 0, n \geq N+1,$$

we have

$$\|v - \Pi^{\alpha/2}_{M,N} v\|^2_{L^2_{-\alpha/2}(\Omega)} \leq (M^{-2s_1} + N^{-2s_2})\sum_{m=0}^{\infty}\sum_{n=0}^{\infty}(m^{2s_1} + n^{2s_2})(|v^{(1)}_{m,n}|^2 + |v^{(2)}_{m,n}|^2)h^{\alpha/2}_{m,n}. \quad (3.4.4)$$

Using the definition of the semi-norm (3.2.9) immediately leads to the desired result. $\qquad\square$

Lemma 3.4.2. Let $(1-r^2)^{-\alpha/2}v \in \mathbf{B}^{s_1+\alpha/2,s_2+\alpha/2}_{\alpha/2}(\Omega)$ with $s_1, s_2 \geq 0$. Then we have the following estimate

$$|v - \Pi^{\alpha/2}_{M,N}v|_{H^{\alpha/2}(\Omega)} \leq (M^{-s_1} + N^{-s_2})|(1-r^2)^{-\alpha/2}v|_{\mathbf{B}^{s_1+\alpha/2,s_2+\alpha/2}_{\alpha/2}(\Omega)}. \quad (3.4.5)$$

Proof. By Lemmas 1.2.3 and 3.3.1, we have

$$|v - \Pi^{\alpha/2}_{M,N}v|^2_{H^{\alpha/2}(\Omega)} \approx ((-\Delta)^{\alpha/2}(v - \Pi^{\alpha/2}_{M,N}v), v - \Pi^{\alpha/2}_{M,N}v)$$

$$\leq (\sum_{m=M+1}^{\infty}\sum_{n=0}^{\infty} + \sum_{m=0}^{\infty}\sum_{n=N+1}^{\infty})\lambda^{\alpha}_{n,m}(|v^{(1)}_{m,n}|^2 + |v^{(2)}_{m,n}|^2)h^{\alpha/2}_{m,n}.$$

Similar to the derivation of (3.4.4), we have

$$|v - \Pi^{\alpha/2}_{M,N}v|^2_{H^{\alpha/2}(\Omega)} \leq (M^{-2s_1} + N^{-2s_2})\sum_{m=0}^{\infty}\sum_{n=0}^{\infty}\lambda^{\alpha}_{m,n}(m^{2s_1} + n^{2s_2})(|v^{(1)}_{m,n}|^2 + |v^{(2)}_{m,n}|^2)h^{\alpha/2}_{m,n}.$$

Using the estimate (3.3.9) and the semi-norm (3.2.9) leads to (3.4.5). $\qquad\square$

We are in position to state the convergence order of spectral Galerkin method (3.4.1).

Theorem 3.4.3 (Optimal convergence order). *Suppose that u and $u_{M,N}$ satisfy the problems (3.2.1) and (3.4.1), respectively. If $f \in \mathbf{B}_{\alpha/2}^{s_1,s_2}(\Omega) \cap H^{-\alpha/2}(\Omega)$ with $s_1, s_2 \geq 0$, we have the following error estimates*

$$\|u - u_{M,N}\|_{L_{-\alpha/2}^2(\Omega)} \leq c(M^{-\gamma_1} + N^{-\gamma_2})|(1 - r^2)^{-\alpha/2}u|_{\mathbf{B}_{\alpha/2}^{\gamma_1,\gamma_2}(\Omega)}, \qquad (3.4.6)$$

$$\|u - u_{M,N}\|_{H^{\alpha/2}(\Omega)} \leq c(M^{\alpha/2-\gamma_1} + N^{\alpha/2-\gamma_2})|(1 - r^2)^{-\alpha/2}u|_{\mathbf{B}_{\alpha/2}^{\gamma_1,\gamma_2}(\Omega)}, \qquad (3.4.7)$$

where $\gamma_1 = s_1 + \alpha/2$ and $\gamma_2 = \alpha + \min(3\alpha/2 + 1 - \epsilon, s_2)$ with arbitrarily small $\epsilon > 0$.

Proof. Denote $u - u_{M,N} = \eta + e$ with $\eta = u - \Pi_{M,N}^{\alpha/2}u$ and $e = \Pi_{M,N}^{\alpha/2}u - u_{M,N}$. By (3.2.1) and (3.4.1), we have

$$a(u - u_{M,N}, v) = 0, \quad \forall v \in U_{M,N}.$$

It follows that

$$a(e, v) = -a(\eta, v), \quad \forall v \in U_{M,N}.$$

Taking $v = e$ and using the fractional Hardy inequality (1.2.4) lead to

$$c\|e\|_{L_{-\alpha/2}^2(\Omega)}^2 \leq \|e\|_{H^{\alpha/2}(\Omega)}^2 \leq a(e, e) = -a(\eta, e) = -((-\Delta)^{\alpha/2}\eta, e) - \mu(\eta, e). \qquad (3.4.8)$$

By Lemma 3.3.1 and the orthogonality property of the basis, we have

$$((-\Delta)^{\alpha/2}\eta, v) = 0, \quad \forall v \in U_{M,N}.$$

Hence we can obtain from (3.4.8) that

$$c\|e\|_{L_{-\alpha/2}^2(\Omega)}^2 \leq -\mu(\eta, e) \leq |\mu|\|\eta\|_{L_{-\alpha/2}^2(\Omega)}\|e\|_{L_{\alpha/2}^2(\Omega)} \leq |\mu|\|\eta\|_{L_{-\alpha/2}^2(\Omega)}\|e\|_{L_{-\alpha/2}^2(\Omega)},$$

where we have used the Cauchy-Schwarz inequality and the definition (3.2.2). Thus we have

$$c\|e\|_{L_{-\alpha/2}^2(\Omega)} \leq |\mu|\|\eta\|_{L_{-\alpha/2}^2(\Omega)}, \quad \|u - u_{M,N}\|_{L_{-\alpha/2}^2(\Omega)} \leq (1 + |\mu|/c)\|\eta\|_{L_{-\alpha/2}^2(\Omega)}.$$

Using the approximation property in Lemma 3.4.1 and the regularity estimate in Theorem 3.3.3, we get (3.4.6). The estimate (3.4.7) in the energy norm can be similarly proved and omitted here. This completes the proof. $\qquad \square$

Remark 3.4.4. *In the proof, we have used the fractional Hardy inequality which requires $\alpha \in (1,2)$ to show the strong error estimate in negative weighted L^2 norm. If we use the well-known fractional Poincare inequality $c\|e\|_{L^2(\Omega)} \leq \|e\|_{H^{\alpha/2}(\Omega)}$, we can relax the assumption $\alpha \in (1,2)$ to $\alpha \in (0,2)$. We then can get the optimal error estimate in the L^2-norm when $\alpha \in (0,2)$: $\|e\|_{L^2(\Omega)} \leq |\mu|/c\|\eta\|_{L^2(\Omega)}$ and thus*

$$\|u - u_{M,N}\|_{L^2(\Omega)} \leq (1 + |\mu|/c)\|\eta\|_{L^2(\Omega)} \leq (1 + |\mu|/c)\|\eta\|_{L_{-\alpha/2}^2(\Omega)} \leq C(M^{\alpha/2-\gamma_1} + N^{\alpha/2-\gamma_2}).$$

3.5 Numerical experiments

In this section, we discuss the implementation of the spectral Galerkin method (3.4.1) and present four numerical examples, which verify our error estimates in Theorem 3.4.3.

3.5.1 Implementation of the spectral Galerkin method

For linear problem (3.4.1), plug $u_{M,N} = \sum_{m=0}^{M} \sum_{n=0}^{N} [u_{m,n}^{(1)} \phi_{m,n}^{(1)} + u_{m,n}^{(2)} \phi_{m,n}^{(2)}] \in U_{M,N}$ into (3.4.1) and take $v_{M,N} = \phi_{m,n}^{(i)}(x)$ for $i = 1, 2$, $m = 0, 1, \ldots M$ and $n = 0, 1, \ldots, N$, where

$$\phi_{m,n}^{(1)}(r, \theta) := (1 - r^2)^{\alpha/2} \cos(m\theta) Q_n^{\alpha/2,m}(r), \quad \phi_{m,n}^{(2)}(r, \theta) := (1 - r^2)^{\alpha/2} \sin(m\theta) Q_n^{\alpha/2,m}(r).$$

By the orthogonality of $\cos(m\theta)$ and $\sin(m\theta)$ in $L^2([0, 2\pi])$, the resulting linear system can be represented as

$$S_m^{(i)} U_m^{(i)} + \mu M_m^{(i)} U_m^{(i)} = F_m^{(i)}, \tag{3.5.1}$$

where $U_m^{(i)} = (u_{m,0}^{(i)}, u_{m,1}^{(i)}, \ldots, u_{m,N}^{(i)})^T$, $0 \le m \le M$ for $i = 1, 2$. The matrices $S_m^{(i)}$, $M_m^{(i)}$ and $F_m^{(i)}$ will be elaborated in the following.

The stiffness matrix $(S_m^{(i)})_{k,n}$ in (6.1.28) are diagonal matrix. By the orthogonality of Jacobi polynomials and Lemma 3.3.1, we have

$$(S_m^{(1)})_{k,n} = ((-\Delta)^{\alpha/2} \phi_{m,n}^{(1)}, \phi_{m,k}^{(1)}) = (\frac{1}{2})^{\alpha/2+m+2} \pi \lambda_{m,n}^{\alpha} h_n^{\alpha/2,m} \delta_{k,n} \delta_m, \quad 0 \le m \le M,$$

where $\delta_{k,n} = 1$ if $k = n$ and 0 otherwise; $\delta_0 = 2$ and $\delta_m = 1$ for $m \ge 1$; $h_n^{\alpha/2,m}$ is defined in (6.1.5) and $\lambda_{m,n}^{\alpha}$ from Lemma 3.3.1. More precisely we have

$$(S_m^{(1)})_{k,n} = \frac{2^{\alpha-1}\pi}{2n + \alpha/2 + m + 1} \left(\frac{\Gamma(1 + \alpha/2 + n)}{\Gamma(n+1)} \right)^2 \delta_{k,n} \delta_m, \quad 0 \le m \le M.$$

Similarly, $(S_m^{(2)})_{k,n} = ((-\Delta)^{\alpha/2} \phi_{m,n}^{(2)}, \phi_{m,k}^{(2)})$ and we have $S_m^{(1)} = S_m^{(2)}$ for $1 \le m \le M$.

We now turn to the right hand side $F_m^{(i)}$. Letting $f = f(r, \theta)$, we have

$$\begin{aligned}
(F_m^{(1)})_k &= \int_0^{2\pi} \int_0^1 f(r, \theta) \cos(m\theta) Q_k^{\alpha/2,m}(r)(1 - r^2)^{\alpha/2} r \, dr \, d\theta \tag{3.5.2} \\
&= \int_0^{2\pi} \int_{-1}^1 G_{m,k}(t, \theta) \cos(m\theta) \omega^{\alpha/2,1}(t) \, dt \, d\theta,
\end{aligned}$$

where $G_{m,k}(t, \theta) = \frac{1}{2^{\alpha+2}} f((1+t)/2, \theta) \hat{Q}_k^{\alpha/2,m}(t)(3+t)^{\alpha/2}$ and $\omega^{\alpha/2,1}(t) = (1-t)^{\alpha/2}(1+t)$. Here

$$\hat{Q}_n^{\alpha/2,m}(t) = Q_n^{\alpha/2,m}(\frac{1+t}{2})$$

can be obtained by the following recurrence relations (see also [87]):

$$\begin{aligned}
\hat{Q}_{n+1}^{\alpha/2,m}(t) &= \left(a_n^{\alpha/2,m}(\frac{(1+t)^2}{2} - 1) - b_n^{\alpha/2,m} \right) \hat{Q}_{n+1}^{\alpha/2,m}(t) - c_n^{\alpha/2,m} \hat{Q}_{n-1}^{\alpha/2,m}(t), \\
\hat{Q}_0^{\alpha/2,m}(t) &= (\frac{1+t}{2})^m, \\
\hat{Q}_1^{\alpha/2,m}(t) &= (\frac{1+t}{2})^m \left(\frac{1}{2}(\alpha/2 + m + 2)(\frac{(1+t)^2}{2} - 1) + \frac{1}{2}(\alpha/2 - m) \right),
\end{aligned}$$

where

$$a_n^{\alpha/2,m} = \frac{(2n+\alpha/2+m+1)(2n+\alpha/2+m+2)}{2(n+1)(n+\alpha/2+m+1)},$$

$$b_n^{\alpha/2,m} = \frac{(m^2-(\alpha/2)^2)(2n+\alpha/2+m+1)}{2(n+1)(n+\alpha/2+m+1)(2n+\alpha/2+m)},$$

$$c_n^{\alpha/2,m} = \frac{(n+\alpha/2)(n+m)(2n+\alpha/2+m+2)}{(n+1)(n+\alpha/2+m+1)(2n+\alpha/2+m)}.$$

To find $(F_m^{(1)})_k$, we use a Gauss-Jacobi quadrature rule in t direction and rectangular rule in θ direction: $(F_m^{(1)})_k \approx \frac{2\pi}{\mathsf{M}} \sum_{k=0}^{\mathsf{M}-1} \sum_{j=0}^{\mathsf{N}} G_{m,k}(t_j, \theta_k) \cos(m\theta_k) \mathsf{w}_j$. Here t_j's are the roots of Jacobi polynomial $P_{\mathsf{N}+1}^{\alpha/2,1}(t)$, w_j's are the corresponding quadrature weights, and $\theta_k = \frac{2\pi k}{\mathsf{M}}$ for $k = 1, 2 \ldots, \mathsf{M}-1$. The right hand side $(F_m^{(2)})_k = \int_0^{2\pi} \int_0^1 f(r,\theta) \sin(m\theta) Q_k^{\alpha/2,m}(r)(1-r^2)^{\alpha/2} r dr d\theta$, can be treated similarly. In the numerical tests, we take quadrature numbers $\mathsf{N} = \max(N+60, 512)$ and $\mathsf{M} = 2(M+1)$.

Remark 3.5.1. *For small modes ($N < 1000$), we use a direct solver. For large N, we can use the classical preconditioned conjugate gradient method with the stiffness matrix $S_m^{(i)}$ as the preconditioner for each linear system in (6.1.28), which was tested but not presented here.*

The computation cost of computing right hand sides $F^{(i)}$ is $\mathcal{O}(M\log(M)N^2)$ operations as fast Fourier transforms can be applied and the iterative solver for the linear system requires the $\mathcal{O}(MN^2)$ operations.

If the right hand side f is smooth in θ direction, only a few modes with a very small M is required to achieve certain accuracy. In this case, the fast solver based on the Hankel-Toeplitz structure proposed by [84] can be used to reduce the computational cost from $\mathcal{O}(N^2)$ to $\mathcal{O}(N \log N)$.

3.5.2 Numerical results

In this section, we present four examples with different source terms f: smooth (Example 3.5.2), weakly singular at interior (Example 3.5.3), weakly singular at the interior circle (Example 3.5.4) and weakly singular at boundary (Example 3.5.5) using the implementation in Section 3.5.1. We take $\mu = 1$ and measure the errors as follows [2] [2]

$$E(M, N) = \|u_{\text{ref}} - u_{M,N}\|_{L^2_{-\alpha/2}(\Omega)} \approx \mathcal{O}(M^{-\gamma_1}) + \mathcal{O}(N^{-\gamma_2}). \tag{3.5.3}$$

Since exact solutions are unavailable, we use reference solutions u_{ref}, which are computed with a very fine resolution using the same method for computing $u_{M,N}$. In all our examples, we take $u_{\text{ref}} := u_{200,256}$, which are fine enough to observe convergence orders. When testing convergence orders in θ direction, we choose different M's in $E(M, 256)$ and vary N's in $E(200, N)$ to test convergence in the radial direction.

Example 3.5.2. *Consider $f = \sin(x_1) + 2x_2$. Here f belongs to $\mathbf{B}_{\alpha/2}^{\infty,\infty}(\Omega)$.*

By Theorem 3.3.3, $(1-r^2)^{-\alpha/2}u \in \mathbf{B}_{\alpha/2}^{\infty,5\alpha/2+1-\epsilon}(\Omega)$ for the problem (1.2.1)-(1.2.2) with $\mu = 1$. According to Theorem 3.4.3, the convergence orders in $L^2_{-\alpha/2}(\Omega)$ norm are expected to be $5\alpha/2+1-\epsilon$
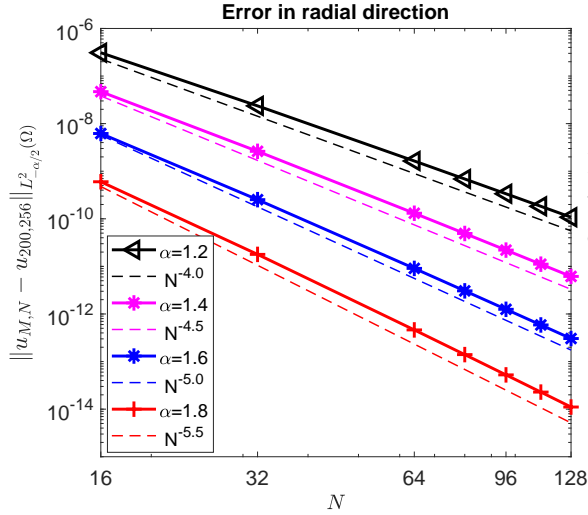
Figure 3.1: For $(-\Delta)^{\alpha/2}u + u = \sin(x_1) + 2x_2$ with u vanishing outside of Ω, the convergence order of the spectral Galerkin method (3.4.1) is $5\alpha/2 + 1 - \epsilon$ in $L^2_{-\alpha/2}(\Omega)$ norm. (c.f. Example 3.5.2)

in the radial direction, which is observed in Figure 3.1.

Example 3.5.3. *Consider* $f = |x_1|^3 + x_2$. *Here* f *belongs to* $\mathbf{B}^{3.5-\epsilon,3.5-\epsilon}_{\alpha/2}(\Omega)$ *for any* $\epsilon > 0$.

From Appendix .5, we have that $f \in \mathbf{B}^{3.5-\epsilon,3.5-\epsilon}_{\alpha/2}(\Omega)$. By Theorem 3.3.3, $(1 - r^2)^{-\alpha/2}u \in \mathbf{B}^{\alpha/2+3.5-\epsilon,\alpha+\min(3\alpha/2+1-\epsilon,3.5-\epsilon)}_{\alpha/2}(\Omega)$ for the problem (1.2.1)-(1.2.2) with $\mu = 1$. According to Theorem 3.4.3, the convergence orders are $\alpha/2 + 3.5 - \epsilon$ in θ and $\alpha + \min(3\alpha/2 + 1 - \epsilon, 3.5 - \epsilon)$ in the radial direction respectively, which can be observed from Tables 3.3-3.4. To test the convergence order in the radial direction, we fix $M = 200$ in θ and let N vary from 16 to 128. From Table 3.3, we can see the convergence order is much close to $\alpha + \min(3\alpha/2 + 1 - \epsilon, 3.5 - \epsilon)$ in the radial direction.

To test the convergence order in θ, we fix $N = 256$ and let M vary from 16 to 112. From Table 3.4, we can see that the convergence order is about $\alpha/2 + 3.5 - \epsilon$ in θ direction. All these numerical results verify the theoretical predictions in Theorem 3.4.3.

Example 3.5.4. *Consider* $f = |0.25 - r^2|\sin(x_1)$. *The function* f *has a weak singularity at internal circle* $r^2 = x_1^2 + x_2^2 = 0.25$ *and* $f \in \mathbf{B}^{\infty,1.5-\epsilon}_{\alpha/2}(\Omega)$ *for any* $\epsilon > 0$.

Using the norm (.3.2), we can verify that $f \in \mathbf{B}^{\infty,1.5-\epsilon}_{\alpha/2}(\Omega)$ for any $\epsilon > 0$. By Theorem 3.3.3, $(1 - r^2)^{-\alpha/2}u \in \mathbf{B}^{\infty,\alpha+\min(3\alpha/2+1,1.5)-\epsilon}_{\alpha/2}(\Omega)$ for the problem (1.2.1)-(1.2.2). According to Theorem 3.4.3, the convergence order in the radial direction for the spectral Galerkin method (3.4.1) is expected to be $\alpha + 1.5 - \epsilon$ in $L^2_{-\alpha/2}(\Omega)$ norm. To test the order in the radial direction, we fix $M = 200$ and let N vary from 16 to 128. From Table 3.5, we can observe that the convergence order for the spectral Galerkin method (3.4.1) is $\alpha + 1.5$, which is in agreement with the theoretical prediction.

Example 3.5.5 (Boundary singularity for the right hand side f). *Consider* $f = (1 - r^2)^{-0.4}\sin(x_1)$.

---

[22] We also measured errors in the energy semi-norm using $((-\Delta)^\alpha u_{\text{ref}} - u_{M,N}, u_{\text{ref}} - u_{M,N})$ which is equivalent to the seminorm $|u_{\text{ref}} - u_{M,N}|_{H^{\alpha/2}}$. The convergence orders in all examples match our theoretical prediction in Theorem 3.4.3. Here we will not present these results for brevity.

Table 3.3: For the diffusion-reaction equation $(-\Delta)^{\alpha/2}u + u = |x_1|^3 + x_2$ with u vanishing outside of Ω. The convergence order of the spectral Galerkin method (3.4.1) is $\alpha + (3\alpha/2 + 1 - \epsilon) \wedge (3.5 - \epsilon)$ in the radial direction using the measurement (3.5.3). Here $M = 200$ in θ direction. (c.f. Example 3.5.3)

N	$\alpha = 1.2$		$\alpha = 1.4$		$\alpha = 1.6$		$\alpha = 1.8$	
	$E(M,N)$	rate	$E(M,N)$	rate	$E(M,N)$	rate	$E(M,N)$	rate
16	8.05e-08		1.79e-08		6.76e-09		3.09e-09	
32	5.81e-09	3.79	8.43e-10	4.41	2.50e-10	4.76	1.00e-10	4.95
64	3.94e-10	3.88	3.72e-11	4.50	8.25e-12	4.92	2.90e-12	5.11
80	1.64e-10	3.92	1.35e-11	4.53	2.71e-12	4.98	9.13e-13	5.18
96	8.02e-11	3.93	5.92e-12	4.53	1.09e-12	5.01	3.53e-13	5.21
112	4.37e-11	3.95	2.94e-12	4.54	5.02e-13	5.02	1.58e-13	5.22
128	2.57e-11	3.96	1.60e-12	4.54	2.56e-13	5.04	7.84e-14	5.24
Order	(Theoretical)	4.00		4.50		5.00		5.30

Table 3.4: For the diffusion-reaction equation $(-\Delta)^{\alpha/2}u + u = |x_1|^3 + x_2$ with u vanishing outside of Ω. The convergence order of the spectral Galerkin method (3.4.1) is $\alpha/2 + 3.5$ in θ direction using the measurement (3.5.3). Here $N = 256$ in the radial direction. (c.f. Example 3.5.3)

M	$\alpha = 1.2$		$\alpha = 1.4$		$\alpha = 1.6$		$\alpha = 1.8$	
	$E(M,N)$	rate	$E(M,N)$	rate	$E(M,N)$	rate	$E(M,N)$	rate
16	2.24e-06		1.24e-06		7.82e-07		4.98e-07	
32	1.30e-07	4.10	7.23e-08	4.10	4.47e-08	4.13	2.85e-08	4.13
64	7.06e-09	4.21	4.00e-09	4.18	2.51e-09	4.15	1.65e-09	4.11
80	2.73e-09	4.26	1.55e-09	4.25	9.89e-10	4.18	6.59e-10	4.12
96	1.24e-09	4.32	7.12e-10	4.27	4.58e-10	4.22	3.07e-10	4.18
112	6.26e-10	4.45	3.70e-10	4.24	2.36e-10	4.29	1.58e-10	4.30
Order	(Theoretical)	4.10		4.20		4.30		4.40

Following the approach in [57] and the norm (.3.2), we obtain that $f \in \mathbf{B}_{\alpha/2}^{\infty,\alpha/2+0.2-\epsilon}(\Omega)$. By Theorem 3.3.3, the theoretical order for the spectral Galerkin method is $3\alpha/2 + 0.2 - \epsilon$, which is observed Figure 3.2. In this example, the observed convergence orders for Galerkin method are in accordance with the theoretical ones when f has boundary singularity. The numerical results verify the regularity estimates and also show that the error estimates for the spectral Galerkin method are optimal.

In summary, we observe in Examples 3.5.2-3.5.5 that the convergence orders of spectral Galerkin method 3.4.1 in $L^2_{-\alpha/2}(\Omega)$ norm are $\alpha/2 + s_1$ in θ and $\alpha + \min(3\alpha/2 + 1, s_2)$ in the radial direction, respectively, which verify the error estimates in Theorem 3.4.3.

3.6 Conclusion and discussion

In this paper, we study regularity and a spectral Galerkin method for a two dimensional fractional diffusion-reaction equation with fractional Laplacian. By factorizing the solution as $u = (1-r^2)^{\alpha/2}\tilde{u}$,

Table 3.5: For the diffusion-reaction equation $(-\Delta)^{\alpha/2}u + u = |0.25 - r^2|\sin(x_1)$ with u vanishing outside of Ω. The convergence order of the spectral Galerkin method (3.4.1) is $\alpha + 1.5 - \epsilon$ in the radial direction using the measurement (3.5.3). Here $M = 200$. (c.f. Example 3.5.4)

N	$\alpha = 1.2$ $E(M,N)$	rate	$\alpha = 1.4$ $E(M,N)$	rate	$\alpha = 1.6$ $E(M,N)$	rate	$\alpha = 1.8$ $E(M,N)$	rate
16	7.26e-06		3.34e-06		1.54e-06		7.08e-07	
32	1.42e-06	2.36	5.82e-07	2.52	2.40e-07	2.68	9.86e-08	2.84
64	2.25e-07	2.66	8.03e-08	2.86	2.87e-08	3.06	1.03e-08	3.26
80	1.27e-07	2.55	4.37e-08	2.73	1.50e-08	2.90	5.19e-09	3.07
96	7.84e-08	2.65	2.59e-08	2.86	8.60e-09	3.07	2.85e-09	3.28
112	5.00e-08	2.91	1.60e-08	3.12	5.16e-09	3.31	1.66e-09	3.51
128	3.50e-08	2.69	1.10e-08	2.86	3.44e-09	3.02	1.08e-09	3.19
Order	(Theoretical)	2.70		2.90		3.10		3.30
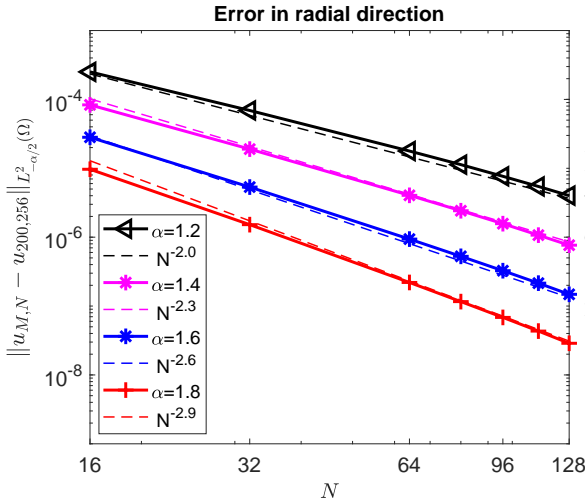
Figure 3.2: For $(-\Delta)^{\alpha/2}u + u = (1-r^2)^{-0.4}\sin(x_1)$ with u vanishing outside of Ω, the convergence order of the spectral Galerkin method (3.4.1) is $3\alpha/2 + 0.2 - \epsilon$ in the radial direction using the measurement (3.5.3). (c.f. Example 3.5.5)

we show that the regularity of solution $\tilde{u}$ in weighted Sobolev spaces can be greatly improved compared to that u in non-weighted Sobolev spaces, with the regularity index being $5\alpha/2 + 1 - \epsilon$ in radial direction when the right hand side function f is sufficiently smooth. Here $\alpha/2 \in (1/2, 1)$ is the order of fractional Laplacian and $\epsilon > 0$ is arbitrarily small. Based on the obtained regularity, we prove optimal error estimates of a spectral Galerkin method in the weighted L^2-norm and energy norm. Numerical results verify our theoretical regularity estimates and optimal convergence orders.

In our numerical experiments, we consider the examples with a constant reaction coefficient under which the resulting linear system can be reduced to independent one-dimensional equations. However, such reduction does not hold for linear equations with variable coefficients or nonlinear equations. For the large truncation numbers M and N, fast solvers with low storage are needed. The difficulty in developing fast solvers arises for the large index m in the Zernike-polynomials $Q_n^{\alpha/2,m}e^{im\theta}$, for which no fast algorithms on the balls are available though it is possible to implement fast algorithms on spheres, e.g., [80].

For future work, we will extend our spectral methods to advection-diffusion problems, e.g., fractional Burgers and Navier-Stokes equations. We are currently working on fractional diffusion-

reaction equations on general domains using domain decomposition techniques.

Chapter 4

Extensions to general domain

In this chapter [1], we will use fictitious domain technique to extend our developed finite difference and spectral methods to general domains. In Section 4.4, we will briefly recall the rationale for fictitious domain methods. In Section 4.2, to get the intuition, we will detailedly investigate the fictitious domain methods for one dimensional problems. In Section 4.3, we will discuss the fictitious domain method for higher dimensions. In the end, we will conclude the chapter with some remarks.

4.1 The rationale for fictitious domain method

Let the fictitious domain D be the unit disk, $D = \{x = (x_1, x_2) \,|\, x_1^2 + x_2^2 < 1\}$. Suppose $\Omega \subset D$ and denote $\Omega_1 = D/\Omega$.

Our approximation is not restricted to the rectangular domain and can be readily extended to other general open bounded domain using classical fictitious or extended domain techniques, to transform the original problems into the one defined on rectangular domain. More precisely, extend the domain Ω into a large rectangular one R such that $\Omega \subset R$ as illustrated in Figure 4.1.
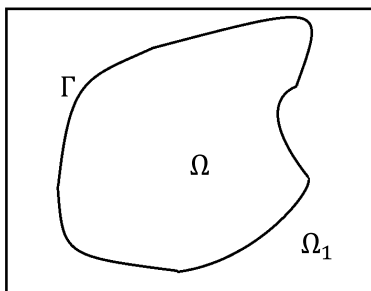
Figure 4.1: The original domain Ω and the extended rectangular domain $R = \Omega \cup \Omega_1$.

The weak formulation of the problem is to find $u \in H_0^{\alpha/2}(\Omega)$, such that

$$((-\Delta)^{\alpha/2}u, v)_\Omega = (f, v)_\Omega, \quad \forall v \in H_0^{\alpha/2}(\Omega). \tag{4.1.1}$$

Here the inner product $(u, v)_\Omega = \int_\Omega u(x)v(x)dx$, and the space $H_0^{\alpha/2}(\Omega)$ $H_0^{\alpha/2}(\Omega) = \{u : u = 0, x \in \Omega^c, u \in H^{\alpha/2}(\mathbb{R}^2)\}$.

---

[1]This chapter is based on the paper: Zhaopeng Hao, Marcus Sarkis and Zhongqiang Zhang, Spectral methods for integral fractional Laplacian on the general domain, preprint, 2019.

Denote the quadratic functional

$$J(v) = ((-\Delta)^{\alpha/2}v, v)_D - 2(\tilde{f}, v)_D$$

where $\tilde{f} \in L^2(D)$ is any extension of f into D such that

$$\tilde{f} = f \, a.e. \, x \in \Omega, \quad \|\tilde{f}\|_{L^2(D)} \leq C_{\Omega,D}\|f\|_{L^2(\Omega)}, \tag{4.1.2}$$

with a positive constant $C_{\Omega,D}$ depending only on D and Ω.

The variational formulation (4.1.1) is equivalent to the following constrained minimization problem, i.e., find $u \in H_0^{\alpha/2}(D)$ such that

$$J(u) \leq J(v), \quad \forall v \in H_0^{\alpha/2}(D), \tag{4.1.3}$$

$$\text{subject to} \quad \int_{\Omega_1} u^2 dx = 0. \tag{4.1.4}$$

For the constrained minimization problem, there are mainly two popular ways to attack it. One is Lagrange multiplier and another one is penalty method. In this paper, we take the second approach, the penalty method, which was motivated by the Babuska's seminal paper in 1973. The Penalty method was introduced by Courant (1943) in the context of the calculus of variation.

Introduce the quadratic functional

$$J_\epsilon(v) = ((-\Delta)^{\alpha/2}v, v)_D - 2(\tilde{f}, v)_D + \frac{1}{\epsilon}\int_{\Omega_1} v^2 dx,$$

where $0 < \epsilon \leq 1$ is the penalty parameter.

The approximated minimization problem to find $u_\epsilon \in H_0^{\alpha/2}(D)$ such that

$$J_\epsilon(u_\epsilon) \leq J_\epsilon(v), \quad \forall v \in H_0^{\alpha/2}(D). \tag{4.1.5}$$

It is clear that the quadratic functional $J_\epsilon(v)$ converges to $J(v)$ when ϵ goes to 0. Thus the solution of constrained minimization problem (4.1.3)-(4.1.4) can be approximated by the one of unconstrained minimization problem (4.1.5).

Then the fictitious domain formulation with L^2 penalization for (4.1.1) is to find $u_\epsilon \in H_0^{\alpha/2}(D)$, such that

$$((-\Delta)^{\alpha/2}u_\epsilon, v)_D + \frac{1}{\epsilon}(u_\epsilon, v)_{\Omega_1} = (\tilde{f}, v)_D, \quad \forall v \in H_0^{\alpha/2}(D). \tag{4.1.6}$$

In the integer case $\alpha = 2$, Saito and Zhou [76] gave the error estimates as follows

$$\|u - u_\epsilon\|_{L^2(\Omega)} \leq C\epsilon^{1/2}\|f\|_{L^2(\Omega)}. \tag{4.1.7}$$

For the fractional case $1 < \alpha < 2$, we assume that

$$\|u - u_\epsilon\|_{L^2(\Omega)} \leq C\epsilon^{\nu_\alpha}\|f\|_{L^2(\Omega)}. \tag{4.1.8}$$

where ν_α is a positive constant which depends on α, and $\nu_\alpha \to 1/2$ when $\alpha \to 2$.

Remark 4.1.1. *Unfortunately, for the time being we can not prove the error estimate since the rigorous proof will involve a lot of knowledge of partial differential equations. We will leave it as an open question and hopefully will address it in our future work.*

Remark 4.1.2. *The classical form is*

$$(-\Delta)^{\alpha/2} u_\epsilon + \frac{\chi}{\epsilon} u_\epsilon = f(x), \quad x \in D, \tag{4.1.9}$$

$$u(x) = 0, \quad x \in D^c \tag{4.1.10}$$

where the characterized function $\chi(x) = 1$ if $x \in \Omega_1$ and $\chi(x) = 0$ if $x \in \Omega$. The classical formulation can provide us a stating point to consider penalized collocation method as alternative approach to solve the original problem.

Remark 4.1.3. *The approximated L^2 formulation is unique. It is possible to consider other penalization form, e.g., the fictitious domain formulation with H^1 penalization for (4.1.1) is to find $u \in H_0^{\alpha/2}(D) \cap H_0^1(\Omega_1)$, such that*

$$((-\Delta)^{\alpha/2} u_\epsilon, v)_D + \frac{1}{\epsilon}(\nabla u_\epsilon, \nabla v)_{\Omega_1} = (\tilde{f}, v)_D, \quad \forall v \in H_0^{\alpha/2}(D) \cap H_0^1(\Omega_1). \tag{4.1.11}$$

Except for its complicate formulation, numerically it is also found that H^1 penalization formulation is not superior than the L^2 version; see Figure 4.6 for comparison.

4.2   Fictitious domain methods based on the spectral method

4.2.1   Spectral Galerkin method for 1D

Take one dimensional case defined on the domain $x \in \Omega = (-r_0, r_0)$ with $r_0 < 1$ for example. We embed the domain Ω into $\Lambda = (-1, 1)$. Then make a partition on the complement domain $\Omega_1 = \Lambda \cap \Omega^c = (-1, -r_0) \cup (r_0, 1)$.

We first present the spectral Galerkin method. According to Lemma 2.3.1, we introduce the following approximated space

$$U_N := (1 - x^2)^{\alpha/2} \mathbb{P}_N = \text{Span}\{\phi_0, \phi_1, \ldots, \phi_N\},$$

where $\phi_k(x) := (1 - x^2)^{\alpha/2} P_k^{\alpha/2, \alpha/2}(x)$ for $0 \leq k \leq N$, and $\mathbb{P}_N$ is the set of all algebraic polynomials of degree at most N. The spectral Galerkin method is to find $u_{\epsilon, N} \in U_N$ such that

$$((-\Delta)^{\alpha/2} u_{\epsilon, N}, v_N)_D + \frac{1}{\epsilon}(u_{\epsilon, N}, v_N)_{\Omega_1} = (\tilde{f}, v_N)_D, \quad \forall v_N \in U_N. \tag{4.2.1}$$

The well-posedness of discrete problem (4.2.1) can be readily shown by the Lax-Milgram theorem. We omit the statement.

We are ready to state the convergence order of the spectral Galerkin method (4.2.1).

Theorem 4.2.1. *Suppose that u_ϵ and $u_{\epsilon, N}$ satisfy the problems (4.1.6) and (4.2.1), respectively. Suppose that f satisfies the assumption (4.1.2). We have the following error estimates:*

$$\|u_\epsilon - u_{\epsilon, N}\|_{L^2(D)} \leq C_\epsilon N^{-\alpha} \|f\|_{L^2(\Omega)}, \tag{4.2.2}$$

where the constant C_ϵ depends on ϵ and $C_\epsilon \to \infty$ as $\epsilon \to 0$.

The proof is similar as [57], here we skip it.

Combining (4.1.7) and (4.2.2), we have

$$
\begin{aligned}
\|u - u_{\epsilon,N}\|_{L^2(\Omega)} &\leq \|u - u_{\epsilon,N}\|_{L^2(D)} \leq \|u - u_\epsilon\|_{L^2(D)} + \|u_\epsilon - u_{\epsilon,N}\|_{L^2(D)} \\
&\leq (C\epsilon^{\nu_\alpha} + C_\epsilon N^{-\alpha})\|f\|_{L^2(\Omega)}.
\end{aligned} \tag{4.2.3}
$$

Remark 4.2.2. *From above error estimate, we can see that the the penalty parameter ϵ can not be arbitrarily chosen small.*

4.2.2 Numerical implementation

We present the implementation of a spectral Galerkin method for 1D fractional reaction equation.

Plugging $u_N = \sum_{n=0}^N \hat{u}_n (1 - x^2)^{\alpha/2} P_n^{\alpha/2,\alpha/2}(x)$ into the extend equation and taking $v_N = (1 - x^2)^{\alpha/2} P_k^{\alpha/2,\alpha/2}(x)$ for $k = 0, 1, \ldots, N$, by the orthogonality of Jacobi polynomials, the equality (2.3.2) we obtain that

$$
(S + M)U = F. \tag{4.2.4}
$$

Here the solution $U = (\hat{u}_0, \hat{u}_1, \cdots, \hat{u}_N)^T$ and the right hand side $F = [F_0, F_1, \cdots, F_N]^T$ is a $N + 1$ by 1 column with

$$
F_k = \int_{-1}^1 (1 - x^2)^{\alpha/2} f(x) P_k^{\alpha/2,\alpha/2}(x)\, dx.
$$

The stiffness matrix $S = diag(s_0, s_1, \cdots, s_N)$, which can be derived from Lemma 2.3.2 and the orthogonality of Jacobi polynomials

$$
\begin{aligned}
S_{k+1,n+1} &= \int_{-1}^1 (-\Delta)^{\alpha/2}[(1 - x^2)^{\alpha/2} P_n^{\alpha/2}(x)] \cdot (1 - x^2)^{\alpha/2} P_k^{\alpha/2}(x) dx \\
&= \int_{-1}^1 \lambda_n^\alpha P_n^{\alpha/2,\alpha/2}(x) \cdot (1 - x^2)^{\alpha/2} P_k^{\alpha/2,\alpha/2}(x) dx := \lambda_n^\alpha h_n^{\alpha/2,\alpha/2} \delta_{k,n}
\end{aligned} \tag{4.2.5}
$$

for $k, n = 0, 1, 2, \cdots, N$, where $\delta_{k,n} = 1$ for $k = n$ and $\delta_{k,n} = 0$ otherwise, λ_n^α defined in (2.3.2) and $h_k^{\alpha/2,\alpha/2}$ is from (6.1.5).

The mass matrix M is $N + 1$ by $N + 1$ with

$$
M_{k+1,n+1} = \frac{1}{\epsilon} \int_{-1}^1 1_{\Omega_1} (1 - x^2)^\alpha P_n^{\alpha/2,\alpha/2}(x) P_k^{\alpha/2,\alpha/2}(x)\, dx, \quad k, n = 0, 1, 2, \cdots, N. \tag{4.2.6}
$$

We can see that the mass matrix M is dense, which seems to be expensive to store and compute. However, there is a hidden structure behind the analytical expression. In fact, the mass matrix can be approximated by the low rank matrix, that is,

$$
M \approx \sum_{j=1}^J \mathsf{w}_j \beta_j \beta_j^T = V^T \Sigma V \tag{4.2.7}
$$

where Σ is J by J diagonal matrix, and its entries w_j's are the corresponding quadrature weights, $V = [\beta_1, \beta_2, \cdots, \beta_J]^T$ is J by $N + 1$ matrix and its j-th row vector is

$$
\beta_j = [P_0^{\alpha/2,\alpha/2}(x_j), P_1^{\alpha/2,\alpha/2}(x_j), \ldots, P_{N+1}^{\alpha/2,\alpha/2}(x_j)] \tag{4.2.8}
$$

with the quadrature points $\{x_j\} \in \Omega_1 = \Omega^c \cap D$.

Thus instead of solving the original matrix (4.2.4), we solve the following approximated equation

$$(S + V^T \Sigma V)U = F. \tag{4.2.9}$$

When J is small, the flowing lemma provides a fast solver to find the solution of matrix.

Lemma 4.2.3 (Sherman-Morrison-Woodbury Identity). *Suppose $A \in \mathbb{R}^{n \times n}$ $D \in \mathbb{R}^{m \times m}$ and $U, V \in \mathbb{R}^{n \times m}$ are invertible square matrices,. Then $A + UDV^T$ is invertible if and only if $D^{-1} + V^T A^{-1} U$ is invertible. In this case,*

$$(A + UDV^T)^{-1} = A^{-1} - [A^{-1}U(D^{-1} + V^T A^{-1}U)^{-1}V^T A^{-1}]. \tag{4.2.10}$$

4.2.3   Numerical results

To examine the accuracy and convergence orders of penalty method, we will present numerical results for one-dimensional case.

Take $f = 1$ and measure the error as follows

$$error(N) = \|u - u_{N,\epsilon}\|_{L^2(\Omega)}$$

where $u_{N,\epsilon} = (1 - x^2)^{\alpha/2} \sum_{n=0}^{N} \hat{u}_n P_n^{\alpha/2}$.

The original problem $(-\Delta)^{\alpha/2}u = 1$, $x \in \Omega = (-r_0, r_0)$. The extended problem $(-\Delta)^{\alpha/2}u + \frac{\chi}{\epsilon}u = 1$, $x \in D = (-1, 1)$ with $0 < r_0 < 1$. The exact solution is known $u = (r_0^2 - x^2)^{\alpha/2}/\Gamma(\alpha + 1)$.

Example 4.2.4. *How to choose the quadrature number J?*

It should be pointed out that the quadrature points $\{x_j\}$ in (4.2.8) can be flexibly chosen. For simplicity, we will study two ways of partition, the uniform mesh and non-uniform graded mesh. Specifically, we will consider the following cases.

- Case 1.   Take uniform mesh $\{x_j = r_0 + (j - 1) * (1 - r_0)/N_1\}$ for $j = 1, 2, \cdots, N_1$ and $\{x_j = -x_{j-N_1}\}$ for $j = N_1 + 1, 2, \cdots, J$ with $J = 2 * N_1$. The corresponding weights are taken equally as $\mathsf{w}_j = (1 - r_0)/N_1$. Here $N_1 = floor(-\log_{0.95}(N))$ which is proportional to $\log_2(N)$.

- Case 2.   Take uniform mesh $\{x_j = r_0 + (j - 1) * (1 - r_0)/N\}$ for $j = 1, 2, \cdots, N$ and $\{x_j = -x_{j-N_1}\}$ for $j = N + 1, 2, \cdots, J$ with $J = 2 * N$ and the corresponding weights $\mathsf{w}_j = (1 - r_0)/N$.

- Case 3.   Take nonuniform geometrically graded mesh $\{x_1 = r_0\}$, $\{x_j = r0 + (1 - r0) * (0.95)^{N_1-j+2}\}$ for $j = 2, \cdots, N_1$ and $\{x_j = -x_{j-N_1}\}$ for $j = N_1 + 1, \cdots 2N_1$. The corresponding weights are taken as $\mathsf{w}_j = x_{j+1} - x_j$ for $j = 1, \cdots, N_1 - 1$ and $\mathsf{w}_{N_1} = 1 - x_{N_1}$; $\mathsf{w}_j = \mathsf{w}_{j-N_1}$ for $j = N_1 + 1, \cdots, 2N_1$.

- Case 4.   Take nonuniform geometrically graded mesh $\{x_1 = r_0\}$, $\{x_j = r0 + (1 - r0) * (0.9)^{N_1-j+2}\}$ for $j = 2, \cdots, N_1$ and $\{x_j = -x_{j-N_1}\}$ for $j = N_1 + 1, \cdots 2N_1$. The corresponding weights are taken as $\mathsf{w}_j = x_{j+1} - x_j$ for $j = 1, \cdots, N_1 - 1$ and $\mathsf{w}_{N_1} = 1 - x_{N_1}$; $\mathsf{w}_j = \mathsf{w}_{j-N_1}$ for $j = N_1 + 1, \cdots, 2N_1$.

- Case 5. Take nonuniform graded mesh $\{x_j = r_0 + (1 - r_0) * ((j-1)/N_1)^2\}$ for $j = 1, 2, \cdots, N_1$ and $\{x_j = -x_{j-N_1}\}$ for $j = N_1 + 1, 2, \cdots, J$ with $J = 2 * N_1$. The corresponding weights are taken as $\mathsf{w}_j = x_{j+1} - x_j$.

- Case 6. Take uniform mesh as Case 1. but with nonuniform weights $\mathsf{w}_j = h/(jh)^{1/2}$ with $h = (1 - r_0)/N_1$ for $j = 1, \cdots, N_1$ $\mathsf{w}_j = \mathsf{w}_{j-N_1}$ for $j = N_1 + 1, \cdots, 2N_1$.

- Case 7. Take uniform mesh as Case 1. but with nonuniform weights $\mathsf{w}_j = h/(jh)^{\alpha/2}$ with $h = (1 - r_0)/N_1$ for $j = 1, \cdots, N_1$ $\mathsf{w}_j = \mathsf{w}_{j-N_1}$ for $j = N_1 + 1, \cdots, 2N_1$.

- Case 8. Take the nonuniform as Case 3 but with the same weight as the Case 1.

The comparison for convergence order and accuracy of different choices will be presented in Table (4.1). From Table (4.1), we can see that, using fewer quadrature points, one can achieve almost the same accuracy as the large number of points in Case 2. However, as N goes large, using fewer quadrature points uniformly but with the same weights in Case 1 will not bring better accuracy while geometrically non-uniform mesh can lead to stable decreasing of the error. Note that the number $-\log_{0.95}(N)$ in Case 3 is greater that $-\log_{0.9}(N)$ in Case 4. The better accuracy in Case 3 can be obtained than the Case 4. However, for uniform mesh partition, if we take graded weights, the large weights near the boundary and the small weights far away, we can get the stable decreasing the error.

To sum up, the numerical results in (4.1) supports the feasibility of taking the fewer number of quadrature points which is proportional to $\log_2(N)$.

Table 4.1: Convergence order and error for different quadrature numbers J. Here the original equation $(-\Delta)^{\alpha/2} u = 1$ for $x \in (-0.5, 0.5)$ with $\alpha = 1.5$. The penalty number $\epsilon = N^{-\alpha}$. Case 1 refers to uniform mesh with $J = -2\log_{0.95}(N) \approx \log_2(N)$; Case 2 refers to uniform mesh with $J = 2N$; Case 3 refers to nonuniform geometrically graded mesh with $J = -2\log_{0.95}(N) \approx \log_2(N)$; Case 4 refers to nonuniform geometrically graded mesh with $J = -2\log_{0.9}(N) \approx \log_2(N)$; ; Case 5 graded mesh with J same as Case 3; Case 6 uniform mesh as Case 1 but different weights; Case 7 uniform mesh as Case 1 but different weights;Case 8 nonuniform mesh as Case 3 but the same weights as Case 1.

N	Case 1 error	rate	Case 2 error	rate	Case 3 error	rate	Case 4 error	rate
64	7.91e-03		7.23e-03		8.45e-03		8.16e-03	
128	3.13e-03	1.34	3.70e-03	0.97	4.27e-03	0.98	4.32e-03	0.92
256	8.91e-04	1.81	1.90e-03	0.96	2.23e-03	0.94	2.23e-03	0.95
512	1.26e-04	2.82	9.67e-04	0.97	1.15e-03	0.95	1.25e-03	0.83
1024	2.50e-04	-0.99	4.91e-04	0.98	6.22e-04	0.89	7.40e-04	0.76

N	Case 5 error	rate	Case 6 error	rate	Case 7 error	rate	Case 8 error	rate
64	9.98e-03		6.56e-03		1.08e-02		1.36e-03	
128	5.01e-03	0.99	4.22e-03	0.64	6.40e-03	0.75	1.51e-03	-0.16
256	2.52e-03	0.99	2.68e-03	0.65	3.65e-03	0.81	1.36e-03	0.16
512	1.25e-03	1.01	1.35e-03	0.99	1.60e-03	1.19	9.44e-04	0.52
1024	6.14e-04	1.02	5.79e-04	1.22	5.97e-04	1.43	6.07e-04	0.64

Example 4.2.5. *What is optimal penalized number and convergence order?*

In this example, we explore the optimal penalized number and convergence order. First we look at the error distribution of solution. From Figure 4.2.3, we can see that the error is very larger near the boundary than that in the interior domain This agrees with our expectation since the solution has weak boundary singularity (the first order derivative blows up).

Second, we take different small penalty parameter $\epsilon = \frac{1}{N^\sigma}$ with differ σ to see the effect of the parameter on convergence order of the solution. To this end, fix the $\alpha = 1.5$ and vary ϵ. From Figure 4.3, we can see that the optimal constant is $\sigma = 1.8$ and the convergence order is around 1.3. When we take large penalty number with $\sigma = 2$, the error will froze. We also test the even large penalty number and found the overdue penalization will not improve accuracy but conversely lead to the deterioration; see the comparison between Figure 4.4 and 4.5. This suggest the penalty number must be carefully chosen. In general it is recommended that the penalty number can be taken as $\epsilon = N^{-\alpha}$ and about the first order convergence can be obtained for different α, which can be seen from Figures 4.4 with $\alpha = 1.2$ and 1.8.
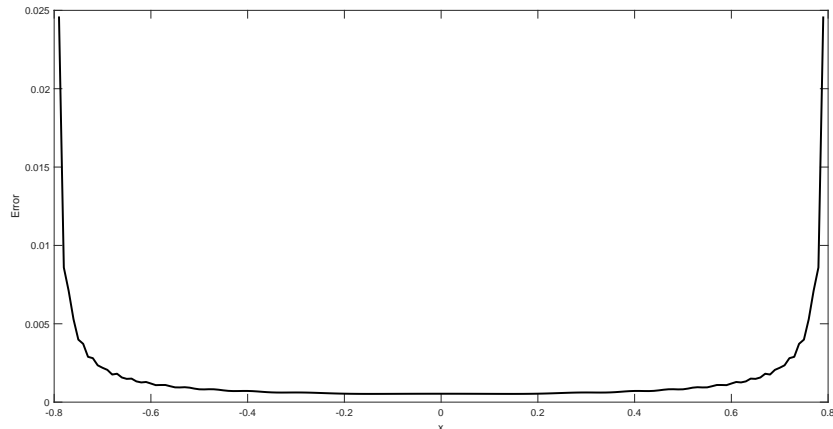
Figure 4.2: In computation, we take truncation number $N = 640$ and $\epsilon = N^{-1.8}$. The error profile of the numerical solution for $\alpha = 1.5$

Example 4.2.6. L^2 *penalty method versus* H^1 *penalty method.*

In this example we show the comparison between L^2 penalty method and H^1 penalty method. From the Figure 4.6, we can see that L^2 penalty method is much better than H^1 version.This explain why we prefer L^2 penalty method over H^1 version in this paper.

4.3 Fictitious domain method based on spectral method for 2D

4.3.1 Spectral Galerkin method for 2D

We consider the unit disk $\Omega = \{(x_1, x_2) \,|\, x_1^2 + x_2^2 < 1\}$. Let $x_1 = r\cos(\theta)$ and $x_2 = r\sin(\theta)$. Then in polar coordinate we will use (r, θ) where $\Omega = \{(r, \theta) \,|\, 0 \le r < 1, \, 0 \le \theta \le 2\pi\}$.
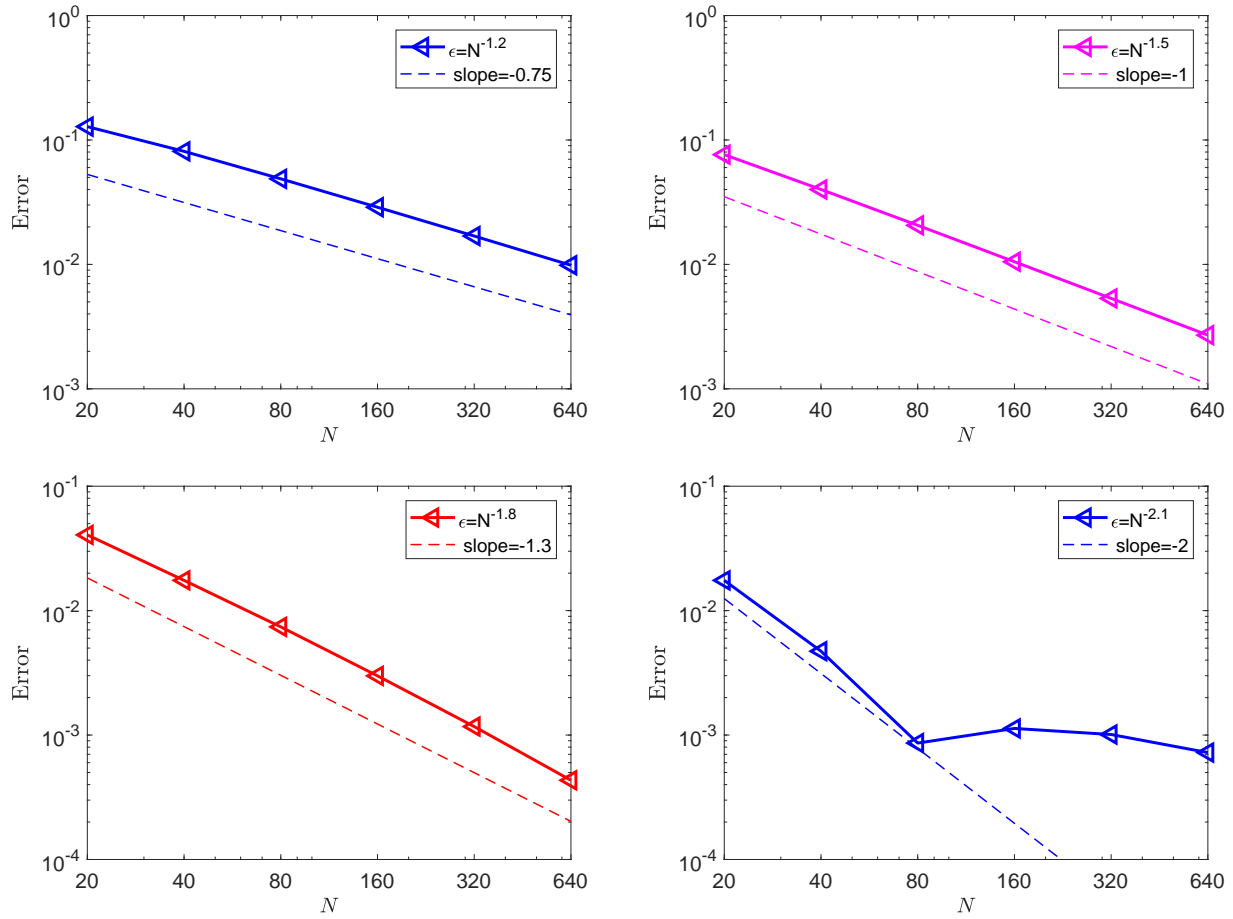
Figure 4.3: The convergence order for different penalty parameter ϵ. In computation, we take $\alpha = 1.5$.
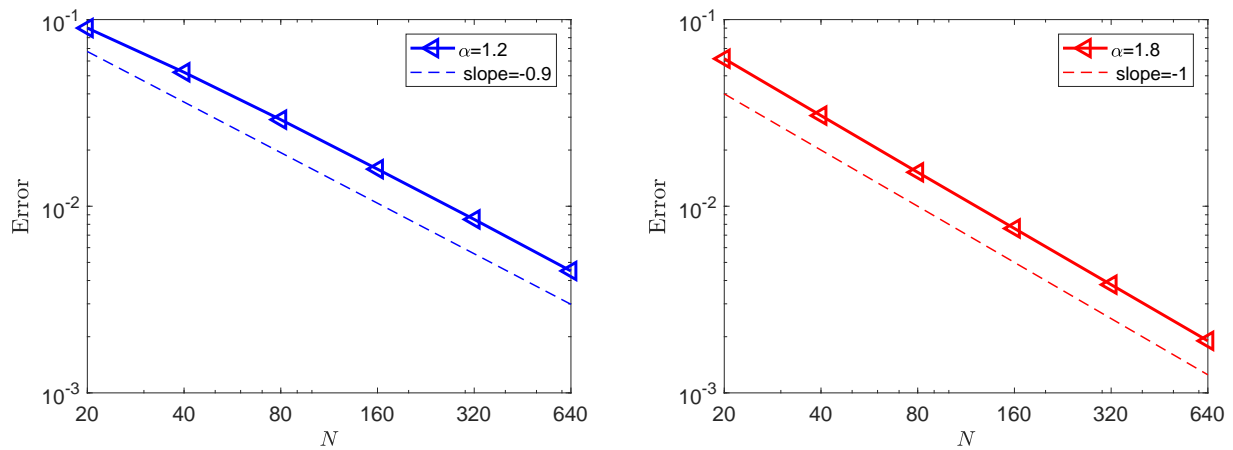
Figure 4.4: The convergence order for different α. In computation, we take $\epsilon = N^{-\sigma}$ with $\sigma = \alpha$.
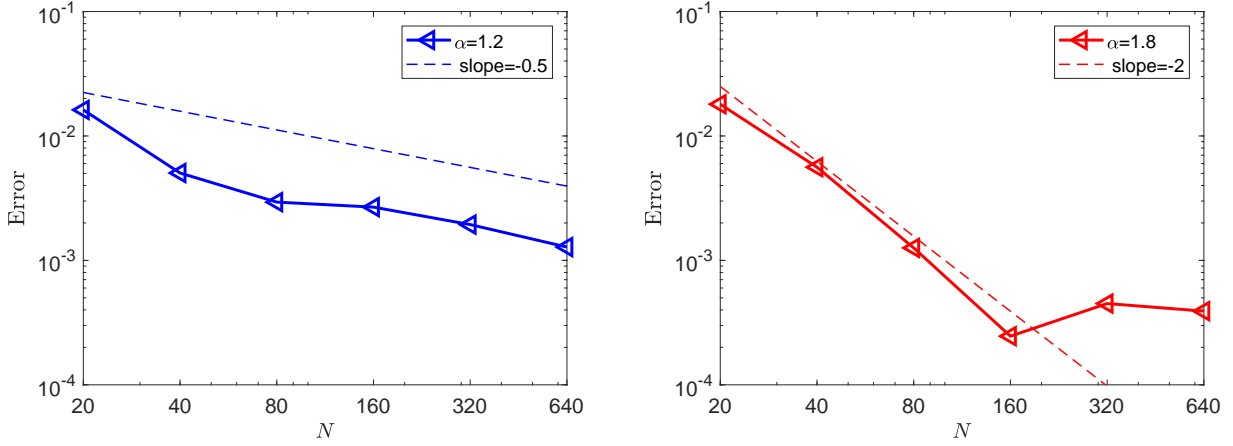
Figure 4.5: The convergence order for different α. In computation, we take $\epsilon = N^{-\sigma}$ with $\sigma = \alpha + 0.6$.
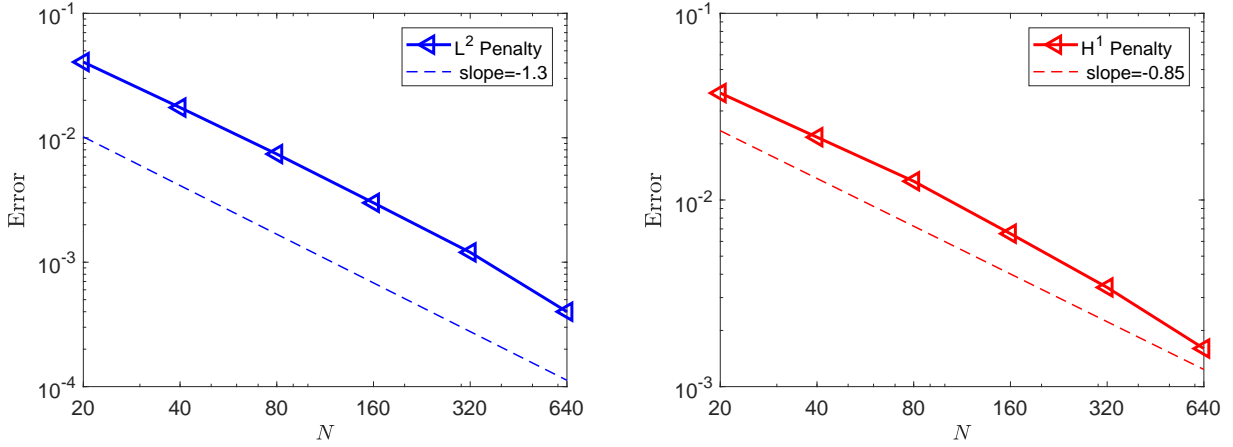
Figure 4.6: Comparison between L^2 penalty method and H^1 version. In computation, we take $\epsilon = N^{-1.8}$ and $\alpha = 1.5$.

According to the pseudo-eigenfunction relation in Lemma (3.3.1), we present the spectral Galerkin method using the non-polynomials, more precisely, the product of weighted function and polynomial basis. Define the finite dimensional space

$$U_{M,N} := \text{Span}\{\phi_{m,n}^{(1)}, \phi_{m,n}^{(2)}, 0 \le m \le M, 0 \le n \le N\},$$

where

$$\phi_{m,n}^{(1)}(x_1, x_2) := (1 - r^2)^{\alpha/2} r^m \cos(m\theta) P_n^{\alpha/2,m}(2r^2 - 1)$$

and

$$\phi_{m,n}^{(2)}(x_1, x_2) := (1 - r^2)^{\alpha/2} r^m \sin(m\theta) P_n^{\alpha/2,m}(2r^2 - 1).$$

It is clear that the dimension number of approximation space $U_{M,N}$ is $(2M + 1) \times (N + 1)$.

Set $u_{0,n}^{(2)} = 0$ for $0 \leq n \leq N$. The spectral Galerkin method is to find $u_{M,N} \in U_{M,N}$ such that

$$((-\Delta)^{\alpha/2} u_{\epsilon,M,N}, v_{M,N})_D + \frac{1}{\epsilon}(u_{\epsilon,M,N}, v_{M,N})_{\Omega_1} = (\tilde{f}, v_{M,N})_D, \quad \forall v_{M,N} \in U_{M,N}. \quad (4.3.1)$$

The well-posdeness of discrete problem (4.2.1) can be readily shown by Lax-Milgram's Theorem. Next we introduce two important lemmas which play key role in the error estimate.

For $u \in L^2_{-\alpha/2}(\Omega)$ we have $(1-r^2)^{-\alpha/2}u \in L^2_{\alpha/2}(\Omega)$ by the definition (3.2.2). Thus it is legitimate to write u as

$$\Pi_{M,N}^{\alpha/2} u \;=\; (1-r^2)^{\alpha/2} \sum_{m=0}^{\infty} \sum_{n=0}^{\infty} \left[u_{m,n}^{(1)} \cos(m\theta) + u_{m,n}^{(2)} \sin(m\theta) \right] r^m P_n^{\alpha/2,m}(2r^2 - 1). \quad (4.3.2)$$

Introduce the projection $\Pi_{M,N}^{\alpha/2} : L^2_{-\alpha/2}(\Omega) \to U_{M,N}$ such that

$$\Pi_{M,N}^{\alpha/2} u \;=\; (1-r^2)^{\alpha/2} \sum_{m=0}^{M} \sum_{n=0}^{N} \left[u_{m,n}^{(1)} \cos(m\theta) + u_{m,n}^{(2)} \sin(m\theta) \right] r^m P_n^{\alpha/2,m}(2r^2 - 1). \quad (4.3.3)$$

We are in position to state the convergence order of spectral Galerkin method (4.2.1).

Theorem 4.3.1 (Optimal convergence order). *Suppose that u and u_N satisfy the problems (3.2.1) and (4.2.1), respectively. Suppose that $f \in L^2(\Omega)$ we have the following error estimate:*

$$\|u_\epsilon - u_{\epsilon,M,N}\|_{L^2(\Omega)} \leq C_\epsilon (M^{-\alpha/2} + N^{-\alpha}) \|f\|_{L^2(\Omega)}.$$

The proof is similar as [54], here we skip it.

4.3.2 Numerical implementation

Set $u_{0,n}^{(2)} = 0$ for $0 \leq n \leq N$. For linear problem (4.3.1), plug $u_{M,N} = \sum_{m=0}^{M} \sum_{n=0}^{N} [\hat{u}_{m,n}^{(1)} \phi_{m,n}^{(1)} + \hat{u}_{m,n}^{(2)} \phi_{m,n}^{(2)}] \in U_{M,N}$ into (4.3.1) and take $v_{M,N} = \phi_{l,k}^{(i)}(x)$ for $i = 1,2$, $l = 0,1,\ldots M$ and $k = 0,1,\ldots,N$. Similar to one dimensional case, we obtain

$$(S + M)U = F. \quad (4.3.4)$$

Here the solution $U = (U_0^{(1)}, U_1^{(1)}, \cdots, U_M^{(1)}, U_1^{(2)}, U_2^{(2)}, \cdots, U_M^{(2)})^T$ with $U_m^{(i)} = (\hat{u}_{m,0}^{(i)}, \hat{u}_{m,1}^{(i)}, \cdots, \hat{u}_{m,N}^{(i)})$ for $i = 1,2$ and $m = 0,1,\cdots,M$. The right hand side $F = (F_0^{(1)}, F_1^{(1)}, \cdots, F_M^{(1)}, F_1^{(2)}, F_2^{(2)}, \cdots, F_M^{(2)})^T$ where $F_m^{(i)}$ are 1 by $N+1$ vectors

$$F_m^{(1)} = \text{Re}(F_m) \quad F_m^{(2)} = \text{Im}(F_m) \quad (4.3.5)$$

with the n-th $(n = 1, 2 \cdots, N+1)$ entry as

$$(F_m)_n \;=\; \int_0^{2\pi} \int_0^1 f(r,\theta) r^m e^{\mathbf{i}m\theta} P_{n-1}^{\alpha/2,m}(2r^2 - 1)(1-r^2)^{\alpha/2} r dr d\theta, \quad \mathbf{i}^2 = -1. \quad (4.3.6)$$

The stiffness $S = diag(S_0^{(1)}, S_1^{(1)}, \cdots, S_M^{(1)}, S_2^{(2)}, , \cdots, S_M^{(2)})$, where $S_m^{(1)} = S_m^{(2)}$ are diagonal matrices as one dimensional case. In fact, by the orthogonality of Jacobi polynomials and Lemma 3.3.1, we have

$$(S_m^{(1)})_{k,n} = ((-\Delta)^{\alpha/2} \phi_{m,n}^{(1)}, \phi_{m,k}^{(1)}) = (\frac{1}{2})^{\alpha/2+m+2} \pi \lambda_{m,n}^{\alpha} h_n^{\alpha/2,m} \delta_{k,n} \delta_m, \quad 0 \leq m \leq M, \quad (4.3.7)$$

where $\delta_{k,n} = 1$ if $k = n$ and 0 otherwise; $\delta_0 = 2$ and $\delta_m = 1$ for $m \geq 1$; $h_n^{\alpha/2,m}$ is defined in (6.1.5) and $\lambda_{m,n}^{\alpha}$ from Lemma 3.3.1. More precisely we have

$$(S_m^{(1)})_{k,n} = \frac{2^{\alpha-1}\pi}{2n+\alpha/2+m+1}\left(\frac{\Gamma(1+\alpha/2+n)}{\Gamma(n+1)}\right)^2 \delta_{k,n}\delta_m, \quad 0 \leq m \leq M, \tag{4.3.8}$$

The mass matrix M is $(2M+1)\times(N+1)$ by $(2M+1)\times(N+1)$, a Gram matrix generated by the basis ordered as $\phi_{0,0}^{(1)}, \phi_{0,1}^{(1)}, \cdots, \phi_{0,N}^{(1)}, \phi_{1,0}^{(1)}, \phi_{1,1}^{(1)}, \cdots, \phi_{1,N}^{(1)}, \cdots \phi_{M,0}^{(1)}, \phi_{M,1}^{(1)}, \cdots, \phi_{M,N}^{(1)}, \phi_{1,0}^{(2)}, \phi_{1,1}^{(2)}, \cdots, \phi_{1,N}^{(2)},$
$\cdots \phi_{M,0}^{(2)}, \phi_{M,1}^{(2)}, \cdots, \phi_{M,N}^{(2)}$, with respect to the inner product $(\cdot,\cdot)_{\Omega_1}$

Like one dimensional case, the dense matrix M can be approximated by the low rank matrix

$$M \approx \sum_{j=1}^{J} \mathsf{w}_j \beta_j \beta_j^T = V^T \Sigma V \tag{4.3.9}$$

where Σ is J by J diagonal matrix, and its entries w_j's are the corresponding quadrature weights, $V = [\beta_1, \beta_2, \cdots, \beta_J]^T$ is J by $(2M+1)\times(N+1)$ matrix and its j-th row vector is

$$\beta_j = [\beta_{j,0}^{(1)}, \beta_{j,1}^{(1)}, \cdots, \beta_{j,M}^{(1)}, \beta_{j,1}^{(2)}, \cdots, \beta_{j,M}^{(2)}],$$

where

$$\beta_{j,m}^{(1)} = \cos(m\theta_j)r_j^m \times [P_0^{\alpha/2,m}(2r_j^2-1), P_1^{\alpha/2,m}(x_j), \ldots, P_{N+1}^{\alpha/2,m}(2r_j^2-1)], \tag{4.3.10}$$

$$\beta_{j,m}^{(2)} = \sin(m\theta_j)r_j^m \times [P_0^{\alpha/2,m}(2r_j^2-1), P_1^{\alpha/2,m}(x_j), \ldots, P_{N+1}^{\alpha/2,m}(2r_j^2-1)], \tag{4.3.11}$$

with the quadrature points $\{(r_j, \theta_j)\} \in \Omega_1 = \Omega^c \cap D$.

The quadrature points can be chosen like this, taking the uniform partition on in the theta direction, then make non-uniform partition in the radial direction as in one dimensional case. In this way, we only need the fewer quadrature points, thus reduce the storage and computational cost greatly.

In the following numerical test, we take $\mathsf{N} = \max(N+60, 512)$ and $\mathsf{N}' = 2(M+1)$.

For large M, we can speed up the calculation by using the FFT algorithm in θ direction.

4.3.3 Numerical results

In this section we exam the convergence order of the proposed method and present the surface and contour of the numerical solution. When the solution is unknown, we use the same method with fine resolution to compute the reference solution.

When we measure the convergence order in radial direction, we take a fixed large number $M = 40$, and let N double from 16 to 128. The error is measured as

$$error(N) = \|U_{40,N} - U_{40,2N}\|.$$

When we measure the convergence order in radial direction, we take a fixed large number $N = 128$, and let N double from 8 to 64. The error is measured as

$$error(M) = \|U_{M,128} - U_{2M,128}\|.$$

Example 4.3.2. *(Convergence order for small circle) Consider* $(-\Delta)^{\alpha/2}u = 2$, $(r,\theta) \in \Omega = (0, 1/\sqrt{2}) \times (0, 2\pi)$.

The analytical solution is $u = (1/2-r^2)^{\alpha/2}/2^{\alpha-1}(\Gamma(\alpha/2+1))^2$. The extended problem $(-\Delta)^{\alpha/2}u + \frac{\chi}{\epsilon}u = 2$, $(r,\theta) \in (0,1) \times (0,2\pi)$. Note that both the right hand side function and the domain is radial symmetrical. In computation, we take truncation number $N = 100$ in radial direction and $M = 0$ in theta direction, and $\epsilon = N^{-1.5}$. From 4.2, we can see that the convergence orders for different α are around 1, which is the same as one dimensional case. We also present the solution profile in the Figure 4.7 for $\alpha = 1.5$, where we can see the solution almost vanishes outside of the original domain. The numerical results show the convergence and accuracy of the proposed method.

Table 4.2: Convergence order for different α. The penalty numbers for outside and boundary are taken as $\epsilon = N^{-\alpha}$.

	$\alpha = 1.1$		$\alpha = 1.5$		$\alpha = 1.9$	
N	$E(N)$	rate	$E(N)$	rate	$E(N)$	rate
16	5.22e-03		4.02e-03		4.34e-03	
32	3.17e-03	0.72	1.36e-03	1.56	1.92e-03	1.18
64	1.92e-03	0.72	4.24e-04	1.69	8.81e-04	1.13
128	1.08e-03	0.83	1.22e-04	1.80	4.12e-04	1.09
256	6.06e-04	0.84	5.83e-05	1.06	1.95e-04	1.08

Example 4.3.3. *(Convergence order for sector domain) Consider* $(-\Delta)^{\alpha/2}u = 2$, $(r,\theta) \in \Omega$

Case 1. $\Omega = (0,1) \times (0,\pi)$; Case 2. $\Omega = (0,1) \times (0,\pi/2)$; Case 3. $\Omega = (0,1) \times (0,3\pi/2)$.

In this example we test the convergence order and accuracy for half circle, sector with rectangular and reentrant corner, respectively. From the Tables 4.3-4.4, we can see that effect of the shape on the convergence orders is almost negligible, and the convergence orders are about one in both radial direction and θ direction when the penalty number is taken as $\epsilon = (N+M)^{-\alpha}$. From Table 4.5, we can see that the convergence orders are around one for different α.

Table 4.3: Convergence order and accuracy in radial direction for different shape. The penalty number is taken as $\epsilon = N^{-\alpha}$ with $\alpha = 1.5$

	rectangular corner		half circle		reentrant corner	
N	$E(40, N)$	rate	$E(40, N)$	rate	$E(40, N)$	rate
32	8.51e-02		7.23e-02		9.20e-02	
64	4.84e-02	0.81	3.72e-02	0.96	5.14e-02	0.84
128	1.83e-02	1.40	1.50e-02	1.31	2.55e-02	1.01

Example 4.3.4. *(Numerical solution for different boundary.) Consider* $(-\Delta)^{\alpha/2}u = 1$, $(r,\theta) \in \Omega$ *with* $\alpha = 1.5$. *Case 1. the small circle* $\Omega = (0,1) \times (0,2\pi)$; *Case 2. the sector with reentrant corner* $\Omega = (0,1) \times (-\pi/2,\pi)$; *Case 3. the square* $\omega = \{(x,y) : |x| < \sqrt{2}/2, |y| < \sqrt{2}/2\}$; *Case 4. the ellipse* $\omega = \{(x,y) : x^2 + 2y^2 < 1\}$.

60

Table 4.4: Convergence order and accuracy in theta direction for different shape. The penalty number is taken as $\epsilon = N^{-\alpha}$ with $\alpha = 1.5$

	rectangular corner		half circle		reentrant corner	
M	$E(M, 128)$	rate	$E(M, 128)$	rate	$E(M, 128)$	rate
32	5.72e-02		5.12e-02		8.84e-02	
64	2.80e-02	1.03	2.75e-02	0.90	4.07e-02	1.12
128	1.48e-02	0.92	1.54e-02	0.84	1.77e-02	1.20

Table 4.5: Convergence order in the radial direction for the sector with rectangular corner. The penalty number is taken as $\epsilon = N^{-\alpha}$

	$\alpha = 1.1$		$\alpha = 1.5$		$\alpha = 1.9$	
N	$E(40, N)$	rate	$E(40, N)$	rate	$E(40, N)$	rate
32	8.51e-02		5.24e-02		8.51e-02	
64	4.84e-02	0.81	2.42e-02	1.11	4.84e-02	0.81
128	1.83e-02	1.40	7.70e-03	1.65	1.83e-02	1.40

In the computation for all cases, we take $\epsilon = N^{-1.5}$. In case 1, we take truncation number $N = 100$ in radial direction and $M = 0$ in theta direction. In Case 2, we take truncation number $N = 80$ in radial direction and $M = 40$ in theta direction, $\epsilon = (N + M)^{-1.5}$. In Case 3, we take truncation number $N = 40$ in radial direction and $M = 40$ in theta direction, $\epsilon = (N + M)^{-1.5}$. In Case 4, we take truncation number $N = 40$ in radial direction and $M = 40$ in theta direction, $\epsilon = (N + M)^{-1.5}$. The numerical solution for different shape are presented in Figures 4.7-4.10.
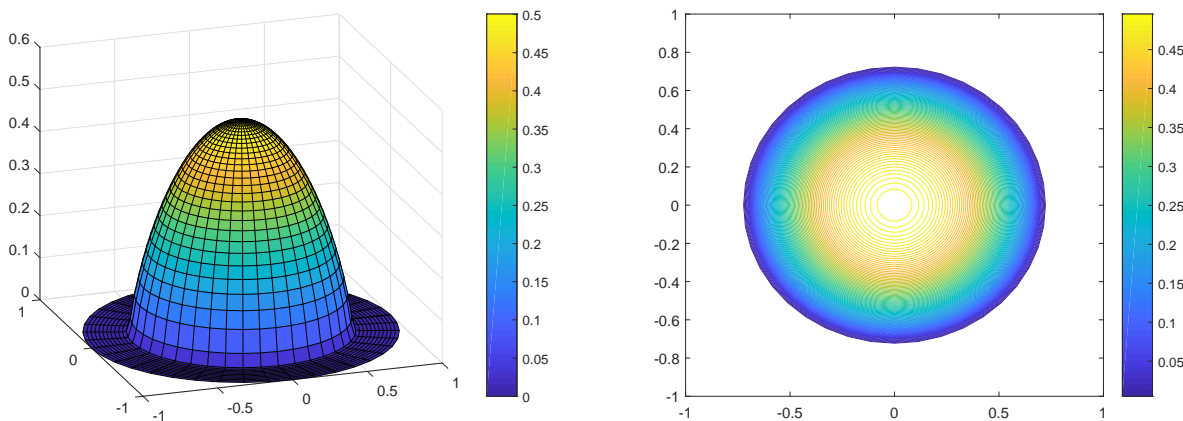
Figure 4.7: Numerical solution for the small circle.
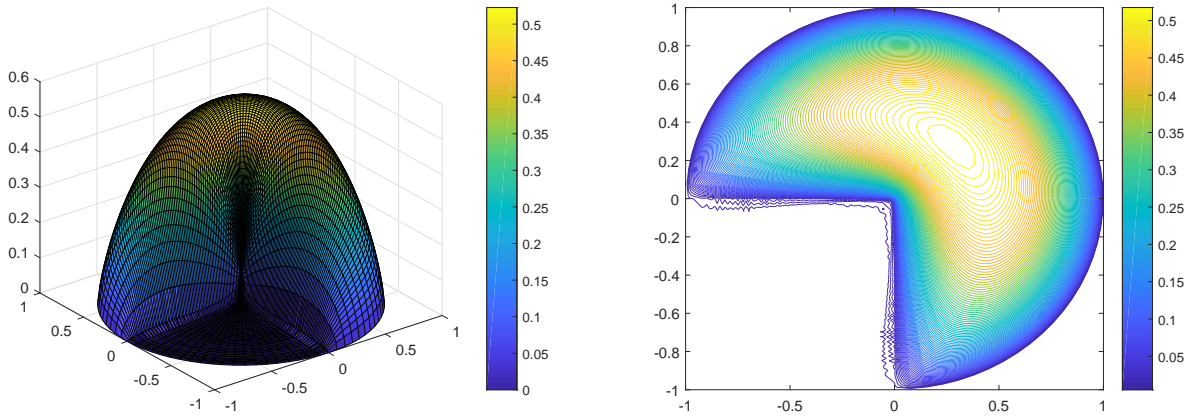
Figure 4.8: The numerical solution for the sector with reentrant corner
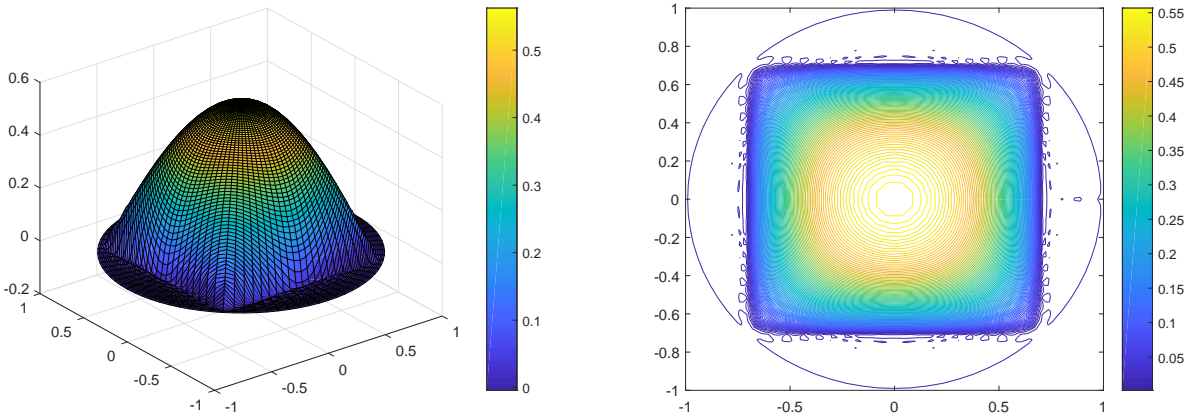
Figure 4.9: The numerical solution for the square domain

4.4 Conclusion

In this chapter, we investigated fictitious domain methods for the fractional Laplacian diffusion equations on the general domain. We provide an ample numerical examples to show the efficiency and accuracy of this method. However we did not present the error estimates for the method since it is much more involved and rather technique to analyze. We will leave this topic for our future research.
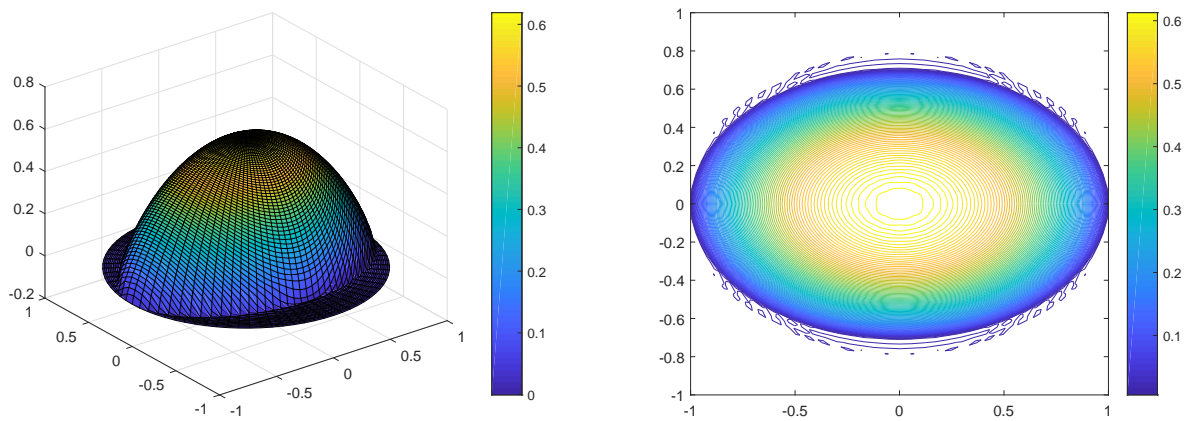
Figure 4.10: The numerical solution for the ellipse

Chapter 5

Finite difference method for fractional Laplacian

In this chapter [1], we propose a simple approach that can significantly reduce the cost for preparing the linear system for solutions. This approach is based on generating functions of finite difference schemes on uniform mesh, analogue to that for the Laplacian operator. More precisely, for the fractional Laplacain operator $(-\Delta)_d^{\alpha/2}$ (In this chapter, we use the subscript d to differentiate the dimensionality), we construct the discrete fractional Laplacian $(-\Delta_h)^{\alpha/2}$ as

$$(-\Delta_h)_d^{\alpha/2}u(x) =: \frac{1}{h^\alpha} \sum_{i_1,i_2,\cdots i_d \in \mathbb{Z}} a_{i_1,i_2,\cdots,i_d}^{(\alpha)} u(x_1 + i_1 h, x_2 + i_2 h, \cdots, x_d + i_d h), \qquad (5.0.1)$$

where h is step-size or spatial discretization parameter, $\mathbb{Z}$ is the set of all integer number, $a_{i_1,i_2,\cdots,i_d}^{(\alpha)}$ are expansion coefficients of generating function $\big[\sum_{j=1}^d 4\sin^2(\frac{k_j}{2})\big]^{\alpha/2}$, i.e.,

$$a_{i_1,i_2,\cdots,i_d}^{(\alpha)} = \frac{1}{(2\pi)^d} \int_{[-\pi,\pi]^d} \big[\sum_{j=1}^d 4\sin^2(\frac{k_j}{2})\big]^{\alpha/2} e^{-\mathbf{i}\sum_{j=1}^d i_j k_j} dk_1 dk_2 \cdots dk_d, \quad \mathbf{i}^2 = -1. \qquad (5.0.2)$$

When $\alpha = 2$, the generating function becomes the one for integer operator. The weights or coefficients $a_{i_1,i_2,\cdots,i_d}^{(\alpha)}$ can be readily computed using the *fast Fourier transform*. This is one of main attractive features and advantages of our method compared to other existing ones in the literature.

For the proposed approximation we prove that it has second-order convergence to the fractional Laplacian when a function is smooth, which is consistent with the classical centered difference approximation for second-order Laplacian. However, we point out that the convergence order of the approximation is not deteriorated in the interior domain when the approximation is applied to the problem (1.2.1)-(1.2.2) even though the solution is not smooth. In fact, we observe the second-order approximation in the interior domain in our numerical examples, see Section 5.4.

Based on the γth-order ($\gamma \le 2$) scheme, a high-order approximation up to fourth-order can be obtained using an extrapolation technique. The γth-order ($\gamma \le 2$) approximation can be further

---

[1]This chapter is based on the paper: Zhaopeng Hao, Zhongqiang Zhang, Rui Du, Fractional centered difference scheme for the high-dimensional integral fractional Laplacian, Journal of Computational Physics, (submitted).

applied to more general problems with fractional Laplacian on rectangle/cube rectangle or even more general domains. For example, we can apply the fictitious or extended domain method (e.g., [60, 12, 43] when $\alpha = 2$) to solve problems on more general domains. Specifically, we first reformulate problems on general domains into problems penalized with an extra reaction term on rectangles covering the considered domains. Then we solve the reformulated problems on the rectangles using our method, see Section 5.4.

When the approximation is applied to (1.2.1), the stability and convergence can be readily proved in a discrete energy norm for $\alpha \in (0, 2)$. For simplicity, we restrict our analysis to the fractional elliptic equations in 2D but the analysis can be extended to 3D problems.

In Section 5.4, we illustrate our new approximation and show its γth-order ($\gamma \leq 2$) convergence and further derive a high-order approximation. In Section 5.1, we consider the finite difference scheme for the diffusion equation with fractional Laplacian and prove its stability and convergence. In Section 5.2, we present a fast solver based on the Fourier transform for the resulting linear systems. Numerical results are shown in Section 5.4 to verify the theoretical convergence and develop a fictitious method for fractional diffusion equations on general domains in Section 5.5 before we make concluding remarks and discussions on possible extensions.

5.1 Approximations for fractional Laplacian

In this section, we first present our fractional centered difference (FCD) formula and then show its γth-order ($\gamma \leq 2$) convergence. We also develop a high-order approximation up to fourth-order based on the Richardson's extrapolation technique.

5.1.1 The fractional centered difference approximation

Take $d = 1$. For $\alpha = 2$, the centered difference approximation based on the uniform mesh is

$$(-\Delta)_1 u(x) = (-\Delta_h)_1 u(x) + \mathcal{O}(h^2) \tag{5.1.1}$$

where h is the step size and

$$(-\Delta_h)_1 u(x) =: \frac{1}{h^2} [a_{-1}^{(2)} u(x-h) + a_0^{(2)} u(x) + a_1^{(2)} u(x+h)], \quad a_0^{(2)} = 2, \, a_{-1}^{(2)} = a_1^{(2)} = -1. \tag{5.1.2}$$

Under suitable regularity condition, e.g., $u \in C^4[x-h, x+h]$, the above second-order approximation can be readily proved by Taylor expansion.

The generating function of this approximation can be derived from the following observation. For any z, we have

$$4\sin^2(\frac{z}{2}) = a_{-1}^{(2)} \exp(-1 \cdot (-\mathbf{i}z)) + a_0^{(2)} \exp(0 \cdot (-\mathbf{i}z)) + a_1^{(2)} \exp(1 \cdot (-\mathbf{i}z)). \tag{5.1.3}$$

Then we can write

$$a_j^{(2)} = \frac{1}{2\pi} \int_{-\pi}^{\pi} 4\sin^2(\frac{k}{2}) e^{-\mathbf{i}jk} \, dk. \tag{5.1.4}$$

We call the function $4\sin^2(\frac{z}{2})$ the generating function of the approximation (5.1.1)-(5.1.2).

For $\alpha \neq 2$, we generalize the discrete fractional Laplacian operator as follows

$$(-\Delta_h)_1^{\alpha/2} u(x) =: \frac{1}{h^\alpha} \sum_{j \in \mathbb{Z}} a_j^{(\alpha)} u(x+jh), \tag{5.1.5}$$

66

where

$$a_j^{(\alpha)} = \frac{1}{2\pi} \int_{-\pi}^{\pi} [4\sin^2(\frac{k}{2})]^{\alpha/2} e^{-\mathbf{i}jk} dk. \tag{5.1.6}$$

In two-dimensional case, the *discrete fractional Laplacian* operator can be generalized as follows

$$(-\Delta_h)_2^{\alpha/2} u(x_1, x_2) =: \frac{1}{h^\alpha} \sum_{i,j \in \mathbb{Z}} a_{i,j}^{(\alpha)} u(x_1 + ih, x_2 + jh), \tag{5.1.7}$$

where $a_{i,j}^{(\alpha)}$ are expansion coefficients of the generating function $[4\sin^2(\frac{k_1}{2}) + 4\sin^2(\frac{k_2}{2})]^{\alpha/2}$, i.e.,

$$a_{i,j}^{(\alpha)} = \frac{1}{4\pi^2} \int_{-\pi}^{\pi} \int_{-\pi}^{\pi} [4\sin^2(\frac{k_1}{2}) + 4\sin^2(\frac{k_2}{2})]^{\alpha/2} e^{-\mathbf{i}(ik_1 + jk_2)} dk_1 dk_2. \tag{5.1.8}$$

In particular, when $\alpha = 2$, the formula (5.1.7) reduces to the classical five-point centered difference approximation for Laplacian. When $d \geq 2$, the coefficients $a_{i_1, i_2, \dots, i_d}^{(\alpha)}$ is written in (5.0.1). These coefficients are computed numerically using the fast Fourier transform, see Section 5.3 for some details.

A natural question here is whether $(-\Delta_h)^{\frac{\alpha}{2}} u$ is an approximation of $(-\Delta)^{\frac{\alpha}{2}} u$ of certain order. In the following, we prove the convergence of FCD approximation to the fractional Laplacian under suitable smooth conditions.

Remark 5.1.1. *If we take the generating function as $[4\sin^2(\frac{k_1}{2})]^{\alpha/2} + [4\sin^2(\frac{k_2}{2})]^{\alpha/2}$ rather than $[4\sin^2(\frac{k_1}{2}) + 4\sin^2(\frac{k_2}{2})]^{\alpha/2}$, we then obtain a γth-order ($\gamma \leq 2$) approximation for the coordinate-dependent fractional derivative (two-sided and symmetrical Riemann-Liouville derivatives or Riesz derivatives in Appendix .9 e.g., see [56, 94]) rather than the integral fractional Laplacian.*

5.1.2 Convergence order

Introduce the following space as in [95]:

$$W^{s,1}(\mathbb{R}^2) = \{u \mid u \in L^1(\mathbb{R}^2), \int_{\mathbb{R}^2} (1 + |k|)^s |\hat{u}(k_1, k_2)| dk_1 dk_2 < \infty\}.$$

Here $|k|^2 = k_1^2 + k_2^2$.

Theorem 5.1.2. *Let $u \in W^{\gamma+\alpha,1}(\mathbb{R}^2)$ with a positive constant $\gamma \leq 2$ and $\hat{u}(k_1, k_2)$ is the Fourier transform of $u(x_1, x_2)$. Then for the fractional centered difference operator $(-\Delta_h)_2^{\alpha/2}$ defined in (5.1.7), it holds that*

$$(-\Delta)_2^{\alpha/2} u(x_1, x_2) = (-\Delta_h)_2^{\alpha/2} u(x_1, x_2) + \mathcal{O}(h^\gamma), \tag{5.1.9}$$

when h is sufficiently small.

Proof   For the generating function $[4\sin^2(\frac{k_1}{2}) + 4\sin^2(\frac{k_2}{2})]^{\alpha/2}$, we have

$$[4\sin^2(\frac{k_1}{2}) + 4\sin^2(\frac{k_2}{2})]^{\alpha/2} = \sum_{i,j \in \mathbb{Z}} a_{i,j}^{(\alpha)} e^{\mathbf{i}(ik_1 + jk_2)}. \tag{5.1.10}$$

67

Applying the Fourier transform, we have

$$h^\alpha \mathcal{F}\{(-\Delta_h)_2^{\alpha/2}u\} = \sum_{i,j\in\mathbb{Z}} a_{i,j}^{(\alpha)} e^{\mathbf{i}(ik_1+jk_2)h}\hat{u}(k_1,k_2)$$

$$= [4\sin^2(\frac{k_1 h}{2}) + 4\sin^2(\frac{k_2 h}{2})]^{\alpha/2}\hat{u}(k_1,k_2). \tag{5.1.11}$$

It follows that

$$\mathcal{F}\{(-\Delta_h)_2^{\alpha/2}u\} = |k|^\alpha \hat{u}(k_1,k_2) + \hat{T}_u(k_1,k_2), \tag{5.1.12}$$

where the Fourier transform of the truncation error T_u is

$$\hat{T}_u(k_1,k_2) = |k|^\alpha \left(\frac{[4\sin^2(\frac{k_1 h}{2}) + 4\sin^2(\frac{k_2 h}{2})]^{\alpha/2}}{|kh|^\alpha} - 1 \right)\hat{u}(k_1,k_2).$$

Set $z_1 = k_1 h$ and $z_2 = k_2 h$. By Taylor expansion we know that

$$\left(\frac{4\sin^2(z_1/2) + 4\sin^2(z_2/2)}{z_1^2 + z_2^2} \right)^{\alpha/2} = [1 + \mathcal{O}(z_1^2 + z_2^2)]^{\alpha/2} = 1 + \mathcal{O}(z_1^2 + z_2^2) \tag{5.1.13}$$

for small $z_1^2 + z_2^2$. Thus there exist constants C_0, C_1 which may depend on α but are independent of h such that

$$|\hat{T}_u(k_1,k_2)| \le |k|^\alpha \cdot C_0 |kh|^2 \cdot |\hat{u}(k_1,k_2)|, \quad |kh| < 1, \tag{5.1.14}$$

and by the boundedness of $\left(\frac{[4\sin^2(\frac{k_1 h}{2})+4\sin^2(\frac{k_2 h}{2})]^{\alpha/2}}{|kh|^\alpha} - 1 \right)$,

$$|\hat{T}_u(k_1,k_2)| \le C_1 |k|^\alpha \cdot |\hat{u}(k_1,k_2)|, \quad |kh| \ge 1. \tag{5.1.15}$$

By the assumption that $u \in W^{\gamma+\alpha,1}(\mathbb{R}^2)$, (5.1.14) and (5.1.15), we have

$$|T_u(x_1,x_2)|$$
$$= \frac{1}{4\pi^2}|\int_{\mathbb{R}^2} e^{-\mathbf{i}(k_1 x_1 + k_2 x_2)}\hat{T}_u(k)dk_1 dk_2| \le \int_{\mathbb{R}^2}|\hat{T}_u(k_1,k_2)|dk_1 dk_2$$
$$\le \int_{|kh|<1}|\hat{T}_u(k_1,k_2)|dk_1 dk_2 + \int_{|kh|\ge 1}|\hat{T}_u(k_1,k_2)|dk_1 dk_2$$
$$\le \int_{|kh|<1} C_0 h^2 (1+|k|)^{\alpha+2}|\hat{u}(k_1,k_2)|dk_1 dk_2 + C_1 h^\gamma \int_{|kh|\ge 1}(1+|k|)^{\alpha+\gamma}|\hat{u}(k_1,k_2)|dk_1 dk_2$$
$$\le (2^{2-\gamma}C_0 + C_1)h^\gamma \int_{\mathbb{R}^2}(1+|k|)^{\alpha+\gamma}|\hat{u}(k_1,k_2)|dk_1 dk_2 =: c_u h^\gamma. \tag{5.1.16}$$

Thus $|T_u| \le c_u h^\gamma$ by the inverse Fourier transform of function. Taking the inverse Fourier transformation of (5.1.12) leads to

$$(-\Delta_h)_2^{\alpha/2}u(x_1,x_2) = (-\Delta)_2^{\alpha/2}u(x_1,x_2) + T_u(x_1,x_2). \tag{5.1.17}$$

This completes the proof. $\square$

If we further assume such that $u \in W^{\delta+\alpha,1}(\mathbb{R}^2)$ with $2 < \delta \le 4$, we can write

$$(-\Delta)_2^{\alpha/2}u(x_1,x_2) = (-\Delta_h)_2^{\alpha/2}u(x_1,x_2) + \Phi_u(x_1,x_2)h^2 + \mathcal{O}(h^\delta), \tag{5.1.18}$$

where Φ_u is independent of h. The estimation (5.1.18) can be derived as in the proof of Theorem 5.1.2 and thus the proof is omitted. Now we can derive a high-order approximation by extrapolation.

68

Theorem 5.1.3. *Let $u \in W^{\delta+\alpha,1}(\mathbb{R}^2)$ with $2 < \delta \leq 4$. Then it holds that*

$$(-\Delta)_2^{\alpha/2} u(x_1, x_2) = \frac{4}{3}(-\Delta_{\frac{h}{2}})_2^{\alpha/2} u(x_1, x_2) - \frac{1}{3}(-\Delta_h)_2^{\alpha/2} u(x_1, x_2) + \mathcal{O}(h^\delta), \qquad (5.1.19)$$

when $h \to 0$. Here the fractional centered difference operator $(-\Delta_h)_2^{\alpha/2}$ is defined in (5.1.7).

Proof　Replacing h by $h/2$ in (5.1.18), we have

$$(-\Delta)_2^{\alpha/2} u(x_1, x_2) = (-\Delta_{\frac{h}{2}})_2^{\alpha/2} u(x_1, x_2) + \frac{1}{4}\Phi_u(x_1, x_2)h^2 + \mathcal{O}(h^\delta). \qquad (5.1.20)$$

Notice that Φ_u is independent of h. By (5.1.18) and (5.1.20), we can obtain the desired result.　□

5.2　Finite difference scheme for model equation

Let us introduce some necessary notations. The set of infinite grid is denoted by $h\mathbb{Z}^2$, with grid points (ih, jh) for integers $i, j \in \mathbb{Z}$, the set of all integers. Consider (1.2.1) at the grid points (ih, jh) and we obtain

$$(-\Delta)_2^{\alpha/2} u(ih, jh) + \mu u(ih, jh) = f(ih, jh). \qquad (5.2.1)$$

5.2.1　Construction of the finite difference scheme

Replacing the fractional Laplacian by the difference operator defined in (5.1.7), (5.2.1) becomes

$$(-\Delta_h)_2^{\alpha/2} u(ih, jh) + \mu u(ih, jh) = f(ih, jh) + T_u(ih, jh),$$
$$(ih, jh) \in \Omega_h, \qquad (5.2.2)$$

with the truncation error T_u depending on the solution u. By Theorem 5.1.2, we assume $u \in W^{\gamma+\alpha,1}(\mathbb{R}^2)$ with a positive constant $\gamma \leq 2$, such that there exists a constant c_u satisfying

$$|T_u| \leq c_u h^\gamma. \qquad (5.2.3)$$

Omitting T_u in (5.2.2) and denoting by $u_{i,j}$ the numerical approximation of $u(ih, jh)$, and $f_{i,j} = f(ih, jh)$, we get the fractional centered difference (FCD) scheme

$$(-\Delta_h)_2^{\alpha/2} u_{i,j} + \mu u_{i,j} = f_{i,j}, \quad (ih, jh) \in \Omega_h, \qquad (5.2.4)$$
$$u_{i,j} = 0, \quad (ih, jh) \in \Omega_h^c. \qquad (5.2.5)$$

5.2.2　Stability and convergence

We analyze the stability and convergence of the fractional centered difference scheme for the fractional diffusion equation.

For any grid functions $u = \{u_{i,j}\}$, $v = \{v_{i,j}\}$ on $h\mathbb{Z}^2$, a discrete inner product and the associated norm are defined as

$$(u, v)_h = h^2 \sum_{i,j \in \mathbb{Z}} u_{i,j} \bar{v}_{i,j}, \quad \|u\|_{L_h^2}^2 = (u, u)_h$$

and the discrete maximum norm is denoted by $\|v\|_{L_h^\infty} = \sup_{i,j\in\mathbb{Z}} |v_{i,j}|$. Here $\bar{v}$ denotes the complex conjugate of v. Set $L_h^2 \equiv \{u \,|\, u = \{u_{i,j}\}, \|u\|_{L_h^2}^2 < +\infty\}$. For $u \in L_h^2$, we define the semi-discrete Fourier transform $\hat{u} : [-\frac{\pi}{h}, \frac{\pi}{h}]^2 \to \mathbb{C}$ by

$$\hat{u}(k_1, k_2) := h^2 \sum_{i,j\in\mathbb{Z}} u_{i,j} e^{-\mathbf{i}(k_1 ih + k_2 jh)}, \tag{5.2.6}$$

and the inverse semi-discrete Fourier transform

$$u_{i,j} = \frac{1}{4\pi^2} \int_{-\pi/h}^{\pi/h} \int_{-\pi/h}^{\pi/h} \hat{u}(k_1, k_2) e^{\mathbf{i}(k_1 ih + k_2 jh)} dk_1 dk_2. \tag{5.2.7}$$

It is not hard to check that Parseval's identity

$$(u, v)_h = \frac{1}{4\pi^2} \int_{-\pi/h}^{\pi/h} \int_{-\pi/h}^{\pi/h} \hat{u}(k_1, k_2) \overline{\hat{v}(k_1, k_2)} dk_1 dk_2$$

holds. For a positive constant s, we define the fractional Sobolev semi-norm $|\cdot|_{H_h^s}$ as

$$|u|_{H_h^s}^2 = \int_{-\pi/h}^{\pi/h} \int_{-\pi/h}^{\pi/h} (k_1^2 + k_2^2)^s |\hat{u}(k_1, k_2)|^2 dk_1 dk_2, \tag{5.2.8}$$

$$\|u\|_{H_h^s}^2 = \int_{-\pi/h}^{\pi/h} \int_{-\pi/h}^{\pi/h} [1 + (k_1^2 + k_2^2)^s] |\hat{u}(k_1, k_2)|^2 dk_1 dk_2. \tag{5.2.9}$$

Set $H_h^s := \{u \,|\, u = \{u_{i,j}\}, \|u\|_{H_h^s} < +\infty\}$.

In the continuous level, we have well-known fractional Poincare inequality $\|u\|_{L^2} \leq C_s |u|_{H^s}$ for $s > 0$. The discrete analogue can be stated as following lemma.

Lemma 5.2.1 (Discrete Sobolev embedding inequality). *For $u \in H_h^s$ with $s > 0$, we have*

$$\|u\|_{L_h^2} \leq C_s |u|_{H_h^s},$$

where C_s is constant independent of h.

Proof Using the fact that

$$\min\{1, 2^{1-s}\}(k_1^2 + k_2^2)^s \leq (k_1^{2s} + k_2^{2s}) \leq \max\{1, 2^{1-s}\}(k_1^2 + k_2^2)^s, \quad s > 0,$$

we can define the coordinate equivalent norms

$$|u|_{H_h^{*,s}}^2 = \int_{-\pi/h}^{\pi/h} \int_{-\pi/h}^{\pi/h} (k_1^2 + k_2^2)^s |\hat{u}(k_1, k_2)|^2 dk_1 dk_2,$$

$$\|u\|_{H_h^{*,s}}^2 = \int_{-\pi/h}^{\pi/h} \int_{-\pi/h}^{\pi/h} [1 + (k_1^2 + k_2^2)^s] |\hat{u}(k_1, k_2)|^2 dk_1 dk_2,$$

which coincides with the norms in [53]. By the discrete fractional embedding equality in [53], we get the conclusion directly. □

To derive the error estimates in discrete energy norm, we need the following lemma.

Lemma 5.2.2 (Discrete Sobolev embedding inequality). *For $u \in H_h^s$ with $s > 1$, we have*

$$\|u\|_{L_h^\infty} \le C_s \|u\|_{H_h^s},$$

where $C_s = \frac{1}{4\pi^2} \big(\int_{-\infty}^{\infty} \int_{-\infty}^{\infty} \frac{1}{1+(k_1^2+k_2^2)^s} dk_1 dk_2 \big)^{\frac{1}{2}}$.

   Proof   By (5.2.7), we have

$$
\begin{aligned}
|u_{i,j}| &= \Big| \frac{1}{4\pi^2} \int_{-\pi/h}^{\pi/h} \int_{-\pi/h}^{\pi/h} \hat{u}(k_1, k_2) e^{\mathbf{i}(k_1 ih + k_1 jh)} dk_1 dk_2 \Big| \\
&\le \frac{1}{4\pi^2} \int_{-\pi/h}^{\pi/h} \int_{-\pi/h}^{\pi/h} |\hat{u}(k_1, k_2)| dk_1 dk_2 \\
&\le \frac{1}{4\pi^2} \Big(\int_{-\pi/h}^{\pi/h} \int_{-\pi/h}^{\pi/h} \frac{1}{1+(k_1^2+k_2^2)^s} dk_1 dk_2 \Big)^{\frac{1}{2}} \Big(\int_{-\pi/h}^{\pi/h} \int_{-\pi/h}^{\pi/h} (1+(k_1^2+k_2^2)^s) |\hat{u}(k_1, k_2)|^2 dk_1 dk_2 \Big)^{\frac{1}{2}} \\
&\le C_s \|u\|_{H_h^s}, \quad i, j \in \mathbb{Z},
\end{aligned}
$$

where we have used the Cauchy-Schwartz inequality. Taking the supremum leads to the desired result. This completes the proof.   □

Lemma 5.2.3 (Fractional semi-norm equivalence). *Supposed u, is a well-defined grid function. For $u \in H_h^{\alpha/2}$, we have*

$$(\frac{2}{\pi})^\alpha |u|_{H_h^{\alpha/2}}^2 \le ((-\Delta_h)_2^{\alpha/2} u, u)_h \le |u|_{H_h^{\alpha/2}}^2. \tag{5.2.10}$$

For $u \in H_h^\alpha$, we have

$$(\frac{2}{\pi})^{2\alpha} |u|_{H_h^\alpha}^2 \le ((-\Delta_h)_2^{\alpha/2} u, (-\Delta_h)_2^{\alpha/2} u)_h \le |u|_{H_h^\alpha}^2. \tag{5.2.11}$$

   Proof   By (5.1.11) and Parseval's identity, we have

$$((-\Delta_h)_2^{\alpha/2} u, u)_h = \frac{1}{4\pi^2} \int_{-\pi/h}^{\pi/h} \int_{-\pi/h}^{\pi/h} \frac{1}{h^\alpha} [4\sin^2(\frac{k_1 h}{2}) + 4\sin^2(\frac{k_2 h}{2})]^{\alpha/2} |\hat{u}(k_1, k_2)|^2 dk_1 dk_2. \tag{5.2.12}$$

By the fact that $\frac{2}{\pi} x < \sin(x) \le x$ for $x \in (0, \pi/2)$, we have

$$(\frac{2}{\pi})^\alpha h^\alpha (k_1^2 + k_2^2)^{\alpha/2} \le [4\sin^2(\frac{k_1 h}{2}) + 4\sin^2(\frac{k_2 h}{2})]^{\alpha/2} \le h^\alpha (k_1^2 + k_2^2)^{\alpha/2}. \tag{5.2.13}$$

Combining the formulas above together, we obtain the desired result (5.2.10). Similarly, (5.2.11) can be proved.   □

   We are now in the position to present the stability and convergence of the scheme (5.2.4)-(5.2.5).

Theorem 5.2.4 (Stability). *For any $h > 0$, the fractional centered difference scheme (5.2.4)-(5.2.5) is uniquely solvable and stable with respect to the right hand side f in the following sense*

$$|u|_{H_h^\alpha} \le (\frac{\pi}{2})^\alpha \|f\|_{L_h^2}, \quad 0 < \alpha \le 2; \tag{5.2.14}$$

$$\|u\|_{L_h^\infty} \le C_\alpha (\frac{\pi}{2})^\alpha \|f\|_{L_h^2}, \quad 1 < \alpha \le 2. \tag{5.2.15}$$

Here C_α is defined in Lemma 5.2.2.

Proof Taking the discrete inner product of (5.2.4) with $(-\Delta_h)_2^{\alpha/2}u$ on both sides gives

$$\big((-\Delta_h)_2^{\alpha/2}u,(-\Delta_h)_2^{\alpha/2}u\big)_h + \mu\big(u,(-\Delta_h)_2^{\alpha/2}u\big)_h = \big(f,(-\Delta_h)_2^{\alpha/2}u\big)_h.$$

Using the semi-positivity in Lemma 5.2.3 and Cauchy-Schwartz inequality, we have

$$\|(-\Delta_h)_2^{\alpha/2}u\|_{L_h^2}^2 \;\leq\; \frac{1}{2}\|f\|_{L_h^2}^2 + \frac{1}{2}\|(-\Delta_h)_2^{\alpha/2}u\|_{L_h^2}^2.$$

Consequently

$$\|(-\Delta_h)_2^{\alpha/2}u\|_{L_h^2} \leq \|f\|_{L_h^2}.$$

Using the norm equivalence in Lemma 5.2.3, we have

$$(\frac{2}{\pi})^\alpha|u|_{H_h^\alpha} \leq \|(-\Delta_h)_2^{\alpha/2}u\|_{L_h^2} \leq \|f\|_{L_h^2}. \tag{5.2.16}$$

Taking $f = 0$ leads to $|u|_{H_h^\alpha} = 0$. By (5.2.8) and (5.2.7) we have $u = 0$, which implies that there exists a unique solution to the scheme (5.2.4)-(5.2.5). This completes the proof. $\qquad\square$

Theorem 5.2.5 (Convergence). *For sufficiently small h, suppose that $U_{i,j} = u(ih,jh)$ be the solution of equation (1.2.1)-(1.2.2) and $u_{i,j}$ be the numerical solution of the difference scheme (5.2.4)-(5.2.5). Let $u \in W^{\gamma+\alpha,1}(\mathbb{R}^2)$ with a positive constant $\gamma \leq 2$, it holds that*

$$|U - u|_{H_h^\alpha} \leq c_u(\frac{\pi}{2})^\alpha h^\gamma, \quad 0 < \alpha \leq 2.$$

$$\|U - u\|_{L_h^\infty} \leq C_u C_\alpha(\frac{\pi}{2})^\alpha h^\gamma, \quad 1 < \alpha \leq 2.$$

Here c_u is defined in (5.2.3) and C_α are defined in Lemma 5.2.2 respectively.

Proof Define the error grid function as $e_{i,j} =: U_{i,j} - u_{i,j}$. Subtracting (5.2.4) from (5.2.2) leads to the error equation

$$(-\Delta_h)_2^{\alpha/2}e_{i,j} + \mu e_{i,j} = (T_u)_{i,j}, \quad (ih,jh) \in \Omega_h, \tag{5.2.17}$$
$$e_{i,j} = 0, \quad (ih,jh) \in \Omega_h^c. \tag{5.2.18}$$

Following the similar argument as the proof for stability, we can obtain

$$|e|_{H_h^\alpha} \leq (\frac{\pi}{2})^\alpha\|T_u\|_{L_h^2} \leq c_u h^\gamma, \quad 0 < \alpha \leq 2. \tag{5.2.19}$$

$$\|e\|_{L_h^\infty} \leq C_\alpha(\frac{\pi}{2})^\alpha\|T_u\|_{L_h^2} \leq C_u h^\gamma, \quad 1 < \alpha < 2. \tag{5.2.20}$$

This completes the proof.

$\qquad\square$

Remark 5.2.6. *By discrete fractional Poincare inequality holds in the discrete norms, we can obtain $\|U - u\|_{L_h^2} \leq ch^\gamma$, with c independent of h for $0 < \alpha \leq 2$.*

By (5.2.19), it suffices to have weaker condition $\|T_u\|_{L_h^2} \leq \tilde{C}_u h^\gamma$ rather than $\|T_u\|_{L_h^\infty} \leq C_u h^\gamma$ to achieve the γ-th convergence order.

5.3 Implementations

In this section we present a matrix-free fast solver for solving the resulting linear system discretized from the rectangular domain.

To illustrate the idea, we rewrite the scheme in matrix form although we never do this in the practical computation. Denote the vector $\mathbf{U} = (\mathbf{U}_1, \mathbf{U}_2, \cdots, \mathbf{U}_{N_2-1})^T$ with $\mathbf{U}_j = (u_{1,j}, u_{2,j}, \cdots, u_{N_1-1,j})$, where N_1 and N_2 are partition numbers in x_1 and x_2 direction respectively. The right hand side vector $\mathbf{b}$ is defined similarly. Then the scheme (5.2.4) can be written as

$$(\mathbf{A} + \mu h^\alpha \mathbf{I})\mathbf{U} = h^\alpha \mathbf{b} \tag{5.3.1}$$

where $\mathbf{I}$ is the identity matrix, $\mathbf{A}$ is a symmetric block Toeplitz matrix with Toeplitz blocks, defined as

$$\mathbf{A} = \begin{pmatrix} \mathbf{A}_0 & \mathbf{A}_1 & \mathbf{A}_2 & \cdots & \mathbf{A}_{N_2-3} & \mathbf{A}_{N_2-2} \\ \mathbf{A}_1 & \mathbf{A}_0 & \mathbf{A}_1 & \cdots & \mathbf{A}_{N_2-4} & \mathbf{A}_{N_2-3} \\ \mathbf{A}_2 & \mathbf{A}_1 & \mathbf{A}_0 & \cdots & \mathbf{A}_{N_2-5} & \mathbf{A}_{N_2-4} \\ \vdots & \vdots & \vdots & \ddots & \vdots & \vdots \\ \mathbf{A}_{N_2-3} & \mathbf{A}_{N_2-4} & \mathbf{A}_{N_2-5} & \cdots & \mathbf{A}_0 & \mathbf{A}_1 \\ \mathbf{A}_{N_2-2} & \mathbf{A}_{N_2-3} & \mathbf{A}_{N_2-4} & \cdots & \mathbf{A}_1 & \mathbf{A}_0 \end{pmatrix}_{N \times N}, \tag{5.3.2}$$

with

$$\mathbf{A}_j = \begin{pmatrix} a_{0,j} & a_{1,j} & a_{2,j} & \cdots & a_{N_1-3,j} & a_{N_1-2,j} \\ a_{1,j} & a_{0,j} & a_{1,j} & \cdots & a_{N_1-4,j} & a_{N_1-3,j} \\ a_{2,j} & a_{1,j} & a_{0,j} & \cdots & a_{N_1-5,j} & a_{N_1-4,j} \\ \vdots & \vdots & \vdots & \ddots & \vdots & \vdots \\ a_{N_1-3,j} & a_{N_1-4,j} & a_{N_1-5,j} & \cdots & a_{0,j} & a_{1,j} \\ a_{N_1-2,j} & a_{N_1-3,j} & a_{N_1-4,j} & \cdots & a_{1,j} & a_{0,j} \end{pmatrix}_{(N_1-1) \times (N_1-1)}. \tag{5.3.3}$$

Note that $\mathbf{A}_j$ is $N_1 - 1$ by $N_1 - 1$ matrix and $\mathbf{A}$ is $N_2 - 1$ by $N_2 - 1$ block matrix. Thus $\mathbf{A}$ is N by N matrix with $N = (N_1 - 1)(N_2 - 1)$ being the number of unknowns.

5.3.1 Preconditioned Conjugated Gradient (PCG) method

In [35], the authors only consider the CG method without preconditioning. However, for the fractional equation (1.2.1), when the coefficient μ is very large (e.g. for the time-dependent problem, $\mu = 1/\Delta t$ with Δt as the step-size in time), the CG method may converge very slowly. Hence, a preconditioner is entailed to reduce the iteration steps and accelerate the convergence of iterative solver.

Notice that the resulting equation equals the Toeplitz matrix plus a diagonal matrix. Denote the $\mathbf{A}_h = (\mathbf{A} + \bar{\mu} h^\alpha \mathbf{I})$ with $\bar{\mu}$ being the average of $\mu_{i,j}$. Then $\mathbf{A}_h$ is almost the same as $\mathbf{A}$ except for the entries of diagonal block matrix $\mathbf{A}_0$ becomes $a_{0,0}^{(\alpha)} + \mu h^\alpha$ instead of $a_{0,0}^{(\alpha)}$. Without confusion, we still use the notation $\mathbf{A}$ to briefly illustrate the choice of preconditioner.

We take the preconditioner $\mathbf{M}$ as block circulant matrix with circulant blocks, which has the same structure as (5.3.2). More specifically, the k-th entry in the j-th block of the first column of

$\mathbf{M}$ is given by

$$c_k^{(j)} = \frac{1}{(N_1-1)(N_2-1)}[(N_2-1-j)(N_1-1-k)a_{k,j} + j(N_1-1-k)a_{k,N_2-1-j}$$
$$+(N_2-1-j)ka_{N_1-1-k,j} + jka_{N_1-1-k,N_2-1-j}] \tag{5.3.4}$$

for $0 \le j < N_2 - 1$ and $0 \le k < N_1 - 1$. Thus it requires only $\mathcal{O}(N)$ ($N = (N_1-1)(N_2-1)$) operations to compute the first column of $\mathbf{M}$. Since $\mathbf{M}$ is a block-circulant-circulant-block matrix, it can be decomposed as (see [22])

$$\mathbf{M} = (\mathbf{F}_{N_2-1} \otimes \mathbf{F}_{N_1-1})^{-1}\text{diag}(\hat{\mathbf{c}})(\mathbf{F}_{N_2-1} \otimes \mathbf{F}_{N_1-1}), \tag{5.3.5}$$

where $\mathbf{F}_{N_2-1} \otimes \mathbf{F}_{N_1-1}$ represents the two-dimensional discrete Fourier transform matrix, and $\hat{\mathbf{c}} = (\mathbf{F}_{N_2-1} \otimes \mathbf{F}_{N_1-1})\mathbf{c}$ with $\mathbf{c}$ being the first column of matrix $\mathbf{M}$, and $\text{diag}(\hat{\mathbf{c}})$ is a diagonal matrix with $(\hat{\mathbf{c}})$ as a diagonal. In each iteration step, we solve the equation $\mathbf{My} = \mathbf{r}$ with the residue vector $\mathbf{r}$, which can be computed as follows

$$\mathbf{y} = \mathbf{M}^{-1}\mathbf{r} = (\mathbf{F}_{N_2-1} \otimes \mathbf{F}_{N_1-1})^{-1}\text{diag}^{-1}(\hat{\mathbf{c}})(\mathbf{F}_{N_2-1} \otimes \mathbf{F}_{N_1-1})\mathbf{r}, \tag{5.3.6}$$

In practice, the matrix-vector multiplication $(\mathbf{F}_{N_2-1} \otimes \mathbf{F}_{N_1-1})\mathbf{r}$ can be efficiently computed via a the two-dimensional fast Fourier transform and its inverse transform. Consequently the total computational cost for $\mathbf{M}^{-1}\mathbf{r}$ can be $\mathcal{O}(N \log N)$ with $N = (N_1-1)(N_2-1)$.

In each iteration step, we still need to perform matrix-vector multiplication $\mathbf{AU}$. As the matrix $\mathbf{A}$ is a block-Toeplitz-Toeplitz matrix, we use the fast Fourier transform to compute the matrix-vector product as in [35]. For convenience of reader, we describe it as follows.

First, we embed the Toeplitz matrix A_j for $(0 \le j < N_2 - 1)$ into a double circulant matrix and obtain

$$\mathbf{C}_j = \begin{pmatrix} \mathbf{A}_j & \mathbf{T}_j \\ \mathbf{T}_j & \mathbf{A}_j \end{pmatrix}_{2(N_1-1)\times 2(N_1-1)}, \tag{5.3.7}$$

where $\mathbf{T}_j$ is a $N_1 - 1$ by $N_1 - 1$ Toeplitz matrix defined by

$$\mathbf{T}_j = \begin{pmatrix} 0 & a_{N_1-2,j} & a_{N_1-3,j} & \cdots & a_{2,j} & a_{1,j} \\ a_{N_1-2,j} & 0 & a_{N_1-2,j} & \cdots & a_{3,j} & a_{2,j} \\ a_{N_1-3,j} & a_{N_1-2,j} & 0 & \cdots & a_{4,j} & a_{3,j} \\ \vdots & \vdots & \vdots & \ddots & \vdots & \vdots \\ a_{2,j} & a_{3,j} & a_{4,j} & \cdots & 0 & a_{N_1-2,j} \\ a_{1,j} & a_{2,j} & a_{3,j} & \cdots & a_{N_1-2,j} & 0 \end{pmatrix}_{(N_1-1)\times(N_1-1)}. \tag{5.3.8}$$

Based on the above setup, we can construct a block-Toeplitz-circulant-block matrix $\tilde{\mathbf{C}}_{2N\times 2N}$ with the same structure as that in (5.3.2) but each block is $\mathbf{C}_j$.

Next, as $\tilde{\mathbf{C}}$ is also a block Toeplitz matrix, we can further embed $\tilde{\mathbf{C}}$ into a double sized block circulant matrix and obtain

$$\mathbf{C} = \begin{pmatrix} \tilde{\mathbf{C}} & \mathbf{T} \\ \mathbf{T} & \tilde{\mathbf{C}} \end{pmatrix}, \tag{5.3.9}$$

where the matrix $\mathbf{T}$ is defined as

$$\mathbf{T} = \begin{pmatrix} 0 & \mathbf{C}_{N_2-2} & \mathbf{C}_{N_2-3} & \cdots & \mathbf{C}_2 & \mathbf{C}_1 \\ \mathbf{C}_{N_2-2} & 0 & \mathbf{C}_{N_2-2} & \cdots & \mathbf{C}_3 & \mathbf{C}_2 \\ \mathbf{C}_{N_2-3} & \mathbf{C}_{N_2-2} & 0 & \cdots & \mathbf{C}_4 & \mathbf{C}_3 \\ \vdots & \vdots & \vdots & \ddots & \vdots & \vdots \\ \mathbf{C}_2 & \mathbf{C}_3 & \mathbf{C}_4 & \cdots & 0 & \mathbf{C}_{N_2-2} \\ \mathbf{C}_1 & \mathbf{C}_2 & \mathbf{C}_3 & \cdots & \mathbf{C}_{N_2-2} & 0 \end{pmatrix}. \tag{5.3.10}$$

Let the vector $\mathbf{V}_j = (\mathbf{U}_j, \mathbf{0}_{1\times(N_1-1)})$, and introduce the block vector $\mathbf{V}^* = (\mathbf{V}_1, \mathbf{V}_2, \cdots, \mathbf{V}_{N_2-1})^T$ and $\mathbf{V} = (\mathbf{V}^*, \mathbf{0}_{1\times 2N})^T$. Thus the matrix-vector product $\mathbf{CV}$ can be efficiently computed as in the last subsection. After finishing the matrix-vector multiplications, we truncate the first $2N$ entries of $\mathbf{CV}$ as $\mathbf{W}$. Then the product $\mathbf{AU}$ can be obtained by removing every other N_1 entries of the vector $\mathbf{W}$. Hence, the computational cost in total is $\mathcal{O}(2N\log N)$ with the storage is linear as $\mathcal{O}(N)$, where $N = (N_1-1)(N_2-1)$.

5.3.2 The computation of the coefficients $a_{i,j}^{(\alpha)}$

In one dimension, the coefficients $a_j^{(\alpha)}$ can be reformulated in term of Gamma function, i.e., (see [72])

$$a_j^{(\alpha)} = \frac{1}{2\pi}\int_{-\pi}^{\pi}[4\sin^2(\frac{k}{2})]^{\alpha/2}e^{-\mathbf{i}jk}dk = \frac{(-1)^j\Gamma(\alpha+1)}{\Gamma(\alpha/2-j+1)\Gamma(\alpha/2+j+1)}. \tag{5.3.11}$$

We apply numerical quadrature to compute the coefficients $a_{i,j}^{(\alpha)}$. Take an integer number $M > \max(N_1, N_2)$ and step-size $\delta = 2\pi/M$. Denote $\varphi(k_1, k_2) = [4\sin^2(\frac{k_1}{2}) + 4\sin^2(\frac{k_2}{2})]^{\alpha/2}$. Applying the trapezoidal rule we have

$$\begin{aligned} a_{i,j}^{(\alpha)} &= \frac{1}{4\pi^2}\int_0^{2\pi}\int_0^{2\pi}\varphi(k_1, k_2)e^{-\mathbf{i}(ik_1+jk_2)}dk_1dk_2 \\ &\approx \frac{1}{M^2}\sum_{p=0}^{M-1}\sum_{q=0}^{M-1}\varphi(p\delta, q\delta)e^{-\mathbf{i}(ip\delta+jq\delta)} = \tilde{a}_{i,j}^{(\alpha)}. \end{aligned} \tag{5.3.12}$$

With the expression above we can use Matlab built-in function 'ifft2' to compute the coefficients $a_{i,j}^{(\alpha)}$ for $0 \leq i, j \leq M-1$ efficiently with the computational cost $\mathcal{O}(M\log M)$. Numerically it is found that the accuracy of approximation (5.3.12) is $\mathcal{O}(M^{-2-\alpha})$, which is observed in Table 5.1. Here the errors are measured as $E(M) = \left(\sum_{i=0}^N\sum_{j=0}^N |a_{i,j}^{(\alpha)}(M) - a_{i,j}^{(\alpha)}(2M)|^2\right)^{1/2}$.

Remark 5.3.1. *The convergence order of computing the coefficients in one-dimensional is $\mathcal{O}(M^{-1-\alpha})$ (not presented). In d-dimension, the convergence order of using the trapezoidal rule is expected to be $\mathcal{O}(M^{-d-\alpha})$.*

Remark 5.3.2. *By Grenander-Szegö Theorem (see [45]), it can be shown that the condition number of fractional difference matrix is $cond(A) = \mathcal{O}(h^{-\alpha})$, which is same as the matrix $(\mathbf{A} + \mu h^\alpha\mathbf{I})$ since the fractional order term dominates the resulting equation. Denote the approximated matrix $\tilde{\mathbf{A}}$ which is related to the coefficients $\tilde{a}_{i,j}^{(\alpha)}$. If take $M \approx h^{-1}$ in (5.3.12), then we have the second-order convergence when solving the approximated matrix equation $(\tilde{\mathbf{A}} + \mu h^\alpha\mathbf{I})\mathbf{U} = h^\alpha\mathbf{b}$ instead of original form (5.3.1). In fact, $\|\mathbf{U} - \tilde{\mathbf{U}}\| \leq cond(A)\epsilon \approx \mathcal{O}(h^2)$ with the tolerance $\epsilon = \mathcal{O}(M^{-\alpha-2})$.*

Table 5.1: The convergence order and the accuracy of computing the coefficients $a_{i,j}^{(\alpha)}$ using fft2.

	$\alpha = 1.8$		$\alpha = 1.4$		$\alpha = 1.0$		$\alpha = 0.6$	
M	$E(M)$	rate	$E(M)$	rate	$E(M)$	rate	$E(M)$	rate
2^8	8.85e-08		1.41e-06		1.22e-05		8.78e-05	
2^9	4.31e-09	4.36	1.01e-07	3.81	1.26e-06	3.27	1.31e-05	2.75
2^{10}	2.84e-10	3.92	8.95e-09	3.49	1.52e-07	3.06	2.11e-06	2.63
2^{11}	2.00e-11	3.83	8.36e-10	3.42	1.88e-08	3.01	3.46e-07	2.61

Here we summarize our method in the following algorithm.

Algorithm 5.3.3. *Given fractional order α, the rectangular domain Ω (containing the x- and y-axes in the first quadrant) and the grid size h.*

Step 1. Generate the grid $(ih, jh) \in h\mathbb{Z}^2$, $0 \leq i \leq N_1 - 1$ and $0 \leq j \leq N_2 - 1$. Compute the coefficient $a_{i,j}^{(\alpha)}$ using (5.3.12). Take $M = h^{-k} \geq \max(N_1, N_2)$, $k \geq 1$.

Step 2. Generate the preconditioner $\mathbf{M}$ with block-circulant-circulant preconditioner as in (5.3.4).

Step 3. Apply the preconditioned conjugate gradient method with the stopping condition $\left| U^{(r)} - U^{(r+1)} \right| \leq \epsilon$, where r is the iteration number and ϵ is at the order of h^3 or even smaller.

As mentioned earlier, the pre-computational cost is $\mathcal{O}(M^2)$ in Step 1. In Step 3, the computational cost is roughly the number of iterations r times the cost of matrix-vector products in each iterations with $\mathcal{O}(rN\log(N))$.

5.4 Numerical examples

In this section, several numerical examples are presented to show the efficiency and accuracy of the schemes. We first examine the convergence order and the accuracy of FCD formula and the high-order approximation in Example 5.4.1. Then we apply the proposed FCD scheme to solving the diffusion equation in Example 5.4.2. To show the wide application of finite difference method, we consider the problems on general domains in Example 5.5.1. In the last example, we apply the proposed FCD scheme to solving the time-dependent problem.

Throughout the examples, M is taken as 2^{14} to compute the coefficients $a_{i,j}^{(\alpha)}$ so that the accuracy of numerical solution will not be polluted. The tolerance of the CG and PCG method is set as 10^{-16} and the initial guess is fixed as zero in our simulations. All the simulations are performed on the personal computer with the configuration of 2.2GHz CPU and 8G RAM.

Example 5.4.1 (Approximations for two dimensional fractional Laplacian)**.** *Consider the function $u(x_1, x_2) = (1 - x_1^2)^\beta (1 - x_2^2)^\beta$ with a compact support $[-1, 1]^2$.*

In Table 5.2, the error is measured as $\|(-\Delta_h)^{\alpha/2}u - (-\Delta_{h/2})^{\alpha/2}u\|_{L_h^\infty}$ and the convergence order is $\log_2(\frac{E(2h)}{E(h)})$.

Table 5.2 shows that for function $u(x_1, x_2) \in W^{2+\alpha,1}(\mathbb{R}^2)$ for $\beta = 4$, our presented FCD scheme is second-order convergence, which verifies the theoretical result in Theorem 5.1.2.

Table 5.2: The convergence orders and errors for the approximation $(-\Delta_h)^{\alpha/2}u$ in (5.1.2). Here $u(x_1, x_2) = (1 - x_1^2)^4(1 - x_2^2)^4$ with a compact support $[-1, 1]^2$. (c.f. Example 5.4.1)

	$\alpha = 1.8$		$\alpha = 1.4$		$\alpha = 1$		$\alpha = 0.6$	
h	Error	Order	Error	Order	Error	Order	Error	Order
1/8	6.94e-01		2.84e-01		1.07e-01		3.44e-02	
1/16	1.80e-01	1.95	7.28e-02	1.96	2.72e-02	1.98	8.65e-03	1.99
1/32	4.53e-02	1.99	1.83e-02	1.99	6.84e-03	1.99	2.16e-03	2.00

Table 5.3: The convergence orders and errors for the approximation $(-\tilde{\Delta}_h)^{\alpha/2}u$ in (5.1.3). Here $u(x_1, x_2) = (1 - x_1^2)^4(1 - x_2^2)^4$ with a compact support $[-1, 1]^2$. (c.f. Example 5.4.1)

	$\alpha = 1.8$		$\alpha = 1.4$		$\alpha = 1$		$\alpha = 0.6$	
h	Error	Order	Error	Order	Error	Order	Error	Order
1/8	1.25e-01		3.83e-02		9.37e-03		1.30e-03	
1/16	1.06e-02	3.56	2.48e-03	3.95	5.92e-04	3.98	7.90e-05	4.04
1/32	7.06e-04	3.91	1.57e-04	3.99	3.71e-05	4.00	4.41e-06	4.16

In Table 5.3, the error is measured as $\|(-\tilde{\Delta}_h)^{\alpha/2}u(x_1, x_2) - (-\tilde{\Delta}_{h/2})^{\alpha/2}u(x_1, x_2)\|_{L_h^\infty}$ with $(-\tilde{\Delta}_h)^{\alpha/2} = \frac{4}{3}(-\Delta_{\frac{h}{2}})_2^{\alpha/2}u(x_1, x_2) - \frac{1}{3}(-\Delta_h)_2^{\alpha/2}u(x_1, x_2)$. Table 5.3 shows that for this example, our extrapolated scheme (5.1.3) is fourth-order as $u(x_1, x_2) \in W^{4+\alpha,1}(\mathbb{R}^2)$, which again verifies the accuracy of Theorem 5.1.3.

Lastly, we examine the convergence order of the fractional Laplacian at the internal point, e.g., $(x_1, x_2) = (0, 0)$ for simplicity. The error is measured as $|(-\Delta_h)^{\alpha/2}u - (-\Delta_{h/2})^{\alpha/2}u|_{(x_1,x_2)=(0,0)}$. Table 5.4 shows that for this function, our presented FCD scheme is second-order for $\beta = 4$ and $\beta = 1.5$, but with the order of 1.5 for $\beta = 0.5$ and the order of 1 for $\beta = 0$. It is illustrated from this example that the condition $u \in W^{2+\alpha,1}(\mathbb{R}^2)$ for $\alpha \in (0, 2)$ is sufficient but unnecessary to achieve the second-order convergence when the approximation at an interior point is interested.

Table 5.4: The convergence orders and errors for second-order approximation $(-\Delta_h)^{\alpha/2}u|_{(x_1,x_2)=(0,0)}$ in (5.1.2). Here $\alpha = 1.5$ and $u(x_1, x_2) = (1 - x_1^2)^\beta(1 - x_2^2)^\beta$ with a compact support $[-1, 1]^2$. (c.f. Example 5.4.1)

	$\beta = 4$		$\beta = 1.5$		$\beta = 0.5$		$\beta = 0$	
h	Error	Order	Error	Order	Error	Order	Error	Order
1/8	9.17e-02		9.89e-03		9.32e-03		3.38e-02	
1/16	2.31e-02	1.99	2.48e-03	1.99	2.97e-03	1.65	1.56e-02	1.12
1/32	5.78e-03	2.00	6.22e-04	2.00	9.82e-04	1.60	7.49e-03	1.06
1/64	1.44e-03	2.00	1.48e-04	2.07	3.45e-04	1.51	3.69e-03	1.02

Example 5.4.2 (FCD scheme for fractional diffusion equations). *Consider a fractional equation* $(-\Delta)^{\alpha/2}u + \mu u = f$ *on* $\Omega = [-1, 1]^2$. *Case 1,* $\mu = 1$ *and the exact solution is set as* $u(x_1, x_2) = (1 - x_1^2)^\beta(1 - x_2^2)^\beta$; *Case 2,* $\mu = 0$, *the exact solution is unknown.*

In our numerical tests, we take $\beta = 4$. The right hand side $f \approx f_h = (-\Delta_h)^{\alpha/2}u + u$ with small $h = 2^{-9}$. We first examine Case 1 to show the accuracy and efficiency of our scheme. The discrete fractional norm of the error is defined by $\sqrt{h^2 \sum_{ij}(\triangle_h^\alpha u_h - \triangle_h^\alpha u_{h/2})^2}$. In Table 5.5, the errors in fractional norm and convergence are listed with different α. From the table, we can see the convergence order is about two which is agreement with the theoretical results. Furthermore, we consider the error in the maximum norm which is measured as $E(h) = \|u_h - u_{h/2}\|_{L_h^\infty}$. Table 5.6 shows the errors and convergence orders with $\alpha = 1.8, 0.8$ for the finite difference scheme (5.2.4)-(5.2.5). From Table 5.6, we can observe that our scheme has the second-order convergence, which verifies Theorem 5.2.5. Furthermore, to show the performance of fast solver presented in this paper, the iteration number and CPU time are presented in Table 5.6 with different α and grid size N. From the Table 5.6, we can see the iteration number of PCG is smaller than that of CG. In particular the efficiency is more significant for large α as it can be expected from the condition number $\mathcal{O}(h^{-\alpha})$. From Table 5.6, we conclude that the CPU time increases roughly as $\mathcal{O}(N \log N)$ in this example.

Table 5.5: The convergence orders and errors in fractional norm of the finite difference scheme (5.2.4)-(5.2.5) for $(-\Delta)^{\alpha/2}u + u = 1$. (c.f. Example 5.4.2)

	$\alpha = 1.6$		$\alpha = 1.2$		$\alpha = 0.8$		$\alpha = 0.4$	
h	Error	Order	Error	Order	Error	Order	Error	Order
1/16	2.56e-02		9.00e-03		2.78e-03		6.34e-04	
1/32	4.32e-03	2.57	1.64e-03	2.45	5.60e-04	2.31	1.43e-04	2.15
1/64	7.08e-04	2.61	2.84e-04	2.53	1.08e-04	2.38	3.14e-05	2.19
1/128	1.38e-04	2.36	5.10e-05	2.48	2.09e-05	2.37	7.29e-06	2.11

Table 5.6: The convergence orders and errors of the finite difference scheme (5.2.4)-(5.2.5) for $(-\Delta)^{\alpha/2}u + u = 1$ in maximum-norm by PCG and CG method. (c.f. Example 5.4.2)

	$\alpha = 1.8$						$\alpha = 0.8$					
	Error	Order	PCG		CG		Error	Order	PCG		CG	
N			Iter	CPU time	Iter	CPU time			Iter	CPU time	Iter	CPU time
32^2	9.32e-03		30	4.24e-02	93	7.16e-02	3.49e-03		17	5.83e-02	33	3.57e-02
64^2	2.32e-03	2.00	45	0.15	170	0.19	8.69e-04	2.00	20	0.05	46	0.07
128^2	5.80e-04	2.00	64	0.55	364	1.92	2.17e-04	2.00	23	0.23	62	0.39
256^2	1.45e-04	2.00	97	2.20	687	10.55	5.39e-05	2.01	27	0.69	85	1.34
512^2	3.62e-05	2.00	153	26.13	1296	137.29	1.04e-05	2.37	30	5.44	114	12.64

Next we consider Case 2 with unknown solution. Especially for the lager grid size, the superiority of PCG over CG has again been illustrated by Table 5.7. However the convergence order is less than second order and is around $\mathcal{O}(h^{\alpha/2})$, which is caused by the weak singularity of the solution. In fact, [46] showed that the solution behaves like $u(x) \approx d^{\alpha/2}(x) + v(x)$ ($d(x)$ is the distance function to the boundary), which is Hölder continuous with the exponent $\alpha/2$. This implies the convergence order is at most $\mathcal{O}(h^{\alpha/2})$. Thus for certain problems with singularity, extra care has to be taken in order to keep the desired accuracy.

Table 5.7: The convergence orders and errors of the finite difference scheme (5.2.4)-(5.2.5) for $(-\Delta)^{\alpha/2}u = 1$ in maximum-norm by PCG and CG method. (c.f. Example 5.4.2)

	$\alpha = 1.8$						$\alpha = 0.8$					
	Error	Order	PCG		CG		Error	Order	PCG		CG	
N			Iter	CPU time	Iter	CPU time			Iter	CPU time	Iter	CPU time
128^2	6.18e-04		65	0.52	345	1.86	1.49e-02		26	0.27	72	0.41
256^2	3.32e-04	0.90	97	2.23	651	9.80	1.13e-02	0.40	30	0.66	97	1.53
512^2	1.79e-04	0.89	156	26.73	1337	147.0	8.59e-03	0.40	34	5.95	138	14.89
1024^2	9.61e-05	0.90	243	115.59	2568	838.08	6.53e-03	0.40	38	18.53	185	60.93

Example 5.4.3 (Application to time-dependent problems)**.** *Consider the fractional equation*

$$u_t + (-\Delta)^{\alpha/2}u = 0, \quad (x,t) \in \mathbb{R}^2 \times (0,T], \tag{5.4.1}$$

$$\lim_{x\to\infty} u(x,t) = 0, \quad t \in (0,T) \tag{5.4.2}$$

with the initial condition $u(x,0) = e^{-|x|^2}, \quad x \in \mathbb{R}^2.$

In this example, we test the convergence order of spatial direction in final time $T = 1$. Since the solution decays to zero, we truncate the finite domain $\Omega = [-8,8]^2$ in space as our computational domain. For time discretization we use backward Euler scheme. Since there is no exact solution we measure the error as $\|u_h(\cdot,T) - u_{h/2}(\cdot,T)\|_{l_h^\infty}$ with $T = n_t\Delta t$. To test the convergence orders in space, we take the small step-zie $\Delta t = 0.01$ so that the error in time will not pollute the accuracy in space.

The convergence orders and errors for different α are shown in Table 5.8, from which the second-order convergence can be observed. This further verifies the second-order approximation of our proposed FCD scheme. This example will help us for future study on Schrödinger equations with fractional Laplacian.

Table 5.8: The spatial convergence orders and errors for initial-boundary value problem (5.4.1)-(5.4.2) at final time $T = 1$. (c.f. Example 5.4.3)

	$\alpha = 1.6$		$\alpha = 1.2$		$\alpha = 0.8$		$\alpha = 0.4$	
h	Error	Order	Error	Order	Error	Order	Error	Order
1/4	3.92e-03		4.76e-03		4.91e-03		3.21e-03	
1/8	9.28e-04	2.08	1.13e-03	2.08	1.18e-03	2.05	7.88e-04	2.03
1/16	2.29e-04	2.02	2.78e-04	2.02	2.93e-04	2.02	1.93e-04	2.03
1/32	5.70e-05	2.01	6.86e-05	2.02	6.92e-05	2.08	3.15e-05	2.61

5.4.1 Fractional dynamics

Example 5.4.4. *Consider the following fractional Allen-Cahn equation*

$$u_t + (-\Delta)^{\alpha/2}u = -\frac{1}{\epsilon^2}(u^3 - u), \quad (x,t) \in \Omega \times (0,T],$$

$$u = -1 \quad (x,t) \in \Omega^c \times (0,T].$$
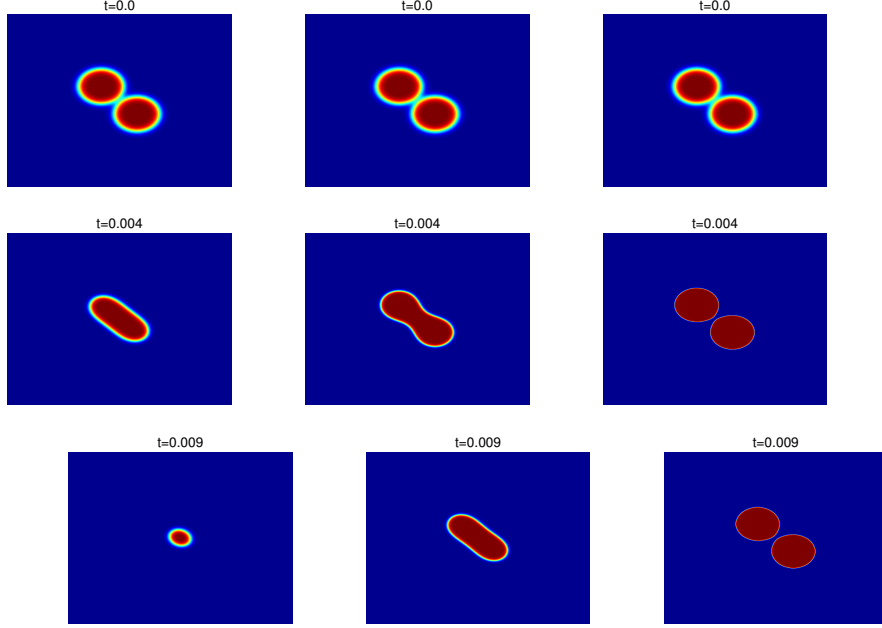
Figure 5.1: Dynamics of the two kissing bubbles for fractional Allen-Cahn equation (Left: $\alpha = 2$; Middle: $\alpha=1.8$; Right: $\alpha=1.4$).
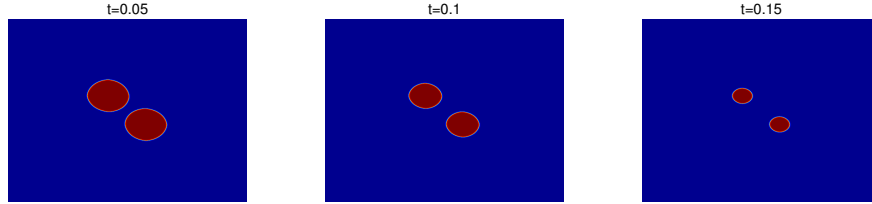
Figure 5.2: Evolution of the two "kissing" bubbles for fractional Allen-Cahn equation with $\alpha = 1.4$.

In the simulation $\Omega = [0,1]^2, \epsilon = 0.01$ and $u(x,0) = 1 - \tanh(\frac{d_1(x_1,x_2)}{2\epsilon}) - \tanh(\frac{d_2(x_1,x_2)}{2\epsilon})$ where $d_i(x_1,x_2) = \sqrt{(x_1 - a_i)^2 + (x_2 - b_i)^2}$ and $a_1 = b_1 = 0.42, a_2 = b_2 = 0.58$. Three level linearized finite-difference scheme (semi-implicit in time) is used in the simulation. Taking $h = 2^{-9}, \Delta t = 10^{-5}$ and letting $\overline{u} = u+1$, we can rewrite the problem as an equation of $\overline{u}$ with the extended homogeneous boundary conditions.

Figure. 5.1 demonstrates the time evolution of the two bubbles in both classical and fractional Allen-Cahn equations. From the picture we can see that the two bubbles first coalesce into one bubble, and then this newly formed bubble shrinks and are eventually absorbed by the fluid when $\alpha = 2.0$. When α is becoming smaller, the process which two bubbles shrink to one bubble is slower. It is interesting to note that when $\alpha = 1.4$, the two kissing bubbles separate into two single bubbles. From Figure. 5.2, we can see the two single bubbles will be absorbed by the fluid with $\alpha = 1.4$. From the simulation, we also can see that the width of the interface is influenced by the value of ϵ and the fractional power α.

5.5 Fictitious domain methods based on the finite difference method

The penalized formulation of the problem (1.2.1)-(1.2.2) with $\mu = 0$ is as follows

$$(-\Delta)^{\alpha/2}u_\epsilon + \frac{\chi}{\epsilon}u_\epsilon = f(x), \quad x \in R, \tag{5.5.1}$$

$$u_\epsilon(x) = 0, \quad x \in R^c, \tag{5.5.2}$$

where the penalized parameter $\epsilon > 0$ is small (depending h in numerical methods) and the characterized function $\chi(x) = 1$ if $x \in \Omega_1 = R \cap \Omega^c$ and $\chi(x) = 0$ if $x \in \Omega$. This formulation allows us to find approximated solutions $u_{\epsilon,h}$ as approximation of u. Since we are working on a rectangular domain, we can apply the fast algorithm in Algorithm 5.3.3.

When $\alpha = 2$, it is shown in [76] that u_ϵ converges to u with order $1/2$ when ϵ goes to 0. Following from [76], we take the penalty parameter $\epsilon = h^2$ and will examine the convergence order and accuracy of the penalty method in Example 5.5.1. Note that the equation (5.5.1) is variable coefficient and the preconditioner (5.3.4) can not be directly used and has to be modified. In this example, for simplicity, we use the CG method to show the feasibility of our method and refer the interested readers to [33] for modified preconditioner for variable coefficients case.

Example 5.5.1 (Applications on general domain). *Consider a fractional Poisson equation* $(-\Delta)^{\alpha/2}u = 1$ *on non-rectangular domain* Ω.

First we consider the circular domain to test the convergence order of fictitious domain method since in this case the exact solution is known as $u = (1 - x^2)^{\alpha/2}/\lambda_0^{\alpha/2}$ with $\lambda_0^{\alpha/2} = 2^\alpha[\Gamma(1 + \alpha/2)]^2$; see [37]. For $\alpha = 2$, the authors in [76] showed that the convergence order in L^2 norm is of first order for finite element method with respect to the original domain. For the fractional case, it can be expected the convergence of finite difference method is also of first order. Since in fractional case the solution has weaker singularity across the boundary, to avoid the effect of low regularity near the boundary on numerical solution, we test the convergence order in the internal domain $\Omega_0 = \{(x_1, x_2) \mid x_1^2 + x_2^2 < (\frac{3}{4})^2\}$ which is away from the boundary. Moreover, the error is measured as $\|u - u_h\|_{L_h^\infty(\Omega_0)}$. In Table 5.9, we can see the convergence order is of first order which agrees with the expected one.

Next we study other non-rectangular domains with unknown solutions. In Figure 5.2, we consider the domain with hole and L shape as benchmark tests, and provide the contour of numerical solution correspondingly. As we can see, the profile of numerical solution is continuously distributed from the internal part to the boundary of domain, which shows that our method is numerically viable and effective. These tests are important preparations toward studying of fractional Navier-Stokes equation in our future work.

5.6 Conclusion and discussion

In this section we proposed a simple and easy-to-implement fractional centered difference approximation to the fractional Laplacian on a uniform mesh using generating functions. We proved the proposed approximation has a γth-order ($\gamma \leq 2$) convergence and further applied it to fractional diffusion equations. For linear fractional diffusion equations, we showed the stability and convergence in a discrete energy norm and maximum norm.

For implementation, we presented a fast iterative solver using the preconditioned conjugated gradient method after applying the fast Fourier transform to compute the coefficients of the finite

Table 5.9: The convergence orders and errors for fictitious domain method. The penalty number ϵ is taken as h^2. The domain is a unit disk. (c.f. Example 5.5.1)

h	$\alpha = 2$		$\alpha = 1.6$		$\alpha = 1.2$		$\alpha = 0.8$	
	Error	Order	Error	Order	Error	Order	Error	Order
1/16	9.37e-03		9.77e-03		8.04e-03		4.15e-03	
1/32	5.23e-03	0.84	5.81e-03	0.75	5.31e-03	0.60	3.44e-03	0.27
1/64	2.58e-03	1.02	2.87e-03	1.02	2.61e-03	1.02	1.69e-03	1.03
1/128	1.26e-03	1.04	1.39e-03	1.04	1.25e-03	1.07	7.70e-04	1.13
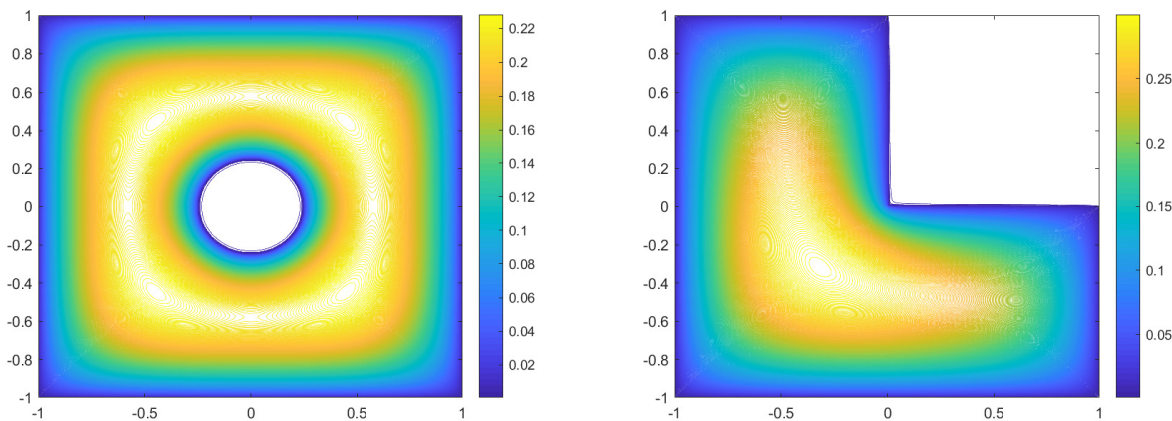
Figure 5.3: The contour of the numerical solution for equation $(-\Delta)^{\alpha/2} u = 1$ defined on the domain with hole (left) and L shape domain (right). Here $\alpha = 1.5$ and $h = 2^{-8}$. (c.f. Example 5.5.1)

difference scheme. We also provided several numerical examples to verify the γth-order ($\gamma \leq 2$) convergence of the new approximation. Based on the fast solver on rectangular domain, we developed an efficient fictitious method for the fraction Poisson equation on the general domain.

In this work, we haven't addressed the boundary singularity of the solutions. In our example using fictitious domain methods, the deterioration of the accuracy is from the oversimplified penalization. To keep the strength of this work using uniform meshes, we want to find an alternative method to adaptive methods such as in [7] while keeping the accuracy. A possible approach is the singularity subtraction techniques as in the extended finite element methods or in our recent work with finite difference methods [52].

Chapter 6

Toward the numerical simulation for the fractional Stokes problem

Our goal of this chapter is to discuss the spectral Galerkin method and its implementation for the steady fractional Stokes problems and non-steady Navier-Stokes problems. We will study the steady fractional stokes equations which describe the motion of incompressible viscous fluid flow at very low Reynolds numbers. For moderate Reynolds numbers the nonlinear convective term is often treated explicitly, while the linear (Stokes) part is treated implicitly. In order for this semi-implicit approach to be attractive, efficient unsteady Stokes solvers are required. In the follow-up sections, we will first concentrate on the model problem of two-term fractional Laplacian on the unit disk. The benefit of using the basis in polar coordinate form is that we essentially solve the one-dimensional problems in radial direction. The implementation is heavily relying on the one-dimensional case. Specifically, we will detailedly investigate the regularity and accuracy of the two-term fractional Laplacian model problem in Section 6.1, first starting from one-dimensional case and then moving on to the two dimensional one later. Next, we will describe the procedure of the implementation for the steady fractional Stokes Problems in Section 6.2. We also include the discussion of time dependent fractional Navier-Stokes problems in Section 6.3 before we conclude this chapter in the last section.

6.1 Two-term fractional Laplacian equations

6.1.1 1D modern problem

Consider the two-term fractional Laplacian model problem,

$$-\Delta u + (-\Delta)^{\alpha/2} u = f, \quad x \in \Omega, \tag{6.1.1}$$

$$u = 0, \quad x \in \partial\Omega. \tag{6.1.2}$$

To examine the accuracy and the efficiency of spectral Galerkin method using the polynomial basis, we will first consider one-dimensional case, $x \in (-1, 1)$.

The basis is taken as $\phi_n(x) = (1 - x^2)P_n^1(x)$ for $n = 0, 1, \cdots, N$. Here N is a discretization parameter for spectral Galerkin method. The fractional derivative of $\phi_n(x)$ can be calculated as follows.

Expand the basis $\phi_n(x)$ in terms of different Jacobi polynomials, i.e.,

$$\phi_n(x) = (1 - x^2)P_n^1(x) = (1 - x^2)^{\alpha/2} \sum_{j=0}^{\infty} \tilde{c}_{j,n}^{\alpha/2 \to 1} P_j^{\alpha/2}(x), \tag{6.1.3}$$

with the connection coefficients

$$\tilde{c}_{j,n}^{\alpha/2 \to 1} = \frac{1}{h_j^{\alpha/2}} \int_{-1}^{1} P_j^{\alpha/2}(x)(1 - x^2)P_n^1(x)dx = \frac{h_n^1}{h_j^{\alpha/2}} c_{j,n}^{\alpha/2 \to 1}, \tag{6.1.4}$$

where we recall that

$$h_n^{\beta} = \left\| P_n^{\beta} \right\|_{\omega^{\beta}}^2 = \frac{2^{2\beta+1}(\Gamma(n + \beta + 1))^2}{(2n + 2\beta + 1)\Gamma(n + 2\beta + 1)\Gamma(n + 1)}. \tag{6.1.5}$$

Here it should be noted that by orthogonality of the Jacobi Polynomials, we know that $c_{j,n}^{\alpha/2 \to 1} = 0$ for $j < n$.

Recall the Pochhammer symbol $(a)_n = a(a + 1) \cdots (a + n - 1) = \Gamma(n + a)/\Gamma(a)$ for any $a \in \mathbb{R}$ and $n \in \mathbb{N}_0$. Note that the explicit analytical derivation of $c_{j,n}^{\alpha/2 \to 1}$ can be derived through the connection matrix; see formula (7.34) in Page 63 in [11].

$$P_n^{\gamma,\gamma} = \sum_{k=0}^{[n/2]} c_{n,n-2k}^{\gamma \to \beta} P_{n-2k}^{\beta,\beta}(x). \tag{6.1.6}$$

where the connection coefficient is

$$c_{n,n-2k}^{\gamma \to \beta} = \frac{(\gamma + 1)_n}{(2\beta + 1)_n} \cdot \frac{(2\beta + 1)_{n-2k}(\gamma + 1/2)_{n-k}(\beta + 3/2)_{n-2k}(\gamma - \beta)_k}{(\beta + 1)_{n-2k}(\beta + 3/2)_{n-k}(\beta + 1/2)_{n-2k}k!} \tag{6.1.7}$$

By the connection relation between different Jacobi polynomials, we can derive

$$c_{j,n}^{\alpha/2 \to 1} = \frac{(\alpha/2 + 1)_j(3)_n[(\alpha + 1)/2]_{(n+j)/2}(5/2)_n(\alpha/2 - 1)_{(j-n)/2}}{(3)_j(2)_n(5/2)_{(n+j)/2}(3/2)_n[(j - n)/2]!} \tag{6.1.8}$$

for $j - n = 2k$ with nonnegative integer k and $c_{j,n}^{\alpha/2 \to 1} = 0$ for others. By (3.3.8), we know that

$$c_{j,n}^{\alpha/2 \to 1} \approx j^{\alpha/2 - 2}n^2(j + n)^{\alpha/2 - 2}(j - n)^{\alpha/2 - 2}, \tag{6.1.9}$$

$$\tilde{c}_{j,n}^{\alpha/2 \to 1} \approx j^{\alpha/2 - 1}n(j + n)^{\alpha/2 - 2}(j - n)^{\alpha/2 - 2}. \tag{6.1.10}$$

Remark 6.1.1. *The analytical expression of connection coefficients may be still a little cumbersome for the computation but it is a key for the regularity estimates of the solution!*

We use the bootstrapping technique to prove the regularity of solution. The key step is to analyze the low-order perturbation term $(-\Delta)^{\alpha/2}u$, which determines the highest regularity index of the solution.

By the pseudo-eigen relation in Lemma 2.3.1, we have

$$(-\Delta)^{\alpha/2}[(1 - x^2)P_n^1(x)] = \sum_{j=n}^{\infty} \lambda_j^{\alpha} \tilde{c}_{j,n}^{\alpha/2 \to 1} P_j^{\alpha/2}(x). \tag{6.1.11}$$

84

Then transforming into the expansion with respect to the basis $P_j^1(x)$ leads to

$$(-\Delta)^{\alpha/2}[(1-x^2)P_n^1(x)] = \sum_{j=n}^{\infty} \lambda_j^{\alpha} \tilde{c}_{j,n}^{\alpha/2 \to 1} \sum_{k=0}^{j} c_{j,k}^{\alpha/2 \to 1} P_k^1(x). \tag{6.1.12}$$

Lemma 6.1.2. *If $v \in B_\omega^s$ with $s \geq 2$, then $-(\Delta)^{\alpha/2}(v\omega) \in B_\omega^{\min(s, 3-\alpha/2-\epsilon)}$ with arbitrarily small $\epsilon > 0$.*

Remark 6.1.3. *Up to this point we haven't finish the proof. Here we provide the outline. Let $v = (1-x^2)\sum_{n=0}^{\infty} \hat{v}_n P_n^1(x)$. Then*

$$\begin{aligned}
(-\Delta)^{\alpha/2} v &= \sum_{n=0}^{\infty} \hat{v}_n \sum_{j=n}^{\infty} \lambda_j^{\alpha} \tilde{c}_{j,n}^{\alpha/2 \to 1} \sum_{k=0}^{j} c_{j,k}^{\alpha/2 \to 1} P_k^1(x) \\
&= \sum_{j=0}^{\infty} \left(\sum_{n=0}^{j} \hat{v}_n \lambda_j^{\alpha} \tilde{c}_{j,n}^{\alpha/2 \to 1} \right) \sum_{k=0}^{j} c_{j,k}^{\alpha/2 \to 1} P_k^1(x) \\
&= \sum_{k=0}^{\infty} \left[\sum_{j=k}^{\infty} \left(\sum_{n=0}^{j} \hat{v}_n \tilde{c}_{j,n}^{\alpha/2 \to 1} \right) \lambda_j^{\alpha} c_{j,k}^{\alpha/2 \to 1} \right] P_k^1(x). \tag{6.1.13}
\end{aligned}$$

Thus it suffices to estimate

$$\sum_{j=k}^{\infty} \left(\sum_{n=0}^{j} \hat{v}_n \tilde{c}_{j,n}^{\alpha/2 \to 1} \right) \lambda_j^{\alpha} c_{j,k}^{\alpha/2 \to 1} \leq C k^? \tag{6.1.14}$$

According to assumption we know $\hat{v}_n \approx n^{-s-\epsilon}$ for any positive number ϵ, and $\lambda_j^{\alpha} \approx j^{\alpha}$. Then by(6.1.9)- (6.1.10) we have

$$\sum_{n=0}^{j} \hat{v}_n \tilde{c}_{j,n}^{\alpha/2 \to 1} \approx j^{\alpha/2-1} \sum_{n=0}^{j} n^{1-s-\epsilon} \cdot (j^2 - n^2)^{\alpha/2-2} \leq C j^? \tag{6.1.15}$$

$$\lambda_j^{\alpha} c_{j,k}^{\alpha/2 \to 1} \approx j^{3\alpha/2-2} k^2 (j^2 - k^2)^{\alpha/2-2}, \tag{6.1.16}$$

It suffices to have the following optimal estimates of finite summation

$$\sum_{n=1}^{j-1} n^t \cdot (j^2 - n^2)^s \leq C j^?, \quad \sum_{j=n+1}^{\infty} j^t \cdot (j^2 - n^2)^s \leq C n^?. \tag{6.1.17}$$

We are now at the position to present the regularity of the two-term fractional Laplacian model problem.

Theorem 6.1.4 (Regularity in weighted Sobolev spaces). *For the problem 6.1.1-6.1.2, if $f \in H^{-1} \cap B_{\omega^1}^r$ with $r \geq 0$, then we have $\omega^{-1} u \in B_\omega^{2+\min(3-\alpha/2-\epsilon, r)}$ with $\epsilon > 0$ arbitrarily small.*

With above regularity results, we can expect our spectral Galerkin method has the convergence order up to $5 - \alpha/2$, which will be verified in the numerical experiments.

6.1.2 The implementation in 1D

In the computation we need to truncate the finite terms and choose the suitable approximation number J, i.e,

$$(-\Delta)^{\alpha/2}\phi_n(x) \approx \sum_{j=n}^{J} \lambda_j^{\alpha/2} \tilde{c}_{j,n}^{\alpha/2 \to 1} P_j^{\alpha/2}(x). \tag{6.1.18}$$

With above preparation, we first present the spectral Galerkin method for two-term Laplacian. Define

$$U_N := \text{Span}\{\phi_0, \phi_1, \ldots, \phi_N\},$$

where $\phi_k(x) := (1-x^2)P_k^1(x)$ for $0 \le k \le N$, and $\mathbb{P}_N$ is the set of all algebraic polynomials of degree at most N. The spectral Galerkin method is to find $u_N \in U_N$ such that

$$a(u_N, v_N) = (f, v_N), \quad \forall v_N \in U_N, \tag{6.1.19}$$

with $a(u_N, v_N) = (-\Delta u_N, v_N) + ((-\Delta)^{\alpha/2} u_N, v_N)$.

Plugging $u_N = \sum_{n=0}^{N} \hat{u}_n \phi_n(x)$ into (6.1.19) and taking $v_N = \phi_k(x)$ for $k = 0, 1, \ldots, N$, we obtain the following linear equation from the orthogonality of Jacobi polynomials and Lemma 2.3.1 that

$$A\hat{u} = \hat{f}, \tag{6.1.20}$$

where $\hat{u} = (\hat{u}_0, \hat{u}_1, \ldots, \hat{u}_N)^T$, $\hat{f} = (\hat{f}_0, \hat{f}_1, \ldots, \hat{f}_N)^T$ with $\hat{f}_k = (f, \phi_k)$. Here the matrix $A = S^{(2)} + M^{(\alpha)}$, where $S^{(\alpha)}$ is a diagonal matrix with

$$S^{(\alpha)} = \text{diag}(\lambda_0^\alpha h_0^{\alpha/2}, \lambda_1^\alpha h_1^{\alpha/2}, \cdots, \lambda_N^\alpha h_N^{\alpha/2}),$$

and the entries of matrices $M^{(\alpha)}$ are

$$M_{k,n}^{(\alpha)} = \int_{-1}^{1} (-\Delta)^{\alpha/2} \phi_n(x) \phi_k(x)\, dx. \tag{6.1.21}$$

If a direct solver is applied to (6.1.20), we then need to find $M_{k,n}^{(\alpha)}$. Here we apply Gauss-Jacobi quadrature rules as follows. For $M_{k,n}^{(\alpha)}$, recalling the notation of (6.1.4), we obtain

$$M_{k,n}^{(\alpha)} \approx \sum_{j=0}^{J} \lambda_j^{\alpha/2} \tilde{c}_{j,n}^{\alpha/2 \to 1} \int_{-1}^{1} P_j^{\alpha/2}(x) P_k^1(x)(1-x^2) dx = \sum_{j=0}^{J} \lambda_j^{\alpha/2} h_j^{\alpha/2} \tilde{c}_{j,n}^{\alpha/2 \to 1} \tilde{c}_{k,j}^{\alpha/2 \to 1},$$

with

$$\tilde{c}_{k,j}^{\alpha/2 \to 1} = \frac{1}{h_j^{\alpha/2}} \int_{-1}^{1} P_j^{\alpha/2}(x) P_k^1(x)(1-x^2) dx \approx \frac{1}{h_j^{\alpha/2}} \sum_{i=0}^{N} P_j^{\alpha/2}(\mathsf{x}_i) P_k^1(\mathsf{x}_i) \mathsf{w}_i,$$

where x_i's are the zeros of Jacobi polynomial $P_{\mathsf{N}+1}^1(x)$ and w_i's are the corresponding quadrature weights. The quadrature rule here is exact since $n + k \le 2\mathsf{N}$ while the quadrature rule is exact for all $(2\mathsf{N}+1)$-th order polynomials.

If we introduce the rectangular matrix C of size $N+1$ by $J+1$, then the matrix equation is

$$(S^{(2)} + CS^{(\alpha)}C^T)\hat{u} = \hat{f} \tag{6.1.22}$$

To find $\hat{f}_k = (f, \phi_k)$, we use a different Gauss-Jacobi quadrature rule: $\hat{f}_k \approx \sum_{j=0}^{N} f(x_j) P_k^1(x_j) w_j$.

Here x_j's are the roots of Jacobi polynomial $P_{N+1}^{\alpha/2}(x)$ and w_j's are the corresponding quadrature weights. We then can solve (6.1.20) using any efficient direct solver.

Note that the optimal relation between J and N are determined by the regularity and error estimates. In our test problem, we will consider the smooth right hand side f. In this case, the reference solution is choose $u_{\text{ref}} = u_N$ with $N = 512$. In the numerical test, we will choose large number J, the different cases as $J = N/4$, $N/2$, N, $2N$ and up to $16N$. We found the numerical results are the same except for $J = N/4$ under which the convergence orders change dramatically and implies that it is not advisable to choose too small number J. We only present the case for $N/2$ and $\alpha \in (1,2)$ in our report since the other cases are almost the same.

6.1.3   Numerical results in 1D

In the computation, we measure the error as follows

$$E(N) = \|u_{\text{ref}} - u_N\|_{L^2_{\omega^{-1}}}, \quad E^*(N) = \|u_{\text{ref}} - u_N\|_{L^2}$$

Table 6.1: Convergence orders and errors of the spectral Galerkin method (6.1.19) for the equation $-\Delta u + (-\Delta)^{\alpha/2}u = \sin x$. The estimated convergence order is $5 - \alpha/2 - \epsilon$ in negative weighted L^2-norm.

| N | $\alpha = 1.2$ | | $\alpha = 1.4$ | | $\alpha = 1.6$ | | $\alpha = 1.8$ | |
	$E(N)$	rate	$E(N)$	rate	$E(N)$	rate	$E(N)$	rate
16	5.45e-07		7.16e-07		7.53e-07		4.85e-07	
32	3.00e-08	4.18	4.35e-08	4.04	5.15e-08	3.87	3.68e-08	3.72
64	1.53e-09	4.29	2.42e-09	4.17	3.17e-09	4.02	2.53e-09	3.86
128	7.55e-11	4.34	1.28e-10	4.24	1.84e-10	4.11	1.64e-10	3.95
256	3.64e-12	4.37	6.65e-12	4.27	1.03e-11	4.15	1.03e-11	4.00
Order		4.40		4.30		4.20		4.10

From the tables, we can see that the convergence order is around $5 - \alpha/2$ in negative weighted L^2-norm and $5 - \alpha/2$ in non-weighted L^2-norm, which suggests the regularity of solution is about $5 - \alpha/2$ or up to $5.5 - \alpha/2$.

From the tables, we can see that the convergence order is around $5 - \alpha/2$ in negative weighted L^2-norm and $5 - \alpha/2$ in non-weighted L^2-norm, which suggests the regularity of solution is about $5 - \alpha/2$ or up to $5.5 - \alpha/2$.

6.1.4   The implementation in 2D

Let

$$c_{n,j,m}^{\alpha/2 \to 1} =: \frac{1}{h_j^{\alpha/2,m}} \int_{-1}^{1} P_n^{1,m}(t) P_j^{\alpha/2,m}(t)(1-t)(1+t)^m dt. \tag{6.1.23}$$

Table 6.2: Convergence orders and errors of the spectral Galerkin method (6.1.19) for the equation $-\Delta u + (-\Delta)^{\alpha/2}u = \sin x$. The estimated convergence order is $5.5 - \alpha/2 - \epsilon$ in L^2-norm.

| N | $\alpha = 1.2$ | | $\alpha = 1.4$ | | $\alpha = 1.6$ | | $\alpha = 1.8$ | |
	$E^*(N)$	rate	$E^*(N)$	rate	$E^*(N)$	rate	$E^*(N)$	rate
16	2.35e-07		3.02e-07		3.09e-07		1.96e-07	
32	1.00e-08	4.56	1.42e-08	4.41	1.62e-08	4.25	1.13e-08	4.11
64	3.80e-10	4.72	5.85e-10	4.60	7.41e-10	4.45	5.74e-10	4.31
128	1.36e-11	4.81	2.26e-11	4.69	3.13e-11	4.56	2.69e-11	4.42
256	4.71e-13	4.85	8.44e-13	4.74	1.27e-12	4.62	1.21e-12	4.48
Order		4.90		4.80		4.70		4.60

Table 6.3: Convergence orders and errors of the spectral Galerkin method (6.1.19) for the equation $-\Delta u + (-\Delta)^{\alpha/2}u = |\sin x|$. The estimated convergence order is $3.5 - \epsilon$ in negative weighted L^2-norm.

| N | $\alpha = 1.2$ | | $\alpha = 1.4$ | | $\alpha = 1.6$ | | $\alpha = 1.8$ | |
	$E(N)$	rate	$E(N)$	rate	$E(N)$	rate	$E(N)$	rate
16	4.70e-05		4.69e-05		4.67e-05		4.62e-05	
32	5.30e-06	3.15	5.30e-06	3.15	5.28e-06	3.14	5.25e-06	3.14
64	5.33e-07	3.31	5.33e-07	3.31	5.33e-07	3.31	5.31e-07	3.31
128	5.04e-08	3.40	5.04e-08	3.40	5.04e-08	3.40	5.03e-08	3.40
256	4.59e-09	3.46	4.59e-09	3.46	4.59e-09	3.46	4.58e-09	3.46
Order		3.50		3.50		3.50		3.50

Table 6.4: Convergence orders and errors of the spectral Galerkin method (6.1.19) for the equation $-\Delta u + (-\Delta)^{\alpha/2}u = |\sin x|$. The estimated convergence order is $3.5 - \epsilon$ in L^2-norm.

| N | $\alpha = 1.2$ | | $\alpha = 1.4$ | | $\alpha = 1.6$ | | $\alpha = 1.8$ | |
	$E^*(N)$	rate	$E^*(N)$	rate	$E^*(N)$	rate	$E^*(N)$	rate
16	4.33e-05		4.32e-05		4.29e-05		4.25e-05	
32	5.06e-06	3.10	5.05e-06	3.09	5.04e-06	3.09	5.01e-06	3.08
64	5.20e-07	3.28	5.20e-07	3.28	5.19e-07	3.28	5.18e-07	3.28
128	4.97e-08	3.39	4.97e-08	3.39	4.97e-08	3.39	4.96e-08	3.38
256	4.56e-09	3.45	4.56e-09	3.45	4.56e-09	3.45	4.55e-09	3.45
Order		3.50		3.50		3.50		3.50

Clearly, $c_{n,j,m}^{\alpha/2 \to 1} = 0$ for $j < n$. Thus we only care about $c_{n,j,m}^{\alpha/2 \to 1}$ for $j \geq n$. Then using the expansion $P_n^{\gamma,\beta}(t) = \sum_{k=0}^{n} c_{n,k,\beta}^{\gamma \to \delta} P_k^{\delta,\beta}(t)$ (see formula (7.33) in [11]) with

$$c_{n,k,\beta}^{\gamma \to \delta} = \frac{(\beta+1)_n(\gamma-\delta)_{n-k}(\delta+\beta+1)_k(\delta+\beta+2)_{2k}(\beta+\gamma+n+1)_k}{(\delta+\beta+2)_n(1)_{n-k}(\beta+1)_k(\delta+\beta+1)_{2k}(\delta+\beta+n+2)_k}, \tag{6.1.24}$$

and the orthogonality property of Jacobi polynomials, then we obtain

$$c_{n,j,m}^{\alpha/2 \to 1} = \frac{h_n^{1,m}}{h_j^{\alpha/2,m}} \frac{(m+1)_j (\alpha/2 - 1)_{(j-n)} (1+m+1)_n (1+m+2)_{2n} (m+\alpha/2+j+1)_n}{(1+m+2)_j (1)_{j-n} (m+1)_n (1+m+1)_{2n} (1+m+j+2)_n}. \quad (6.1.25)$$

Using the (3.3.8) leads to

$$c_{n,j,m}^{\alpha/2 \to 1} \approx \frac{n(2j+m)}{j^{\alpha/2}(j-n)^{2-\alpha/2}(m+n+j)^{2-\alpha/2}}. \quad (6.1.26)$$

The above estimate plays an essential role to analyze the regularity of the solution for two-dimensional problem on a disk.

We first present the spectral Galerkin method using the basis from the pseudo-eigenfunction in Lemma 3.3.1. Define the finite dimensional space

$$U_{M,N} := \mathrm{Span}\{(1-r^2)\cos(m\theta)Q_n^{1,m}(r), (1-r^2)\sin(m\theta)Q_n^{1,m}(r), 0 \le m \le M, 0 \le n \le N\},$$

where $Q_n^{1,m}(r)$'s are from Lemma 3.3.1. The spectral Galerkin method is to find $u_{M,N} \in U_{M,N}$ such that

$$a(u_{M,N}, v_{M,N}) = (f, v_{M,N}), \quad \forall v_{M,N} \in U_{M,N}, \quad (6.1.27)$$

with $a(u_{M,N}, v_{M,N}) := (-\Delta u_{M,N}, v_{M,N}) + ((-\Delta)^{\alpha/2} u_{M,N}, v_{M,N})$.

For linear problem (6.1.27), plug $u_{M,N} = \sum_{m=0}^{M} \sum_{n=0}^{N} [u_{m,n}^{(1)} \phi_{m,n}^{(2,1)} + u_{m,n}^{(2)} \phi_{m,n}^{(2,2)}] \in U_{M,N}$ into (6.1.27) and take $v_{M,N} = \phi_{m,n}^{(i)}(x)$ for $i = 1, 2$, $m = 0, 1, \ldots M$ and $n = 0, 1, \ldots, N$, where

$$\phi_{m,n}^{(\alpha,1)}(r,\theta) := (1-r^2)\cos(m\theta)Q_n^{1,m}(r), \quad \phi_{m,n}^{(\alpha,2)}(r,\theta) := (1-r^2)\sin(m\theta)Q_n^{1,m}(r).$$

By the orthogonality of $\cos(m\theta)$ and $\sin(m\theta)$ in $L^2([0,2\pi])$, the resulting linear system can be represented as

$$S_m^{(2,i)} U_m^{(i)} + M_m^{(\alpha,i)} U_m^{(i)} = F_m^{(i)}, \quad (6.1.28)$$

where $U_m^{(i)} = (u_{m,0}^{(i)}, u_{m,1}^{(i)}, \ldots, u_{m,N}^{(i)})^T$, $0 \le m \le M$ for $i = 1, 2$. The matrices $S_m^{(\alpha,i)}$, $M_m^{(\alpha,i)}$ for $\alpha \in (0,2]$, and $F_m^{(i)}$ will be elaborated in the following.

The stiffness matrix $(S_m^{(\alpha,i)})_{k,n}$ in (6.1.28) are diagonal matrix. By the orthogonality of Jacobi polynomials and Lemma 3.3.1, we have

$$(S_m^{(\alpha,1)})_{k,n} = ((-\Delta)^{\alpha/2}\phi_{m,n}^{(\alpha,1)}, \phi_{m,k}^{(\alpha,1)}) = (\frac{1}{2})^{\alpha/2+m+2}\pi\lambda_{m,n}^{\alpha} h_n^{\alpha/2,m} \delta_{k,n}\delta_m, \quad 0 \le m \le M,$$

where $\delta_{k,n} = 1$ if $k = n$ and 0 otherwise; $\delta_0 = 2$ and $\delta_m = 1$ for $m \ge 1$; $h_n^{\alpha/2,m}$ is defined in (6.1.5) and $\lambda_{m,n}^{\alpha}$ from Lemma 3.3.1. More precisely we have

$$(S_m^{(\alpha,1)})_{k,n} = \frac{2^{\alpha-1}\pi}{2n+\alpha/2+m+1} \left(\frac{\Gamma(1+\alpha/2+n)}{\Gamma(n+1)}\right)^2 \delta_{k,n}\delta_m, \quad 0 \le m \le M.$$

Similarly, $(S_m^{(\alpha,2)})_{k,n} = ((-\Delta)^{\alpha/2}\phi_{m,n}^{(\alpha,2)}, \phi_{m,k}^{(\alpha,2)})$ and we have $S_m^{(\alpha,1)} = S_m^{(\alpha,2)}$ for $1 \le m \le M$.

89

Following the similar argument in 1D, we can derive the lower order fractional mass matrix Introduce the connection matrix C_m of the size $N+1$ by $J+1$ with entries as $(C_m)_{n,j} = c_{n,j,m}$. Then

$$(M_m^{(\alpha,1)})_{k,n} = ((-\Delta)^{\alpha/2}\phi_{m,n}^{(\alpha,1)}, \phi_{m,k}^{(\alpha,1)}) \approx 2^{\alpha/2-1}\sum_{j=0}^{J} c_{n,j,m}c_{k,j,m}(\frac{1}{2})^{\alpha/2+m+2}\pi\lambda_{m,j}^{\alpha}h_j^{\alpha/2,m}\delta_m. \quad (6.1.29)$$

Thus $M_m^{(\alpha,1)} \approx 2^{\alpha/2-1}C_m S^{(\alpha,1)}C_m^T$ and the resulting matrix equations are

$$(S_m^{(2,1)} + 2^{\alpha/2-1}C_m S^{(\alpha,1)}C_m^T)U_m^{(1)} = F_m^{(1)}, \quad (6.1.30)$$

Similarly, $(M_m^{(\alpha,2)})_{k,n} = ((-\Delta)^{\alpha/2}\phi_{m,n}^{(\alpha,2)}, \phi_{m,k}^{(\alpha,2)})$ and we have $M_m^{(1)} = M_m^{(2)}$ for $0 \leq m \leq M$. The right hand side can be treated similarly as that in Chapter 3.

In the numerical tests, we take quadrature numbers $\mathsf{N} = \max(N+60, 512)$ and $\mathsf{M} = 2(M+1)$.

Table 6.5: Convergence orders and errors of the spectral Galerkin method (6.1.19) for the equation $-\Delta u + (-\Delta)^{\alpha/2}u = \sin x_1 + 2x_2$. The estimated convergence order is $5 - \alpha/2 - \epsilon$ in nonnegative weighted L^2-norm.

	$\alpha = 0.2$		$\alpha = 0.4$		$\alpha = 0.6$		$\alpha = 0.8$	
N	$E(N)$	rate	$E(N)$	rate	$E(N)$	rate	$E(N)$	rate
16	1.40e-09		4.99e-09		1.69e-08		6.03e-08	
32	4.65e-11	4.92	1.61e-10	4.95	4.16e-10	5.34	1.02e-09	5.89
64	1.73e-12	4.75	6.43e-12	4.65	1.75e-11	4.57	4.15e-11	4.62
128	6.13e-14	4.82	2.44e-13	4.72	7.13e-13	4.62	1.80e-12	4.53
256	2.13e-15	4.85	9.01e-15	4.76	2.82e-14	4.66	7.64e-14	4.56
Order		4.90		4.80		4.70		4.60

In this example we consider the smooth data. Since the regularity reveals that the solution is smooth in theta direction, we only need to study the accuracy of the solution in radial direction. From Table 6.5, we can observe that the convergence order of the solution is $5 - \alpha/2$ which is consistent with that in one dimensional case. The incorporation of the principle term lift the regularity of the solution for the fractional order term dominant problems. We will give a full analysis of such error estimates in the future work.

6.2 Extension to steady fractional-stokes problems

Consider the axisymmetric steady model problem

$$-\Delta\mathbf{u} + (-\Delta)^{\alpha/2}\mathbf{u} + \nabla p = \mathbf{F}, \quad x \in \Omega, \quad (6.2.1)$$

$$\nabla \cdot \mathbf{u} = 0, \quad x \in \Omega, \quad (6.2.2)$$

$$\mathbf{u} = \mathbf{0}, \quad x \in \partial\Omega. \quad (6.2.3)$$

where the domain Ω is a unit disk. Since the disk in our problem is tensorized domain and the finite dimensional basis is formulated in polar coordinate, it is convenient to transform the problems.

In order to make sure the uniqueness of solution, we assume that

$$\int_\Omega p dx = 0. \tag{6.2.4}$$

We follow the well-known $\mathbb{P}_{N'} - \mathbb{P}_{N'-2}$ (Here N' is maximum degree of the polynomial in 2D) spectral Petrov-Galerkin method to discretize the stokes equation; see the monograph by Bernardi and Maday in [17]. For the rectangular domain both in 2D and 3D, Bernardi and Maday detailedly investigated the spectral Galerkin method with the tensorial basis of Legendre polynomials. They pointed out the main features of such method are:

- the velocity is not exactly divergence-free

- the method is variational formulation

- but there is not spurious mode for the pressure

- the best constant of the inf-sup conditions on the pressure is of order $(N')^{-1/2}$

Define the finite dimensional space

$$V_{M,N} := \text{Span}\{\cos(m\theta)Q_n^{0,m}(r), \sin(m\theta)Q_n^{0,m}(r), 0 \le m \le M-1, 0 \le n \le N\},$$

where $Q_n^{1,m}(r)$'s are from Lemma 3.3.1. Let $\mathbf{U}_{M,N} = U_{M,N} \times U_{M,N}$ and $V_{0,M,N} := \{v \in V_{M,N} : \int_\Omega v dx = 0\}$. The spectral Petrov-Galerkin method is to find $\mathbf{u}_{M,N} \in U_{M,N}$ and $p_{M,N} \in V_{0,M,N}$ such that

$$a(\mathbf{u}_{M,N}, \mathbf{v}_{M,N}) + b(\mathbf{v}_{M,N}, p_{M,N}) = (\mathbf{F}, \mathbf{v}_{M,N}), \quad \forall \mathbf{v}_{M,N} \in \mathbf{U}_{M,N}, \tag{6.2.5}$$

$$b(\mathbf{u}_{M,N}, q_{M,N}) = 0, \quad \forall q_{M,N} \in V_{0,M,N}, \tag{6.2.6}$$

with $a(\mathbf{u}_{M,N}, \mathbf{v}_{M,N}) := (-\Delta \mathbf{u}_{M,N}, \mathbf{v}_{M,N}) + ((-\Delta)^{\alpha/2}\mathbf{u}_{M,N}, \mathbf{v}_{M,N})$ and $b(\mathbf{u}_{M,N}, q_{M,N}) = (\mathbf{u}_{M,N}, \nabla q_{M,N})$.

The key to the stability of the spectral method is to establish the well-known inf-sup condition or Ladyzenskaya-Babuska-Brezzi condition:

$$\sup_{\mathbf{v}_{M,N} \in \mathbf{U}_{M,N}} \frac{b(\mathbf{v}_{M,N}, p_{M,N})}{\|\mathbf{v}_{M,N}\|_{\mathbf{H}^1(\Omega)}} \ge \beta_{M,N} \|p_{M,N}\|_{L^2(\Omega)}, \quad \forall p_{M,N} \in V_{0,M,N}. \tag{6.2.7}$$

In the tensorial rectangular domain, the inf-sup constant is optimal and depends on the discretization number. However, for the our problem defined on the smooth geometry domain, unit disk, the ideal condition which is independent of discretization number can be reached.

The key to prove the inf-sup condition here is Fortin's criterion [41] which is well known in the context of finite element methods. The spectral version can be stated as follows.

Lemma 6.2.1. *Let X and Y be Hilbert spaces. Suppose that the bilinear form $b : X \times Y \to \mathbb{R}$ satisfies the inf-sup condition. In addition, suppose that for the subspaces $X_{M,N}, Y_{M,N}$, there exists a bounded linear projector $\Pi_{M,N} : X \to X_{M,N}$ such that*

$$b(v - \Pi_{M,N}v, w_{M,N}) = 0, \quad \forall w_{M,N} \in Y_{M,N}.$$

If $\|\Pi_{M,N}\| \le c$ for some constant c independent of the discretization numbers M, N, then the spectral spaces satisfy the inf-sup condition.

91

Proof.

$$
\begin{aligned}
\beta \| w_{M,N} \|_Y \quad &\leq \quad \sup_{v \in X} \frac{b(v, w_{M,N})}{\|v\|_X} = \sup_{v \in X} \frac{b(\Pi_{M,N} v, w_{M,N})}{\|v\|_X} \\
&\leq \quad c \sup_{v \in X} \frac{b(\Pi_{M,N} v, w_{M,N})}{\|\Pi_{M,N} v\|_X} = \sup_{v_{M,N} \in X_{M,N}} \frac{b(v, w_{M,N})}{\|v_{M,N}\|_X}.
\end{aligned} \tag{6.2.8}
$$

$\square$

For any $\mathbf{v} \in H_0^1(\Omega) \times H_0^1(\Omega)$ defined on the disk, it is legitimate to write

$$
\mathbf{v} = (1 - r^2) \sum_{m=0}^{\infty} \sum_{n=0}^{\infty} [\mathbf{v}_{m,n}^{(1)} \phi_{m,n}^{(2,1)} + \mathbf{v}_{m,n}^{(2)} \phi_{m,n}^{(2,2)}]. \tag{6.2.9}
$$

The projection operator is taken as

$$
\Pi_{M,N} \mathbf{v} =: (1 - r^2) \sum_{m=0}^{M} \sum_{n=0}^{N} [\mathbf{v}_{m,n}^{(1)} \phi_{m,n}^{(2,1)} + \mathbf{v}_{m,n}^{(2)} \phi_{m,n}^{(2,2)}]. \tag{6.2.10}
$$

Using the pseudo eigen-relation in 3, we can obtain that

$$
\| \Pi_{M,N} \mathbf{v} \|_{H_0^1} \leq \| \mathbf{v} \|_{H_0^1}. \tag{6.2.11}
$$

With the projection operator $\Pi_{M,N}$ introduced above, by the orthogonality of polynomials in theta direction, it is readily to check $\mathbf{u}_{M,N}$ and $V_{0,M,N}$ satisfy the Fortin's criterion and inf-sup condition holds.

Remark 6.2.2. *Recently, the authors in [24, 81] considered stokes problem in triangle and proved the optimal inf-sup constant. For the special geometry disk, we are not aware of any work discussing about the disk. The result shown here is surprising.*

6.2.1 Implementation of spectral method

For linear problem (6.2.5)-(6.2.6), plug

$$
\mathbf{u}_{M,N} = \sum_{m=0}^{M} \sum_{n=0}^{N} [\mathbf{u}_{m,n}^{(1)} \phi_{m,n}^{(2,1)} + \mathbf{u}_{m,n}^{(2)} \phi_{m,n}^{(2,2)}] \in \mathbf{U}_{M,N}
$$

into (6.2.5), and

$$
p_{M,N} = \sum_{m=1}^{M-1} \sum_{n=0}^{N} [p_{m,n}^{(1)} \cos(m\theta) Q_n^{0,m}(r) + p_{m,n}^{(2)} \sin(m\theta) Q_n^{0,m}(r)] + \sum_{n=1}^{N} p_{0,n}^{(1)} Q_n^{0,0}(r) \in V_{0,M,N}
$$

into (6.2.6), respectively, and take $v_{M,N} = \phi_{m,n}^{(i)}(x)$ for $i = 1, 2$, $m = 0, 1, \ldots M$ and $n = 0, 1, \ldots, N$, we get the matrix equation

$$
\begin{bmatrix} \mathbf{A} & \mathbf{B} \\ \mathbf{B}^T & \mathbf{0} \end{bmatrix} \begin{bmatrix} \mathbf{u} \\ \mathbf{p} \end{bmatrix} = \begin{bmatrix} \mathbf{f} \\ \mathbf{0} \end{bmatrix} \tag{6.2.12}
$$

with

$$\mathbf{A} = \begin{bmatrix} \mathbf{A}_1 & \mathbf{0} \\ \mathbf{0} & \mathbf{A}_2 \end{bmatrix}, \quad \mathbf{B} = \begin{bmatrix} \mathbf{B}_1 \\ \mathbf{B}_2 \end{bmatrix}, \tag{6.2.13}$$

Here the matrix $\mathbf{A}_1$ and $\mathbf{A}_2$ a re $(2M+1)$ by $(2M+1)$ diagonal block matrix with each block being $N+1$ by $N+1$ matrix, which are shown in the last section. Next we only need to determine the matrix $\mathbf{B}_1$ and $\mathbf{B}_2$. By the orthogonality, we know that

$$\mathbf{B}_1 = \begin{bmatrix} \mathbf{B}_{1,1} & \mathbf{0} \\ \mathbf{0} & \mathbf{B}_{1,2} \end{bmatrix}, \quad \mathbf{B}_2 = \begin{bmatrix} \mathbf{0} & \mathbf{B}_{2,1} \\ \mathbf{B}_{2,2} & \mathbf{0} \end{bmatrix} \tag{6.2.14}$$

where $\mathbf{B}_{i,j}$ are sparse matrices with tri-diagonal block. More precisely, we have

$$\mathbf{B}_{1,1} = \begin{bmatrix} \mathbf{0} & * & \mathbf{0} & \cdots & \mathbf{0} & \mathbf{0} \\ * & \mathbf{0} & * & \cdots & \mathbf{0} & \mathbf{0} \\ \mathbf{0} & * & \mathbf{0} & \ddots & \mathbf{0} & \mathbf{0} \\ \vdots & \vdots & \ddots & \ddots & \ddots & \mathbf{0} \\ \vdots & \vdots & \vdots & \ddots & \mathbf{0} & * \\ \mathbf{0} & \mathbf{0} & \mathbf{0} & \cdots & * & \mathbf{0} \\ \mathbf{0} & \mathbf{0} & \mathbf{0} & \cdots & \mathbf{0} & * \end{bmatrix}_{(M+1)\times M}, \quad \mathbf{B}_{1,2} = \begin{bmatrix} \mathbf{0} & * & \mathbf{0} & \cdots & \mathbf{0} & \mathbf{0} \\ * & \mathbf{0} & * & \cdots & \mathbf{0} & \mathbf{0} \\ \mathbf{0} & * & \mathbf{0} & \ddots & \mathbf{0} & \mathbf{0} \\ \vdots & \vdots & \ddots & \ddots & \ddots & \mathbf{0} \\ \vdots & \vdots & \vdots & \ddots & \mathbf{0} & * \\ \mathbf{0} & \mathbf{0} & \mathbf{0} & \cdots & * & \mathbf{0} \\ \mathbf{0} & \mathbf{0} & \mathbf{0} & \cdots & \mathbf{0} & * \end{bmatrix}_{M\times(M-1)} \tag{6,2.15}$$

and

$$\mathbf{B}_{2,1} = \begin{bmatrix} * & \mathbf{0} & \mathbf{0} & \cdots & \mathbf{0} \\ \mathbf{0} & * & \mathbf{0} & \cdots & \mathbf{0} \\ * & \mathbf{0} & * & \ddots & \mathbf{0} \\ \vdots & \ddots & \ddots & \ddots & \ddots \\ \vdots & \vdots & \ddots & \ddots & * \\ \mathbf{0} & \mathbf{0} & \mathbf{0} & \ddots & \mathbf{0} \\ \mathbf{0} & \mathbf{0} & \mathbf{0} & \cdots & * \end{bmatrix}_{(M+1)\times(M-1)}, \quad \mathbf{B}_{2,2} = \begin{bmatrix} * & \mathbf{0} & * & \mathbf{0} & \cdots & \cdots & \mathbf{0} \\ \mathbf{0} & * & \mathbf{0} & * & \cdots & \cdots & \mathbf{0} \\ \mathbf{0} & \mathbf{0} & * & \mathbf{0} & \ddots & \cdots & \mathbf{0} \\ \vdots & \ddots & \ddots & \ddots & \ddots & \ddots & \vdots \\ \vdots & \vdots & \ddots & \ddots & \ddots & \ddots & * \\ \mathbf{0} & \mathbf{0} & \mathbf{0} & \ddots & \mathbf{0} & * & \mathbf{0} \\ \mathbf{0} & \mathbf{0} & \mathbf{0} & \cdots & \mathbf{0} & \mathbf{0} & * \end{bmatrix}_{M\times M} \tag{6.2.16}$$

where $*$ stands for the non-zero block matrix with size $(N+1) \times (N+1)$. The notation $*$ in blue denotes a matrix with size $(N+1) \times N$. To solve the system, we can use the direct solver Gaussian elimination to find

$$\begin{aligned} \mathbf{p} &= (\mathbf{B}^T \mathbf{A}^{-1} \mathbf{B})^{-1} \mathbf{B}^T \mathbf{A}^{-1} \mathbf{f} \\ \mathbf{u} &= \mathbf{A}^{-1} \mathbf{f} - \mathbf{A}^{-1} \mathbf{B} \mathbf{p} \end{aligned} \tag{6.2.17}$$

From above we can see that the computational cost will be $\mathcal{O}(MN^2)$ if we use the iterative method.

Note that the matrix $\mathbf{B}^T \mathbf{A}^{-1} \mathbf{B}$ is called Schur-complement. The above system is usually solved by using a preconditioned conjugated gradient method. It is well known that the condition number of $\mathbf{B}^T \mathbf{A}^{-1} \mathbf{B}$ is $1/\beta_{M,N}^2$ with $\beta_{M,N}$ as the inf-sup constant; see [17].

Next, we derive the entries of the block matrices $\mathbf{B}_{i,j}$. For the right hand side data $\mathbf{F}$ is sufficiently smooth in theta direction, that is, only small number modes in theta direction is needed

and in this case fast solver can be developed and computation cost can be reduced to $\mathcal{O}(N \log^2(N))$ as our previous paper.

In polar coordinate, let $x = r \cos(\theta)$ and $y = r \sin(\theta)$, then we have

$$\partial_x = \cos(\theta)\partial_r - \frac{\sin(\theta)}{r}\partial_\theta, \quad \partial_y = \sin(\theta)\partial_r + \frac{\cos(\theta)}{r}\partial_\theta. \tag{6.2.18}$$

Thus

$$\partial_r p_{M,N} = \sum_{m=1}^{M-1} \sum_{n=0}^{N} [p_{m,n}^{(1)} \cos(m\theta)\partial_r Q_n^{0,m}(r) + p_{m,n}^{(2)} \sin(m\theta)\partial_r Q_n^{0,m}(r)] + \sum_{n=1}^{N} p_{0,n}^{(1)} \partial_r Q_n^{0,0}(r)$$

$$\partial_\theta p_{M,N} = \sum_{m=1}^{M-1} \sum_{n=0}^{N} [(-m)p_{m,n}^{(1)} \sin(m\theta)Q_n^{0,m}(r) + m p_{m,n}^{(2)} \cos(m\theta)Q_n^{0,m}(r)].$$

Consequently,

$$
\begin{aligned}
\partial_x p_{M,N} &= \cos(\theta)\partial_r p_{M,N} - \frac{\sin(\theta)}{r}\partial_\theta p_{M,N} \\
&= \sum_{m=1}^{M-1} \sum_{n=0}^{N} [p_{m,n}^{(1)} \cos(\theta) \cos(m\theta)\partial_r Q_n^{0,m}(r) + p_{m,n}^{(2)} \cos(\theta) \sin(m\theta)\partial_r Q_n^{0,m}(r)] \\
&\quad - \sum_{m=1}^{M-1} \sum_{n=0}^{N} [(-m)p_{m,n}^{(1)} \sin(\theta) \sin(m\theta)r^{-1}Q_n^{0,m}(r) + m p_{m,n}^{(2)} \sin(\theta) \cos(m\theta)r^{-1}Q_n^{0,m}(r)] \\
&\quad + \sum_{n=1}^{N} p_{0,n}^{(1)} \cos(\theta)\partial_r Q_n^{0,0}(r) \\
&= \sum_{m=1}^{M-1} \sum_{n=0}^{N} p_{m,n}^{(1)} [\cos(\theta) \cos(m\theta)\partial_r Q_n^{0,m}(r) + m \sin(\theta) \sin(m\theta)r^{-1}Q_n^{0,m}(r)] \\
&\quad + \sum_{m=1}^{M-1} \sum_{n=0}^{N} p_{m,n}^{(2)} [\cos(\theta) \sin(m\theta)\partial_r Q_n^{0,m}(r) - m \sin(\theta) \cos(m\theta)r^{-1}Q_n^{0,m}(r)] \\
&\quad + \sum_{n=1}^{N} p_{0,n}^{(1)} \cos(\theta)\partial_r Q_n^{0,0}(r) \tag{6.2.19}
\end{aligned}
$$

and

$$\partial_y p_{M,N} = \sin(\theta)\partial_r p_{M,N} + \frac{\cos(\theta)}{r}\partial_\theta p_{M,N}$$

$$= \sum_{m=1}^{M-1}\sum_{n=0}^{N}[p_{m,n}^{(1)}\sin(\theta)\cos(m\theta)\partial_r Q_n^{0,m}(r) + p_{m,n}^{(2)}\sin(\theta)\sin(m\theta)\partial_r Q_n^{0,m}(r)]$$

$$+ \sum_{m=1}^{M-1}\sum_{n=0}^{N}[(-m)p_{m,n}^{(1)}\cos(\theta)\sin(m\theta)r^{-1}Q_n^{0,m}(r) + mp_{m,n}^{(2)}\cos(\theta)\cos(m\theta)r^{-1}Q_n^{0,m}(r)]$$

$$+ \sum_{n=1}^{N}p_{0,n}^{(1)}\sin(\theta)\partial_r Q_n^{0,0}(r)$$

$$= \sum_{m=1}^{M-1}\sum_{n=0}^{N}p_{m,n}^{(1)}[\sin(\theta)\cos(m\theta)\partial_r Q_n^{0,m}(r) - m\cos(\theta)\sin(m\theta)r^{-1}Q_n^{0,m}(r)]$$

$$+ \sum_{m=1}^{M-1}\sum_{n=0}^{N}p_{m,n}^{(2)}[\sin(\theta)\sin(m\theta)\partial_r Q_n^{0,m}(r) + m\cos(\theta)\cos(m\theta)r^{-1}Q_n^{0,m}(r)]$$

$$+ \sum_{n=1}^{N}p_{0,n}^{(1)}\sin(\theta)\partial_r Q_n^{0,0}(r). \tag{6.2.20}$$

The entries of $\mathbf{B}_{1,1}$, $m = 0$, $1 \leq n \leq N$; $1 \leq m \leq M-1$ and $0 \leq n \leq N$, $0 \leq l \leq M$, $0 \leq k \leq N$:

$$\mathbf{B}_{1,1}(l,m;k,n) = \int_0^{2\pi}\int_0^1 \cos(\theta)\cos(m\theta)\partial_r Q_n^{0,m}(r)(1-r^2)Q_k^{1,l}(r)\cos(l\theta)rdrd\theta$$

$$+ \int_0^{2\pi}\int_0^1 m\sin(\theta)\sin(m\theta)r^{-1}Q_n^{0,m}(r)(1-r^2)Q_k^{1,l}(r)\cos(l\theta)rdrd\theta$$

$$= \int_0^{2\pi}\cos(\theta)\cos(m\theta)\cos(l\theta)d\theta \cdot \int_0^1 \partial_r Q_n^{0,m}(r)(1-r^2)Q_k^{1,l}(r)rdr$$

$$+ m\int_0^{2\pi}\sin(\theta)\sin(m\theta)\cos(l\theta)d\theta \cdot \int_0^1 Q_n^{0,m}(r)(1-r^2)Q_k^{1,l}(r)dr. \tag{6.2.21}$$

For $1 \leq m \leq M-1$ and $0 \leq n \leq N$, $1 \leq l \leq M$, $0 \leq k \leq N$, the (k,n)-th entry of (l,m)-block of $\mathbf{B}_{1,2}$ are:

$$\mathbf{B}_{1,2}(l,m;k,n) = \int_0^{2\pi}\int_0^1 \cos(\theta)\sin(m\theta)\partial_r Q_n^{0,m}(r)(1-r^2)Q_k^{1,l}(r)\sin(l\theta)rdrd\theta$$

$$- \int_0^{2\pi}\int_0^1 m\sin(\theta)\cos(m\theta)r^{-1}Q_n^{0,m}(r)(1-r^2)Q_k^{1,l}(r)\sin(l\theta)rdrd\theta$$

$$= \int_0^{2\pi}\cos(\theta)\sin(m\theta)\sin(l\theta)d\theta \cdot \int_0^1 \partial_r Q_n^{0,m}(r)(1-r^2)Q_k^{1,l}(r)rdr$$

$$- m\int_0^{2\pi}\sin(\theta)\cos(m\theta)\sin(l\theta)d\theta \cdot \int_0^1 Q_n^{0,m}(r)(1-r^2)Q_k^{1,l}(r)dr. \tag{6.2.22}$$

95

For $1 \le m \le M-1$ and $0 \le n \le N$, $0 \le l \le M$, $0 \le k \le N$, the entries of $\mathbf{B}_{2,1}$ are

$$
\begin{aligned}
\mathbf{B}_{2,1}(l,m;k,n) &= \int_0^{2\pi}\int_0^1 \sin(\theta)\sin(m\theta)\partial_r Q_n^{0,m}(r)(1-r^2)Q_k^{1,l}(r)\cos(l\theta)r\,dr\,d\theta \\
&\quad + \int_0^{2\pi}\int_0^1 m\cos(\theta)\cos(m\theta)r^{-1}Q_n^{0,m}(r)(1-r^2)Q_k^{1,l}(r)\cos(l\theta)r\,dr\,d\theta \\
&= \int_0^{2\pi}\sin(\theta)\sin(m\theta)\cos(l\theta)d\theta \cdot \int_0^1 \partial_r Q_n^{0,m}(r)(1-r^2)Q_k^{1,l}(r)r\,dr \\
&\quad + m\int_0^{2\pi}\cos(\theta)\cos(m\theta)\cos(l\theta)d\theta \cdot \int_0^1 Q_n^{0,m}(r)(1-r^2)Q_k^{1,l}(r)dr. \quad (6.2.23)
\end{aligned}
$$

For $m=0$, $1 \le n \le N$; $1 \le m \le M-1$ and $0 \le n \le N$, $1 \le l \le M$, $0 \le k \le N$, the entries of $\mathbf{B}_{2,2}$,

$$
\begin{aligned}
\mathbf{B}_{2,2}(l,m;k,n) &= \int_0^{2\pi}\int_0^1 \sin(\theta)\cos(m\theta)\partial_r Q_n^{0,m}(r)(1-r^2)Q_k^{1,l}(r)\sin(l\theta)r\,dr\,d\theta \\
&\quad - \int_0^{2\pi}\int_0^1 m\cos(\theta)\sin(m\theta)r^{-1}Q_n^{0,m}(r)(1-r^2)Q_k^{1,l}(r)\sin(l\theta)r\,dr\,d\theta \\
&= \int_0^{2\pi}\sin(\theta)\cos(m\theta)\sin(l\theta)d\theta \cdot \int_0^1 \partial_r Q_n^{0,m}(r)(1-r^2)Q_k^{1,l}(r)r\,dr \\
&\quad - m\int_0^{2\pi}\cos(\theta)\sin(m\theta)\sin(l\theta)d\theta \cdot \int_0^1 Q_n^{0,m}(r)(1-r^2)Q_k^{1,l}(r)dr. \quad (6.2.24)
\end{aligned}
$$

From above integrals, by the orthogonality, we are only interested in the case $l = m+1$ and $l = m-1$ since it vanishes for other case.

The following relations hold for Jacobi polynomials $P_n^{\alpha,\beta}(x)$, see e.g. [11],

$$
\partial_x P_n^{\alpha,\beta}(x) = \frac{n+\alpha+\beta+1}{2}P_{n-1}^{\alpha+1,\beta+1}(x), \quad \alpha,\beta > -1. \quad (6.2.25)
$$

Thus we have $Q_n^{0,m} = r^m P_n^{0,m}(2r^2-1)$ and

$$
\begin{aligned}
\partial_r Q_n^{0,m} &= mr^{m-1}P_n^{0,m}(2r^2-1) + 2(n+m+1)r^{m+1}P_{n-1}^{1,m+1}(2r^2-1) \\
&= mr^{-1}Q_n^{0,m}(r) + 2(n+m+1)Q_{n-1}^{1,m+1}(r). \quad (6.2.26)
\end{aligned}
$$

Thus, for $l = m+1, m-1$, it holds

$$
\begin{aligned}
&\int_0^1 \partial_r Q_n^{0,m}(r)(1-r^2)Q_k^{1,l}(r)r\,dr \\
&= m\int_0^1 Q_n^{0,m}(r)(1-r^2)Q_k^{1,l}(r)dr + 2(n+m+1)\int_0^1 Q_{n-1}^{1,m+1}(r)(1-r^2)Q_k^{1,l}(r)r\,dr\,(6.2.27)
\end{aligned}
$$

Here the integrals $\int_0^1 Q_n^{0,m}(r)(1-r^2)Q_k^{1,l}(r)dr$ and $\int_0^1 Q_{n-1}^{1,m+1}(r)(1-r^2)Q_k^{1,l}(r)r\,dr$ can be computed as that in the last section.

To simply the notation, denotes

$$\mathbb{I}_1^{m,l}(k,n) = \int_0^1 Q_n^{0,m}(r)(1-r^2)Q_k^{1,l}(r)dr = \frac{1}{8}\int_{-1}^1 Q_n^{0,m}(\frac{1+t}{2})Q_k^{1,l}(\frac{1+t}{2})(1-t)(3+t)dt,$$

$$\mathbb{I}_2^{m,l}(k,n) = \int_0^1 Q_{n-1}^{1,m+1}(r)(1-r^2)Q_k^{1,l}(r)rdr$$

$$= \frac{1}{16}\int_{-1}^1 Q_{n-1}^{1,m}(\frac{1+t}{2})Q_k^{1,l}(\frac{1+t}{2})(1-t)(1+t)(3+t)dt.$$

Then substituting (6.2.27) into (6.2.21)-(6.2.24), using the following basic equalities,

$$2\cos(m\theta)\cos(\theta) = \cos((m-1)\theta) + \cos((m+1)\theta),$$
$$2\sin(m\theta)\sin(\theta) = \cos((m-1)\theta) - \cos((m+1)\theta),$$
$$2\cos(\theta)\sin(m\theta) = \sin((m+1)\theta) + \sin((m-1)\theta),$$
$$2\sin(\theta)\cos(m\theta) = \sin((m+1)\theta) - \sin((m-1)\theta), \tag{6.2.28}$$

we can obtain

$$\begin{aligned}
\mathbf{B}_{1,1}(l,m;k,n) \;=\;& m\int_0^{2\pi}\cos((m-1))\theta)\cos(l\theta)d\theta \cdot \mathbb{I}_1^{m,l}(k,n) \\
& +(n+m+1)\int_0^{2\pi}\cos((m-1))\theta)\cos(l\theta)d\theta \cdot \mathbb{I}_2^{m,l}(k,n) \\
& +(n+m+1)\int_0^{2\pi}\cos((m+1))\theta)\cos(l\theta)d\theta \cdot \mathbb{I}_2^{m,l}(k,n), \tag{6.2.29}
\end{aligned}$$

where $0 \le m \le M-1$, $0 \le l \le M$, $0 \le n \le N$, $0 \le k \le N$; $m = 0$, $1 \le n \le N$.

$$\begin{aligned}
\mathbf{B}_{1,2}(l,m;k,n) \;=\;& m\int_0^{2\pi}\sin((m-1))\theta)\sin(l\theta)d\theta \cdot \mathbb{I}_1^{m,l}(k,n) \\
& +(n+m+1)\int_0^{2\pi}\sin((m-1))\theta)\sin(l\theta)d\theta \cdot \mathbb{I}_2^{m,l}(k,n) \\
& +(n+m+1)\int_0^{2\pi}\sin((m+1))\theta)\sin(l\theta)d\theta \cdot \mathbb{I}_2^{m,l}(k,n), \tag{6.2.30}
\end{aligned}$$

where $1 \le m \le M-1$, $1 \le l \le M$ and $0 \le n \le N$, $0 \le k \le N$.

$$\begin{aligned}
\mathbf{B}_{2,1}(l,m;k,n) \;=\;& m\int_0^{2\pi}\cos((m-1))\theta)\cos(l\theta)d\theta \cdot \mathbb{I}_1^{m,l}(k,n) \\
& +(n+m+1)\int_0^{2\pi}\cos((m-1))\theta)\cos(l\theta)d\theta \cdot \mathbb{I}_2^{m,l}(k,n) \\
& -(n+m+1)\int_0^{2\pi}\cos((m+1))\theta)\cos(l\theta)d\theta \cdot \mathbb{I}_2^{m,l}(k,n), \tag{6.2.31}
\end{aligned}$$

where $1 \le m \le M-1$, $0 \le l \le M$, and $0 \le n \le N$, $0 \le k \le N$.

$$\mathbf{B}_{2,2}(l,m;k,n) \quad = \quad -m \int_0^{2\pi} \sin((m-1))\theta) \sin(l\theta) d\theta \cdot \mathbb{I}_1^{m,l}(k,n)$$

$$-(n+m+1) \int_0^{2\pi} \sin((m-1))\theta) \sin(l\theta) d\theta \cdot \mathbb{I}_2^{m,l}(k,n)$$

$$+(n+m+1) \int_0^{2\pi} \sin((m+1))\theta) \sin(l\theta) d\theta \cdot \mathbb{I}_2^{m,l}(k,n), \quad (6.2.32)$$

where $0 \leq m \leq M-1$, $1 \leq l \leq M$ and $0 \leq n \leq N$, $0 \leq k \leq N$; $m = 0$, $1 \leq n \leq N$.

6.3 Unsteady fractional Navier-Stokes equation

The goal of this section is devoted to the discussion of unsteady fractional Navier-Stokes equation as follows:

$$\partial_t \mathbf{u} + \mathbf{u} \cdot \nabla \mathbf{u} - \nu \Delta \mathbf{u} + \gamma(-\Delta)^{\alpha/2}\mathbf{u} + \nabla p = 0,$$
$$\nabla \cdot \mathbf{u} = 0,$$

where $\nu > 0$, $\alpha > 0$ are real numbers.

Using the first-order backward implicit-explicit difference scheme,

$$\frac{\mathbf{u}^{n+1} - \mathbf{u}^n}{\Delta t} + \mathbf{u}^n \cdot \nabla \mathbf{u}^{n+1} - \nu \Delta \mathbf{u}^{n+1} + \gamma(-\Delta)^{\alpha/2}\mathbf{u}^{n+1} + \nabla p^{n+1} = 0. \quad (6.3.1)$$

Thus at each time step, the problem is reduced to fractional stokes problems discussed in above section.

In the literature, another efficient and popular method, splitting step or projection step method was developed to solve unsteady Navier-Stokes equations. We will discuss and adapt it to our problem below.

6.3.1 First order splitting method

To proceed with the splitting method, we follow the four-step substeps satisfying the (6.3.1), i.e.,

$$\frac{\mathbf{u}^{(1)} - \mathbf{u}^n}{\Delta t} + \mathbf{u}^n \cdot \nabla \mathbf{u}^{(1)} = 0 \quad \text{in } \Omega, \quad (6.3.2)$$

$$\frac{\mathbf{u}^{(2)} - \mathbf{u}^{(1)}}{\Delta t} + \nabla p^{n+1} = 0 \quad \text{in } \Omega, \quad (6.3.3)$$

$$\frac{\mathbf{u}^{(3)} - \mathbf{u}^{(2)}}{\Delta t} + \gamma(-\Delta)^{\alpha/2}\mathbf{u}^{(3)} = 0 \quad \text{in } \Omega, \quad (6.3.4)$$

$$\frac{\mathbf{u}^{(n+1)} - \mathbf{u}^{(3)}}{\Delta t} - \nu \Delta \mathbf{u}^{n+1} = 0 \quad \text{in } \Omega. \quad (6.3.5)$$

Here $\mathbf{u}^{(i)}$ are intermediate velocity fields and $\mathbf{u}^{(2)}$ satisfy the incompressibility constraint, and thus

$$\nabla \cdot \mathbf{u}^{(2)} = 0, \quad \text{in } \Omega. \quad (6.3.6)$$

Incorporating the above assumption, we arrive at the elliptical equation for the pressure with Neumann boundary conditions in the form,

$$\nabla^2 p^{n+1} = \nabla \cdot (\frac{\mathbf{u}^{(1)}}{\Delta t}) \quad \text{in } \Omega, \tag{6.3.7}$$

$$\frac{\partial p^{n+1}}{\partial n} = \mathbf{n} \cdot \left[\mathbf{u}^n \cdot \nabla \mathbf{u}^n + \nu(-\nabla \times (\nabla \times \mathbf{u}^n)) \right]. \tag{6.3.8}$$

The above method will be very efficient to deal with unsteady stokes equations. Here the treatment of boundary condition of pressure follows from the work by karniadakis et al. in 1991, see [61]. For more information, we can also refer to the review paper by Guermond et al. in [48].

For the four-sub step splitting method, the boundary conditions will be an issue for the first step. To address this difficulty, we propose the following three-sub step method.

$$\frac{\mathbf{u}^{(1)} - \mathbf{u}^n}{\Delta t} + \mathbf{u}^n \cdot \nabla \mathbf{u}^{(1)} - \nu \Delta \mathbf{u}^{(1)} = 0 \quad \text{in } \Omega \tag{6.3.9}$$

$$\frac{\mathbf{u}^{(2)} - \mathbf{u}^{(1)}}{\Delta t} + \nabla p^{n+1} = 0 \quad \text{in } \Omega \tag{6.3.10}$$

$$\frac{\mathbf{u}^{(n+1)} - \mathbf{u}^{(2)}}{\Delta t} + \gamma(-\Delta)^{\alpha/2} \mathbf{u}^{(n+1)} = 0 \quad \text{in } \Omega \tag{6.3.11}$$

From Chapter 2, we know that the convergence order of spectral method is $2.5\alpha + 1$. When α is pretty small, the accuracy will degrade dramatically. In this case, we are encouraged to use the following two step splitting method

$$\frac{\mathbf{u}^{(1)} - \mathbf{u}^n}{\Delta t} + \mathbf{u}^n \cdot \nabla \mathbf{u}^{(1)} - \nu \Delta \mathbf{u}^{(1)} + \gamma(-\Delta)^{\alpha/2} \mathbf{u}^{(1)} = 0 \quad \text{in } \Omega \tag{6.3.12}$$

$$\frac{\mathbf{u}^{(n+1)} - \mathbf{u}^{(1)}}{\Delta t} + \nabla p^{n+1} = 0 \quad \text{in } \Omega. \tag{6.3.13}$$

6.3.2   Stability of time discretization

In this subsection we use the energy argument to prove the stability of splitting scheme (6.3.2)-(6.3.5). In the analysis, we repeatedly use the following facts,

$$(a - b) * 2a = (a^2 - b^2) + (a - b)^2 \tag{6.3.14}$$

$$(\mathbf{v} \cdot \nabla \mathbf{w}, \mathbf{w}) = 0 \quad \text{for} \quad \nabla \cdot \mathbf{v} = 0. \tag{6.3.15}$$

Here the inner products is defined for any vector $\mathbf{u}, \mathbf{v} \in H_0(\omega)^d$ as

$$(\mathbf{u}, \mathbf{v}) = \int_\Omega \sum_{i=1}^d u_i v_i d\Omega. \tag{6.3.16}$$

Taking the inner product of (6.3.2) with $2\Delta t \mathbf{u}^{(1)}$ and using facts (6.3.14)-(6.3.15) gives

$$(u^{(1)})^2 - (u^n)^2 \leq 0 \quad \text{in } \Omega. \tag{6.3.17}$$

Taking the inner product of (6.3.2) with $2\Delta t \mathbf{u}^{(2)}$ and noticing $(\nabla p^{n+1}, \mathbf{u}^{(2)}) = 0$ for $\nabla \cdot \mathbf{u}^{(2)} = 0$ yields

$$(u^{(2)})^2 - (u^1)^2 \leq 0 \quad \text{in } \Omega. \tag{6.3.18}$$

Similarly, taking the inner product of (6.3.4)- (6.3.5) with $2\Delta t$ respectively, and combining the results with the above estimates lead to the stability result.

99

6.3.3   The second order splitting method

Using the second-order backward difference scheme,

$$\frac{3/2\mathbf{u}^{n+1} - 2\mathbf{u}^n + 1/2\mathbf{u}^{n-1}}{\Delta t} + 2\mathbf{u}^n \cdot \nabla \mathbf{u}^n - \mathbf{u}^{n-1} \cdot \nabla \mathbf{u}^{n-1} - \nu \Delta \mathbf{u}^{n+1} + \gamma(-\Delta)^{\alpha/2} \mathbf{u}^{n+1} + \nabla p^{n+1} = 0.$$

$$(6.3.19)$$

To proceed with the splitting method, we follow the four-step substeps satisfying the (6.3.19), i.e.,

$$\frac{\mathbf{u}^{(1)} - 2\mathbf{u}^n + 1/2\mathbf{u}^{n-1}}{\Delta t} + 2\mathbf{u}^n \cdot \nabla \mathbf{u}^n - \mathbf{u}^{n-1} \cdot \nabla \mathbf{u}^{n-1} = 0 \quad \text{in } \Omega, \tag{6.3.20}$$

$$\frac{\mathbf{u}^{(2)} - \mathbf{u}^{(1)}}{\Delta t} + \nabla p^{n+1} = 0 \quad \text{in } \Omega, \tag{6.3.21}$$

$$\frac{\mathbf{u}^{(3)} - \mathbf{u}^{(2)}}{\Delta t} + \gamma(-\Delta)^{\alpha/2} \mathbf{u}^{(3)} = 0 \quad \text{in } \Omega, \tag{6.3.22}$$

$$\frac{3/2\mathbf{u}^{(n+1)} - \mathbf{u}^{(3)}}{\Delta t} - \nu \Delta \mathbf{u}^{n+1} = 0 \quad \text{in } \Omega. \tag{6.3.23}$$

Here $\mathbf{u}^{(i)}$ are intermediate velocity fields and $\mathbf{u}^{(2)}$ satisfy the incompressibility constraint, and thus

$$\nabla \cdot \mathbf{u}^{(2)} = 0, \quad \text{in } \Omega. \tag{6.3.24}$$

Incorporating the above assumption, we arrive at the elliptical equation for the pressure with Neumann boundary conditions in the form,

$$\nabla^2 p^{n+1} = \nabla \cdot \left(\frac{\mathbf{u}^{(1)}}{\Delta t}\right) \quad \text{in } \Omega, \tag{6.3.25}$$

$$\frac{\partial p^{n+1}}{\partial n} = \mathbf{n} \cdot \left[2\mathbf{u}^n \cdot \nabla \mathbf{u}^n - \mathbf{u}^{n-1} \cdot \nabla \mathbf{u}^{n-1} + 2\nu(-\nabla \times (\nabla \times \mathbf{u}^n)) + \nu(\nabla \times (\nabla \times \mathbf{u}^{n-1}))\right].$$

$$(6.3.26)$$

The first

6.3.4   Three sub-steps rotational velocity correction schemes

When $\gamma = 0$, the equation reduces to the classical integer-order Navier-Stokes equations and a lot of schemes has been proposed in the literature. Prior to presenting our schemes, we first recall the two-substeps rotational velocity correction schemes, which comes from [32, 23].

Assume that at each time step, $\{\mathbf{u}^k, \tilde{\mathbf{u}}^k, p^k\}$ are given and one seeks $\{\mathbf{u}^{k+1}, \tilde{\mathbf{u}}^{k+1}, p^{k+1}\}$. In the first substep, we solve for (u^{k+1}, p^{k+1}) from:

$$\frac{\mathbf{u}^{k+1} - \tilde{\mathbf{u}}^k}{\Delta t} + \mathbf{u}^k \cdot \nabla \tilde{\mathbf{u}}^k + \nu \nabla \times \nabla \times \tilde{\mathbf{u}}^k + \nabla p^{k+1} = \mathbf{f}^{k+1}, \tag{6.3.27}$$

$$\nabla \cdot \mathbf{u}^{k+1} = 0,$$

$$\mathbf{u}^{k+1} \cdot \mathbf{n}|_\Gamma = 0. \tag{6.3.28}$$

In the second substep, we correct $\mathbf{u}^{k+1}$ by solving $\tilde{\mathbf{u}}^{k+1}$ from

$$\frac{\tilde{\mathbf{u}}^{k+1} - \mathbf{u}^{k+1}}{\Delta t} + \mathbf{u}^{k+1} \cdot \nabla \tilde{\mathbf{u}}^{k+1} - \mathbf{u}^k \cdot \nabla \tilde{\mathbf{u}}^k - \nu \Delta \tilde{\mathbf{u}}^{k+1} - \nu \nabla \times \nabla \times \tilde{\mathbf{u}}^k = 0, \qquad (6.3.29)$$

$$\mathbf{u}^{k+1}|_\Gamma = \mathbf{0}. \qquad (6.3.30)$$

The above schemes can be easily extended to second-order as follows in the first substep, we solve for $(\mathbf{u}^{k+1}, p^{k+1})$ from:

$$\frac{3\mathbf{u}^{k+1} - 4\tilde{\mathbf{u}}^k + \tilde{\mathbf{u}}^{k-1}}{2\Delta t} + \mathbf{u}^k \cdot \nabla \tilde{\mathbf{u}}^k + \nu \nabla \times \nabla \times \tilde{\mathbf{u}}^k + \nabla p^{k+1} = \mathbf{f}^{k+1}, \qquad (6.3.31)$$

$$\nabla \cdot \mathbf{u}^{k+1} = 0,$$

$$\mathbf{u}^{k+1} \cdot \mathbf{n}|_\Gamma = 0. \qquad (6.3.32)$$

In the second substep, we correct $\mathbf{u}^{k+1}$ by solving $\tilde{\mathbf{u}}^{k+1}$ from

$$\frac{3\tilde{\mathbf{u}}^{k+1} - 3\mathbf{u}^{k+1}}{2\Delta t} + \mathbf{u}^{k+1} \cdot \nabla \tilde{\mathbf{u}}^{k+1} - \mathbf{u}^k \cdot \nabla \tilde{\mathbf{u}}^k - \nu \Delta \tilde{\mathbf{u}}^{k+1} - \nu \nabla \times \nabla \times \tilde{\mathbf{u}}^k = 0, \qquad (6.3.33)$$

$$\mathbf{u}^{k+1}|_\Gamma = \mathbf{0}. \qquad (6.3.34)$$

Introduce a Gauge variable, $\{q^k\}$, and an axillary variable, $\{\mathbf{w}^k\}$, defined by

$$q^0 = 0; \quad q^{k+1} = \nabla \cdot \tilde{u}^{k+1} + q^k, \quad k \geq 0, \qquad (6.3.35)$$

$$\mathbf{w}^k = \nu \nabla \times \nabla \times \tilde{\mathbf{u}}^k + \mathbf{u}^k \cdot \nabla \tilde{\mathbf{u}}^k - \nu \nabla q^k. \qquad (6.3.36)$$

For the fist order scheme, the stability and convergence have been proved by Chen and Shen in [23], which are presented as follows.

Theorem 6.3.1. *The scheme with $\mathbf{f} \equiv 0$ is unconditionally energy stable in the sense that, for all $0 \leq k \leq T/\Delta t - 1$, we have:*

$$\varepsilon_{k+1}^{(1)} - \varepsilon_k^{(1)} \leq -\nu \Delta t \|\nabla \tilde{\mathbf{u}}^{k+1}\|^2, \qquad (6.3.37)$$

where:

$$\varepsilon_k^{(1)} = \|\tilde{\mathbf{u}}^k\|^2 + \Delta t^2 \|\mathbf{w}^k\|^2 + \nu \Delta t \|q^k\|^2 \qquad (6.3.38)$$

is modified energy at time step k.

Theorem 6.3.2. *Assuming that the exact solution satisfies suitable regularity assumption, we have the following error estimates for the schemes: for all $0 \leq m \leq T/\Delta t - 1$, we have:*

$$\|\tilde{\mathbf{e}}^{m+1}\|^2 + \|\mathbf{e}^{m+1}\|^2 + \frac{1}{2}\sum_{k=0}^{m}(\nu \Delta t \|\nabla \tilde{\mathbf{e}}^{k+1}\|^2 + \|\mathbf{e}^{k+1} - \tilde{\mathbf{e}}^k\|^2) \leq c\Delta t^2, \qquad (6.3.39)$$

where c is a constant independent of k,

$$\mathbf{e}^k = \mathbf{u}(\cdot, t_k) - \mathbf{u}^k, \quad \tilde{\mathbf{e}}^k = \mathbf{u}(\cdot, t_k) - \tilde{\mathbf{u}}^k. \qquad (6.3.40)$$

For our problem with fractional Laplacian, we present three-substeps methods. The first two substep is same as the previous method except that we keep on correcting the $\tilde{\mathbf{u}}^{k+1}$ by $\hat{\mathbf{u}}^{k+1}$ in the substep as follows:

$$\frac{\hat{\mathbf{u}}^{k+1} - \tilde{\mathbf{u}}^{k+1}}{\Delta t} + \gamma(-\Delta)^{\alpha/2}\hat{\mathbf{u}}^{k+1} = 0. \tag{6.3.41}$$

Equation (6.3.41) gives

$$\hat{\mathbf{u}}^{k+1} + \Delta t\gamma(-\Delta)^{\alpha/2}\hat{\mathbf{u}}^{k+1} = \tilde{\mathbf{u}}^{k+1}. \tag{6.3.42}$$

Taking the inner product of (6.3.42) with itself on both sides, we obtain:

$$\|\hat{\mathbf{u}}^{k+1}\|^2 + \Delta t(\hat{\mathbf{u}}^{k+1}, \gamma(-\Delta)^{\alpha/2}\hat{\mathbf{u}}^{k+1}) + \Delta t^2\|\gamma(-\Delta)^{\alpha/2}\hat{\mathbf{u}}^{k+1}\|^2$$
$$= \|\hat{\mathbf{u}}^{k+1} + \Delta t\gamma(-\Delta)^{\alpha/2}\hat{\mathbf{u}}^{k+1}\|^2 = \|\tilde{\mathbf{u}}^{k+1}\|^2. \tag{6.3.43}$$

Combining with Theorem 6.3.1, we get the stability of our scheme, which is stated as following theorem.

Theorem 6.3.3. *The scheme with $\mathbf{f} \equiv 0$ is unconditionally energy stable in the sense that, for all $0 \le k \le T/\Delta t - 1$, we have:*

$$\varepsilon_{k+1}^{(1)} - \varepsilon_k^{(1)} \le -\nu\Delta t\|\nabla\tilde{\mathbf{u}}^{k+1}\|^2, \tag{6.3.44}$$

where:

$$\varepsilon_k^{(1)} = \|\hat{\mathbf{u}}^k\|^2 + \gamma\Delta t(\hat{\mathbf{u}}^k, (-\Delta)^{\alpha/2}\hat{\mathbf{u}}^k) + \gamma\Delta t^2\|(-\Delta)^{\alpha/2}\hat{\mathbf{u}}^{k+1}\|^2 + \Delta t^2\|\mathbf{w}^k\|^2 + \nu\Delta t\|q^k\|^2 \tag{6.3.45}$$

is modified energy at time step k.

Next, we consider the error estimates of our scheme. Introduce the following notation

$$\mathbf{e}^k = \mathbf{u}(\cdot, t_k) - \hat{\mathbf{u}}^k. \tag{6.3.46}$$

From (6.3.41), we have

$$\frac{\hat{\mathbf{e}}^{k+1} - \tilde{\mathbf{e}}^{k+1}}{\Delta t} + \gamma(-\Delta)^{\alpha/2}\hat{\mathbf{e}}^{k+1} = \gamma(-\Delta)^{\alpha/2}\mathbf{u}(\cdot, t_k)^{k+1}, \tag{6.3.47}$$

which gives

$$\hat{\mathbf{e}}^{k+1} + \gamma(-\Delta)^{\alpha/2}\hat{\mathbf{e}}^{k+1} = \tilde{\mathbf{e}}^{k+1} + \Delta t\gamma(-\Delta)^{\alpha/2}\mathbf{u}(\cdot, t_k)^{k+1}. \tag{6.3.48}$$

Taking the inner product of (6.3.48) with itself on both sides, we obtain

$$\|\hat{\mathbf{e}}^{k+1}\|^2 \le \|\hat{\mathbf{e}}^{k+1} + \gamma(-\Delta)^{\alpha/2}\hat{\mathbf{e}}^{k+1}\|^2 \le 2\|\tilde{\mathbf{e}}^{k+1}\|^2 + \Delta t^2\|\gamma(-\Delta)^{\alpha/2}\mathbf{u}(\cdot, t_k)^{k+1}\|^2. \tag{6.3.49}$$

Combining the convergence Theorem (6.3.4) and the regularity assumption of the solution

Theorem 6.3.4. *Assuming that the exact solution satisfies suitable regularity assumption, we have the following error estimates for the schemes: for all $0 \le m \le T/\Delta t - 1$, we have:*

$$\|\mathbf{e}^{m+1}\|^2 + \|\tilde{\mathbf{e}}^{m+1}\|^2 + \|\hat{\mathbf{e}}^{m+1}\|^2 \le c\Delta t^2, \tag{6.3.50}$$

where c is a constant independent of Δt.

6.4 Conclusion

In this chapter, we presented the preliminary results about the numerical solution for the steady Stokes problems and time-dependent Navier-Stokes equations. To this end, we first investigated the two-term Laplacian model problems, provide some analysis, and showed some numerical examples to verify our conjectures. Based on the results of two-term fractional Laplacian model problems, we generalized the result to steady fractional stokes problems and described the implementation. Furthermore, we extended it to the time-dependent case. We applied the well-known splitting method to our fractional equations and showed the stability of the semi-discretization scheme.

With the preparations above, we are readily to perform the simulation for both steady Stokes and unsteady Navier-Stokes equations. We will leave them as ongoing works.

Chapter 7

Conclusions and Future Work

7.1 Summary and discussions

In this work, we present two methods, spectral and finite difference methods for fractional diffusion equations on the special geometry and extend these methods to general domain using the fictitious domain techniques.

For the spectral method to FADR in Chapter 2, the main findings and contributions are as follows.

• For the ADR equation (2.0.1), where $\mu_1 \neq 0$, we show the higher regularity of $\tilde{u}$ in terms of the right hand side function f in the weighted Sobolev spaces than the regularity of the solution u in non-weighted Sobolev spaces. Specifically, the regularity index for $\tilde{u}$ is $5\alpha/2 - 1 - \epsilon$ with $\epsilon > 0$ arbitrary small when f is smooth enough.

• For the DR equation (2.0.1), where $\mu_1 = 0$ and $\mu_2 > 0$, we improve the regularity estimate of $\tilde{u}$ in the weighted Sobolev spaces, higher than in [93]. Specifically, the regularity index for $\tilde{u}$ is $5\alpha/2 + 1 - \epsilon$ instead of $2\alpha + 1$ when f is smooth enough.

• We prove optimal error estimates of the spectral Galerkin method for (2.0.1)-(2.0.2) both in $H^{\alpha/2}$-norm and weighted $L^2_{\omega^{-\alpha/2}}$-norm; see Theorem 3.4.3.

• We present a fast iterative solver with the complexity $\mathcal{O}(N \log^2 N)$; see Section 5. The same complexity is reported in [7] on an adaptive finite element method, where the convergence order in the L^2-norm is 2 and the order in the $H^{\alpha/2}$-norm is $2 - \alpha/2$. For DR equations, our method has better convergence orders, as our order in the $L^2_{\omega^{-\alpha/2}}$-norm) is $5\alpha/2 + 1 - \epsilon$ and the order in the $H^{\alpha/2}$-norm is $2\alpha + 1 - \epsilon$. Even for ADR equations, our convergence orders are higher than the orders in [7] when $\alpha > 6/5$ in both L^2- and $H^{\alpha/2}$-norms.

It is surprising that the regularity index of $\tilde{u}$ for ADR case ($\mu_1 \neq 0$) is essentially different from the DR case ($\mu_1 = 0, \mu_2 > 0$) in (2.0.1). However, the regularity estimates are sharp and have been verified numerically using the spectral Galerkin method in Section 3.5.

In Chapter 3, for the spectral method in 2D, the main findings and contributions of this work are as follows.

• For the two-dimensional diffusion-reaction equation (1.2.1), we show the higher regularity of $\tilde{u} = u(1 - r^2)^{-\alpha/2}$ in terms of the right hand side function f in the weighted Sobolev spaces than the regularity of solution u in non-weighted Sobolev spaces. Specifically, the regularity index in radial direction for $\tilde{u}$ is $5\alpha/2 + 1 - \epsilon$ with $\epsilon > 0$ arbitrary small when f is smooth enough.

• We prove the optimal error estimates of spectral Galerkin method for (1.2.1)-(1.2.2) in weight-

ed $L^2_{-\alpha/2}(\Omega)$ norm and $H^{\alpha/2}(\Omega)$ norm; see Theorem 3.4.3. The error estimates are sharp and have been numerically verified using a spectral Galerkin method in Section 2.4.

For the finite difference method proposed in Chapter 5, the contributions are summarized as follows.

- We present a fractional centered difference scheme based on the generating function to discretize the fractional Laplacian.

- We show the stability and convergence analysis of the finite difference scheme (1.2.1)-(1.2.2) in a discrete energy norm.

- We provide a fast solver using a preconditioned conjugate gradient method.

- We develop a fictitious domain method for fractional diffusion equations on the general domains.

Our current work includes applying the proposed fractional centered difference approximation to various problems, e.g., high dimensional fractional Schrödinger equations, fractional Navier-Stokes equations on the general domains and fractional optimization problems.

Using the extended domain techniques we can retain the efficiency of the finite difference method or spectral method. However, the advantage of high accuracy will no longer exist when it goes to the general domain as the solution has been extended and weak singularity came across the original boundary of the domain. Heuristically, the convergence order of extended finite difference or spectral method is only of first order convergence, which pretty lower when the high-order accuracy numerical solution is needed. We remedy this, we revisit the finite element method. It is well known that, compared to the finite difference method and spectral methods, the finite element is well-suited to the complex geometry like hyper-polygonal domain and easier to design high-order method as it is derived from the Galerkin formulation. For the standard finite element method, however, the convergence order is very low and less than $\alpha/2 + 0.5$. Using the singular functions to enrich the approximation basis, higher orer convergence order up to second-order can be expected.

7.2 Other potential applications

The methods presented in this work can be directly applied to solve the fractional diffusion equations. An example will be given as follows. Fractional quasi-geostrophic has the following form [26]:

$$\frac{D\theta}{Dt} = \frac{\partial\theta}{\partial t} + v \cdot \nabla\theta = 0, \tag{7.2.1}$$

where, $v = (v_1, v_2)$ is a two-dimensional velocity field which is decided by the streaming function

$$v_1 = -\frac{\partial\psi}{\partial x_2}, \quad v_2 = \frac{\partial\psi}{\partial x_1}. \tag{7.2.2}$$

Here the current function ψ and θ has the relationship

$$(-\Delta)^{\frac{1}{2}}\psi = -\theta. \tag{7.2.3}$$

106

Here θ is the potential temperature, v is current velocity, ψ can be regarded as the pressure. When the viscous term and an external force term are considered, the following equation can be derived

$$\theta_t + v \cdot \nabla\theta + \kappa(-\Delta)^{\alpha/2}\theta = f \tag{7.2.4}$$

The solution in holder spaces has been studied by [90].

7.3   Ongoing and other future work

- Error estimates for full discretization of convergence orders observed for the fractional elliptic equations with random noise in Chapter 2.

- Regularity estimates and error estimates for two-term fractional Laplacian for two-dimensional case in Chapter 3.

- Error estimates for the fictitious methods with respect to the penalty parameter Chapter 4

- Optimal error estimates and interior estimates for the finite difference methods in Chapter 5.

- Regularity estimates and error estimates for two-term fractional Laplacian for one-dimensional case in Chapter 6.

- We will apply the fast finite difference solver developed in Chapter 5 to solve the fractional Stokes problems and time-dependent fractional Navier-Stokes equations in Chapter 6.

- *Nonlocal problems with other boundary conditions* Can we extend the numerical methods and the techniques to the nonlocal problems with other boundary conditions in [31].

- Optimal error regularity estimates and convergence orders for other asymmetrical fractional operators like two-sided Riemann-Liouville derivatives in [55].

Appendices

.1 Interpolation of weighted Sobolev spaces

Let us recall the K-interpolation for weighted Sobolev spaces. Let $\mathcal{B}_{2,q}^{s,\alpha/2}$ with $s > 0$ be interpolation spaces defined by

$$[B_{\omega^{\alpha/2}}^l, B_{\omega^{\alpha/2}}^k]_{\theta,q}, \tag{.1.1}$$

where $0 < \theta < 1$, $1 \le q \le \infty$, $s = (1-\theta)l + \theta k$, l and k are nonnegative integers (here k, l can be nonnegative real numbers which can be verified by the reiteration theorem; see e.g. Chapter 3 in [15]), $l < k$. When $q = \infty$, $\|u\|_{\mathcal{B}_{2,\infty}^{s,\alpha/2}} = \sup_{t>0} t^{-\theta} K(t, u)$; and

$$\|u\|_{\mathcal{B}_{2,q}^{s,\alpha/2}} = \left(\int_0^\infty t^{-q\theta} |K(t,u)|^q \frac{dt}{t} \right)^{1/q}, \ 1 \le q < \infty, \ \text{where}$$
$$K(t, u) = \inf_{u=v+w} (\|v\|_{B_{\omega^{\alpha/2}}^l} + t\|w\|_{B_{\omega^{\alpha/2}}^k}). \tag{.1.2}$$

In this paper, we are interested in the case $q = 2$.

Theorem .1.1 ([13]). *When $q = 2$, it holds that $\mathcal{B}_{2,2}^{s,\alpha/2} = B_{\omega^{\alpha/2}}^s$, $\quad s \ge 0$.*

In [40], it is shown that the norm in $B_{\omega^\beta}^s$ ($s = m + \sigma$, where the integer $m \ge 0$ and $0 < \sigma < 1$ and $s \ne 1 + \beta$ if $-1 < \beta < 0$) is equivalent to the following

$$\|u\|_{B_{\omega^\beta}^s} = (\|u\|_{B_{\omega^\beta}^m}^2 + |D^m u|_{B_{\omega^{\beta+m}}^\sigma}^2)^{1/2}, \tag{.1.3}$$
$$|D^m u|_{B_{\omega^{\beta+m}}^\sigma}^2 = \iint_{\Omega_a} \omega^{\beta+s}(x) \frac{|D^m u(x) - D^m u(y)|^2}{|x - y|^{1+2\sigma}} dx dy,$$

where $\omega^{\beta+s}(x) = (1 - x^2)^{\beta+s}$ and the set Ω_a ($a > 1$) is defined by

$$\Omega_a = \{(x, y) \in \Omega \otimes \Omega \mid a^{-1}(1 - |x|) < 1 - \text{sgn}(x)y < a(1 - |x|)\}. \tag{.1.4}$$

Here a can be any number large than 1 and we take $a = 2$.

In the analysis of regularity, we need the following weighted Sobolev spaces.

$$W_{\omega^\beta}^{m,p} := \left\{ u \mid \int_\Omega |D^k u|^p \omega^\beta dx < \infty, \ k = 0, 1, \dots, m \right\} \tag{.1.5}$$

with $1 \le p < \infty$ and m a nonnegative integer, which is equipped with the following norm

$$\|u\|_{W_{\omega^\beta}^{m,p}} = \left(\sum_{k=0}^m |u|_{W_{\omega^\beta}^{k,p}}^p \right)^{1/p}, \quad |u|_{W_{\omega^\beta}^{k,p}} = \left(\int_\Omega |D^k u|^p \omega^\beta dx \right)^{1/p}. \tag{.1.6}$$

When $m = s$ is not an integer, the space can be defined via the classical interpolation method, e.g. K- method; see [15, 16].

The next lemma connects the weighted Sobolev spaces (.1.5) and the weighted Sobolev spaces (2.1.3) used in the current work.

Lemma .1.2 (Theorem 3.3 in [71]). *For an nonnegative integer l, the spaces $W_{\omega^{\beta+l}}^{l,2}$ and $B_{\omega^\beta}^l$ are equivalent, which is denoted as $W_{\omega^{\beta+l}}^{l,2} \approx B_{\omega^\beta}^l$.*

In the proof of the regularity of problem (2.0.1)-(2.0.2), we have used the following lemmas.

Lemma .1.3 (Theorem 7.2 in [16]). *Let β, γ be two real numbers which are greater than -1, $1 < p, q < \infty$, and s, t two real numbers such that $0 \leq t \leq s$. If the next two conditions are satisfied (i) $t - \frac{1}{q} < s - \frac{1}{p}$ or $t - \frac{1}{q} = s - \frac{1}{p}$ with $p \leq q$, (ii) $t - \frac{\beta}{q} - \frac{1}{q} < s - \frac{\gamma}{p} - \frac{1}{p}$ or $t - \frac{\beta}{q} - \frac{1}{q} = s - \frac{\gamma}{p} - \frac{1}{p}$ with $p \leq q$ and $s - \frac{\gamma}{p} - \frac{1}{p} \notin \mathbb{N}$, the following embedding holds:*

$$W_{\omega^\gamma}^{s,p} \subset W_{\omega^\beta}^{t,q}. \tag{.1.7}$$

With above lemmas we can prove Lemma .1.4.

Lemma .1.4 (Connection with the non-weighted Sobolev space). *For all $s = l + \sigma \geq 0$ with l an integer, $0 \leq \sigma < 1$ and $-1 < \gamma \leq l \leq s$, we have that $B_{\omega^\gamma}^s \subset H^{\frac{s-\gamma}{2}}$.*

Proof   We know from Lemma .1.2 that

$$B_{\omega^\gamma}^s = [B_{\omega^\gamma}^l, B_{\omega^\gamma}^{l+1}]_{\sigma,2} \approx [W_{\omega^{\gamma+l}}^{l,2}, W_{\omega^{\gamma+l+1}}^{l+1,2}]_{\sigma,2} \tag{.1.8}$$

with $\sigma = s - l$. Take $p = q = 2$ and $\beta = 0$ and then applying Lemma .1.3 leads to

$$[W_{\omega^{\gamma+l}}^{l,2}, W_{\omega^{\gamma+l+1}}^{l+1,2}]_{\sigma,2} \subset [H^{\frac{l-\gamma}{2}}, H^{\frac{l+1-\gamma}{2}}]_{\sigma,2} = H^{\frac{s-\gamma}{2}}. \tag{.1.9}$$

By (.1.8) and (.1.9), we get the desired conclusion.   □

To prove Lemmas 2.2.5 and .3.1 we need the following two lemmas.

Lemma .1.5 ([93]). *Let $v \in L_{\omega^{\gamma+1-\beta+2s}}^2$, where $\beta < 3$ and $\gamma, s \in \mathbb{R}$. Then*

$$\iint_{\Omega_a} \omega^\gamma(x) v^2(x) \frac{|\omega^s(x) - \omega^s(y)|^2}{|x-y|^\beta} \, dx \, dy \ \leq \ C \, \|v\|_{\omega^{\gamma+1-\beta+2s}}^2 .$$

Lemma .1.6. *Let $v \in B_{\omega^{2\gamma+\beta}}^s \cap L_{\omega^{2\gamma+\beta-s}}^2$, where $0 < s < 1$ and $\beta, \gamma \in \mathbb{R}$. Then*

$$|v\omega^\gamma|_{B_{\omega^\beta}^s}^2 \leq C(|v|_{B_{\omega^{2\gamma+\beta}}^s}^2 + |v|_{L_{\omega^{2\gamma+\beta-s}}^2}^2).$$

Proof   By definition of the fractional norm (.1.3), we have

$$
\begin{aligned}
|v\omega^\gamma|_{B_{\omega^\beta}^s}^2 &= \iint_{\Omega_a} \omega^{\beta+s}(x) \frac{|\omega^\gamma(x)v(x) - \omega^\gamma(y)v(y)|^2}{|x-y|^{1+2s}} dxdy \\
&\leq 2 \iint_{\Omega_a} \omega^{\beta+s}(x)\omega^{2\gamma}(y) \frac{|v(x) - v(y)|^2}{|x-y|^{1+2s}} dxdy \\
&\quad + 2 \iint_{\Omega_a} \omega^{\beta+s}(x)v^2(x) \frac{|\omega^\gamma(x) - \omega^\gamma(y)|^2}{|x-y|^{1+2s}} dxdy \\
&\leq C|v|_{B_{\omega^{2\gamma+\beta}}^s}^2 + 2 \iint_{\Omega_a} \omega^{\beta+s}(x)v^2(x) \frac{|\omega^\gamma(x) - \omega^\gamma(y)|^2}{|x-y|^{1+2s}} dxdy,
\end{aligned}
$$

where we have used the fact that $\omega^\rho(y) \leq C\omega^\rho(x)$ for any ρ on Ω_a in the last inequality. By Lemma .1.5, we have

$$\iint_{\Omega_a} \omega^{\beta+s}(x)v^2(x) \frac{|\omega^\gamma(x) - \omega^\gamma(y)|^2}{|x-y|^{1+2s}} dxdy \leq C\|v\|_{L_{\omega^{2\gamma+\beta-s}}^2}^2. \tag{.1.10}$$

Combining above together leads to the desired results. □

In the following proof, we first prove that Lemma 2.2.5 holds for $s = 0$. Then we prove that Lemma 2.2.5 still holds for $s = 3\alpha/2 - 1 - \epsilon$ with arbitrarily small $\epsilon > 0$. In the last, we use the interpolation technique to show that Lemma 2.2.5 holds for $s \in [0, 3\alpha/2 - 1)$.

Proof Step 1. When $s = 0$, we have

$$\|v\omega^{\alpha/2-1}\|_{L^2_{\omega^{\alpha/2}}}^2 = \int_{-1}^1 v^2 \omega^{\alpha-2}(x)\omega^{\alpha/2}dx \leq \int_{-1}^1 v^2 \omega^{\alpha/2-1}(x)dx = \|v\|_{L^2_{\omega^{\alpha/2-1}}}^2. \tag{.1.11}$$

The desired conclusion holds for $s = 0$.

Step 2. Next we prove that Lemma 2.2.5 holds for $s = 3\alpha/2 - 1 - \epsilon$ with arbitrary small $\epsilon > 0$. We discuss two cases depending on the range of α: $1 < \alpha \leq 4/3$ and $4/3 < \alpha < 2$.

Case 1. If $1 < \alpha \leq 4/3$, then $s = 3\alpha/2 - 1 - \epsilon < 1$ for arbitrary small $\epsilon > 0$. Applying Lemma .1.6 gives

$$|v\omega^{\alpha/2-1}|_{B^s_{\omega^{\alpha/2}}}^2 \leq C(|v|_{B^s_{\omega^{3\alpha/2-2}}}^2 + \|v\|_{L^2_{\omega^{3\alpha/2-2-s}}}^2). \tag{.1.12}$$

First, it holds by Definition (.1.1) that $B^s_{\omega^{\alpha/2-1}} = [B^0_{\omega^{\alpha/2-1}}, B^1_{\omega^{\alpha/2-1}}]_{s,2}$ and $B^s_{\omega^{3\alpha/2-2}} = [B^0_{\omega^{3\alpha/2-2}}, B^1_{\omega^{3\alpha/2-2}}]_{s,2}$. By the definition of the weighted Sobolev space (2.1.3) we have $B^k_{\omega^{\alpha/2-1}} \subset B^k_{\omega^{3\alpha/2-2}}$ for $k = 0, 1$. Then it follows that $B^s_{\omega^{\alpha/2-1}} \subset B^s_{\omega^{3\alpha/2-2}}$, i.e.

$$|v|_{B^s_{\omega^{3\alpha/2-2}}} \leq C|v|_{B^s_{\omega^{\alpha/2-1}}}. \tag{.1.13}$$

Second, we have

$$\|v\|_{L^2_{\omega^{3\alpha/2-2-s}}}^2 \leq c_\epsilon \|v\|_{L^\infty}^2, \quad \text{where } c_\epsilon = \int_{-1}^1 (1-x^2)^{\epsilon-1}dx. \tag{.1.14}$$

Applying Lemma .1.4 we have that the space $B^s_{\omega^{\alpha/2-1}} \subset H^{\alpha/2-\epsilon}$ for $\epsilon > 0$. Thus it gives $B^s_{\omega^{\alpha/2-1}} \subset L^\infty$, i.e.

$$\|v\|_{L^\infty}^2 \leq C|v|_{B^s_{\omega^{\alpha/2-1}}}^2. \tag{.1.15}$$

By (.1.12)-(.1.15), we have

$$\begin{aligned} |v\omega^{\alpha/2-1}|_{B^s_{\omega^{\alpha/2}}}^2 &\leq C(|v|_{B^s_{\omega^{3\alpha/2-2}}}^2 + \|v\|_{L^2_{\omega^{3\alpha/2-2-s}}}^2) \\ &\leq C(|v|_{B^s_{\omega^{\alpha/2-1}}}^2 + \|v\|_{L^\infty}^2) \leq C\|v\|_{B^s_{\omega^{\alpha/2-1}}}^2. \end{aligned} \tag{.1.16}$$

By (.1.11), (.1.16) and the definition of the norm (.1.3) in the weighted Sobolev space, we have the desired conclusion for $1 < \alpha \leq 4/3$.

Case 2. If $4/3 < \alpha < 2$, then $s = 3\alpha/2 - 1 - \epsilon \in (1, 2)$ for sufficiently small $\epsilon > 0$. By the norm of weighted Sobolev space (.1.3), we need to bound three terms: $\left\|v\omega^{\alpha/2-1}\right\|_{L^2_{\omega^{\alpha/2}}}$, $\|D(v\omega^{\alpha/2-1})\|_{L^2_{\omega^{\alpha/2+1}}}$ and $|D(v\omega^{\alpha/2-1})|_{B^{s-1}_{\omega^{\alpha/2+1}}}$.

First, we have $D(v\omega^{\alpha/2-1}) = \omega^{\alpha/2-1}Dv + (2-\alpha)x\omega^{\alpha/2-2}v$ and thus

$$\begin{aligned} \|D(v\omega^{\alpha/2-1})\|_{L^2_{\omega^{\alpha/2+1}}} &\leq \|\omega^{\alpha/2-1}Dv\|_{L^2_{\omega^{\alpha/2+1}}} + \|(2-\alpha)x\omega^{\alpha/2-2}v\|_{L^2_{\omega^{\alpha/2+1}}} \\ &\leq C\|Dv\|_{L^2_{\omega^{\alpha/2}}} + C\|v\|_\infty. \end{aligned}$$

113

Here by Lemma .1.4 and the Sobolev embedding inequality, we have

$$\|v\|_{L^\infty} \leq C\|v\|_{B^s_{\omega^{\alpha/2-1}}}. \tag{.1.17}$$

Thus, it holds that

$$\|D(v\omega^{\alpha/2-1})\|_{L^2_{\omega^{\alpha/2+1}}} \leq C\|Dv\|_{L^2_{\omega^{\alpha/2}}} + C\|v\|_\infty \leq C\|v\|_{B^s_{\omega^{\alpha/2-1}}} \tag{.1.18}$$

Second, we have

$$|D(v\omega^{\alpha/2-1})|_{B^{s-1}_{\omega^{\alpha/2+1}}} \leq |\omega^{\alpha/2-1}Dv|_{B^{s-1}_{\omega^{\alpha/2+1}}} + |(2-\alpha)x\omega^{\alpha/2-2}v|_{B^{s-1}_{\omega^{\alpha/2+1}}} =: \text{I} + \text{II}. \tag{.1.19}$$

Applying Lemma .1.6 gives

$$\begin{aligned}
\text{I} = |\omega^{\alpha/2-1}Dv|^2_{B^{s-1}_{\omega^{\alpha/2+1}}} &\leq C(|Dv|^2_{B^{s-1}_{\omega^{3\alpha/2-1}}} + \|Dv\|^2_{L^2_{\omega^{3\alpha/2-s}}}) \\
&\leq C(|Dv|^2_{B^{s-1}_{\omega^{\alpha/2}}} + \|Dv\|^2_{L^2_{\omega^{\alpha/2}}}) \leq C\|v\|^2_{B^s_{\omega^{\alpha/2-1}}}.
\end{aligned} \tag{.1.20}$$

For the term II, we have

$$\text{II} = |(2-\alpha)x\omega^{\alpha/2-2}v|_{B^{s-1}_{\omega^{\alpha/2+1}}} \leq |\omega^{\alpha/2-2}v|^2_{B^{s-1}_{\omega^{\alpha/2+1}}}. \tag{.1.21}$$

The term in the last inequality can be bounded by applying Lemma .1.6 and

$$|\omega^{\alpha/2-2}v|^2_{B^{s-1}_{\omega^{\alpha/2+1}}} \leq C(|v|^2_{B^{s-1}_{\omega^{3\alpha/2-3}}} + \|v\|^2_{L^2_{\omega^{3\alpha/2-2-s}}}) \leq C(|v|^2_{B^{s-1}_{\omega^{3\alpha/2-3}}} + \|v\|^2_{L^\infty}).$$

Then by $\|v\|_{L^\infty} \leq C\|v\|_{B^s_{\omega^{\alpha/2-1}}}$ in (.1.17), we have

$$|\omega^{\alpha/2-2}v|^2_{B^{s-1}_{\omega^{\alpha/2+1}}} \leq C(|v|^2_{B^{s-1}_{\omega^{3\alpha/2-3}}} + \|v\|^2_{B^s_{\omega^{\alpha/2-1}}}). \tag{.1.22}$$

We claim and prove shortly that

$$|v|_{B^{s-1}_{\omega^{3\alpha/2-3}}} \leq C\|v\|_{B^s_{\omega^{\alpha/2-1}}}, \tag{.1.23}$$

and thus by (.1.21) and (.1.22), we have

$$\text{II} \leq |\omega^{\alpha/2-2}v|^2_{B^{s-1}_{\omega^{\alpha/2+1}}} \leq C\|v\|^2_{B^s_{\omega^{\alpha/2-1}}}. \tag{.1.24}$$

Further, we have from (.1.19), (.1.20) and (.1.24) that

$$|D(v\omega^{\alpha/2-1})|_{B^{s-1}_{\omega^{\alpha/2+1}}} = \text{I} + \text{II} \leq C\|v\|_{B^s_{\omega^{\alpha/2-1}}}. \tag{.1.25}$$

By the norm of weighted Sobolev space (.1.3), (.1.18), and (.1.25),

$$\begin{aligned}
\left\|v\omega^{\alpha/2-1}\right\|_{B^s_{\omega^{\alpha/2}}} &\leq \left\|v\omega^{\alpha/2-1}\right\|_{L^2_{\omega^{\alpha/2}}} + \|D(v\omega^{\alpha/2-1})\|_{L^2_{\omega^{\alpha/2+1}}} + |D(v\omega^{\alpha/2-1})|_{B^{s-1}_{\omega^{\alpha/2+1}}} \\
&\leq \|v\|_{L^2_{\omega^{\alpha/2-1}}} + C\|v\|_{B^s_{\omega^{\alpha/2-1}}} \leq C\|v\|_{B^s_{\omega^{\alpha/2-1}}}.
\end{aligned}$$

114

This is the desired conclusion for $4/3 < \alpha < 2$.

It remains to check the claim (.1.23). In fact, we have by Lemma .1.2 that

$$B^s_{\omega^{\alpha/2-1}} = [B^1_{\omega^{\alpha/2-1}}, B^2_{\omega^{\alpha/2-1}}]_{\sigma,2} \approx [W^{1,2}_{\omega^{\alpha/2}}, W^{2,2}_{\omega^{\alpha/2+1}}]_{\sigma,2}, \tag{.1.26}$$

$$B^{s-1}_{\omega^{3\alpha/2-3}} = [B^0_{\omega^{3\alpha/2-3}}, B^1_{\omega^{3\alpha/2-3}}]_{\sigma,2} \approx [W^{0,2}_{\omega^{3\alpha/2-3}}, W^{1,2}_{\omega^{3\alpha/2-2}}]_{\sigma,2}, \tag{.1.27}$$

where $\sigma = s - 1$. By Lemma .1.3, we have

$$[W^{1,2}_{\omega^{\alpha/2}}, W^{2,2}_{\omega^{\alpha/2+1}}]_{\sigma,2} \subset [W^{0,2}_{\omega^{3\alpha/2-3}}, W^{1,2}_{\omega^{3\alpha/2-2}}]_{\sigma,2}. \tag{.1.28}$$

Then by (.1.26)-(.1.28), we have $B^s_{\omega^{\alpha/2-1}} \subset B^{s-1}_{\omega^{3\alpha/2-3}}$ and thus (.1.23) is proved. This completes the proof in Case 2 of Step 2.

Step 3. For $s \in [0, 3\alpha/2 - 1 - \epsilon]$, we use the interpolation technique to show that $\omega^{\alpha/2-1}v \in B^s_{\omega^{\alpha/2-1}}$ if $v \in B^s_{\omega^{\alpha/2-1}}$.

By the definition (.1.2), $B^s_{\omega^{\alpha/2-1}} = [B^0_{\omega^{\alpha/2-1}}, B^{3\alpha/2-1-\epsilon}_{\omega^{\alpha/2-1}}]_{\sigma,2}$ with $\sigma = 3\alpha/2 - 1 - \epsilon$. Thus for any $v \in B^s_{\omega^{\alpha/2-1}}$, there exists a decomposition $v = v_1 + v_2$ with $v_1 \in B^0_{\omega^{\alpha/2-1}}$ and $v_2 \in B^{3\alpha/2-1-\epsilon}_{\omega^{\alpha/2-1}}$ such that

$$\int_0^\infty t^{-2\theta} \left(\|v_1\|_{B^0_{\omega^{\alpha/2-1}}} + t\|v_2\|_{B^{3\alpha/2-1-\epsilon}_{\omega^{\alpha/2-1}}} \right)^2 \frac{dt}{t} < 2\|v\|^2_{B^s_{\omega^{\alpha/2-1}}}. \tag{.1.29}$$

As we have proved the conclusion of Lemma 2.2.5 for $s = 0$ and $s = 3\alpha/2 - 1 - \epsilon$, it holds

$$\|\omega^{\alpha/2-1}v_1\|_{B^0_{\omega^{\alpha/2}}} \le C\|v_1\|_{B^0_{\omega^{\alpha/2-1}}}, \tag{.1.30}$$

$$\|\omega^{\alpha/2-1}v_2\|_{B^{3\alpha/2-1-\epsilon}_{\omega^{\alpha/2}}} \le C\|v_2\|_{B^{3\alpha/2-1-\epsilon}_{\omega^{\alpha/2-1}}}. \tag{.1.31}$$

Together with (.1.29), we have

$$\int_0^\infty t^{-2\theta} \left(\|\omega^{\alpha/2-1}v_1\|_{B^0_{\omega^{\alpha/2}}} + t\|\omega^{\alpha/2-1}v_2\|_{B^{3\alpha/2-1-\epsilon}_{\omega^{\alpha/2}}} \right)^2 \frac{dt}{t}$$

$$\le C \int_0^\infty t^{-2\theta} \left(\|v_1\|_{B^0_{\omega^{\alpha/2-1}}} + t\|v_2\|_{B^{3\alpha/2-1-\epsilon}_{\omega^{\alpha/2-1}}} \right)^2 \frac{dt}{t} < 2\|v\|^2_{B^s_{\omega^{\alpha/2-1}}}. \tag{.1.32}$$

This inequality suggests the decomposition $\omega^{\alpha/2-1}v = \omega^{\alpha/2-1}v_1 + \omega^{\alpha/2-1}v_2$ with $\omega^{\alpha/2-1}v_1 \in B^0_{\omega^{\alpha/2-1}}$ and $\omega^{\alpha/2-1}v_2 \in B^{3\alpha/2-1-\epsilon}_{\omega^{\alpha/2-1}}$. By the equivalent definition (.1.2), we have $\omega^{\alpha/2-1}v \in B^s_{\omega^{\alpha/2-1}}$. This completes the proof. $\square$

Since the Lemma .3.1 can be proved similarly as the Lemma 2.2.5, we provide a sketch.

Proof **Step 1.** It is clear that $v\omega^{\alpha/2} \in B^s_{\omega^{\alpha/2}}$ for $s = 0$ if $v \in B^s_{\omega^{\alpha/2}}$.

Step 2. For $s = 3\alpha/2 + 1 - \epsilon$ and $v \in B^s_{\omega^{\alpha/2}}$, using Lemma .1.4 we have $v \in L^\infty$.

Case 1. $1 < \alpha < 4/3$ and $3\alpha/2 + 1 - \epsilon \in (2,3)$. Note that $D(v\omega^{\alpha/2}) = Dv\omega^{\alpha/2} + vD\omega^{\alpha/2}$ and $D^2(v\omega^{\alpha/2}) = D^2v\omega^{\alpha/2} + 2DvD\omega^{\alpha/2} + vD^2\omega^{\alpha/2}$. By direct calculation and the L^∞ bound of v, we know that $v\omega^{\alpha/2} \in B^k_{\omega^{\alpha/2}}$ for $v \in B^k_{\omega^{\alpha/2}}$ and $k = 0, 1, 2$. For $k = s \in (2,3)$, by the definition (.1.3), it suffices to show the semi-norm

$$|v\omega^{\alpha/2}|^2_{B^s_{\omega^{\alpha/2}}} = |D^2(v\omega^{\alpha/2})|^2_{B^{s-2}_{\omega^{\alpha/2+2}}} \tag{.1.33}$$

$$\le |\omega^{\alpha/2}D^2v|^2_{B^{s-2}_{\omega^{\alpha/2+2}}} + C|\omega^{\alpha/2-1}Dv|^2_{B^{s-2}_{\omega^{\alpha/2+2}}} + C|\omega^{\alpha/2-2}v|^2_{B^{s-2}_{\omega^{\alpha/2+2}}} < \infty,$$

where each term can be bounded, by Lemma .1.6.

Case 2. When $4/3 \leq \alpha < 2$ and $s = 3\alpha/2 + 1 - \epsilon \in [3, 4)$, the proof follows similar arguments in Case 1.

Step 3. For $0 < s < 3\alpha/2 + 1$, we use the interpolation technique to derive the desired result.

□

.2 Using the combinations of Gegenbauer polynomial $C_n^\nu(x)$ and elementary functions

Gegenbauer polynomial $C_n^\nu(x)$ are normalized by

$$\int_{-1}^{1} (1 - x^2)^{\nu - 1/2} [C_n^\nu(x)]^2 dx = \frac{\pi 2^{1-2\nu} \Gamma(n + 2\nu)}{n!(n + \nu)[\Gamma(\nu)]^2}. \tag{.2.1}$$

By (2.1.4) and (.2.1), we have

$$P_n^{\alpha/2} = b_n^{\alpha/2} C_n^{\alpha/2 + 1/2}, \quad b_n^{\alpha/2} = \frac{2^{\alpha + 1/2} \Gamma(n + \alpha/2 + 1)\Gamma(\alpha/2 + 1)}{\sqrt{\pi}\Gamma(n + \alpha + 1)}. \tag{.2.2}$$

For any a, it holds that (see Page 797 in [44])

$$\int_{-1}^{1} (1 - x^2)^{\nu - 1/2} e^{iax} C_n^\nu(x) dx = \Phi(a, n, \nu) i^n, \quad \Phi(a, n, \nu) := \frac{\pi 2^{1-\nu} \Gamma(2\nu + n)}{n! \Gamma(\nu)} a^{-\nu} J_{\nu + n}(a), \tag{.2.3}$$

where $\mathrm{Re}(\nu) > -1/2$.

Lemma .2.1. *For positive real numbers ν and z it holds that*

$$|J_\nu(z)| \leq C_l (\frac{z}{\nu})^l z^{-1/2}, \tag{.2.4}$$

where C_l is a constant which depends on the positive number l.

Proof. It suffices to show that (.2.4) holds when l is integer as the non-integer case can be straight-forwardly proved by standard interpolation. Noting that for the Bessel function $J_\nu(z)$, we have (https://dlmf.nist.gov/10.6 and https://dlmf.nist.gov/10.7)

$$J_{\nu+1}(z) + J_{\nu-1}(z) = \frac{2\nu}{z} J_\nu(z), \tag{.2.5}$$

$$J_\nu(z) = \sqrt{2/(\pi z)}(\cos(z - \frac{1}{2}\nu\pi - \frac{\pi}{4}) + e^{|\mathrm{Imag}(z)|}\mathcal{O}(1)), \quad z \to \infty. \tag{.2.6}$$

Thus we have

$$|J_v(z)| = |\frac{z}{2\nu}(J_{\nu+1}(z) + J_{\nu-1}(z))| \leq C(\frac{z}{\nu})z^{-1/2}. \tag{.2.7}$$

Repeatedly using (.2.7) l times gives $|J_\nu(z)| \leq C_l(\frac{z}{\nu})^l z^{-1/2}$. □

116

With all preparations above we now can estimate the $a_{n,k}^{\alpha/2}$. Take the basis function $e_k(x) = \sin(k\pi(\frac{x+1}{2})) = \sin(\frac{k\pi x}{2})\cos(\frac{k\pi}{2}) + \cos(\frac{k\pi x}{2})\sin(\frac{k\pi}{2})$. Then letting $a = \frac{k\pi}{2}$ and $\nu = \alpha/2 + 1/2$ yields

$$
\begin{aligned}
a_{n,k}^{\alpha/2} &= \frac{1}{h_n^{\alpha/2}}\int_{-1}^{1}(1-x^2)^{\alpha/2}e_k(x)P_n^{\alpha/2}(x)dx = \frac{b_n^{\alpha/2}}{h_n^{\alpha/2}}\int_{-1}^{1}(1-x^2)^{\alpha/2}e_k(x)C_n^{\alpha/2+1/2}(x)dx \\
&\leq \frac{b_n^{\alpha/2}}{h_n^{\alpha/2}}\Phi(\frac{k\pi}{2},n,\frac{\alpha+1}{2}) = \frac{b_n^{\alpha/2}}{h_n^{\alpha/2}}\frac{\pi 2^{1-\nu}\Gamma(2\nu+n)}{n!\Gamma(\nu)}a^{-\nu}J_{\nu+n}(a) \\
&\leq C\frac{n^{\alpha/2+1}}{k^{(\alpha+1)/2}}J_{n+(\alpha+1)/2}(\frac{k\pi}{2}),
\end{aligned}
\tag{.2.8}
$$

where we have used the formula (3.3.8). By the estimate (.2.4), we have

$$
a_{n,k}^{\alpha/2} \leq C\frac{n^{\alpha/2+1}}{k^{(\alpha+1)/2}}J_{n+(\alpha+1)/2}(\frac{k\pi}{2}) \leq C\frac{n^{\alpha/2+1}}{k^{(\alpha+1)/2}}(\frac{k}{n})^l k^{-1/2} = Cn^{\alpha/2+1-l}k^{l-\alpha/2-1},
\tag{.2.9}
$$

where C may change each line but independent of n and k. Substituting (.2.9) into (2.5.9) and combining with (2.1.8) leads to

$$
\|\dot{W}^\beta\|_{\mathbb{L}^2(\Omega;B_\beta^s)}^2 = \sum_{k,n=0}^{\infty}k^{-\beta}|a_{n,k}^{\alpha/2}|^2 h_n^{\alpha/2}(1+n^2)^s \leq C\sum_{k,n=0}^{\infty}k^{-\beta}n^{\alpha+2-2l}k^{2l-\alpha-2}h_n^{\alpha/2}(1+n^2)^s.
\tag{.2.10}
$$

Observe that $h_n^{\alpha/2} \approx n^{-1}$, which can be derived by (3.3.8). In order to $\|\dot{W}^\beta\|_{\mathbb{L}^2(\Omega;B_\beta^s)}^2 < \infty$ it suffices to let $l < \alpha/2 + \beta$ and $2s + \alpha/2 + 1 - l < 0$, which implies $s < \frac{\beta}{2} - \frac{1}{2}$. This shows the regularity index of color noise $\dot{W}^\beta(x)$ is $\frac{\beta}{2} - \frac{1}{2} - \epsilon$ for any $\epsilon > 0$.

.3 The proof of Lemma 3.3.4

The Jacobi polynomials $P_n^{\gamma,\beta}(z)$ defined as hyper-geometric form

$$
P_n^{\gamma,\beta}(z) = \begin{pmatrix} n+\gamma \\ n \end{pmatrix} {}_2F_1(-n,n+\gamma+\beta+1;\gamma+1,\frac{1-z}{2})
\tag{.3.1}
$$

are mutually orthogonal.

Denote $a_m(r) = \sum_{n=0}^{\infty}a_{m,n}^{\alpha/2}P_n^{\alpha/2,m}(2r^2-1)$ and $b_m(r) = \sum_{n=0}^{\infty}b_{m,n}^{\alpha/2}P_n^{\alpha/2,m}(2r^2-1)$. Then (3.2.4) can be rewritten as

$$
v = \sum_{m=0}^{+\infty}a_m(r)r^m\cos(m\theta) + \sum_{m=0}^{+\infty}b_m(r)r^m\sin(m\theta).
$$

Analogous to the 1d case in [57], we have an equivalent semi-norm of $|\cdot|_{\mathbf{B}_{\alpha/2}^{s_1,s_2}(\Omega)}$ and

$$
|v|_{\mathbf{B}_{\alpha/2}^{s_1,s_2}(\Omega)}^2 = \sum_{m=0}^{\infty}m^{2s_1}(\|\tilde{a}_m\|_{L_{\alpha/2,m}^2(\Lambda)}^2 + \|\tilde{b}_m\|_{L_{\alpha/2,m}^2(\Lambda)}^2) + \sum_{m=0}^{\infty}(|\tilde{a}_m|_{B_{\alpha/2,m}^{s_2}(\Lambda)}^2 + |\tilde{b}_m|_{B_{\alpha/2,m}^{s_2}(\Lambda)}^2),
$$

$$
\tag{.3.2}
$$

where $\tilde{a}_m(z) = a_m((\frac{1+z}{2})^{1/2})/2^{m/2}$ and $\tilde{b}_m(z) = b_m((\frac{1+z}{2})^{1/2})/2^{m/2}$. Here we denote the weighted space of all functions defined on the unit interval $\Lambda = (-1, 1)$ by $L^2_{\gamma,\beta}(\Lambda)$ with the associated norm $\|\cdot\|_{L^2_{\gamma,\beta}(\Lambda)}$ $(\gamma, \beta \in \mathbb{R})$ in one dimension as

$$\|u\|^2_{L^2_{\gamma,\beta}(\Lambda)} = \int_{-1}^{1} u^2(z)(1-z)^\gamma(1+z)^\beta dz < \infty.$$

The non-uniformly Jacobi-weighted Sobolev space $B^J_{\gamma,\beta}(\Lambda)$, when J is a nonnegative integer, is defined by

$$B^J_{\gamma,\beta}(\Lambda) := \left\{ u \,|\, \partial^j_r u \in L^2_{\gamma+j,\beta+j}(\Lambda), \, j = 0, 1, \dots, J \right\},$$

which is equipped with the following norm

$$\|u\|_{B^J_{\gamma,\beta}(\Lambda)} = \Big(\sum_{j=0}^{J} |u|^2_{B^j_{\gamma,\beta}(\Lambda)} \Big)^{1/2}, \quad |u|_{B^j_{\gamma,\beta}(\Lambda)} = \big\|\partial^j_r u\big\|_{L^2_{\gamma,\beta}(\Lambda)}.$$

When $J = s$ is not an integer, the space can be defined via classical interpolation method, e.g. K-method; see [5]. For more details see [55].

To prove Lemma 3.3.4, we need the following lemma.

Lemma .3.1 ([57]). *If $v(z) \in B^s_{\alpha/2,m}(\Lambda)$, then $(1 - r^2(z))^{\alpha/2}v(z) \in B^{\min(s,3\alpha/2+1-\epsilon)}_{\alpha/2,m}(\Lambda)$. Here $r(z) = (\frac{1+z}{2})^{1/2}$ and $\epsilon > 0$ arbitrarily small.*

With all preparations above, we are ready to prove Lemma 3.3.4.

Proof of Lemma 3.3.4. Since $v \in \mathbf{B}^{s_1,s_2}_{\alpha/2}(\Omega)$ with $s_1, s_2 \geq 0$, we can write v in the form of (3.2.4) and the semi-norm (.3.2) of v can be bounded,

$$|v|^2_{\mathbf{B}^{s_1,s_2}_{\alpha/2}(\Omega)} = \sum_{m=0}^{\infty} m^{2s_1}(\|\tilde{a}_m\|^2_{L^2_{\alpha/2,m}(\Lambda)} + \|\tilde{b}_m\|^2_{L^2_{\alpha/2,m}(\Lambda)}) + \sum_{m=0}^{\infty}(|\tilde{a}_m|^2_{B^{s_2}_{\alpha/2,m}(\Lambda)} + |\tilde{b}_m|^2_{B^{s_2}_{\alpha/2,m}(\Lambda)}) < \infty$$

where $\tilde{a}_m(z) = a_m(r(z))/2^{m/2}$ and $\tilde{b}_m(z) = b_m(r(z))/2^{m/2}$. It suffices to show the semi-norm of product $(1 - r^2(z))^{\alpha/2}v$ can also be bounded. Applying Lemma .3.1, we have

$$|(1 - r^2)^{\alpha/2}\tilde{a}_m|^2_{B^{\min(s_2,3/2\alpha+1-\epsilon)}_{\alpha/2,m}(\Lambda)} \leq c|\tilde{a}_m|^2_{B^{s_2}_{\alpha/2,m}(\Lambda)}, \quad |(1 - r^2)^{\alpha/2}\tilde{b}_m|^2_{B^{\min(s_2,3/2\alpha+1-\epsilon)}_{\alpha/2,m}(\Lambda)} \leq c|\tilde{b}_m|^2_{B^{s_2}_{\alpha/2,m}(\Lambda)}.$$

Thus we have $|(1 - r^2)^{\alpha/2}v|^2_{\mathbf{B}^{s_1,s_2}_{\alpha/2}(\Omega)} \leq C|v|^2_{\mathbf{B}^{s_1,s_2}_{\alpha/2}(\Omega)}$. This completes the proof. $\qquad\square$

.4 Calculations of integrals arising in the orthogonal expansion

To compute the fractional norm of the functions in numerical test, we need the following formulas for the calculation of integrals to obtain the expansion coefficients $a_{m,n}$ in (3.2.5) and $b_{m,n}$ in (3.2.6).

Define

$$I_{m,n,k} =: \int_0^1 r^{k+m} P^{\alpha/2,m}_n(2r^2 - 1)(1 - r^2)^{\alpha/2} r \, dr. \tag{.4.1}$$

Lemma .4.1. *Let k, m, n be nonnegative integers. When $(k - m)/2 \geq n$, it holds that*

$$I_{m,n,k} = \frac{\Gamma(\alpha/2 + n + 1)}{2\Gamma(n + 1)} \frac{\Gamma((m + k)/2 + 1)}{\Gamma((k - m)/2 - n + 1)} \frac{\Gamma((k - m)/2 + 1)}{\Gamma(\alpha/2 + n + (m + k)/2 + 2)}. \quad (.4.2)$$

When $(k - m)/2 < n$ and $(k - m)/2$ is not a non-negative integer, it holds that

$$I_{m,n,k} = (-1)^n \frac{\Gamma(\alpha/2 + n + 1)}{2\Gamma(n + 1)} \cdot \frac{\Gamma((m + k)/2 + 1)}{\Gamma((m - k)/2)} \cdot \frac{\Gamma((m - k)/2 + n)}{\Gamma(\alpha/2 + n + (m + k)/2 + 2)}. \quad (.4.3)$$

When $(k - m)/2 < n$ and $(k - m)/2$ is a non-negative integer, it holds that $I_{m,n,k} = 0$.

Proof By a change of variable $z = 2r^2 - 1$ in the integral $I_{m,n,k}$, we have

$$I_{m,n,k} = \frac{1}{2^{(m+k)/2 + \alpha/2 + 2}} \int_{-1}^{1} (1 + z)^{(m+k)/2} P_n^{\alpha/2, m}(z)(1 - z)^{\alpha/2} dz$$

$$= \frac{1}{2^{(m+k)/2 + \alpha/2 + 2}} \int_{-1}^{1} (1 + z)^{(k-m)/2} P_n^{\alpha/2, m}(z)(1 - z)^{\alpha/2}(1 + z)^m dz$$

$$= \frac{1}{2^{(m+k)/2 + \alpha/2 + 2}} \int_{-1}^{1} (1 + z)^{(k-m)/2} \cdot \frac{(-1)^n}{2^n \Gamma(n + 1)} \frac{d^n}{dx^n} \left((1 - z)^{\alpha/2 + n}(1 + z)^{m+n} \right) dz.$$

where we have used the Rodrigues' Formula for the Jacobi polynomials in the last equality. Then using the integration by parts repeatedly, we have

$$I_{m,n,k} = \frac{1}{2^{(m+k)/2 + n + \alpha/2 + 2} \Gamma(n + 1)} \int_{-1}^{1} \frac{d^n}{dx^n} \left((1 + z)^{(k-m)/2} \right) (1 - z)^{\alpha/2 + n}(1 + z)^{m+n} dz. \quad (.4.4)$$

Case 1. When $(k - m)/2 \geq n$, it holds that

$$\frac{d^n}{dx^n} \left((1 + z)^{(k-m)/2} \right) = \frac{k - m}{2}(\frac{k - m}{2} - 1) \cdots (\frac{k - m}{2} - n + 1)(1 + z)^{(k-m)/2 - n}$$

$$= \frac{\Gamma((k - m)/2 + 1)}{\Gamma((k - m)/2 - n + 1)}(1 + z)^{(k-m)/2 - n}.$$

Substituting the above equality into (.4.4) gives

$$I_{m,n,k} = \frac{1}{2^{(m+k)/2 + n + \alpha/2 + 2} \Gamma(n + 1)} \cdot \frac{\Gamma((k - m)/2 + 1)}{\Gamma((k - m)/2 - n + 1)} \int_{-1}^{1} (1 - z)^{\alpha/2 + n}(1 + z)^{(m+k)/2} dz.$$

Observing that $\int_{-1}^{1} (1 - z)^{\alpha/2 + n}(1 + z)^{(m+k)/2} dz = h_0^{\alpha/2 + n, (m+k)/2}$ and by (6.1.5), we obtain

$$I_{m,n,k} = \frac{1}{2^{(m+k)/2 + n + \alpha/2 + 2} \Gamma(n + 1)} \cdot \frac{\Gamma((k - m)/2 + 1)}{\Gamma((k - m)/2 - n + 1)} \cdot \frac{2^{\alpha/2 + n + (m+k)/2 + 1}}{\alpha/2 + n + (m + k)/2 + 1}$$

$$\cdot \frac{\Gamma(\alpha/2 + n + 1)\Gamma((m + k)/2 + 1)}{\Gamma(\alpha/2 + n + (m + k)/2 + 1)}.$$

The desired result in (.4.2) is obtained after some simplification of the above equality.

Case 2. When $(k-m)/2 < n$ and $(k-m)/2$ is not non-negative integer, it holds that

$$
\begin{aligned}
\frac{d^n}{dx^n}\left((1+z)^{(k-m)/2}\right) &= (-1)^n \frac{m-k}{2}(\frac{m-k}{2}+1)\cdots(\frac{m-k}{2}+n-1)(1+z)^{(k-m)/2-n} \\
&= (-1)^n \frac{\Gamma((m-k)/2+n)}{\Gamma((m-k)/2)}(1+z)^{(k-m)/2-n}.
\end{aligned}
$$

Substituting the above equality into (.4.4) gives

$$
I_{m,n,k} = \frac{1}{2^{(m+k)/2+n+\alpha/2+2}\Gamma(n+1)} \cdot (-1)^n \frac{\Gamma((m-k)/2+n)}{\Gamma((m-k)/2)} \int_{-1}^{1} (1-z)^{\alpha/2+n}(1+z)^{(m+k)/2}dz.
$$

By this equality, and (6.1.5), we obtain (.4.3).

Case 3. When $(k-m)/2 < n$ and $(k-m)/2$ is a non-negative integer, $\frac{d^n}{dx^n}\left((1+z)^{(k-m)/2}\right) = 0$ and thus $I_{m,n,k} = 0$. $\qquad\square$

Lemma .4.2. *It holds that for integers $k > m$, and $k - m$ is even,*

$$
I^1_{m,k} = \int_0^{2\pi} \cos^k(\theta)\cos(m\theta)d\theta = \frac{2\pi}{2^m} \frac{\Gamma(k+1)}{\Gamma(k-m+1)} \frac{\Gamma((k-m)/2+1/2)}{\Gamma((k+m)/2+1)},
$$

and otherwise $I^1_{m,k} = 0$. For all integers $k \geq 0$ and m,

$$
I^2_{m,k} = \int_0^{2\pi} \cos^k(\theta)\sin(m\theta)d\theta = 0.
$$

Proof By the formula (see Page 166 in [44]),

$$
\int \cos^k(\theta)\cos(m\theta)d\theta = \frac{1}{k+m}\left\{\cos^k(\theta)\sin(m\theta) + k\int \cos^{k-1}(\theta)\cos((m-1)\theta)d\theta\right\}, \quad (.4.5)
$$

we have the relationship $I^1_{m,k} = \frac{k}{k+m}I^1_{m-1,k-1}$. For $k \geq m$, using this relationship repeatedly, we have

$$
\begin{aligned}
I^1_{m,k} &= \frac{k}{k+m}\frac{k-1}{k+m-2}\cdots\frac{k-m+1}{k-m+2}\int_0^{2\pi}\cos^{k-m}(x)dx \\
&= \frac{\Gamma(k+1)}{\Gamma(k-m+1)}\frac{1}{2^m}\frac{\Gamma((k+m)/2-m+1)}{\Gamma((k+m)/2+1)}\int_0^{2\pi}\cos^{k-m}(x)dx.
\end{aligned}
$$

If $k - m = 2l - 1$ with integer l, then $\int_0^{2\pi}\cos^{k-m}(x)dx = 0$. If $k - m = 2l$, we have the following formula (see Page 152 in [44])

$$
\int_0^{2\pi} \cos^{k-m}(x)dx = 2\pi\frac{(2l-1)!!}{2^l l!} = 2\pi\frac{\Gamma(l+1/2)}{\Gamma(l+1)} = 2\pi\frac{\Gamma((k-m)/2+1/2)}{\Gamma((k-m)/2+1)}.
$$

For $k > m$ and $k - m = 2l$, it follows that

$$
I^1_{m,k} = \frac{2\pi}{2^m}\frac{\Gamma(k+1)}{\Gamma(k-m+1)}\frac{\Gamma((k-m)/2+1/2)}{\Gamma((k+m)/2+1)}.
$$

120

For $k < m$, $I^1_{m,k} = 0$ as it follows from (.4.5) that

$$I^1_{m,k} = \frac{k}{k+m}\frac{k-1}{k+m-2}\cdots\frac{k-m+1}{k-m+2}\int_0^{2\pi}\cos((m-k)x)dx = 0.$$

Since the integrand is an odd function over a symmetric domain, it follows that $I^2_{m,k} = 0$. $\quad\square$

Lemma .4.3. *For integers k, m, it holds that when k, m are nonnegative even numbers and $k - m \geq 0$,*

$$\begin{aligned}
I^3_{m,k} &= \int_0^{2\pi}\sin^k(\theta)\cos(m\theta)d\theta, \\
&= \frac{2\pi(-1/8)^{m/2}\Gamma(k+1)\Gamma((k-m)/2+1/2)\Gamma((k-m)/2+3/2)\Gamma((k-m)/4+1/2)}{\Gamma(k-m+1)\Gamma((k-m)/2+1)\Gamma(k/2+3/2)\Gamma((k+m)/4+1/4)},
\end{aligned}$$

and otherwise $I^3_{m,k} = 0$. When k, m are odd numbers and $k - m \geq 0$, it holds that

$$\begin{aligned}
I^4_{m,k} &= \int_0^{2\pi}\sin^k(\theta)\sin(m\theta)d\theta \\
&= \frac{2\pi(-1/8)^{(m-1)/2}\Gamma(k+1)\Gamma((k-m)/2+1/2)\Gamma((k-m)/2+3/2)\Gamma((k-m)/4+1/2)}{(k+m)\Gamma(k-m+1)\Gamma((k-m)/2+1)\Gamma(k/2+3/2)\Gamma((k+m)/4-1/4)}.
\end{aligned}$$

Proof Using the formulas (see Page 163-164 in [44])

$$\int\sin^k(\theta)\cos(m\theta)d\theta = \frac{1}{k+1}\left\{\sin^k(\theta)\sin(m\theta) - k\int\sin^{k-1}(\theta)\sin((m-1)\theta)d\theta\right\},$$

$$\int\sin^k(\theta)\sin(m\theta)d\theta = \frac{1}{k+m}\left\{-\sin^k(\theta)\cos(m\theta) + k\int\sin^{k-1}(\theta)\cos((m-1)\theta)d\theta\right\},$$

we have $I^3_{m,k} = -\frac{k}{k+1}I^4_{m-1,k-1}$ and $I^4_{m,k} = \frac{k}{k+m}I^3_{m-1,k-1}$. Consequently, it holds that

$$I^3_{m,k} = -\frac{k}{k+1}I^4_{m-1,k-1} = -\frac{k}{k+1}\cdot\frac{k-1}{k-1+m-1}I^3_{m-2,k-2}. \tag{.4.6}$$

When k, m are even numbers and $k \geq m$, repeatedly using the relation (.4.6), we have

$$I^3_{m,k} = \frac{(-1)^{m/2}k(k-1)(k-2)(k-3)\cdots(k-m+2)(k-m+1)}{(k+1)(k+m-2)(k-1)(k+m-6)\cdots(k-m+3)(k-m+2)}I^3_{0,k-m}. \tag{.4.7}$$

When $k - m$ is even, by the formulas (see Page 152)

$$\int\sin^{2l}(\theta)d\theta$$

$$= -\frac{\cos(\theta)}{2l}\left\{\sin^{2l-1}(\theta) + \sum_{k=1}^{l-1}\frac{(2l-1)(2l-3)\cdots(2l-2k+1)}{2^k(l-1)(l-2)\cdots(l-k)}\sin^{2l-2k-1}(\theta)\right\} + \frac{(2l-1)!!}{(2l)!!}\theta,$$

$$\int\sin^{2l+1}(\theta)d\theta = -\frac{\cos(\theta)}{2l+1}\left\{\sin^{2l}(\theta) + \sum_{k=0}^{l-1}\frac{2^{k+1}l(l-1)\cdots(l-k)}{(2l-1)(2l-3)\cdots(2l-2k-1)}\sin^{2l-2k-2}(\theta)\right\},$$

we have

$$I^3_{0,k-m} = \int_0^{2\pi} \sin^{k-m}(\theta)d\theta = \frac{2\pi(k-m-1)!!}{(k-m)!!} = \frac{2\pi\Gamma((k-m)/2+1/2)}{\Gamma(1/2)\Gamma((k-m)/2+1)}. \qquad (.4.8)$$

Substituting (.4.8) into (.4.7) and combining the following formulas,

$$k(k-1)(k-2)(k-3)\cdots(k-m+2)(k-m+1) = \frac{\Gamma(k+1)}{\Gamma(k-m+1)},$$

$$(k+1)(k+m-2)(k-1)(k+m-6)\cdots(k-m+3)(k-m+2)$$
$$= 2^{m/2}\frac{\Gamma(k+3/2)}{\Gamma(k-m+3/2)}4^{m/2}\frac{\Gamma((k+m)/4-1/4)}{\Gamma((k-m)/4+1/2)},$$

we obtain the desired result. When $k < m$, $I^3_{m,k} = 0$ as $I^3_{m-k,0} = \int_0^{2\pi}\sin((m-k)\theta) = 0$.

As $I^4_{m,k} = \frac{k}{k+m}I^3_{m-1,k-1}$, the desired result follows from the calculation of $I^3_{m-1,k-1}$. This completes the proof. $\square$

.5   The proof of regularity of non-smooth function $|x_1|^3$

It is clear that $v \in L^2_{\alpha/2}(\Omega)$, i.e.,

$$|v|^2_{L^2_{\alpha/2}(\Omega)} \approx \sum_{m=0}^{\infty}\sum_{n=0}^{\infty}(|a_{m,n}|^2 + |b_{m,n}|^2)\mathbf{h}^{\alpha/2}_{m,n} < \infty.$$

To show that $|x_1|^3 \in \mathbf{B}^{s_1,s_2}_{\alpha/2}(\Omega)$ with $s_1 = 3.5 - \epsilon$ and $s_2 = 3.5 - \epsilon$, it suffices to verify the semi-norm of v is bounded, that is

$$|v|^2_{\mathbf{B}^{s_1,s_2}_{\alpha/2}(\Omega)} \approx \sum_{m=1}^{\infty}\sum_{n=1}^{\infty}(m^{2s_1} + n^{2s_2})(|a_{m,n}|^2 + |b_{m,n}|^2)h^{\alpha/2}_{m,n} < \infty,$$

where $a_{m,n}$'s and $b_{m,n}$'s are from the expansion (3.2.4) for the function $|x_1|^3$.

Note that $|x_1|^3 = r^3|\cos^3(\theta)|$. By (3.2.4), $b_{m,n} = 0$ and $a_{m,n} = I_{m,n,3} \cdot J_m/h^{\alpha/2}_{m,n}$ with

$$I_{m,n,3} = \int_0^1 r^{3+m}P^{\alpha/2,m}_n(2r^2-1)(1-r^2)^{\alpha/2}rdr, \quad J_m = \int_0^{2\pi}|\cos(\theta)|^3\cos(m\theta)d\theta.$$

By (.4.3) and the formula (3.3.8), we have

$$\begin{aligned}
I_{m,n,3} &= (-1)^n\frac{\Gamma(\alpha/2+n+1)}{2\Gamma(n+1)} \cdot \frac{\Gamma((m+3)/2+1)}{\Gamma((m-3)/2)} \cdot \frac{\Gamma((m-3)/2+n)}{\Gamma(\alpha/2+n+(m+3)/2+2)} \\
&\approx (-1)^n n^{\alpha/2} \cdot m^4 \cdot \frac{1}{(n+m/2)^{5+\alpha/2}} = \frac{(-1)^n n^{\alpha/2}m^4}{(n+m/2)^{5+\alpha/2}}.
\end{aligned}$$

Using the formula (3.3.8), we have

$$\begin{aligned}
J_m &= \int_{-\pi/2}^{3\pi/2}|\cos(\theta)|^3\cos(m\theta)d\theta = \left(\int_{-\pi/2}^{\pi/2} - \int_{\pi/2}^{3\pi/2}\right)\cos^3(\theta)\cos(m\theta)d\theta \\
&= 6(3-(-1)^{m+1})\sin((m+1)\pi/2) \cdot \frac{1}{(m^2-1)(m^2-9)} \approx \frac{1}{m^4}, \quad m > 3.
\end{aligned}$$

By the formula (3.3.8) we have $h_{m,n}^{\alpha/2} = \delta_m \pi (\frac{1}{2})^{m+\alpha/2+2} h_n^{\alpha/2,m} \approx \frac{n^{\alpha/2}}{(n+m/2)(n+m)^{\alpha/2}}$. By (3.2.7) and using the formula (3.3.8) again, it holds that

$$(|a_{m,n}|^2 + |b_{m,n}|^2)h_{m,n}^{\alpha/2} \approx \frac{|I_{m,n,3}J_m|^2}{h_{m,n}^{\alpha/2}} \approx \frac{n^{\alpha/2}(n+m)^{\alpha/2}}{(n+m/2)^{9+\alpha}} \approx \frac{1}{(n^2+m^2)^{4.5}}.$$

Thus

$$|v|_{\mathbf{B}_{\alpha/2}^{s_1,s_2}(\Omega)}^2 \approx \sum_{m=1}^{\infty}\sum_{n=1}^{\infty}(m^{2s_1}+n^{2s_2})(|a_{m,n}|^2+|b_{m,n}|^2)h_{m,n}^{\alpha/2} \approx \sum_{m=1}^{\infty}\sum_{n=1}^{\infty}\frac{m^{2s_1}+n^{2s_2}}{(n^2+m^2)^{4.5}}.$$

Observe that when $s_1 = 3.5 - \epsilon$,

$$\sum_{m=1}^{\infty}\sum_{n=1}^{\infty}\frac{m^{2s_1}}{(n^2+m^2)^{4.5}} \leq C\int_1^{+\infty}\int_1^{+\infty}\frac{x_1^{2s_1}}{(x_1^2+x_2^2)^{4.5}}dx_1 dx_2$$
$$= C\int_0^{2\pi}\int_1^{\infty}\frac{(r\cos(\theta))^{2s_1}}{(r^2)^{4.5}}r dr d\theta \leq C\int_1^{\infty}\frac{1}{r^{8-2s_1}}dr < \infty.$$

Similarly, we have $\sum_{m=1}^{\infty}\sum_{n=1}^{\infty}\frac{n^{2s_2}}{(n^2+m^2)^{4.5}} < \infty$ for $s_2 = 3.5 - \epsilon$. Thus $|v|_{\mathbf{B}_{\alpha/2}^{s_1,s_2}(\Omega)}^2 < \infty$. This completes the proof.

.6 Fast Jacobi transform

For any $u_N(x) = \sum_{n=0}^{N}\hat{u}_n^{\gamma,\beta}P_n^{\gamma,\beta}(x) = \sum_{n=0}^{N}\hat{u}_n^{\gamma,\delta}P_n^{\gamma,\delta}(x)$. Denote the vectors

$$\hat{u}^{\gamma,\beta} =: (\hat{u}_0^{\gamma,\beta}, \hat{u}_1^{\gamma,\beta}, \ldots, \hat{u}_N^{\gamma,\beta})^T, \quad \hat{u}^{\gamma,\delta} =: (\hat{u}_0^{\gamma,\delta}, \hat{u}_1^{\gamma,\delta}, \ldots, \hat{u}_N^{\gamma,\delta})^T.$$

The goal of this section is to provide the fast transform from the vector $\hat{u}^{\gamma,\delta}$ to $\hat{u}^{\gamma,\beta}$ with $\beta > \delta$, or the approximation of $\hat{u}^{\gamma,\beta}$ with the acceptable accuracy.

The authors in [84] provided a quasilinear fast solver with the computational cost $\mathcal{O}(N\log^2 N)$. However, there is hidden constant $\beta - \delta$ in the computational cost. For example, in our problem with $\beta = m$ and $\delta = 0$, the computational cost will be $\mathcal{O}(M^2 N\log^2 N)$ when we count in theta direction in total. This motivates us to develop a new solver which can remove the hidden constant or at least relax it (e.g., the constant grows like $\log m$ instead of m) so that the total computational cost will be $\mathcal{O}(MN\log^2 N)$ or $\mathcal{O}(M\log MN\log^2 N)$ instead of $\mathcal{O}(M^2 N\log^2 N)$.

Recall the Pochhammer symbol $(a)_n = a(a+1)\cdots(a+n-1) = \Gamma(n+a)/\Gamma(a)$ for any $a \in \mathbb{R}$ and $n \in \mathbb{N}_0$. By the formula

$$P_n^{\gamma,\delta}(x) = \sum_{k=0}^{n}c_{n,k}(\gamma,\beta,\delta)P_k^{\gamma,\beta}(x)$$

(see formula (7.32) in [11]) with the connection coefficient

$$c_{n,k}(\gamma,\beta,\delta) =: \frac{(\gamma+1)_n}{(\gamma+\beta+2)_n}\frac{(-1)^{n-k}(\delta-\beta)_{n-k}(\gamma+\beta+1)_k(\gamma+\beta+2)_{2k}(n+\gamma+\delta+1)_k}{(-1)_{n-k}(\gamma+1)_k(\gamma+\beta+1)_{2k}(n+\gamma+\beta+2)_k}.$$

Define the upper triangular matrix M with entries $M_{k,n} = c_{n,k}(\gamma, \beta, \delta)$. Then

$$\hat{u}^{\alpha/2,m} = M\hat{u}^{\alpha/2,0}, \quad M = D_1(T \circ H)D_2. \tag{.6.1}$$

where D_1 and D_2 are diagonal matrices, T is Toeplitz matrix, H is a Hankel matrix, and '$\circ$' is the Hadamard matrix product,i.e., entrywise multiplication between two matrices. More precisely,

$$(D_1)_{k,n} = \rho_1(k)\delta_{k,n}, \quad (D_2)_{k,n} = \rho_2(n)\delta_{k,n}, \quad (T)_{k,n} = \rho_3(n-k), \quad (H)_{k,n} = \rho_4(k+n), \tag{.6.2}$$

where $0 \le k \le n \le N$ and

$$\rho_1(k) = \frac{(\gamma + \beta + 1)_k (\gamma + \beta + 2)_{2k}}{(\gamma + 1)_k (\gamma + \beta + 1)_{2k}}, \quad \rho_2(n) = \frac{(\gamma + 1)_n}{(\gamma + \beta + 2)_n}, \tag{.6.3}$$

$$\rho_3(n-k) = \frac{(-1)^{n-k}(\delta - \beta)_{n-k}}{(-1)_{n-k}}, \quad \rho_4(k+n) = \frac{(n + \gamma + \delta + 1)_k}{(n + \gamma + \beta + 2)_k}. \tag{.6.4}$$

Since $(-m)_{n-k} = 0$ for $n - k \ge m$ with $m \le N$, then the conversion matrix M is banded one with bandwith $2M + 1$. Direct calculation requires the storage $\mathcal{O}(mN)$ and the computational cost $\mathcal{O}(mN)$. Next we develop a fast solver with quasilinear complexity for large m.

For the Hankel matrix, we have following property.

Theorem .6.1. *For $\gamma + \delta > -1$ and $\beta - \delta > -1$, the Hankel matrix, H, in (.6.2) is positive semidefinite.*

Proof Note that

$$\rho_4(k+n) = \frac{\Gamma(n + k + \gamma + \delta + 1)}{\Gamma(n + k + \gamma + \beta + 2)} = \frac{B(n + k + \gamma + \delta + 1)}{\Gamma(\beta - \delta + 1)} = \frac{\int_0^1 t^{n+k+\gamma+\delta}(1 - t)^{\beta - \delta}dt}{\Gamma(\beta - \delta + 1)}. \tag{.6.5}$$

Following the similar argument as that in proof of the Theorem in [84], we have desired conclusion. $\square$

Since the Hankel matrix H is positive semidefinite, we can use the pivoted Cholesky algorithm described in Section 5.1 to construct low rank approximation.

.7 The derivation of mass matrix for spectral method in 2D

Recall that $P_k^{\alpha/2,m}(t)$'s are Jacobi polynomials with $\alpha/2 > 0$, $m \ge 0$ and let $P_k^{\alpha/2-n,m+n}(t)$ be the generalized Jacobi polynomial as discussed in [82] (Section 4.22) whenever $\alpha/2 - n \le -1$.

Lemma .7.1.

$$\frac{d^n}{dt^n}[P_k^{\alpha/2,m}(t)(1 - t)^{\alpha/2}] = (-1)^n(k - n + \alpha/2 + 1)_n(1 - t)^{\alpha/2-n}P_k^{\alpha/2-n,m+n}(t) \tag{.7.1}$$

Here $(k - n + \alpha/2 + 1)_n$ is the Pochnamner factorial, which means $(k - n + \alpha/2 + 1)_n = (k - n + \alpha/2 + 1)(k - n + \alpha/2) \cdots (k + \alpha/2 - 1)(k - n + \alpha/2).$

Proof Recall the property of hyper-geometric function $_2F_1(a, b; , c, z)$ derived from Page 123, Exercise 43(b) in [10]

$$\frac{d}{dz}[z^{c-1}\,_2F_1(a, b; c, z)] = (c-1)z^{c-2}\,_2F_1(a, b; c-1, z), \tag{.7.2}$$

which is equivalent to the following form

$$\frac{d}{dz}[(\frac{1-z}{2})^{c-1}\,_2F_1(a, b; c, \frac{1-z}{2})] = (c-1)(\frac{1-z}{2})^{c-2}\,_2F_1(a, b; c-1, \frac{1-z}{2}). \tag{.7.3}$$

Using the above equality repeatedly together with hyper-geometric representation (.3.1) leads to the desired result. □

With the above lemma, we are ready to prove the explicit expression of the mass matrix.

Proof Recall $\phi_{m,n}^{(1)} = (1-r^2)^{\alpha/2}\cos(m\theta)r^m P_n^{\alpha/2,m}(2r^2-1)$. Then

$$
\begin{aligned}
(M_m^{(1)})_{k,n} &= (\phi_{m,n}^{(1)}, \phi_{m,k}^{(1)}) \\
&= \int_0^{2\pi}\int_0^1 (1-r^2)^{\alpha/2}\cos(m\theta)Q_n^{\alpha/2,m}(r)(1-r^2)^{\alpha/2}\cos(m\theta)Q_k^{\alpha/2,m}(r)rdrd\theta \\
&= \delta_m\pi\int_0^1 P_n^{\alpha/2,m}(2r^2-1)P_k^{\alpha/2,m}(2r^2-1)(1-r^2)^\alpha r^{2m+1}dr. \tag{.7.4}
\end{aligned}
$$

Letting $t = 2r^2 - 1$, we have

$$
\begin{aligned}
(M_m^{(1)})_{k,n} &= \frac{\delta_m\pi}{2^{\alpha+m+2}}\int_{-1}^1 P_n^{\alpha/2,m}(t)P_k^{\alpha/2,m}(t)(1-t)^\alpha(1+t)^m dt \\
&= \frac{\delta_m\pi}{2^{\alpha+m+2}}\frac{(-1)^n}{2^n n!}\int_{-1}^1 \frac{d^n}{dt^n}[(1-t)^{\alpha/2+n}(1+t)^{m+n}]P_k^{\alpha/2,m}(t)(1-t)^{\alpha/2}dt \\
&= \frac{\delta_m\pi}{2^{\alpha+m+n+2}n!}\int_{-1}^1 [(1-t)^{\alpha/2+n}(1+t)^{m+n}]\frac{d^n}{dt^n}[P_k^{\alpha/2,m}(t)(1-t)^{\alpha/2}]dt. \tag{.7.5}
\end{aligned}
$$

Using the Lemma .7.1, we have

$$
\begin{aligned}
&\int_{-1}^1 [(1-t)^{\alpha/2+n}(1+t)^{m+n}]\frac{d^n}{dt^n}[P_k^{\alpha/2,m}(t)(1-t)^{\alpha/2}]dt \\
&= (-1)^n(k-n+\alpha/2+1)_n\int_{-1}^1 (1-t)^\alpha(1+t)^{n+m}P_k^{\alpha/2-n,m+n}(t)dt. \tag{.7.6}
\end{aligned}
$$

Then using the expansion $P_n^{\gamma,\beta}(z) = \sum_{k=0}^n c_{n,k}(\gamma, \delta, \beta)P_k^{\delta,\beta}(z)$ (see formula (7.33) in [11]) with

$$c_{n,k}(\gamma, \delta, \beta) = \frac{(\beta+1)_n(\gamma-\delta)_{n-k}(\delta+\beta+1)_k(\delta+\beta+2)_{2k}(\beta+\gamma+n+1)_k}{(\delta+\beta+2)_n(1)_{n-k}(\beta+1)_k(\delta+\beta+1)_{2k}(\delta+\beta+n+2)_k}, \tag{.7.7}$$

and the orthogonality property of Jacobi polynomials, we have

$$
\begin{aligned}
&\int_{-1}^1 [(1-t)^{\alpha/2+n}(1+t)^{m+n}]\frac{d^n}{dt^n}[P_k^{\alpha/2,m}(t)(1-t)^{\alpha/2}]dt \\
&= (-1)^n\frac{\Gamma(k+\alpha/2+1)}{\Gamma(k-n+\alpha/2+1)}\int_{-1}^1 (1-t)^\alpha(1+t)^{n+m}c_{k,0}(\alpha/2-n, n+m, \alpha)P_0^{\alpha,n+m}(t)dt \\
&= (-1)^n(k-n+\alpha/2+1)_n c_{k,0}(\alpha/2-n, n+m, \alpha)h_0^{\alpha,n+m} \tag{.7.8}
\end{aligned}
$$

Substituting the above equality into (.7.5) and recalling (.7.7), (6.1.5) gives

$$(M_m^{(1)})_{k,n} = \delta_m \pi \frac{(-1)^{n+k}\Gamma(k+\alpha/2+1)\Gamma(n+\alpha/2+1)\Gamma(k+n+m+1)\Gamma(\alpha+1)}{2n!k!\Gamma(k-n+\alpha/2+1)\Gamma(n-k+\alpha/2+1)\Gamma(k+n+m+\alpha+2)}. \tag{.7.9}$$

Using the Euler reflection's formula, we have

$$\frac{1}{\Gamma(k-n+\alpha/2+1)\Gamma(n-k+\alpha/2+1)} = \frac{\sin((|k-n|-\alpha/2)\pi)\Gamma(|k-n|-\alpha/2+1)}{(|k-n|-\alpha/2)\pi\Gamma(|k-n|+\alpha/2+1)}. \tag{.7.10}$$

Combining the equality (.7.9) and (.7.10), we get the desired result. □

.8   Equivalence between the space $B_{\frac{\alpha}{2}}^{s,s}(\Omega)$ and the space $\mathbf{H}_{*,\frac{\alpha}{2}}^{s}(\Omega)$

We will show the equivalence of the weighted space $\mathbf{H}_{*,\frac{\alpha}{2}}^{s}(\Omega)$ and the weighted space $B_{\frac{\alpha}{2}}^{s,s}(\Omega)$ when s is a natural number.

Let $\Omega = \{(x_1, x_2) \in \mathbb{R}^2 : x_1^2 + x_2^2 < 1\}$ be the unit disc. For convenience, we use the complex coordinates $z = x_1 + \mathbf{i}x_2$, $\bar{z} = x_1 - \mathbf{i}x_2$, $\mathbf{i}^2 = -1$. Then $\Omega = \{z \in \mathbb{C}^2 : z\bar{z} < 1\}$. Denote $\omega^\beta = (1 - z\bar{z})^\beta = (1 - x_1^2 - x_2^2)^\beta$ as the Jacobi weighted function on Ω.

For $\beta > -1$, the generalized Zernike or disc polynomials on Ω are defined by

$$P_{l,n}^{*,\beta}(z,\bar{z}) = c_{l,n} P_n^{\beta,l-n}(2z\bar{z}-1)z^{l-n}, \quad c_{l,n} = \frac{\Gamma(l+n+1)\Gamma(l+\beta+1)}{\Gamma(l+n+\beta+1)\Gamma(l+1)}, \quad l,n \geq 0. \tag{.8.1}$$

where $P_n^{\beta,l-n}$ is the generalized Jacobi polynomial for $l \leq n$; see [82]. Denote $h_{l,n}^{*,\beta}$ as

$$h_{l,n}^{*,\beta} =: \|P_{l,n}^{*,\beta}\|_{L^2_{\omega^\beta}}^2 = \frac{\pi}{l+n+\beta+1}\left[\frac{\Gamma(l+n+1)}{\Gamma(l+n+\beta+1)}\right]^2 \frac{\Gamma(l+\beta+1)}{\Gamma(l+1)}\frac{\Gamma(n+\beta+1)}{\Gamma(n+1)}. \tag{.8.2}$$

Recall $h_{l-n,n}^\beta$ defined in (3.2.7), we have

$$h_{l,n}^{*,\beta} = (c_{l,n})^2 h_{|l-n|,n}^\beta, \quad l \neq n; \quad h_{l,n}^{*,\beta} = \frac{1}{2}(c_{l,n})^2 h_{0,n}^\beta, \quad l = n. \tag{.8.3}$$

Lemma .8.1 ([65]). *For any integers l, n, $k_i \geq 0$ with $i = 1, 2, 3$, it holds that*

$$\partial_z^{k_1}\partial_{\bar{z}}^{k_2}(z\partial z - \bar{z}\partial_{\bar{z}})^{k_3} P_{l,n}^{*,\beta}(z,\bar{z}) = (l-n)^{k_3}(l+n-k_1-k_2+1)_{k_1+k_2} P_{l-k_1,n-k_2}^{*,\beta+k_1+k_2}(z,\bar{z}). \tag{.8.4}$$

Lemma .8.2 (Equivalent semi-norms, [65]). *For any $u \in \mathbf{H}_{*,\beta}^s$ with $s \geq 0$, it holds that*

$$\sum_{|\mathbf{k}|=s} \binom{s}{\mathbf{k}} \left\|\partial_{x_1}^{k_1}\partial_{x_2}^{k_2}(x_1\partial_{x_2} - x_2\partial_{x_1})^{k_3} u\right\|_{L^2_{\beta+k_1+k_2}}^2 = 2^s \sum_{|\mathbf{k}|=s} \binom{s}{\mathbf{k}} \left\|\partial_z^{k_1}\partial_{\bar{z}}^{k_2}(z\partial_{\bar{z}} - \bar{z}\partial_z)^{k_3} u\right\|_{L^2_{\beta+k_1+k_2}}^2. \tag{.8.5}$$

For any $u \in \mathbf{H}_{*,\beta}^s$ with $s \geq 0$, it holds that

$$u = \sum_{l \geq 0}\sum_{n \geq 0} u_{l,n}^{*,\beta} P_{l,n}^{*,\beta}, \quad u_{l,n}^{*,\beta} = \frac{1}{h_{l,n}^{*,\beta}}(u, P_{l,n}^{*,\beta})_\beta. \tag{.8.6}$$

Recalling (3.2.5)-(3.2.6) and using the relation (.8.3), we have

$$u_{l,n}^{*,\beta} = \frac{1}{c_{l,n}}(a_{l-n,n}^{\beta} - \mathbf{i}b_{l-n,n}^{\beta}), \quad l \geq n, \quad u_{l,n}^{*,\beta} = \frac{1}{c_{l,n}}(a_{n-l,n}^{\beta} + \mathbf{i}b_{n-l,n}^{\beta}), \quad l \leq n. \tag{.8.7}$$

Then by Lemma .8.1, we have

$$\begin{aligned}
\partial_z^{k_1}\partial_{\bar{z}}^{k_2}(z\partial z - \bar{z}\partial_{\bar{z}})^{k_3}u &= \sum_{l\geq 0}\sum_{n\geq 0}u_{l,n}^{*,\beta}\partial_z^{k_1}\partial_{\bar{z}}^{k_2}(z\partial z - \bar{z}\partial_{\bar{z}})^{k_3}P_{l,n}^{*,\beta} \\
&= \sum_{l\geq 0}\sum_{n\geq 0}u_{l,n}^{*,\beta}(l-n)^{k_3}(l+n-k_1-k_2+1)_{k_1+k_2}P_{l-k_1,n-k_2}^{*,\beta+k_1+k_2}.
\end{aligned}$$

Thus it follows from the orthogonality that

$$\|\partial_z^{k_1}\partial_{\bar{z}}^{k_2}(z\partial\bar{z} - z\partial_{\bar{z}})^{k_3}u\|_{L^2_{\beta+k_1+k_2}}^2 = \sum_{l\geq k_1}\sum_{n\geq k_2}\Phi(l,n,k)|u_{l,n}^{*,\beta}|^2h_{l,n}^{*,\beta}. \tag{.8.8}$$

Here $\Phi(l,n,k) = [(l-n)^{k_3}(l+n-k_1-k_2+1)_{k_1+k_2}]^2 h_{l-k_1,n-k_2}^{*,\beta+k_1+k_2}/h_{l,n}^{*,\beta}$ can be simplified as

$$\begin{aligned}
\Phi(l,n,k) &= (l-n)^{2k_3}\frac{\Gamma(l+\beta+1+k_2)\Gamma(l+1)}{\Gamma(l-k_1+1)\Gamma(l+\beta+1)}\frac{\Gamma(n+\beta+1+k_1)\Gamma(n+1)}{\Gamma(n-k_2+1)\Gamma(n+\beta+1)} \\
&\approx (l-n)^{2k_3}(ln)^{k_1+k_2},
\end{aligned} \tag{.8.9}$$

where we applied the formula (3.3.8). From (.8.8) and (.8.9), we can see that

$$\begin{aligned}
\sum_{|\mathbf{k}|=s}\binom{s}{\mathbf{k}}\|\partial_z^{k_1}\partial_{\bar{z}}^{k_2}(z\partial\bar{z} - z\partial_{\bar{z}})^{k_3}u\|_{L^2_{\omega\beta+k_1+k_2}}^2 &\approx \sum_{|\mathbf{k}|=s}\binom{s}{\mathbf{k}}\sum_{l\geq 0}\sum_{n\geq 0}(l-n)^{2k_3}(ln)^{k_1+k_2}|u_{l,n}^{*,\beta}|^2h_{l,n}^{\beta} \\
&= \sum_{l\geq 0}\sum_{n\geq 0}((l-n)^2 + 2ln)^s|u_{l,n}^{*,\beta}|^2h_{l,n}^{*,\beta} \\
&= \sum_{l\geq 0}\sum_{n\geq 0}(l^2+n^2)^s|u_{l,n}^{*,\beta}|^2h_{l,n}^{*,\beta},
\end{aligned}$$

where $s = k_1 + k_2 + k_3$. Let $m = l - n$ and then

$$\sum_{|\mathbf{k}|=s}\binom{s}{\mathbf{k}}\|\partial_z^{k_1}\partial_{\bar{z}}^{k_2}(z\partial\bar{z} - z\partial_{\bar{z}})^{k_3}u\|_{L^2_{\beta+k_1+k_2}}^2 \approx \sum_{m\geq -n}\sum_{n\geq 0}(m^{2s}+n^{2s})|u_{m+n,n}^{*,\beta}|^2h_{m+n,n}^{*,\beta}.$$

From here, (.8.3) and (.8.7), we have

$$\sum_{|\mathbf{k}|=s}\binom{s}{\mathbf{k}}\|\partial_z^{k_1}\partial_{\bar{z}}^{k_2}(z\partial\bar{z} - z\partial_{\bar{z}})^{k_3}u\|_{L^2_{\beta+k_1+k_2}}^2 \approx \sum_{m\geq 0}\sum_{n\geq 0}(m^{2s}+n^{2s})(|a_{m,n}^{\beta}|^2 + |b_{m,n}^{\beta}|^2)h_{m,n}^{\beta}.$$

This implies the equivalence of the space $\mathbf{B}_{\beta}^{s_1,s_2}(\Omega)$ and the weighted space $\mathbf{H}_{*,\beta}^s(\Omega)$ when $s_1 = s_2 = s$.

127

.9 Another popular definition in the fractional community

The left- and right-sided Riemann-Liouville fractional integrals are defined as

$$_aD_x^{-\alpha}f(x) = \frac{1}{\Gamma(\alpha)} \int_a^x \frac{f(\xi)}{(x-\xi)^{1-\alpha}} d\xi, \quad x > a, \quad \alpha > 0,$$

and

$$_xD_b^{-\alpha}f(x) = \frac{1}{\Gamma(\alpha)} \int_x^b \frac{f(\xi)}{(\xi-x)^{1-\alpha}} d\xi, \quad x < b, \quad \alpha > 0.$$

respectively. Let $g(x) = \frac{1}{\Gamma(\alpha)} x^{\alpha-1}$,

$$_aD_x^{-\alpha}f(x) = \int_a^x f(\xi)g(x-\xi)d\xi$$

For $0 < \alpha < 1$,

$$_aD_x^{\alpha}f(x) = \frac{1}{\Gamma(1-\alpha)} \frac{d}{dx} \int_a^x \frac{f(\xi)}{(x-\xi)^{\alpha}} d\xi,$$

$$_xD_b^{\alpha}f(x) = \frac{-1}{\Gamma(1-\alpha)} \frac{d}{dx} \int_x^b \frac{f(\xi)}{(\xi-x)^{\alpha}} d\xi.$$

For more information, the readers can consult the monograph [77] or [74].

Left side and right side Riemann-Liouville (RL) derivative are defined as

$$_aD_x^{\alpha}f(x) = {}_aD_x^n {}_aD_x^{\alpha-n}f(x), \quad x > a,$$

$$_xD_b^{\alpha}f(x) = {}_xD_b^n {}_xD_b^{\alpha-n}f(x), \quad x < b$$

for $n-1 < \alpha < n$. If $\alpha = n$, then

$$_aD_x^{\alpha}f(x) = \frac{d^n}{dx^n}f(x), \text{ and } {}_xD_b^{\alpha}f(x) = (-1)^n \frac{d^n}{dx^n}f(x).$$

For $\alpha \in (0,2)$ there is equivalence between the Riesz derivative(two-sided symmetrical Riemann-Liouville derivative) and fractional Laplacian in one dimension

$$(-\Delta)^{\alpha/2}u(x) = C_\alpha[_{-\infty}D_x^\alpha u(x) + {}_xD_{+\infty}^\alpha u(x)] = C_\alpha \frac{d^2}{dx^2} \int_{-\infty}^{+\infty} \frac{u(y)}{|x-y|^{\alpha-1}} dy$$

where $C_\alpha = -\frac{1}{2} \frac{1}{2\cos\frac{\alpha\pi}{2}}$. The equivalence between Riesz fractional derivative and fractional Laplacian can be stated as follows.

Lemma .9.1. *Consider twice continuously bounded functions $u \in C_b^2(\mathbb{R})$. If $\alpha \in [1,2)$ or $\alpha \in (0,1)$ and $\lim_{|x|\to\infty} u_x(x) = 0$, then*

$$(-\Delta)^{\alpha/2}u(x) = \begin{cases} \frac{1}{\pi} \int_{-\infty}^{\infty} \frac{u_x(y)}{|x-y|} dy, & \alpha = 1, \\ \frac{c_{1,\alpha}}{\alpha(1-\alpha)} \int_{-\infty}^{\infty} \frac{u_{xx}(y)}{|x-y|^{\alpha-1}} dy, & \alpha \neq 1, \end{cases} \tag{.9.1}$$

which leads to the equivalence between the fractional Laplacian and the Riesz derivative.

Proof Let us express the fractional Laplacian as the integral over $[0, \infty)$:

$$
\begin{aligned}
(-\Delta)^{\alpha/2} u(x) &= c_\alpha \int_0^\infty \frac{u(x) - u(x-y) + u(x) - u(x+y)}{y^{1+\alpha}} dy \\
&= c_{1,\alpha} \int_0^\infty \int_0^y \frac{u_x(x-z) - u_x(x+z)}{y^{1+\alpha}} dz dy \\
&= c_{1,\alpha} \int_0^\infty [u_x(x-z) - u_x(x+z)] \int_z^\infty \frac{1}{y^{1+\alpha}} dz dy \\
&= \frac{c_{1,\alpha}}{\alpha} \int_0^\infty \frac{u_x(x-z) - u_x(x+z)}{z^\alpha} dz \qquad (.9.2)
\end{aligned}
$$

where we have changed the order of integration. We distinguish three different cases. When $\alpha = 1$ and $c_{1,1} = 1/\pi$, so

$$
(-\Delta)^{1/2} u(x) = \frac{1}{\pi} \int_0^\infty \frac{u_x(x-y) - u_x(x+y)}{y} dy = \frac{1}{\pi} \int_{-\infty}^\infty \frac{u_x(y)}{y} dy, \qquad (.9.3)
$$

$(-\Delta)^{1/2} u(x)$ is precisely the Hilbert transform of $u(x)$. On the other hand, when $\alpha \in (1,2)$,

$$
\begin{aligned}
(-\Delta)^{\alpha/2} u(x) &= \frac{c_{1,\alpha}}{\alpha} \int_0^\infty \frac{u_x(x-z) - u_x(x) + u_x(x) - u_x(x+z)}{z^\alpha} dz \\
&= -\frac{c_{1,\alpha}}{\alpha} \int_0^\infty \int_0^z \frac{u_{xx}(x-y) + u_{xx}(x+y)}{z^\alpha} dy dz \\
&= -\frac{c_{1,\alpha}}{\alpha} \int_0^\infty (u_{xx}(x-y) + u_{xx}(x+y)) \int_y^\infty \frac{1}{z^\alpha} dz dy \\
&= -\frac{c_{1,\alpha}}{\alpha(\alpha-1)} \int_0^\infty \frac{u_{xx}(x-y) + u_{xx}(x+y)}{y^{\alpha-1}} dy \\
&= \frac{c_{1,\alpha}}{\alpha(\alpha-1)} \int_{-\infty}^\infty \frac{u_{xx}(x+y)}{y^{\alpha-1}} dy = \frac{c_\alpha}{\alpha(\alpha-1)} \int_{-\infty}^\infty \frac{u_{xx}(y)}{|x-y|^{\alpha-1}} dy. \qquad (.9.4)
\end{aligned}
$$

When $\alpha \in (0,1)$, the condition $\lim_{x\to\infty} u_x(x) = 0$ is required.

$$
\begin{aligned}
(-\Delta)^{\alpha/2} u(x) &= \frac{c_{1,\alpha}}{\alpha} \int_0^\infty \frac{u_x(x-z) - u_x(x) + u_x(x) - u_x(x+z)}{z^\alpha} dz \\
&= \frac{c_{1,\alpha}}{\alpha} \int_0^\infty \int_z^\infty \frac{u_{xx}(x-y) + u_{xx}(x+y)}{z^\alpha} dy dz \\
&= \frac{c_{1,\alpha}}{\alpha} \int_0^\infty (u_{xx}(x-y) + u_{xx}(x+y)) \int_0^y \frac{1}{z^\alpha} dz dy \\
&= \frac{c_{1,\alpha}}{\alpha(\alpha-1)} \int_0^\infty \frac{u_{xx}(x-y) + u_{xx}(x+y)}{y^{\alpha-1}} dy \\
&= \frac{c_{1,\alpha}}{\alpha(\alpha-1)} \int_{-\infty}^\infty \frac{u_{xx}(y)}{|x-y|^{\alpha-1}} dy. \qquad (.9.5)
\end{aligned}
$$

On the other hand for the Riesz derivative, by the conditions of twice continuously bounded function, we have

$$
(-\Delta)_x^{\alpha/2} u(x) = c_\alpha \frac{\partial^2}{\partial x^2} \int_{-\infty}^\infty \frac{u(x+y)}{|y|^{\alpha-1}} dy = c_\alpha \int_{-\infty}^\infty \frac{u_{xx}(x+y)}{|y|^{\alpha-1}} dy = c_\alpha \int_{-\infty}^\infty \frac{u_{xx}(y)}{|x-y|^{\alpha-1}} dy. \quad (.9.6)
$$

□ Next we show the connection between the Riesz derivative and fractional Laplacian. In 2D, they are not equivalent which can be seen from the Fourier symbol

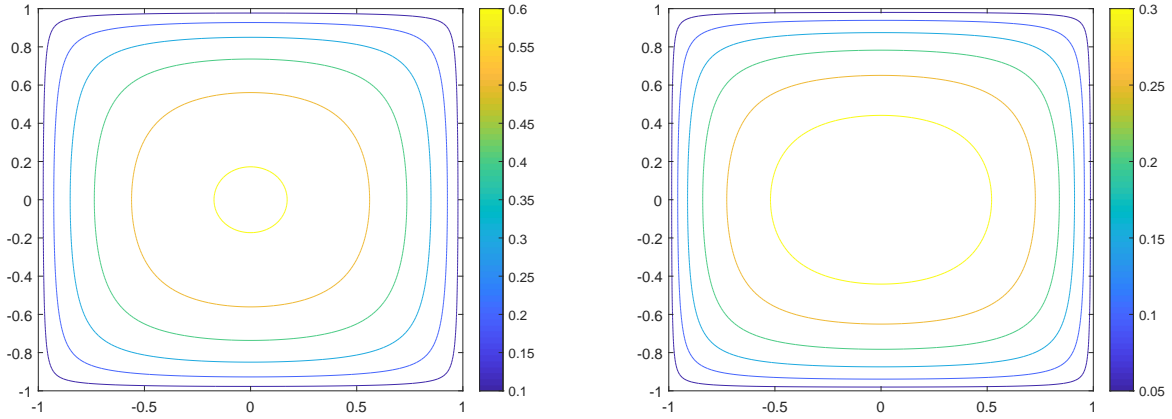$$|k_1|^\alpha + |k_2|^\alpha \neq |k|^\alpha, \quad |k|^2 = k_1^2 + k_2^2.$$

Figure 1: Isotropic vs non-isotropic for $\alpha = 1.2$. Left: $(-\Delta)_2^{\alpha/2} u = 1$; Right: $[2(-\Delta)_{x_1}^{\alpha/2} + (-\Delta)_{x_2}^{\alpha/2}]u = 1$

Bibliography

[1] Nicola Abatangelo and Enrico Valdinoci. Getting acquainted with the fractional Laplacian. In *Contemporary research in elliptic PDEs and related topics*, volume 33 of *Springer INdAM Ser.*, pages 1–105. Springer, Cham, 2019.

[2] Gabriel Acosta, Francisco M. Bersetche, and Juan Pablo Borthagaray. A short FE implementation for a 2d homogeneous Dirichlet problem of a fractional Laplacian. *Comput. Math. Appl.*, 74(4):784–816, 2017.

[3] Gabriel Acosta and Juan Pablo Borthagaray. A fractional Laplace equation: regularity of solutions and finite element approximations. *SIAM J. Numer. Anal.*, 55(2):472–495, 2017.

[4] Gabriel Acosta, Juan Pablo Borthagaray, Oscar Bruno, and Martín Maas. Regularity theory and high order numerical methods for the (1D)-fractional Laplacian. *Math. Comp.*, 87(312):1821–1857, 2018.

[5] Robert A. Adams. *Sobolev spaces*. Academic Press [A subsidiary of Harcourt Brace Jovanovich, Publishers], New York-London, 1975. Pure and Applied Mathematics, Vol. 65.

[6] Mark Ainsworth and Christian Glusa. Aspects of an adaptive finite element method for the fractional Laplacian: a priori and a posteriori error estimates, efficient implementation and multigrid solver. *Comput. Methods Appl. Mech. Engrg.*, 327:4–35, 2017.

[7] Mark Ainsworth and Christian Glusa. Towards an efficient finite element method for the integral fractional Laplacian on polygonal domains. In *Contemporary computational mathematics—a celebration of the 80th birthday of Ian Sloan. Vol. 1, 2*, pages 17–57. Springer, Cham, 2018.

[8] Giovanni Alberti and Giovanni Bellettini. A nonlocal anisotropic model for phase transitions. I. The optimal profile problem. *Math. Ann.*, 310(3):527–560, 1998.

[9] Giovanni Alberti, Guy Bouchitté, and Pierre Seppecher. Phase transition with the line-tension effect. *Arch. Rational Mech. Anal.*, 144(1):1–46, 1998.

[10] George E. Andrews, Richard Askey, and Ranjan Roy. *Special functions*, volume 71 of *Encyclopedia of Mathematics and its Applications*. Cambridge University Press, Cambridge, 1999.

[11] Richard. Askey. *Orthogonal polynomials and special functions*. SIAM, Philadelphia, Pa., 1975.

[12] Ivo Babuška. The finite element method with penalty. *Math. Comp.*, 27:221–228, 1973.

[13] Ivo Babuška and Benqi Guo. Direct and inverse approximation theorems for the p-version of the finite element method in the framework of weighted Besov spaces. I. Approximability of functions in the weighted Besov spaces. *SIAM J. Numer. Anal.*, 39(5):1512–1538, 2001/02.

[14] Peter W. Bates. On some nonlocal evolution equations arising in materials science. In *Nonlinear dynamics and evolution equations*, volume 48 of *Fields Inst. Commun.*, pages 13–52. Amer. Math. Soc., Providence, RI, 2006.

[15] Jöran Bergh and Jörgen Löfström. *Interpolation spaces. An introduction.* Springer-Verlag, Berlin-New York, 1976. Grundlehren der Mathematischen Wissenschaften, No. 223.

[16] Christine Bernardi, Monique Dauge, and Yvon Maday. *Polynomials in the Sobolev World.* 2007.

[17] Christine Bernardi and Yvon Maday. Spectral methods. In *Handbook of numerical analysis, Vol. V*, Handb. Numer. Anal., V, pages 209–485. North-Holland, Amsterdam, 1997.

[18] Andrea Bonito, Juan Pablo Borthagaray, Ricardo H. Nochetto, Enrique Otárola, and Abner J. Salgado. Numerical methods for fractional diffusion. *Comput. Vis. Sci.*, 19(5-6):19–46, 2018.

[19] Andrea Bonito, Wenyu Lei, and Joseph E. Pasciak. Numerical approximation of the integral fractional Laplacian. *Numer. Math.*, 142(2):235–278, 2019.

[20] John P. Boyd and Fu Yu. Comparing seven spectral methods for interpolation and for solving the Poisson equation in a disk: Zernike polynomials, Logan-Shepp ridge polynomials, Chebyshev-Fourier series, cylindrical Robert functions, Bessel-Fourier expansions, square-to-disk conformal mapping and radial basis functions. *J. Comput. Phys.*, 230(4):1408–1438, 2011.

[21] Claudio Canuto, M. Yousuff Hussaini, Alfio Quarteroni, and Thomas A. Zang. *Spectral methods in fluid dynamics.* Springer Series in Computational Physics. Springer-Verlag, New York, 1988.

[22] Raymond H. Chan and Xiao-Qing Jin. A family of block preconditioners for block systems. *SIAM J. Sci. Statist. Comput.*, 13(5):1218–1235, 1992.

[23] Feng Chen and Jie Shen. Stability and convergence analysis of rotational velocity correction methods for the Navier-Stokes equations. *Adv. Comput. Math.*, 45(5-6):3123–3136, 2019.

[24] Lizhen Chen, Jie Shen, and Chuanju Xu. A triangular spectral method for the Stokes equations. *Numer. Math. Theory Methods Appl.*, 4(2):158–179, 2011.

[25] Óscar Ciaurri, Luz Roncal, Pablo Raúl Stinga, José L. Torrea, and Juan Luis Varona. Nonlocal discrete diffusion equations and the fractional discrete Laplacian, regularity and applications. *Adv. Math.*, 330:688–738, 2018.

[26] Peter Constantin, Andrew J. Majda, and Esteban Tabak. Formation of strong fronts in the 2-D quasigeostrophic thermal active scalar. *Nonlinearity*, 7(6):1495–1533, 1994.

[27] Peter Constantin and Jiahong Wu. Behavior of solutions of 2D quasi-geostrophic equations. *SIAM J. Math. Anal.*, 30(5):937–948, 1999.

[28] Rama Cont and Peter Tankov. *Financial modelling with jump processes.* Chapman & Hall/CRC Financial Mathematics Series. Chapman & Hall/CRC, Boca Raton, FL, 2004.

[29] Marta D'Elia, Qiang Du, Christian Glusa, Max Gunzburger, Xiaochuan Tian, and Zhi Zhou. Numerical methods for nonlocal and fractional models. 2020.

[30] Marta D'Elia and Max Gunzburger. The fractional Laplacian operator on bounded domains as a special case of the nonlocal diffusion operator. *Comput. Math. Appl.*, 66(7):1245–1260, 2013.

[31] Serena Dipierro, Xavier Ros-Oton, and Enrico Valdinoci. Nonlocal problems with neumann boundary conditions. *arXiv*, 2014.

[32] S. Dong and J. Shen. An unconditionally stable rotational velocity-correction scheme for incompressible flows. *J. Comput. Phys.*, 229(19):7013–7029, 2010.

[33] Ning Du, Hai-Wei Sun, and Hong Wang. A preconditioned fast finite difference scheme for space-fractional diffusion equations in convex domains. *Comput. Appl. Math.*, 38(1):Art. 14, 13, 2019.

[34] Siwei Duo, Hans Werner van Wyk, and Yanzhi Zhang. A novel and accurate finite difference method for the fractional Laplacian and the fractional Poisson problem. *J. Comput. Phys.*, 355:233–252, 2018.

[35] Siwei Duo and Yanzhi Zhang. Finite difference methods for two and three dimensional fractional Laplacian with applications to solve the fractional reaction-diffusion equations. *arXiv*, 2018.

[36] Bartł omiej Dyda. Fractional calculus for power functions and eigenvalues of the fractional Laplacian. *Fract. Calc. Appl. Anal.*, 15(4):536–555, 2012.

[37] Bartł omiej Dyda, Alexey Kuznetsov, and Mateusz Kwaśnicki. Eigenvalues of the fractional Laplace operator in the unit ball. *J. Lond. Math. Soc. (2)*, 95(2):500–518, 2017.

[38] Brenden P. Epps and Benoit Cushman-Roisin. Turbulence modeling via the fractional laplacian. *arxiv*, 2018.

[39] Lawrence C. Evans. *Partial differential equations*, volume 19 of *Graduate Studies in Mathematics*. American Mathematical Society, Providence, RI, 1998.

[40] G. Fdez-Manin and R. Munoz-Sola. Polynomial approximation of some singular solutions in weighted sobolev space. *Houston J. Math.*, 1995.

[41] Michel Fortin. An analysis of the convergence of mixed finite element methods. *RAIRO Anal. Numér.*, 11(4):341–354, iii, 1977.

[42] Paolo Gatto and Jan S. Hesthaven. Numerical approximation of the fractional Laplacian via *hp*-finite elements, with an application to image denoising. *J. Sci. Comput.*, 65(1):249–270, 2015.

[43] Roland Glowinski, Tsorng-Whay Pan, and Jacques Périaux. A fictitious domain method for Dirichlet problem and applications. *Comput. Methods Appl. Mech. Engrg.*, 111(3-4):283–303, 1994.

[44] I. S. Gradshteyn and I. M. Ryzhik. *Table of integrals, series, and products.* Elsevier/Academic Press, Amsterdam, seventh edition, 2007. Translated from the Russian, Translation edited and with a preface by Alan Jeffrey and Daniel Zwillinger, With one CD-ROM (Windows, Macintosh and UNIX).

[45] Ulf Grenander and Gábor Szegő. *Toeplitz forms and their applications.* Chelsea Publishing Co., New York, second edition, 1984.

[46] Gerd Grubb. Fractional Laplacians on domains, a development of Hörmander's theory of μ-transmission pseudodifferential operators. *Adv. Math.*, 268:478–528, 2015.

[47] Gerd Grubb. Regularity of spectral fractional Dirichlet and Neumann problems. *Math. Nachr.*, 289(7):831–844, 2016.

[48] J. L. Guermond, P. Minev, and Jie Shen. An overview of projection methods for incompressible flows. *Comput. Methods Appl. Mech. Engrg.*, 195(44-47):6011–6045, 2006.

[49] Max Gunzburger, Nan Jiang, and Feifei Xu. Analysis and approximation of a fractional Laplacian-based closure model for turbulent flows and its connection to Richardson pair dispersion. *Comput. Math. Appl.*, 75(6):1973–2001, 2018.

[50] Ben-yu Guo and Li-lian Wang. Jacobi approximations in non-uniformly Jacobi-weighted Sobolev spaces. *J. Approx. Theory*, 128(1):1–41, 2004.

[51] Boling Guo, Xueke Pu, and Fenghui Huang. *Fractional partial differential equations and their numerical solutions.* World Scientific Publishing Co. Pte. Ltd., Hackensack, NJ, 2015. Originally published by Science Press in 2011.

[52] Zhaopeng Hao and Wanrong Cao. An improved algorithm based on finite difference schemes for fractional boundary value problems with nonsmooth solution. *J. Sci. Comput.*, 73(1):395–415, 2017.

[53] Zhaopeng Hao, Wanrong Cao, and Shengyue Li. Numerical correction of finite difference solution for two-dimensional space-fractional diffusion equations with boundary singularity. *Numer. Algo.*, 2020.

[54] Zhaopeng Hao, Huiyuan Li, Zhimin Zhang, and Zhongqiang Zhang. Sharp error estimates of a spectral galerkin method for a diffusion-reaction equation with integral fractional laplacian on a disk. *preprint*, 2019.

[55] Zhaopeng Hao, Guang Lin, and Zhongqiang Zhang. Regularity in weighted sobolev spaces and spectral methods for a two-sided fractional reaction-diffusion equation. 2017.

[56] Zhaopeng Hao, Zhi-zhong Sun, and Wan-rong Cao. A fourth-order approximation of fractional derivatives with its applications. *J. Comput. Phys.*, 281:787–805, 2015.

[57] Zhaopeng Hao and Zhongqiang Zhang. Optimal regularity and error estimates of a spectral galerkin method for fractional advection-diffusion-reaction equations. 2018.

[58] Zhaopeng Hao, Zhongqiang Zhang, and Rui Du. Fractional centered difference scheme for high-dimensional integral fractional laplacian. 2019. https://www.researchgate.net/publication/335888811.

[59] Yanghong Huang and Adam Oberman. Numerical methods for the fractional Laplacian: a finite difference–quadrature approach. *SIAM J. Numer. Anal.*, 52(6):3056–3084, 2014.

[60] Morton A. Hyman. Non-iterative numerical solution of boundary-value problems. *Appl. Sci. Research B.*, 2:325–351, 1952.

[61] George Em. Karniadakis, Moshe Israeli, and Steven A. Orszag. High-order splitting methods for the incompressible Navier-Stokes equations. *J. Comput. Phys.*, 97(2):414–443, 1991.

[62] Mateusz Kwaśnicki. Ten equivalent definitions of the fractional Laplace operator. *Fract. Calc. Appl. Anal.*, 20(1):7–51, 2017.

[63] Nick Laskin. Nonlocal quantum mechanics: fractional calculus approach. In *Handbook of fractional calculus with applications. Vol. 5*, pages 207–236. De Gruyter, Berlin, 2019.

[64] Nikolai Laskin. Fractional quantum mechanics and Lévy path integrals. *Phys. Lett. A*, 268(4-6):298–305, 2000.

[65] Huiyuan Li. Direct Galerkin spectral methods using orthogonal polynomials on the disc, 2019. In preparation.

[66] Huiyuan Li and Yuan Xu. Spectral approximation on the unit ball. *SIAM J. Numer. Anal.*, 52(6):2647–2675, 2014.

[67] A. Lischke, G. Pang, M. Gulian, F. Song, X. Glusa, C.and Zheng, Z. Mao, W. Cai, M. M. Meerschaert, M. Ainsworth, and G. E. Karniadakis. What is the fractional laplacian? 2017.

[68] Michael Loss and Craig Sloane. Hardy inequalities for fractional integrals on general domains. *J. Funct. Anal.*, 259(6):1369–1379, 2010.

[69] Ralf Metzler and Joseph Klafter. The random walk's guide to anomalous diffusion: a fractional dynamics approach. *Phys. Rep.*, 339(1):77, 2000.

[70] Victor Minden and Lexing Ying. A simple solver for the fractional Laplacian in multiple dimensions. *arXiv*, 2018.

[71] Serge Nicaise. Jacobi polynomials, weighted Sobolev spaces and approximation results of some singularities. *Math. Nachr.*, 213:117–140, 2000.

[72] Manuel Duarte Ortigueira. Riesz potential operators and inverses via fractional centred derivatives. *Int. J. Math. Math. Sci.*, pages Art. ID 48391, 12, 2006.

[73] Guofei Pang, Wen Chen, and K. Y. Sze. Gauss-Jacobi-type quadrature rules for fractional directional integrals. *Comput. Math. Appl.*, 66(5):597–607, 2013.

[74] Igor Podlubny. *Fractional differential equations*, volume 198 of *Mathematics in Science and Engineering*. Academic Press, Inc., San Diego, CA, 1999. An introduction to fractional derivatives, fractional differential equations, to methods of their solution and some of their applications.

[75] Xavier Ros-Oton and Joaquim Serra. The Dirichlet problem for the fractional Laplacian: regularity up to the boundary. *J. Math. Pures Appl. (9)*, 101(3):275–302, 2014.

[76] Norikazu Saito and Guanyu Zhou. Analysis of the fictitious domain method with an L^2-penalty for elliptic problems. *Numer. Funct. Anal. Optim.*, 36(4):501–527, 2015.

[77] Stefan G. Samko, Anatoly A. Kilbas, and Oleg I. Marichev. *Fractional integrals and derivatives*. Gordon and Breach Science Publishers, Yverdon, 1993. Theory and applications, Edited and with a foreword by S. M. Nikol′skiĭ, Translated from the 1987 Russian original, Revised by the authors.

[78] Raffaella Servadei and Enrico Valdinoci. On the spectrum of two different fractional operators. *Proc. Roy. Soc. Edinburgh Sect. A*, 144(4):831–855, 2014.

[79] Jie Shen, Tao Tang, and Li-Lian Wang. *Spectral methods*, volume 41 of *Springer Series in Computational Mathematics*. Springer, Heidelberg, 2011. Algorithms, analysis and applications.

[80] Richard Mikaël Slevinsky, Hadrien Montanelli, and Qiang Du. A spectral method for nonlocal diffusion operators on the sphere. *J. Comput. Phys.*, 372:893–911, 2018.

[81] Yanhui Su, Lizhen Chen, Xianjuan Li, and Chuanju Xu. On the inf-sup constant of a triangular spectral method for the Stokes equations. *Comput. Methods Appl. Math.*, 16(3):507–522, 2016.

[82] Gabor Szegö. *Orthogonal Polynomials*. American Mathematical Society, New York, 1939. American Mathematical Society Colloquium Publications, v. 23.

[83] Xiaochuan Tian, Qiang Du, and Max Gunzburger. Asymptotically compatible schemes for the approximation of fractional Laplacian and related nonlocal diffusion problems on bounded domains. *Adv. Comput. Math.*, 42(6):1363–1380, 2016.

[84] Alex Townsend, Marcus Webb, and Sheehan Olver. Fast polynomial transforms based on Toeplitz and Hankel matrices. *Math. Comp.*, 87(312):1913–1934, 2018.

[85] Hans Triebel. *Interpolation theory, function spaces, differential operators*. North-Holland Publishing Co., Amsterdam-New York, 1978.

[86] Enrico Valdinoci. From the long jump random walk to the fractional laplacian. 2009. `http://www.dartmouth.edu/~cushman/papers/2018-JFM-FractionalLaplacian.pdf`.

[87] W. T. M. Verkley. A spectral model for two-dimensional incompressible fluid flow in a circular basin. I. Mathematical formulation. *J. Comput. Phys.*, 136(1):100–114, 1997.

[88] Christian Vollmann and Volker Schulz. Exploiting multilevel Toeplitz structures in high dimensional nonlocal diffusion. *Comput. Vis. Sci.*, 20(1-2):29–46, 2019.

[89] Wojbor A. Woyczyński. Lévy processes in the physical sciences. In *Lévy processes*, pages 241–266. Birkhäuser Boston, Boston, MA, 2001.

[90] Jiahong Wu. Solutions of the 2D quasi-geostrophic equation in Hölder spaces. *Nonlinear Anal.*, 62(4):579–594, 2005.

[91] Alfred Wünsche. Generalized Zernike or disc polynomials. *J. Comput. Appl. Math.*, 174(1):135–163, 2005.

[92] Kailai Xu and Eric Darve. Spectral method for the fractional Laplacian in 2D and 3D. *arXiv*, 2018.

[93] Zhongqiang Zhang. Error Estimates of Spectral Galerkin Methods for a Linear Fractional Reaction–Diffusion Equation. *J. Sci. Comput.*, 78(2):1087–1110, 2019.

[94] Xuan Zhao, Zhi-zhong Sun, and Zhaopeng Hao. A fourth-order compact ADI scheme for two-dimensional nonlinear space fractional Schrödinger equation. *SIAM J. Sci. Comput.*, 36(6):A2865–A2886, 2014.

[95] Vladimir A. Zorich. *Mathematical analysis. II.* Universitext. Springer, Heidelberg, second edition, 2016.